

**University of Windsor
Scholarship at UWindsor**

Electronic Theses and Dissertations

2003

Siphon removal of cohesionless materials.

Syeed Mahbub. Ullah

University of Windsor

Follow this and additional works at: <http://scholar.uwindsor.ca/etd>

Recommended Citation

Ullah, Syeed Mahbub., "Siphon removal of cohesionless materials." (2003). *Electronic Theses and Dissertations*. Paper 3475.

This online database contains the full-text of PhD dissertations and Masters' theses of University of Windsor students from 1954 forward. These documents are made available for personal study and research purposes only, in accordance with the Canadian Copyright Act and the Creative Commons license—CC BY-NC-ND (Attribution, Non-Commercial, No Derivative Works). Under this license, works must always be attributed to the copyright holder (original author), cannot be used for any commercial purposes, and may not be altered. Any other use would require the permission of the copyright holder. Students may inquire about withdrawing their dissertation and/or thesis from this database. For additional inquiries, please contact the repository administrator via email (scholarship@uwindsor.ca) or by telephone at 519-253-3000 ext. 3208.

SIPHON REMOVAL OF COHESIONLESS MATERIALS

by

Syeed Mahbub Ullah

A Thesis

Submitted to the Faculty of Graduate Studies and Research
through the Department of Civil and Environmental Engineering
in Partial Fulfillment of the Requirements for the Degree of Master of Applied Science
at the University of Windsor

August, 2003
Windsor, Ontario, Canada
© 2003, Syeed Mahbub Ullah

National Library
of Canada

Acquisitions and
Bibliographic Services

395 Wellington Street
Ottawa ON K1A 0N4
Canada

Bibliothèque nationale
du Canada

Acquisitions et
services bibliographiques

395, rue Wellington
Ottawa ON K1A 0N4
Canada

Your file *Votre référence*

ISBN: 0-612-84550-8

Our file *Notre référence*

ISBN: 0-612-84550-8

The author has granted a non-exclusive licence allowing the National Library of Canada to reproduce, loan, distribute or sell copies of this thesis in microform, paper or electronic formats.

L'auteur a accordé une licence non exclusive permettant à la Bibliothèque nationale du Canada de reproduire, prêter, distribuer ou vendre des copies de cette thèse sous la forme de microfiche/film, de reproduction sur papier ou sur format électronique.

The author retains ownership of the copyright in this thesis. Neither the thesis nor substantial extracts from it may be printed or otherwise reproduced without the author's permission.

L'auteur conserve la propriété du droit d'auteur qui protège cette thèse. Ni la thèse ni des extraits substantiels de celle-ci ne doivent être imprimés ou autrement reproduits sans son autorisation.

Canada

ABSTRACT

This thesis discusses the removal of cohesionless sediments by siphoning. A significant part of this study involves the analysis of equilibrium scour hole dimensions under different siphon flow characteristics. Scour holes of the sediments were formed by a siphon tube of three different sizes (9.65, 13.86 and 20.4 mm) positioned vertically at different positions relative to the surface of the sand bed. A total of 174 tests were performed, where the position of the tube ranged from 101.6 mm below the original bed to 6.4 mm above it. The latter part of the study investigates the heights for critical and general movement of the sediment particles.

Initially, dimensional analysis was used to examine all length parameters relating the equilibrium scour hole dimensions and the heights for critical and general movements with the characteristics of the flow through the siphon tube. These relations fit well with the densimetric Froude number when an individual sediment is considered. However, when data for different materials are compared, the curves show quite distinct relations. After using dimensional analysis, an effort was made using theory to determine what other parameters might affect the scouring process. This analysis is based on the threshold movement of a sediment particle moved by the viscous shear stress in a laminar boundary layer. It is evident from the theory that besides the densimetric Froude number, the angle of repose, dimensionless size and the Reynolds number of the sediment particle, as well as the Reynolds number of the flow through the tube should be taken into account to predict all the lengths parameters of scour hole dimensions and heights for critical and general movements of the particles. General relations are found for the length parameters obtained from different sediment materials used in the present study as well as in the

studies by Mazurek and Rajaratnam (unpublished) and Brahme (1983). Similarity is found for all the scour hole profiles when the radius of the scour hole at the tube level and the relative maximum equilibrium scour hole depth are used as scales in the radial and axial directions respectively.

To My Parents

ACKNOWLEDGEMENTS

The author wishes to express his sincere and profound gratitude to his supervisor, Dr. K. A. Mazurek, for her encouragement, advice and invaluable suggestions throughout the experiments and preparation of this thesis. The author is also grateful to her financial assistance in the research and compassionate support in different personal issues which have highly motivated him, and helped him to put behind all worries and difficulties.

Gratitude is also extended to other members of the thesis committee, Dr. S. Reitsma and Dr. D. Ting for their help and suggestions. The author is also obliged to Dr. N. Biswas for his encouragement and motivation.

Most importantly the author would like to thank all those people that kept him going. He would like to remember the fellow graduate students for their openhanded help during the experiments. He also appreciates the help from Mr. R. Clark and Mr. L. Pop for building the experimental setup.

Lastly, the author would like to thank his parents. Their love, support, and advice always helped to put things in perspective and keep him focused.

TABLE OF CONTENTS

ABSTRACT.....	iii
DEDICATION.....	v
ACKNOWLEDGEMENTS.....	vi
LIST OF TABLES.....	x
LIST OF FIGURES.....	xi
LIST OF SYMBOLS.....	xiv
CHAPTER 1: INTRODUCTION	1
1.1 Introduction	1
1.2 Objectives of the Study	3
1.3 Contents of Thesis	4
CHAPTER 2: BACKGROUND AND LITERATURE REVIEW	6
2.1 Introduction	6
2.2 Definition of Variables	6
2.3 Flow Characteristics around a Siphon Inlet	7
2.3.1 Siphon Tube set above the Bed	7
2.3.1.1 Inlet Flow having no Boundary ($z_0/d \gg 0$).....	7
2.3.1.2 Inlet Flow above a Rigid Boundary ($z_0/d > 0$).....	8
2.3.2 Siphon Tube at Bed ($z_0/d = 0$)	10
2.3.3 Siphon Tube within Bed ($z_0 < 0$).....	12
2.4 Incipient Motion of Sediment.....	13
2.5 Previous Studies of Scour by Siphon Suction	18

2.5.1 Slotta (1968)	18
2.5.2 Gladigau (1975).....	20
2.5.3 Salzmann (1977).....	22
2.5.4 Brahme (1983).....	23
2.5.5 Rehbinder (1994)	27
2.6 Summary	30
CHAPTER 3: EXPERIMENTAL SETUP AND EXPERIMENTS.....	39
3.1 Introduction	39
3.2 Experimental Setup and Experiments of Present Study	39
 3.2.1 Experimental Setup	39
 3.2.2 Testing Program and Measurements.....	40
 3.2.3 Soil Sample	42
3.3 Experimental Setup and Experiments of Mazurek and Rajaratnam	42
 3.3.1 Experimental Setup	42
CHAPTER 4: RESULTS, ANALYSIS, AND DISCUSSION.....	55
4.1 Introduction	55
4.2 Observations	55
4.3 Results and Analysis.....	58
 4.3.1 Analysis Using Dimensional Arguments	58
 4.3.1.1 Development of a Dimensionless Length Scale.....	58
 4.3.1.2 Analysis of Scour Hole Dimensions at Equilibrium.....	62
 4.3.1.3 Analysis of Heights of Threshold Conditions	65
 4.3.2 Analysis Using Theory	66

<i>4.3.2.1 Development of Functional Relationships for Equilibrium Scour Hole Radii</i>	66
<i>4.3.2.2 Validation of the Theory using Experimental Data.....</i>	77
<i>4.3.2.3 Applying the Theory for Predicting the Equilibrium Scour Hole Depth... </i>	79
<i>4.3.2.4 Applying the Theory for Predicting the Threshold Heights</i>	80
4.6 The Scour Hole Profiles at Equilibrium State	81
4.7 Analysis of Errors.....	83
4.8 Discussion	85
CHAPTER 5: CONCLUSIONS.....	121
5.1 Summary of Observations	121
5.2 Conclusions	124
5.3 Recommendations for Future Research.....	124
REFERENCES	126
APPENDIX A Experimental Results.....	129
APPENDIX B Explanation of the Derived Equations	234
VITA AUCTORIS	240

LIST OF TABLES

Table 3.1	Details of the experiments of the scour hole geometry (Present Study).	44
Table 3.2	Details of experiments for height of critical and general movement (Present Study).	49
Table 3.3	Details of experiments of Mazurek and Rajaratnam (unpublished).	50
Table 4.1	The maximum relative scour hole depth and scour hole radius at equilibrium for the tube set on or below the bed level (Present Study).	87
Table 4.2	The maximum relative scour hole depth and scour hole radius at equilibrium for the tube set above the bed level (Present Study).	91
Table 4.3	Height for critical movement (Present Study).	93
Table 4.4	Height for general movement (Present Study).	94
Table 4.5	The maximum relative scour hole depth and the scour hole radius at equilibrium for the tube set on or below the bed of fine sand.	95
Table 4.6	Critical and general movement heights from Mazurek and Rajaratnam (unpublished).	96
Table 4.7	The maximum relative scour hole depth and the aerial scour hole radius at equilibrium for the tube set above the bed of fine sand (Brahme 1983).	97
Table 4.8	The maximum relative scour hole depth and the aerial scour hole radius at equilibrium for the tube set above the bed of medium sand (Brahme 1983).	98
Table 4.9	The maximum relative scour hole depth and scour hole radius at equilibrium for the tube set above the bed of microbeads (Brahme 1983).	99
Table 4.10	Calculation for dimensionless particle diameter (D_*) for different studies.	100
Table 4.11	Maximum errors in measured and derived quantities.	101

LIST OF FIGURES

Fig. 1.1	Flushing of sediment from the bottom of a reservoir over the dam crest with a siphon.	5
Fig. 2.1	Definition sketch.	31
Fig. 2.2	Three possible cases for the tube position.	31
Fig. 2.3	Three-dimensional co-ordinate system in a sink flow and equipotential line.	32
Fig. 2.4	Final flow configuration for Apgar and Basco's experiment.	32
Fig. 2.5	Typical velocity distribution and boundary layer growth due to a line sink flow near bed.	33
Fig. 2.6	Typical velocity distribution and boundary layer growth due to a point sink flow near bed.	33
Fig. 2.7	Forces on an exposed grain.	34
Fig. 2.8	Shields diagram for incipient motion.	34
Fig. 2.9	Schematic of Slotta's flat bed experiment.	35
Fig. 2.10	Suction tube – sand bed configuration for Gladigau's experiment.	35
Fig. 2.11	Various stages of development of scour hole in sediment removal studies by Brahme.	36
Fig. 2.12	The dimensionless height above bed vs. the dimensionless flow on log-log paper for different materials of Brahme's experiment.	37
Fig. 2.13	Formation of the crater in the Rehbinder's experiment.	38
Fig. 3.1	Experimental setup of the present study.	51
Fig. 3.2	Schematic of the experimental setup of present study.	52
Fig. 3.3	Grain size distribution of the sand sample (present study).	53
Fig. 3.4	Experimental setup of Mazurek and Rajaratnam.	54

Fig. 4.1	Photograph of the some typical scour hole at equilibrium.	102
Fig. 4.2	Typical scour hole profiles for three different inlet heights.	103
Fig. 4.3	Typical scour hole profiles when vortex was generated below tube inlet.	104
Fig. 4.4	The dimensionless equilibrium scour radius, at the tube level, with the densimetric Froude number, for the cases where the tube is set on or below the bed level.	105
Fig. 4.5	The dimensionless equilibrium aerial scour radius, at the tube level, with the densimetric Froude number, for the case where the tube is set above the bed level.	106
Fig. 4.6	The dimensionless equilibrium scour depth, measured from the tube inlet level, with densimetric Froude number.	107
Fig. 4.7	The dimensionless height for critical movement with the densimetric Froude number.	108
Fig. 4.8	The dimensionless height for general movement with the densimetric Froude number.	109
Fig. 4.9	Typical scour hole profile for the case when tube is set on or below bed level.	110
Fig. 4.10	Typical scour hole profile for the case when tube is set above the bed.	110
Fig. 4.11	Possible effect of tube diameter on flow convergence at bed.	111
Fig. 4.12	The dimensionless equilibrium scour radius at inlet level with the theoretical function for the case where the tube is set on or below bed.	112
Fig. 4.13	The dimensionless aerial scour radius at equilibrium with the theoretical function for the case where the tube is set above the bed.	113
Fig. 4.14	The dimensionless relative maximum scour depth with the dimensionless scour radius measured at tube level at equilibrium.	114
Fig. 4.15	The dimensionless equilibrium maximum scour depth measured the tube inlet with the theoretical function.	115
Fig. 4.16	The dimensionless height for the critical movement with the theoretical function.	116

Fig. 4.17	The dimensionless height for general movement with the theoretical function.	117
Fig. 4.18	Curves fit for the dimensionless scour hole profile for the case when tube is set below the bed level (Present Study).	118
Fig. 4.19	Curve fits for the dimensionless scour hole profile for the case when tube is set on the bed level (Present Study).	119
Fig. 4.20	Curve fits for the dimensionless scour hole profile for the case when tube is set above the bed level (Present Study).	120

LIST OF SYMBOLS

The following symbols are used in this thesis:

a, b, c = exponents

c_1, c_2, c_3 = constants

C_d = drag coefficient

C_1, C_2 = constants

d = inner diameter of the tube inlet

D = mean grain diameter

D_{fs} = mean diameter of fine sand

D^* = dimensionless grain diameter

D_{10} = diameter of the particle that 10% the material is finer than to that diameter

D_{60} = diameter of the particle that 60% the material is finer than to that diameter

$f, f', f_1, f_2, \dots, f_8$ = functions

F_0 = the densimetric Froude number

F_d = drag force on a particle

F_g = submerged weight of a sediment particle

F_L = lift force on a particle

g = acceleration due to gravity

g_1 = a function

h = thickness of sediment strata or thickness of sand column inside the tube

i = hydraulic gradient for the seepage flow

i_c = critical hydraulic gradient for the soil

k_1, k_2, k_3 = constants

K	=	hydraulic conductivity of the sediment particle
K', K'', K'''	=	functions
l	=	length term
L	=	dimension of length
M	=	dimension of Mass
M_d	=	the moment due to the drag force exerted by the fluid
M_g	=	the moment due to the submerged weight of the particle
Q	=	flow rate through the tube inlet
Q_a	=	part of discharge resulting from other than seepage flow
r	=	radial distance from the centerline
r_a	=	aerial radius of equilibrium scour hole considering a definite inlet diameter
r_{a0}	=	aerial radius of equilibrium scour hole considering inlet as a point sink
r_b	=	radius of the equilibrium scour hole at bed level
r_t	=	radius of the equilibrium scour hole at inlet level
r_{tl}	=	a radius for an imaginary circle
R_0	=	Reynolds number of the flow through the inlet
Re_*	=	local Reynolds number
R_s	=	particle Reynolds number
S_g	=	specific gravity of the sediment material
T	=	dimension of time
u , and u'	=	velocity in the boundary layer at a distance z and z' respectively
u_*	=	shear velocity of the sediment grain
u_{*c}	=	critical shear velocity of the sediment grain

U_0	=	average flow velocity through the inlet
v	=	quantity of water flowing in unit time through a unit cross-section of soil
v_θ	=	tangential component of velocity
v_r	=	radial component of velocity
v_{rb}	=	flow velocity over sediment bed at a distance r from the tube centerline
V	=	a velocity term, relative velocity between fluid and solid particle
w_s	=	settling velocity of the particle
W	=	actual weight of a sediment particle
W_g	=	submerged weight of a sediment particle
x	=	Cartesian axis over z-plane
y	=	Cartesian axis over z-plane
z	=	vertical direction of from the bed
z'	=	normal direction of from the bed
z_0	=	vertical position of tube inlet from the bed
z_c	=	height of the tube inlet at which critical movement of the sediment occurs
z_g	=	height of the tube inlet at which general movement of the sediment occurs
Z	=	depth of water above the bed
β	=	represents the effects of turbulence
δ	=	thickness of the boundary layer
ε	=	the scour depth on any point measured from the original bed surface
ε_c	=	scour depth measured from the original bed level along the tube centerline
ε_m	=	the maximum scour depth measured from the original bed surface
ε_{rm}	=	the maximum scour depth measured from the tube inlet

ε_r	=	scour depth on any point measured from the inlet
η	=	dimensionless height from the bed in boundary layer
θ	=	slope of sediment bed at tube level, streamwise bed slope
θ'	=	direction about z-axis
μ	=	dynamic viscosity of the fluid
ν	=	kinematic viscosity of the fluid
$\pi_1, \pi_2, \pi_3, \pi_4$	=	dimensionless number
ρ	=	density of the fluid
ρ_s	=	density of the sediment particle
ρ_{sf}	=	density of fine sand
σ_g	=	geometric standard deviation of sand particle
τ^*	=	critical shear stress of the sediment particle
τ_{*c}	=	dimensionless critical shear stress of the sediment particle
τ_0	=	wall shear stress
τ_A	=	shear stress on the point A of the scour hole boundary
τ_c	=	critical shear stress of the sediment particle
$\tau_{c\theta}$ and $\tau_{c\theta s}$	=	critical shear stress of the sediment particle in an inclined plane with no seepage flow and with seepage flow respectively
ϕ	=	velocity potential function
φ	=	angle of repose of the sediment grain
ψ	=	the angle between the aerial radius and the centerline

CHAPTER 1: INTRODUCTION

1.1 Introduction

Siphoning is an important technique for the removal of sediment from channel and reservoir beds. A simple siphon device consists of circular tubing through which water is pumped out at a certain rate, so that the resulting flow erodes the bed sediments creating scour at the bed. Sometimes a siphon is created by means of the difference of water levels between upstream and downstream of dams, instead of mechanical pumps, to remove sediment from the reservoir. An example of this situation is shown in the Fig. 1.1. Although some experimental studies of this phenomenon have been carried out in cohesionless sediment, they are not well supported by theory.

The significant applications of sediment removal by suction are (Herbich 2000; Herbich and Brahme 1991): (1) contaminated and toxic sediment removal, (2) removal of clogging in wastewater channels, (3) dredging for navigation and mining, (4) land reclamation and beach nourishment, and (5) removal of deposited sediment in reservoirs and dams. Of these, contaminated sediment and its removal have been identified as major environmental concerns in many areas in Ontario, especially the Great Lakes (IJC 1985). Persistent toxic substances that have accumulated in bottom sediments from industrial, municipal, and non-point sources cause potential threat to the survival of benthic organisms, fishes, and their consumers. This pollution can also impair the quality of surrounding water, which may be difficult to treat for drinking purposes. Most inorganic and organic contaminants are preferentially adsorbed onto finer grained sediment, such as silts and clays. The concern is that finer grained sediments are more

readily disturbed during dredging than coarse-grained sediments (sand and gravels). Resuspension of contaminated sediments and potential contaminant release to the water column are the most important issues during dredging operations (Herbich 2000).

The classic techniques of sediment removal consist of both mechanical and hydraulic dredging. Mechanical dredges use direct mechanical force to dislodge and excavate the material whereas the hydraulic dredges remove and transport sediments in the form of a slurry. The type of dredging used mainly depends on the area of the location, the water depth, sediment characteristics, and thickness of the sediment layer to be removed (Herbich 2000).

Hydraulic dredging normally involves slurring of the sediments with water usually in a one-part sediment to four-part water mixture where this mixture is typically then pumped as slurry to either open water or to a confined upland disposal or sometimes to a hopper of a hydraulic dredge (Herbich 2000). Thus, it can contain a limited amount of dredged material. For hydraulic dredging, there are many techniques which differ in that portion of the hydraulic dredging system that is in contact with the bed (the dredgehead). Depending on the dredgehead, the hydraulic dredges can be classified as the cutterhead dredges, suction dredges, and hybrid dredges (Herbich and Brahme 1991). The cutterhead dredge is equipped with a rotating cutter apparatus surrounding the intake end of the suction pipe. These dredges are capable of digging and pumping all types of alluvial materials and compacted deposits such as clay and hardpan (Herbich 2000). Suction dredges include those hydraulic dredges that do not consist of a cutterhead. For the suction dredges, the dredgehead can be classified into plain suction, modified suction and matchbox suction (USEPA 1994). The plain suction dredge, the simplest of the

hydraulic suction dredges, employs a long suction pipe to dig and lift the sediment material to the surface. Sometimes this digging may be supplemented by water jets at the suction pipe mouth. Hybrid dredges use a combination of mechanical action and hydraulic pumping.

A plain suction dredge, operating in soft, free-flowing and unconsolidated material, usually causes little solids suspension than those supplemented by water jets or a cutterhead. In general, plain suction is still a preferred methodology because of its capability to dredge material with less resuspension, thereby creating less turbidity, than other types of hydraulic dredging (Herbich 2000; Herbich and Brahme 1991). The prediction of amount of dislodged material should be sufficiently accurate. The geometry of the scour hole produced due to siphoning of a certain flow condition needs to be predicted to get the precise extent of dredging without excessive removal of non-contaminated material. Accuracy in prediction of scour in both the horizontal and vertical directions might be important to ensure economic dredging and minimal impact on environment (Epskamp and Nedam 1995).

The mechanics behind the scour or removal of sediment in case of plain suction is still not well understood. There apparently no published literature that focused on the profile of the scour hole under different siphon characteristics and flows. This study is therefore meant to expand the knowledge of scour phenomena due to suction.

1.2 Objectives of the Study

The main objectives of this study are:

- (1) To study the geometry of the scour hole created by a siphon flow through a circular tube fixed above the soil surface in the equilibrium condition, with

varying suction tube diameter, flow rate (velocity), sediment size, and height of the tube above a cohesionless sand bed.

- (2) To develop semi-empirical equations to predict the dimensions of the scoured out area created by the suction flow, through the use of dimensional analysis and previous research on scour of cohesionless material.
- (3) To attempt to use theoretical fluid mechanics (potential flow in combination with boundary layer theory) to predict the scour hole dimensions and compare this with the experimental results.

1.3 Contents of Thesis

This thesis consists of five chapters. Chapter 2 introduces the variables involved in scouring by siphons and a background discussion on the flow behavior under different possible tube configurations. This chapter also illustrates criteria of incipient sediment motion and a review of previous literature related to scouring by siphons. Chapter 3 describes the details of the experimental setup and experiments of the present study and that of Mazurek and Rajaratnam (unpublished). Chapter 4 provides the observations and results of the experiments. The results contain both a dimensional and theoretical analysis of the experimental data. Chapter 5 gives the conclusions of the overall study, as well as a number of recommendations for the future studies relating to scour by siphon flows.

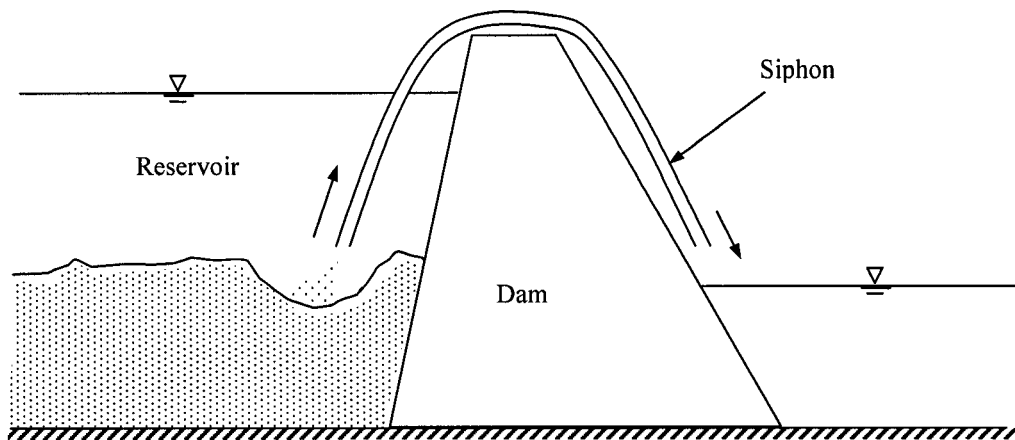


Fig. 1.1: Flushing of sediment from the bottom of a reservoir over the dam crest with a siphon (adapted from Rehbinder 1994).

CHAPTER 2: BACKGROUND AND LITERATURE REVIEW

2.1 Introduction

Before one can understand the scour of sediments created by siphon flows, it is necessary to have some knowledge of the velocity field at the mouth of a suction tube, as well as the characteristics of the flow over the sediment bed. The purpose of this chapter is thus to provide some background to understand the flow around a pipe inlet, as well as the criteria for the erosion of cohesionless sediment grains. There is also a review of the previous research studies that have focused on scour by siphons.

2.2 Definition of Variables

A sketch defining the variables related to scour created by a siphon flow is shown in Fig. 2.1. Important variables are the diameter of the tube inlet d , the vertical distance from its open end to the initial sediment bed surface z_0 , the radial distance of any point from the tube centerline r , the radius of the scour hole at bed level r_b , the radius of the scour hole at tube inlet level r_t , the distance between the center of inlet and the edge of the scour hole r_a (aerial radius), scour depth ε at radial distance r , the maximum depth of the scour hole ε_m , the depth of scour hole along the centerline ε_c , and the depth of the fluid above the bed Z . The mean grain diameter of the sand bed is denoted by D and the density of sand and the fluid are given as ρ_s and ρ , respectively. The rate of flow through the intake pipe is Q and the average velocity is U_0 . The dynamic viscosity and kinematic viscosity of the fluid are μ and ν respectively.

2.3 Flow Characteristics around a Siphon Inlet

There are three conditions for the siphon tube that will be studied herein:

- (1) a tube that is set at some height above the bed,
- (2) a tube that rests on the surface of the sand bed,
- (3) a tube that is set within the bed.

For every tube position, this study considers that the inlet of the tube is deeply submerged. Therefore, the surface boundary conditions are the same for every case and do not have any significant affect on the scouring process. A sketch of the three possible cases is shown in Fig. 2.2.

2.3.1 Siphon Tube set above the Bed

There are two scenarios possible in the case where the siphon tube is above a horizontal boundary. If the distance between the siphon inlet and the bed is very much greater than the inner diameter of the siphon tube, the flow into the siphon is essentially free from any effect of the boundary. When the tube is near the bed, bed effects must be considered. However, what should be considered as “near the bed” has not been explicitly defined in the literature.

2.3.1.1 Inlet Flow having no Boundary ($z_0/d \gg 0$)

The flow towards the suction tube where there is no bed or boundary is typically described by potential flow theory. The absence of any boundary precludes the formation of shear stresses and therefore little turbulence might occur in the converging flow. The flow pattern in this case may be described by potential flow theory since this theory

neglects viscous effects and follows Euler's equations of motion. Potential flow theory also assumes that fluid is ideal and the flow is irrotational and without turbulence.

The three-dimensional flow near the suction inlet without having a solid boundary can be regarded as that created from a point sink flow (Apgar and Basco 1973; Rehbinder 1994). The three-dimensional point sink is given by the potential function (Vallentine 1959)

$$\phi = \frac{Q}{4\pi r} \quad (2.1)$$

where ϕ is the velocity potential function, Q is the rate of flow through the point sink. The co-ordinate system for the three-dimensional sink flow is shown in Fig. 2.3. If v_r = radial velocity component and v_θ = tangential velocity then

$$v_r = \frac{\partial \phi}{\partial r} = -\frac{Q}{4\pi r^2} \quad (2.2)$$

and

$$v_{\theta'} = -\frac{\partial \phi}{r \partial \theta'} = 0 \quad (2.3)$$

where r is the radial distance from the point sink, x and y are two mutually perpendicular axis on the z -plane for Cartesian coordinates, and $\theta' = \tan^{-1}(y/x)$. From Eq. 2.2, we can see that the velocity is the maximum at the mouth of circular inlet and this velocity is inversely proportional to the square of the radial distance. Therefore, the velocity decreases rapidly with the distance from the inlet center.

2.3.1.2 Inlet Flow above a Rigid Boundary ($z_0/d > 0$)

Apgar and Basco (1973) used theory and experiments to examine the flow characteristics around a tube inlet near a flat, horizontal, and smooth rigid bed. The flow

into the tube was described by using potential flow theory. The inlet was represented as a sink and the boundary was simulated by an imaginary “mirror sink”, which was placed at the same distance beneath boundary as the tube is above it. By the principle of superposition, by adding the expressions for point sinks at $z = z_0$ and $z = -z_0$, a plane of symmetry is formed which represents the boundary. Since the flow field below the plane of symmetry is a mirror image of that above, no flow is possible across that plane and it represents a solid boundary. Considering this situation, they showed that the velocity components of the flow to a tube with a smooth rigid boundary can be expressed as

$$v_r = -\frac{Q}{4\pi} \left[\frac{r}{[(z-z_0)^2 + r^2]^{3/2}} + \frac{r}{[(z+z_0)^2 + r^2]^{3/2}} \right] \quad (2.4)$$

and

$$v_z = -\frac{Q}{4\pi} \left[\frac{z-z_0}{[(z-z_0)^2 + r^2]^{3/2}} + \frac{z+z_0}{[(z+z_0)^2 + r^2]^{3/2}} \right] \quad (2.5)$$

where v_r = the component of velocity in the radial direction and v_z = the component of velocity in the vertical direction, r = radial distance from centerline of the tube and z = distance measured upward from the boundary.

After determining the velocity above field from the potential flow theory, Apgar and Basco (1973) carried out experimental studies of the flow patterns around tube inlet to compare the theory with the actual flow. The flow rate was varied from 3.12 to 4.23 L/s and the inlet heights z_0 were 35.7, 71.0 and 142.0 mm above the bed. Only one tube was used, which had an inner diameter of 35.7 mm. The velocity was measured within the first few minutes of each test run. The streaklines and velocities were then plotted for nine flow cases, each of which was a composite of at least six test runs. For $z_0/d = 1$ and

$Q = 3.12$ and 4.23 L/s, the measured velocities agreed fairly well with theory. However, at $z_0/d = 2$ and 4 , far from the tube (nearly at $16d$ from the inlet), a large number of velocity values were significantly higher (up to 3 times) than predicted.

Apgar and Basco (1973) also observed that with time the flow situation changed gradually. The streaklines started to move and become unstable and the values for velocities also changed. This instability occurred in every case until a “general turbulence” set in. As well, after “few minutes”, a horizontal plane of separation developed above the tube inlet position (Fig. 2.4). Below the plane of separation, the streak lines tended to align themselves parallel to the boundary near the inlet. Above the inlet, the flow was weak, and above the plane of separation upward vertical flow takes place. The final flow patterns around the inlet were also similar to theoretical predictions, except that velocities measured below the inlet and near the boundary were larger than what theory predicted (1.5-2 times higher than calculated values).

It is evident from the above discussion that the justification to describe the inlet flow near a smooth boundary as a sink flow by the potential flow theory is related to the elapsed time of the flow through the inlet. The flow around the tube inlet on a rigid bed could be described well by potential flow theory, if we consider the situation just after start-up of the flow. However, the shear stress on the boundary due to this sink flow is apparently absent in the previous literature.

2.3.2 Siphon Tube at Bed ($z_0/d = 0$)

Theoretically, if the tube is exactly on a rigid bed and there is no opening between the pipe inlet and the interface, flow cannot occur. However, if we assume that the tube is located at very small distance above the rigid and smooth bed, it might be considered

as a point sink located on the bed. Schlichting and Gersten (2000) demonstrates a theoretical analysis to determine the boundary layer thickness due to a line sink. Fig. 2.5 shows a typical boundary layer formed over a bed due to the line sink flow. Schlichting and Gersten (2000) gives the velocity distribution in the laminar boundary layer due to the sink flow on the smooth bed as

$$\frac{u}{v_r} = f'(\eta) = 3 \tanh^2 \left(\frac{\eta}{\sqrt{2}} + \operatorname{arctanh} \sqrt{\frac{2}{3}} \right) - 2 \quad (2.6)$$

where the dimensionless distance from the smooth bed

$$\eta = z \sqrt{\frac{-v_r}{rv}} \quad (2.7)$$

and v_r = the radial velocity at a distance r towards the tube centerline, u = the velocity at a vertical distance z from the boundary, and ν = kinematic viscosity of the fluid.

According to Parthasarathy (1969), the dimensionless distance in the boundary layer formed due to a point sink located on the smooth bed (Fig. 2.6) can be taken as

$$\eta = \frac{z}{r} \sqrt{\frac{Q}{4\pi\nu r}} \quad (2.8)$$

Using this velocity distribution described in Eq. 2.6, the wall shear stress τ_0 can be estimated according to Newton's law by

$$\tau_0(r) = -\mu \left(\frac{\partial u}{\partial z} \right)_0 \quad (2.9)$$

where $\tau_0(r)$ is the wall shear stress at a radial distance r from the sink position, μ is the dynamic viscosity of the fluid, and $\left(\frac{\partial u}{\partial z} \right)_0$ is the gradient of the velocity distribution at the boundary . The above relations will be discussed further in Chapter 4.

2.3.3 Siphon Tube within Bed ($z_0 < 0$)

In the last two cases flow around siphon tube has been explained assuming that the bed is impermeable, smooth and rigid. But in the actual situation the soil itself is permeable and the initial flow around suction tube within permeable bed is different from the previous cases. Salzmann (1977) developed an electro-analog model to describe the potential flow net in soil beneath cylindrical suction tube. He mentioned that the amount of flow into the suction pipe prior to scour depends upon the permeability of the soil and the magnitude of the negative pressure acting upon the bed surface. The flow initially will be governed by Darcy's formula for seepage flow through the bed (Das 2002)

$$v = Ki \quad (2.10)$$

where v = the quantity of water flowing in unit time through a unit gross cross-sectional area of soil at right angles to the direction of flow, K = hydraulic conductivity, and i = hydraulic gradient. However, it must be noted that Darcy's law specifically neglects the kinetic energy of the flow through the porous medium.

Suppose, the tube is vertically inserted through the bed and the thickness of sand column inside the tube is h (Fig. 2.2(c)). Due to an upward flow through the tube, the stability of the sand particle any point inside the tube will be lost when the hydraulic gradient, i at that point reaches its critical value (Das 2002). This phenomenon is commonly referred as "quick conditions" and this critical hydraulic gradient is commonly denoted by i_c . Normally for most soils, the critical value of hydraulic gradient is close to 1. However, the flow through the tube must be great enough to carry the particles away. Theoretically, this occurs if the average velocity of flow is larger than the settling

velocity of the particle in the fluid. After some removal of particles takes place, the tube inlet eventually becomes free of sand.

This study concerns only the geometry of the scour hole by siphon flow when the scouring process reaches equilibrium. Therefore, details of the initial flow configuration through the soil are not provided.

2.4 Incipient Motion of Sediment

Cohesionless grains composing the surface of the sediment bed are subjected to a weight force and forces applied by the flowing fluid. The initiation of motion of a particle on a horizontal bed occurs by the action of fluid flow when the forces applied on the particle by fluid flow (drag and lift), exceed the stabilizing force due to particle weight (Raudkivi 1998). Thresholds for particle erosion from any horizontal bed can be calculated using average values for hydraulic parameters if the fluid and sediment properties are known. The important fluid properties are specific weight and viscosity. Significant properties of cohesionless sediments are particle size, shape, specific gravity, and position in the matrix of surrounding particles. Major hydraulic forces are bed shear stress, lift, pressure fluctuations related to turbulence and impact from other particles.

If the flow near the boundary is laminar, the individual grains will not shed eddies and the drag force will be mainly due to viscous shear. At a higher velocity more exposed grains shed eddies and a wake is formed in the lee of the grain (Raudkivi 1998). The drag force in this case becomes the resultant of the surface drag (viscous skin friction) and the form drag due to pressure difference in front and behind the particle. The point of application of the drag force depends on the magnitude of lift and drag

components which in turn are functions of the shape and locations of the particle, and the local Reynolds number (Raudkivi 1998).

Fig. 2.7 shows a typical diagram of an exposed grain subject to fluid force, where the weight of the particle, lift force and drag force are denoted by W , F_d and F_L respectively. For the purpose of analysis Mih and Kabir (1983) assumed that the solid particles are spherical in shape, the drag force F_d , on a solid sphere of diameter D , is

$$F_d = C_d \frac{\pi}{4} D^2 \rho \frac{V^2}{2} \quad (2.11)$$

where C_d = the drag coefficient, ρ = fluid density, and V is the relative velocity between the fluid and the solid particles. If we consider the initiation of the motion of the solid particles along the stationary stream bed, V will represent the velocity of the fluid. The net gravitational force or the submerged weight of the particle is

$$F_g = W - F_L = \frac{\pi}{6} D^3 g (\rho_s - \rho) \quad (2.12)$$

where g = acceleration due to gravity and ρ_s = density of the sediment particle. The dimensionless ratio of the drag force to the net gravitational force, $\frac{F_d}{F_g}$, is an important parameter in the initiation of motion (Mih and Kabir 1983) and this can be expressed as

$$\frac{F_d}{F_g} = \frac{3C_d}{4} \frac{V^2}{gD \left(\frac{\rho_s - \rho}{\rho} \right)} \quad (2.13)$$

The drag coefficient in Eq. 2.11 and 2.13 is a function of Reynolds number and the particle shape. The square root of the ratio $\frac{V^2}{gD\left(\frac{\rho_s - \rho}{\rho}\right)}$ in Eq. 2.13 is termed as the densimetric Froude number (Mih and Kabir 1983) which is denoted by F_0 .

White (1940) considered the initiation of the particle movement would occur by the rolling of one particle over another due to instability in moments only. The point O is the center of gravity of the grain and the point C the pivotal point of rotation (Fig. 2.7). The moment due to the submerged weight of the particle, M_g , and the moment due to the fluid motion, M_d , was expressed as

$$M_g = \frac{\pi D^3}{4} g (\rho_s - \rho) \frac{D}{2} \sin \varphi \quad (2.14)$$

and

$$M_d = \beta \rho u_*^2 \frac{\pi D^2}{4} \frac{D}{2} \cos \varphi \quad (2.15)$$

where ρ_s = particle density of the sediment, D = sediment size, g = gravitational acceleration, ρ = fluid density, φ = angle formed by the line OC with the vertical axis, and β represents the effects of turbulence, the point of application of drag force, etc., i.e.

all the effects besides the weight and drag and the shear velocity, $u_* = \sqrt{\frac{\tau_0}{\rho}}$. The

moments M_g and M_d must be equal for the sediment grain to rotate over the downstream grain about the pivotal point C . Considering this situation, the direction which makes an angle φ with the downstream should be the direction of easiest movement. The angle φ is defined as the angle of repose of the sediment grain. Equating moments described in Eq. 2.14 and 2.15, the shear velocity u_* for the threshold condition can be found (White 1940)

$$u_{*c} = \left(\frac{2 \tan \phi}{3\beta} \right)^{1/2} \left[\left(\frac{\rho_s - \rho}{\rho} \right) g D \right]^{1/2} \quad (2.16)$$

where u_{*c} is the threshold or critical value of u_* . Note that u_{*c} is the dimensionless form of critical shear stress.

Shields (1936) applied dimensional analysis to determine some dimensionless parameters and established his well-known diagram for incipient motion (Fig. 2.8). He proposed the following functional relationship

$$\tau_* = f(Re_*) \quad (2.17)$$

where $\tau_* = \frac{\tau_0}{(\rho_s - \rho)Dg}$ (Shields parameter) and Re_* is the local Reynolds number (or the

particle Reynolds number at the boundary) $= \frac{u_* D}{v}$. Here, τ_* represents a dimensionless

shear stress.

Fig. 2.8 shows the experimental results obtained by Shields and other investigators at incipient motion of cohesionless sediments. At points above the curve, the particle will move, whereas points below the curve the flow is unable to move the particle. The curve represents the critical value of the Shields parameter τ_{*c} that corresponds to the incipient motion ($\tau_0 = \tau_c$).

Julien (1998) showed that the critical value of the Shields parameter τ_{*c} is a function of both the particle Reynolds number at boundary, Re_* , and the angle of repose of the sediment grain, ϕ . He attempted to replace the abscissa of the Shields diagram by using dimensionless particle diameter which can be expressed as

$$D_* = D \left[\frac{(\rho_s - \rho)g}{\rho v^2} \right]^{1/3} \quad (2.18)$$

Using D_* , the critical values of the Shields parameter τ_{*c} can be approximated as follows

$$\tau_{*c} = 0.5 \tan \varphi ; \text{ when } D_* < 0.3 \quad (2.19)$$

$$\tau_{*c} = 0.25 D_*^{-0.6} \tan \varphi ; \text{ when } 0.3 < D_* < 19 \quad (2.20)$$

$$\tau_{*c} = 0.013 D_*^{0.4} \tan \varphi ; \text{ when } 19 < D_* < 50 \quad (2.21)$$

$$\tau_{*c} = 0.06 \tan \varphi ; \text{ when } D_* > 50 \quad (2.22)$$

where $\tau_{*c} = \frac{\tau_c}{(\rho_s - \rho)Dg}$ is the dimensionless critical shear stress.

Note that the Shields curve does not apply to where the soil bed has a slope. The following equation was proposed by Chiew and Parker (1994) in order to account for the effect of bed slope on Shields critical shear stress as

$$\left(\frac{u_{*c\theta}}{u_{*c}} \right)^2 = \cos \theta \left(1 - \frac{\tan \theta}{\tan \varphi} \right) \quad (2.23)$$

where $u_{*c\theta}$ is the critical shear velocity for the particle on a bed with a streamwise slope θ , u_{*c} is the critical velocity for a horizontal sediment bed, and φ is the angle of repose of the particle submerged in water.

Cheng and Chiew (1999) performed a force analysis for the threshold condition of sediment transport by including the effect of a force due to upward seepage flow. They suggested that the ratio of the critical shear stress with the seepage flow in the sediment to that without the seepage flow depends on the hydraulic gradient for seepage just below the surface of the bed. From a theoretical analysis, they gave

$$\left(\frac{u_{*c\theta s}}{u_{*c\theta}} \right)^2 = 1 - \frac{i}{i_c} \quad (2.24)$$

where $u_{*c\theta s}$ is critical the shear stress of the particle with a streamwise bed slope θ and where the seepage flow exists, $u_{*c\theta}$ is the critical shear velocity of the particle with a streamwise bed slope θ and without any seepage flow, i is the hydraulic gradient for seepage, and i_c is the critical hydraulic gradient at which quick conditions occur. From Eq. 2.24, it is apparent that an increase in the hydraulic gradient results in a reduction of the critical shear stress, and the critical velocity decreases to zero when quick conditions occur. If the hydraulic gradient for the seepage is small compared to its critical hydraulic gradient, then the seepage effect on the scouring process can be neglected.

2.5 Previous Studies of Scour by Siphon Suction

Only a few studies have been found that investigated scour by suction flows. Most studies have been experimental in nature and those were mainly intended to predict the relationships of the radius of scour hole under given flow conditions. There have been few studies that have specifically focused on geometric profile or the depth of the scour hole produced by siphon flows.

2.5.1 Slotta (1968)

Slotta (1968) made an attempt to determine similarity criteria for the suction of sediment into the entrance of a dredge pump intake. He analyzed the fluid flow around a vertical intake over single grain layer on a flat board and found a relationship between r_b , and the governing variables Q , d , z_0 , D , U_0 , ρ , μ , and, w_s (the terminal settling velocity of the particle). A schematic of the experiments is shown in Fig. 2.9. Slotta used two different pipe sizes of 14.2 and 28.5 mm inner diameter and granular materials of three different specific gravities (plastic BB's ($S_g = 1.28$), sand ($S_g = 2.65$) and coal ($S_g = 1.3$)).

Slotta suggested the dimensionless variables important to the problem were $\frac{r_b}{z_0}$,

$\frac{U_0^2}{gz_0}$ and $\frac{r_b^2 v}{Q^{1/2} w_s^{1/2} D z_0}$. The second parameter, $\frac{U_0^2}{gz_0}$ is in the form of a Froude number.

Plotting the experimental data in terms of this Froude criterion gave a “poor” correlation for the scour data. However, for these three different sediment materials, almost straight-

line relationships were found between $\frac{r_b}{z_0}$ and $\frac{r_b^2 v}{Q^{1/2} w_s^{1/2} D z_0}$.

Slotta considered the last term as a Reynolds number, since this can also be written as

$$\frac{L^2 v}{LV^{1/2}V^{1/2}L^2} \approx \frac{v}{VL} \quad (2.25)$$

where V is the velocity term, L , is a length and v is a viscosity term. Therefore, he suggested that a Reynolds scaling criteria should control model similitude criteria for dredge suction inlets.

For the three materials he obtained straight lines of three different slopes. The straight lines were described by these equations

$$1. \text{ For plastic BB's} : \frac{r_b}{z_0} = 0.71 + 0.52 \left(\frac{r_b^2 v}{Q^{1/2} w_s^{1/2} D z_0} \right) \quad (2.26)$$

$$2. \text{ for sand} : \frac{r_b}{z_0} = 0.46 + 0.39 \left(\frac{r_b^2 v}{Q^{1/2} w_s^{1/2} D z_0} \right) \quad (2.27)$$

$$3. \text{ for coal} : \frac{r_b}{z_0} = 0.41 + 0.23 \left(\frac{r_b^2 v}{Q^{1/2} w_s^{1/2} D z_0} \right) \quad (2.28)$$

It is apparent that the data for the radius for the sand falls between those for plastic BB's and coal, although the specific gravity of sand is the largest. This study does not explain

this behavior. It is evident that the term $\frac{r_b}{z_0}$ is present in both the dimensionless parameters which could make a spurious relationship. Also, the second term contains the terminal particle settling velocity, w_s , diameter of the sediment grain, D , and the kinematic viscosity, ν . Here, the terminal settling velocity of the particle can be expressed as (Yang 1996)

$$w_s = \frac{1}{18} \left(\frac{\rho_s - \rho}{\rho} \right) g \frac{D^2}{\nu} \quad (2.29)$$

From Eq. 2.29 it is evident that the terms D and ν are included in particle settling velocity w_s . Therefore repeating these variables in the parameter $\frac{r_b^2 \nu}{Q^{1/2} w_s^{1/2} D z_0}$ might have caused over specification. As well, the suction tube diameter d is not present in these dimensionless parameters. Therefore, the importance of suction velocity is ignored. No experimental data is given in this paper.

2.5.2 Gladigau (1975)

Gladigau, in an extension of Slotta's (1968) study, used a similar experimental setup to Slotta (1968) but used more tube diameters and inlet shapes and had a sand bed, as well as the rigid bed with a layer of particles. The main purpose was to assess the flow behavior for a variety of cutter head types and to develop some similarity criteria for the amount of the sediment removed for each case. Two tube inlets were used having internal diameters of 69.9 and 38.1 mm, with straight and bellmouth inlet shapes. The sand used was clean sand with a mean diameter of 0.24 mm, a specific gravity of 2.67, and a settling velocity of 26.7 mm/s in water at 21°C. The experiments were conducted in a tank containing a submerged horizontal sand tray. The first set of experiments was

performed using the sand bed to determine the threshold of the particle movement for a stationary tube (case A1) and a traversing tube (case A2) and the second set was used to determine the scour hole radius and the rate of scour for a stationary tube (case A3) and a traversing tube (case A4). The four configurations for his experiment are shown in the Fig. 2.10.

Gladigau (1975) observed there could be two situations where the particles on the bed were picked up by the flow, as the flow rate increased in the stationary tube experiments (case A1 in Fig 10). The first was the “Horizontal Threshold Movement” where the first grains moved and then more grains were transported towards the center of the flow. The other case was the “Spiral Threshold Pickup” where a small vortex picked up sand and moved it upwards into the tube. From observations of the flow net around the suction inlet using the hydrogen bubble technique, Gladigau determined that the horizontal movement and spiral pickup were completely independent phenomenon. Based on Kramer’s (1935) criteria for defining the threshold when a bed of particles are moving, the “Horizontal Threshold movement” was further divided into “weak movement”, where the movement of the first grain was assessed, and “general movement”, where the overall sand grain movement was observed and which resulted in the formation of a conical heap at the center of the flow. He suggested that with general movement the radius of the scour could be distinguished and measured, whereas in case of the weak movement scour radius was not distinguishable.

For case A3 configuration (where a stationary tube was placed close to sediment bed), for a constant flow rate, sand was removed from the bed at a decreasing rate creating a scour hole. The velocity inside the scour hole was reduced continually as the

scouring progressed. After a certain time, an equilibrium condition was reached where the shear force tending to move the grain balanced the gravity forces holding the grain in position. The “equilibrium profile” was defined as the scour hole profile that occurred when no further sand grain movement could be observed. He showed from his measurements of the velocity field, that the velocity at the bed which just caused particle movement was not greater than the velocity within the scour hole in the equilibrium condition.

In another set of experiments, Gladigau (1975) reconstructed Slotta’s experimental set up and measured the scour hole radius for varying flows and height of the tube inlet above the bed using a 69.9 mm tube inlet. Gladigau observed when z_0 is held constant and Q is varied, the relationship between $\frac{r_b}{d}$ and $\frac{r_b^2 v}{Q^{1/2} w_s^{1/2} D z_0}$ is straight-line. It was also found that the shape of the suction inlet did not produce any difference in scour.

2.5.3 Salzmann (1977)

Salzmann (1977) conducted model studies on hydraulic suction systems and developed a method for computing the solids output of hydraulic dredging equipment. The study included a simple electrical-analog experiment to describe qualitatively the potential flow net beneath a cylinder suction pipe. He also attempted to investigate the interrelation between fluid and soil mechanics as well as the influence of soil type, the influence of the shape of the suction head, and of the supplementary-pressure water leading the output of solid material during hydraulic dredging. He used different pipe sizes and suction inlet shapes such as pear-shape, funnel shape, cylindrical, oval and tube

inlet shapes and determined the intake loss coefficients for different suction head shapes.

The inlet pipe diameters tested were 21, 32, 40.5 and 50.5 mm.

He suggested that a straight circular pipe or cylindrical suction head represents a Borda's outlet. The suction flow becomes constricted as it enters the inlet and at certain distance from the inlet cross section, the constriction of the suction stream is no longer noticeable. Hydraulic model studies were also carried out to determine the pressure and velocity conditions around the intake of a suction pipe. The velocity and pressure distribution beneath the cylindrical inlet above a horizontal and above a funnel shaped rigid bed was measured and graphically presented. In case of funnel shaped rigid bed, Salzmann observed that the flow velocity increases sharply only in the immediate vicinity of the tube inlet. From the results of his studies, he also concluded that:

1. The suction flow is a potential flow and the soil to be loosened is only taken up by flow streamlines that touch the soil surface.
2. The water flows towards the suction pipe not only across the surface of soil but also through the soil. The tendency to constant hydraulic soil movement is due to a large pressure gradient at the soil surface below the suction pipe.

2.5.4 Brahme (1983)

The main objective of Brahme's (1983) study was to understand the basic hydrodynamic conditions in the vicinity of a rotating suction cutterhead and to determine the various factors that contribute to the turbidity generation, the resulting environmental problems and means to reduce the turbidity. The study included flow visualization at the suction intake, measurement of velocity near the intake and an evaluation of sediment removal due to suction.

Brahme used dimensional analysis and conducted similar experiments to Apgar and Basco (1973) to determine the velocity field. In his experiment, Brahme used a steel tank 2440 mm long, 1220 mm wide and 1220 mm deep and three pipe diameters (e.g. 30, 41 and 50.8 mm) at three different heights (e.g. 101.6, 152.4 and 203.2 mm) above the bottom. The pipes were cylindrical shaped and positioned at angles 90° and 60° to the horizontal. Three discharge conditions (e.g. 2.53, 3.03 and 3.53 L/s) were used and the depth of water over the bed throughout the experiment was 914 mm. A flat steel plate was placed at the bottom of the test section.

Brahme observed that initially the effect of shear stress at the boundary was not significant. After some time, the flow away from the intake showed a tendency to become more and more parallel to the boundary than before (which is similar to that observed by Apgar and Basco (1973)). However, like in Apgar and Basco (1973), there is no data for the transient effect of the flow pattern. Brahme mentioned that velocity in the flow field, in general, increased with an increase in the discharge and that the velocity was fairly high very near the intake of the pipe, although it dropped rapidly with distance away from the pipe. He also observed that the region of high velocity near the intake of the pipe moved upwards with an increase in the distance between intake and bottom of the tank, and the velocity field changes very little for the same suction discharge, but different pipe diameters. Brahme also found that the values of the dimensionless number

$$\frac{Q}{r^2 v}$$
 at any location in the velocity field for different flow conditions were similar.

Again the pattern of the flow field and the magnitude of velocities remained more or less unchanged for similar conditions with pipe at 90° to the horizontal.

To study the similitude criteria for the removal of sediment through a suction inlet, Brahme used the same values of parameters as before, except the height of the inlet in this case were 12.7, 22.9 and 31.8 mm, and the cohesionless bed materials used were made up of either microbeads ($S_g = 2.45$), fine sand ($S_g = 2.66$), medium sand ($S_g = 2.64$) or coal ($S_g = 1.38$). The sediment under study was placed over the steel plate at bottom of the tank. In most cases, the scour hole dimensions were observed at 30, 45, 60 and 75 min from the start of the test. He observed that the movement of the sediment to the center of the scour hole continued until the depth at center reached an equilibrium, which took about 1.5 hrs. When the equilibrium was reached, there is no further increase in the scour hole diameter. He discussed four stages of development of scour hole as shown in Fig. 2.11. In the beginning of a test, the sediment starts to move towards the point exactly below the suction pipe and then enter through the inlet. He thought that due to sudden application of vacuum pressure in the center, the bed was found to be slightly raised (Fig. 2.11(a)). He noticed that the sediment was removed mostly from the central portion of the scour hole area just below the pipe. Later on the sediment at the center of the hole was picked up thus creating a deep hole (Fig. 2.11(b)). With time the depth of this portion gradually increased (Fig. 2.11(c)), resulting in more sediment that slipped into the hole when the angle of the slope equaled the angle of repose of the sediment. The movement of the sediment towards the center continued until the geometry of the scour hole reached the equilibrium (Fig. 2.11(d)). Brahme proposed two possible reasons for which the sediment at the periphery of the scour hole was found to be moving towards the center: (1) due to increase in the slope of the scour hole the particle slips to the center of the scour hole; and (2) movement of particle due to the radial flow towards the center

of the pipe. Brahme thought that the contribution of the latter towards the total movement of sediment into the suction pipe appeared to be small compared to the former since the magnitude of velocities at the bottom was small.

Brahme used three dimensionless parameters $\frac{r_b^2 v}{w_s d^2 z_0}$, $\frac{r_b v}{w_s dz_0}$ and $\frac{Qz_0}{r_b^2 v}$. These dimensionless parameters have been plotted against $\frac{r_b}{z_0}$, $\frac{r_b}{d}$ and $\frac{z_0}{d}$ to determine the possible correlations among the various parameters. The relation between the dimensionless parameters $\frac{r_b^2 v}{w_s d^2 z_0}$ and $\frac{r_b v}{w_s dz_0}$ with $\frac{z_0}{d}$ showed that there is a clear dependence on d in both cases. The other dimensionless term $\frac{Qz_0}{r_b^2 v}$ was also related with $\frac{z_0}{d}$. The relation showed a dependence on d for all the materials studied. All the best-fit curves for the different materials, plotted in log-log graph paper, were almost parallel to each other (Fig. 2.12). The relations for the three materials are given below:

$$1. \text{ Microbeads: } \frac{z_0}{d} = 0.1037 \left(\frac{Qz_0}{r_b^2 v} \times 10^{-3} \right)^{0.6892} \quad (2.30)$$

$$2. \text{ Fine sand: } \frac{z_0}{d} = 0.0762 \left(\frac{Qz_0}{r_b^2 v} \times 10^{-3} \right)^{0.7184} \quad (2.31)$$

$$3. \text{ Medium sand: } \frac{z_0}{d} = 0.0639 \left(\frac{Qz_0}{r_b^2 v} \times 10^{-3} \right)^{0.7309} \quad (2.32)$$

However, it has been noticed from this plot that, although the term $\frac{Qz_0}{r_b^2 v}$ was increased gradually from some value the term $\frac{z_0}{d}$ has the same value. This behavior in

the plot was not clarified in this literature. Brahme mentioned that the variation in the slope of the equations (Fig. 2.12) for different materials was mainly due to the difference in the diameter and the specific gravity of the particle. The normalized data for particle diameter and specific gravity using fine sand as the basis were plotted on a log-log paper and the equation for the best-fit line for all the data is

$$\frac{z_0}{d} = 0.0819 \left[\left(\frac{Qz_0}{r_b^2 v} \times 10^{-3} \right) \left(\frac{D_{fs}}{D} \right)^{0.3} \left(\frac{\rho_{fs} - \rho}{\rho_s - \rho} \right)^{0.5} \right]^{0.693} \quad (2.33)$$

where D_{fs} and ρ_{fs} are diameter and density of fine sands and ρ_s is the density of the sediment grains under study. This equation has a correlation coefficient of 0.79. Since the term $\frac{Qz_0}{r_b^2 v}$ is a form of Reynolds number, Brahme concluded that, the sediment scour by siphon flows did not follow the Froude-type relationship, but was basically a phenomenon governed by a Reynolds criteria.

2.5.5 Rehbinder (1994)

Rehbinder (1994) demonstrated both theoretical and experimental analysis to study the threshold conditions of sediment removal by siphons and to examine the effect of pressure due to seepage flow and shear stress on lift of the removed particle. He defined the critical flux through a siphon tube as the flux when the uppermost particles from a horizontal bed barely start to move. The theoretical analysis initially considered the flux which is less than critical flux (which is defined as subcritical flux) and was based on some assumptions: the sediment is homogenous and isotropic; the grains are rounded; and the sediment forms an infinitely extended stratum which rests upon an

impervious horizontal bottom of a semi infinite water reservoir. It was also considered that $r \gg z_0$, which made it reasonable to assume the flow into the inlet as a sink flow.

Rehbinder explained that the flow of water exerts hydraulic forces on the sediment grains in the stratum. These forces are mainly two kinds: (1) forces caused by the flow in the stratum (seepage flow) and (2) shear forces generated in the boundary layer. From the basis of potential theory, Rehbinder calculated the velocity and pressure distribution on the sediment bed along the radial direction. He showed that the radial

velocity near the boundary varies linearly up to a certain axial distance ($r = z_0 \frac{\sqrt{2}}{4}$) and

reaches its maximum value at $r = z_0 \frac{\sqrt{2}}{2}$. He suggested that the viscous flow exists only

within a cylindrical shaped region located in the vicinity of the mouthpiece of siphon ($0 \leq r \leq z_0 \frac{\sqrt{2}}{4}$; $0 \leq r \leq z_0 \frac{\sqrt{2}}{4}$). Using these relations, the pressure distribution and hence the shear force on the particle in the soil water interface was deduced.

Rehbinder also mentioned that the lift force on a particle is a function of the pressure distribution in the soil stratum, porosity, and the volume of the particle grains. He derived vertical pressure distribution on the basis of the pressure distribution at the interface (as discussed before) and Darcy's law. Using the vertical pressure gradient, the hydraulic force has been derived by means of Archimedes' lift.

Combining the two forces (shear force due to viscous effect and lift due to hydraulic pressure gradient), Rehbinder explained that the location for the initiation of motion is only possible at $0.8 < r/z_0 < 1.4$. He showed that the magnitude of the resultant

force has a local maximum at $r \approx 0.8z_0$ and at critical flux the removal of sediment starts in this annular region.

In his experimental analysis, Rehbinder used quartz sand of density 2500 kg/m^3 and diameter 0.2 mm. The suction pipe had an inner diameter of 5 mm and the flow rate Q of 0.49 L/s. He found that as the tube is lowered slowly and at a distance $z_0 \approx 15 \text{ mm}$, a ring shaped crater is rapidly formed around the stagnation point under the tube inlet (Fig. 2.13).

Using the input data of the experiment, Rehbinder calculated from his theory that the ratio of the lift force to the shear force exerted on the sediment grain is from 2 to 20, the thickness of the boundary layer was 0.6 mm. From this point of view, he suggested that the removal of grains in sediment is initiated by lift force due to the creep flow in the saturated sediment and the shear stress at the surface of the sediment has a relatively small influence on the removal. He also concluded that the lift force acting on the grains is proportional to the square of the flow and inversely proportional to about the fifth power of the distance between the tube inlet and the sediment. It should be noted that, although the variables used in the experiment more or less satisfy the assumptions and simplification considered for the theoretical derivation, only one set of flow parameters and sediment size was used in the experiment. The only parameter that was varied in the experiment is the height of the siphon inlet from the bed, z_0 , which was decreased slowly in order to achieve the critical flux. The primary outcome which is relevant to the theoretical analysis is the formation of a crater which was used as a justification for the theory.

2.6 Summary

From a review of the literature, it is evident that studies relating siphon scour on cohesionless materials are limited and generally empirical in nature. There has been limited success in supporting those empirical formulae by theoretical explanation. So far potential flow theory has been the basis for assessing the flow conditions around the siphon inlet near the sand bed. Little effort has been made to determine the maximum scour hole depth or the scour hole profile at equilibrium condition.

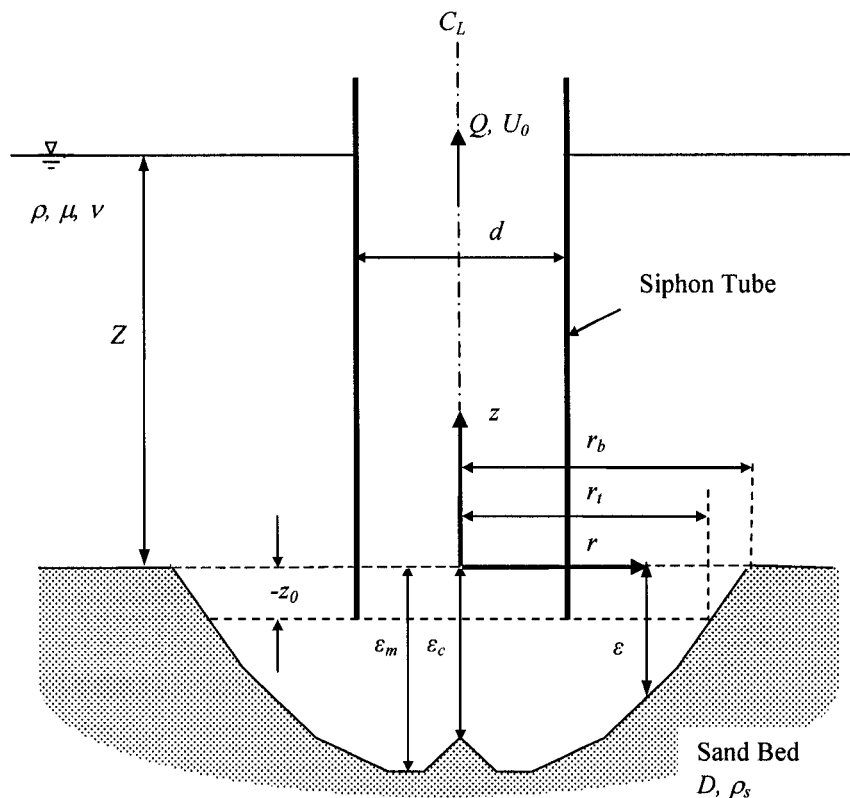


Fig. 2.1: Definition sketch.

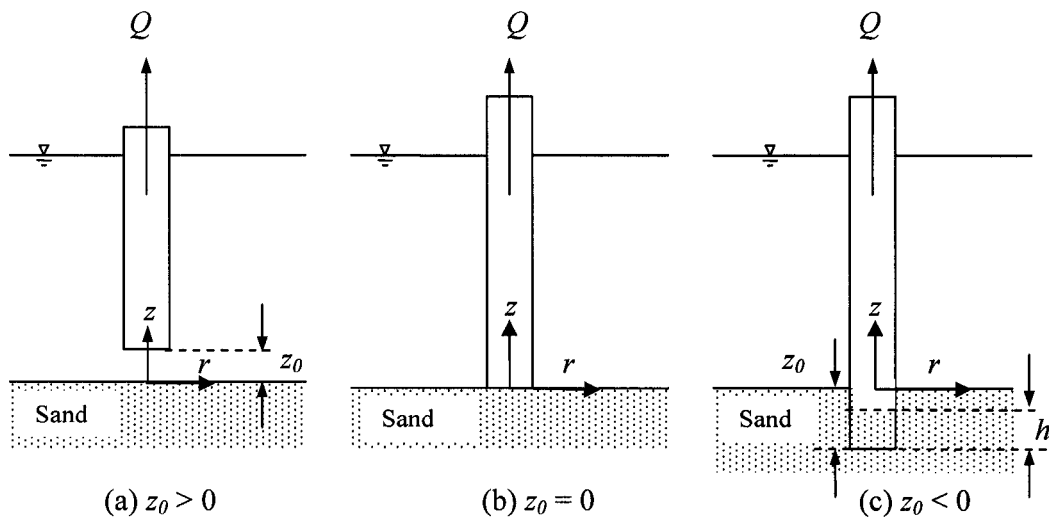


Fig. 2.2: Three possible cases for the tube position.

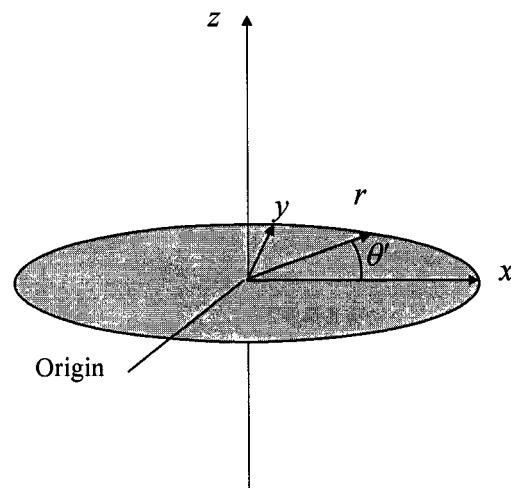


Fig. 2.3: Three-dimensional co-ordinate systems in a sink flow and equipotential line.

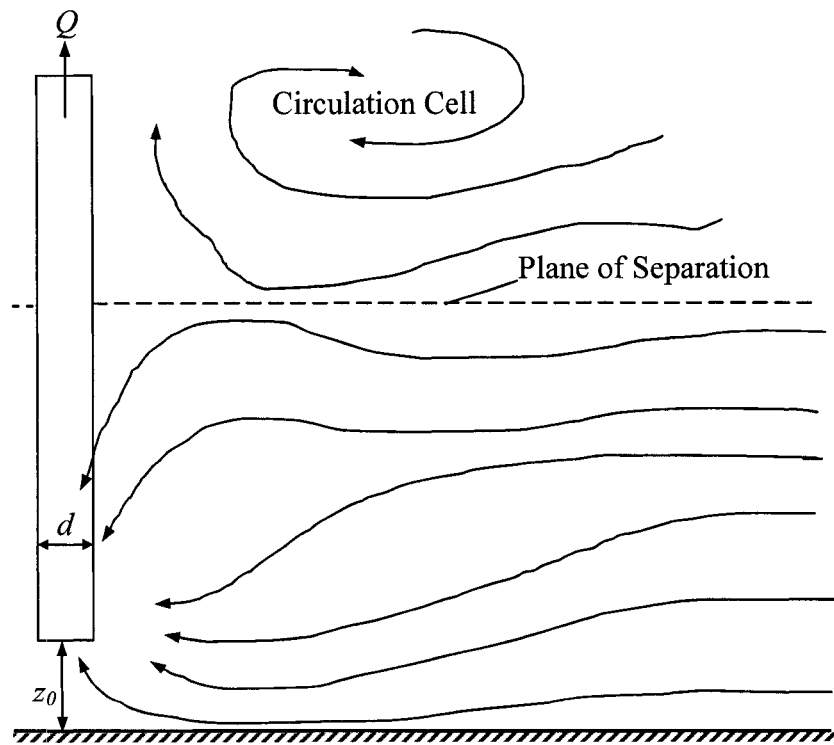


Fig. 2.4: Final flow configuration of Apgar and Basco's experiment
(adapted from Apgar and Basco 1973).

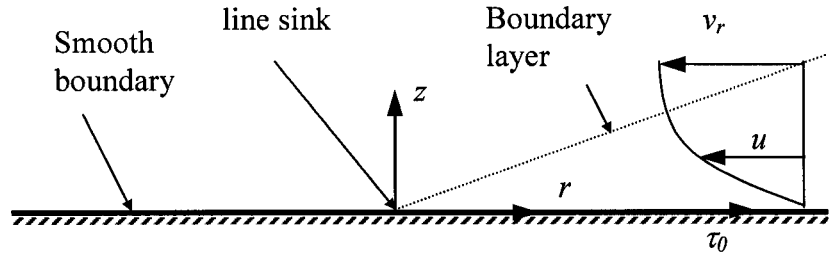


Fig. 2.5: Typical velocity distribution and boundary layer growth due to a line sink flow near bed (adapted from Schlichting and Gersten 2000).

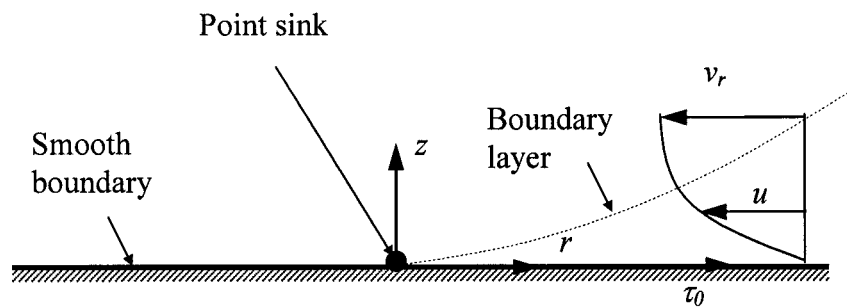


Fig. 2.6: Typical velocity distribution and boundary layer growth due to a point sink flow near bed (adapted from Parthasarathy 1969).

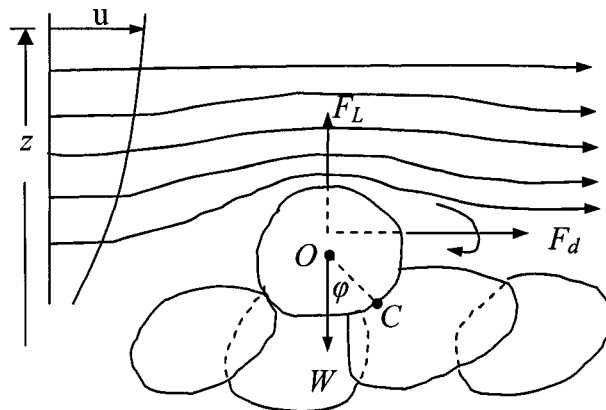


Fig. 2.7: Forces on an exposed grain (adapted from Raudkivi 1998).

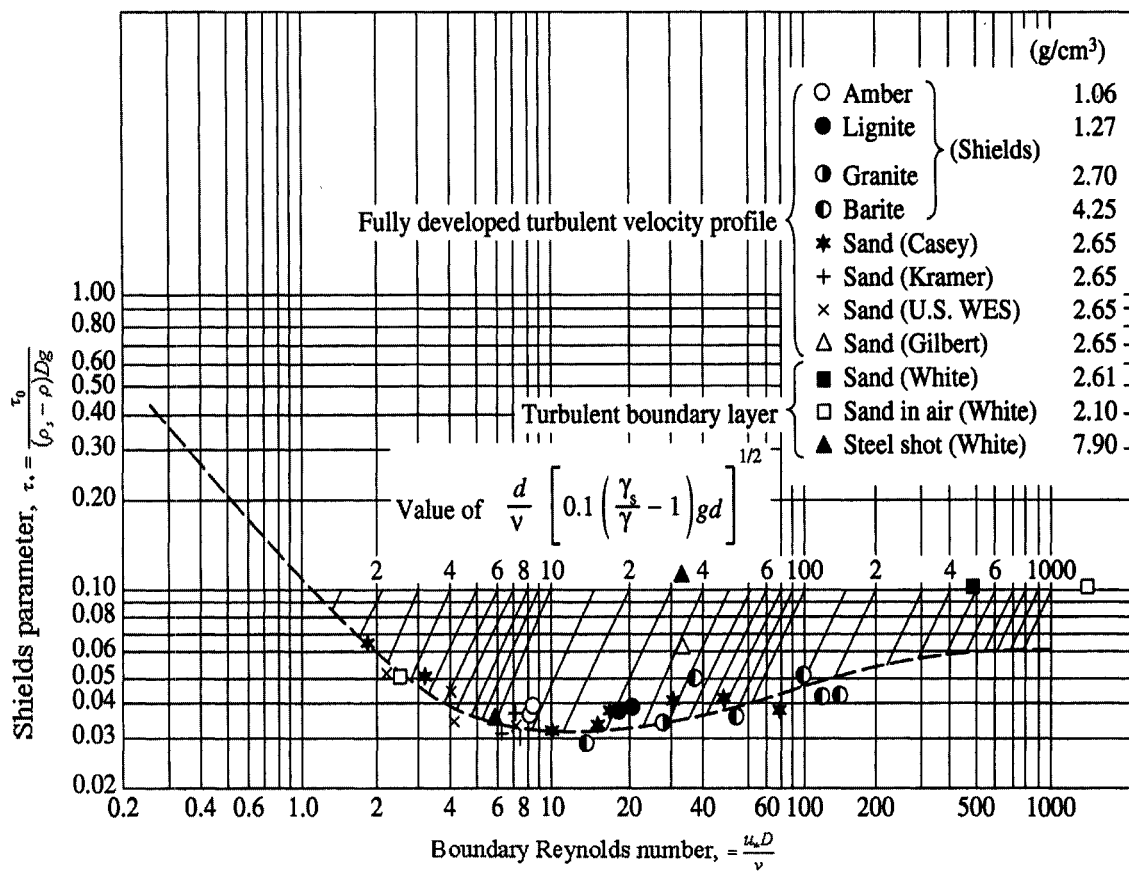


Fig. 2.8: Shields diagram for incipient motion (reproduced from Vanoni and Brooks 1975).

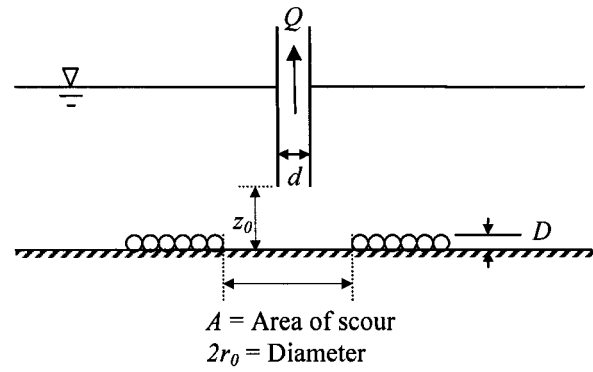


Fig. 2.9: Schematic of Slotta's flat bed Experiment (adapted from Slotta 1968).

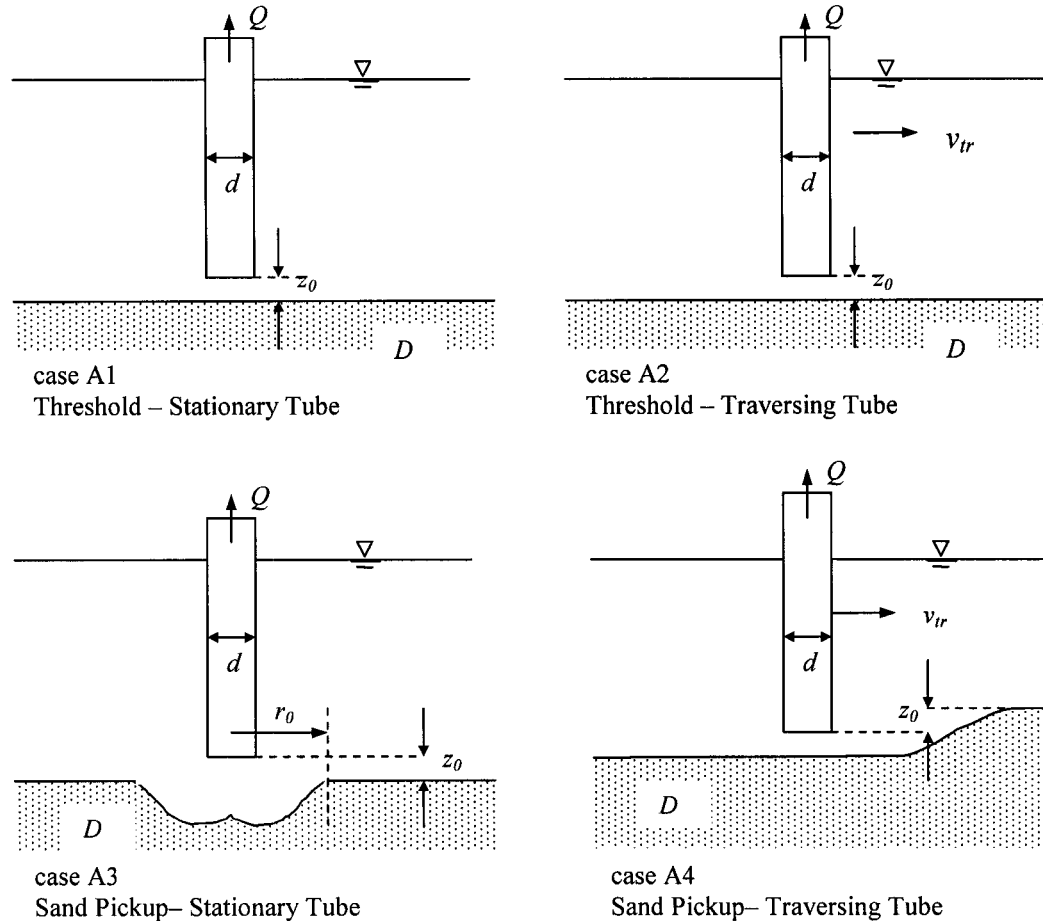


Fig. 2.10: Suction tube and sand bed configuration for Gladigau's experiment (adapted from Gladigau 1975).

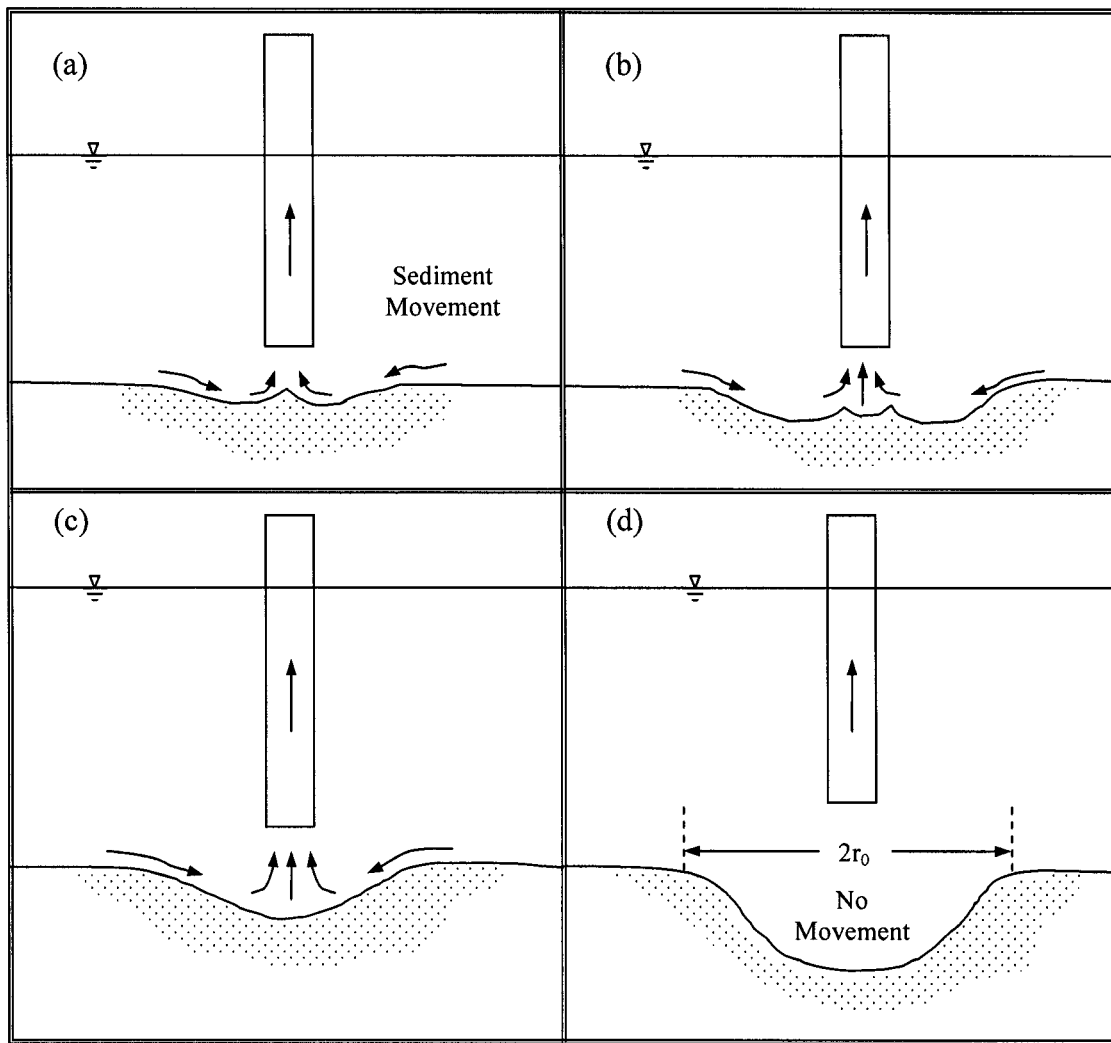


Fig. 2.11: Various stages of development of scour hole in sediment removal studies by Brahme (adapted from Brahme 1983).

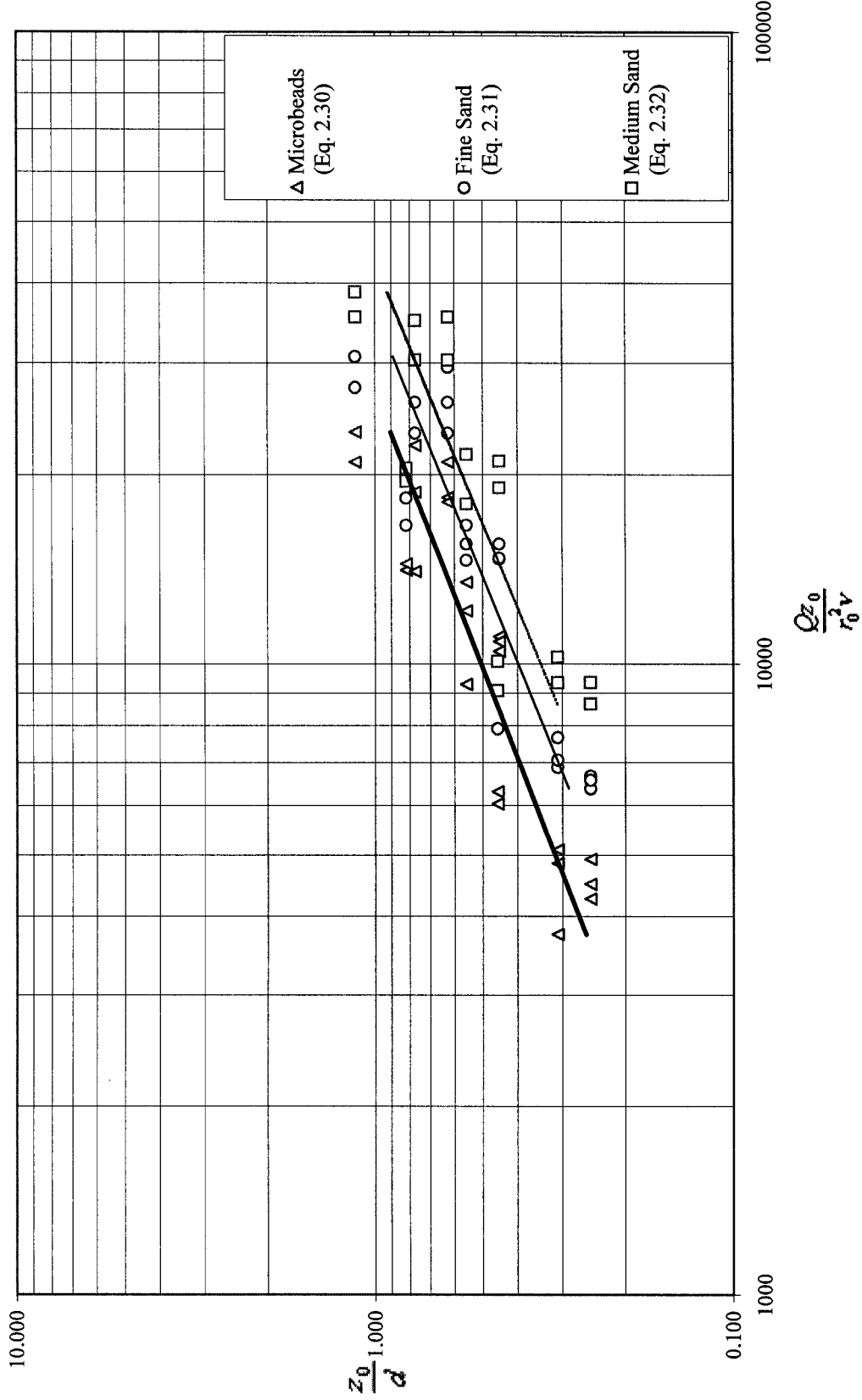


Fig. 2.12: The dimensionless height above bed vs. the Dimensionless flow on log-log paper for different materials of Brahma's experiment (adapted from Brahma 1983).

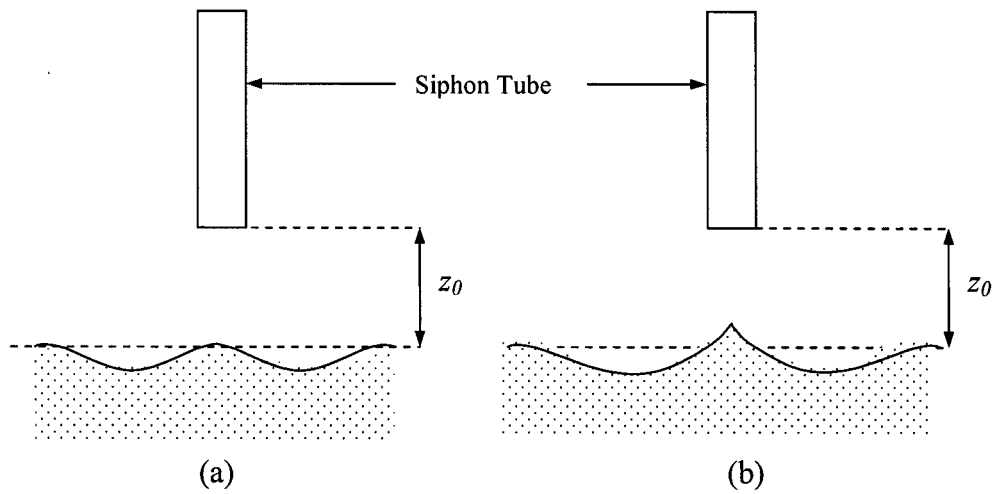


Fig. 2.13: Formation of the crater in the Rehbinder's experiment (a) immediately after the removal of grains has started and (b) when the removal of grains has stabilized (adapted from Rehbinder 1994).

CHAPTER 3: EXPERIMENTAL SETUP AND EXPERIMENTS

3.1 Introduction

In this thesis, experimental data of the present study as well as that of Mazurek and Rajaratnam (unpublished) are presented and analyzed. The experimental setups and procedures are similar and were meant to determine the profile of the scour holes of cohesionless sediments under different siphon flow conditions. No tests were performed in Mazurek and Rajaratnam (unpublished) for the case when tube is set above bed. The experimental setups, measurements, testing programs, and soil properties are described in this chapter.

3.2 Experimental Setup and Experiments of Present Study

3.2.1 Experimental Setup

The tests were performed in the hydraulics laboratory at the University of Windsor. The experiments were conducted in a cylindrical plastic tank of 1219 mm diameter and 1219 mm depth. A smaller cylindrical tank of 550 mm diameter and 705 mm depth was set within the bigger tank at a distance of 100 mm from its right edge and contained the cohesionless sand used for the scour experiments. The depth of water above the sand bed was about 230 mm for all the tests. The siphon tube of 9.65, 13.86, or 20.40 mm diameter was suspended vertically above the smaller tank through the use of a horizontal traversing system set across the larger tank. The siphon tube was connected through the use of 12.7 mm I.D. PVC tubing to a settling basin, which was used to collect the scoured material. This settling basin, a large (50 Liters volume) cylindrical glass jar

having a 450 mm diameter, was placed within the bigger tank. The bigger tank and the glass jar were filled with tap water prior to commencing tests and the glass jar was sealed with a rubber stopper. The flow through the siphon tube was created by using different combinations of two centrifugal pumps and a jet pump, with the flow being drawn from the settling basin. The flow rate was controlled by means of a 25.4 mm gate valve connected at the outlet of the pump. The flow through the pump was returned to the bottom of the large cylindrical tank. The setup is shown in Fig. 3.1 and is sketched in Fig. 3.2.

3.2.2 Testing Program and Measurements

Before performing each test, the bigger tank and the glass jar were filled with water and sand bed in the smaller tank was manually delved so that there was no trapped air inside the sediment. The sediment surface was then leveled. The siphon tube was positioned vertically at a desired distance from the original sediment bed. Scour was initiated by starting the pump. The discharge was measured by volumetric measurements at the pump outlet (using a bucket of volume 11.56 L and a stopwatch). The range of discharge obtained from the pumps was 0.05 to 4.1 L/s using alternately the siphon tubes of three different sizes, the range for the average velocity at the tube inlet of 0.34 to 6.5 m/s.

Two series of tests were carried out. In the first series, the tube was slowly lowered at a given flow rate until a few particles of sand moved below the tube (noted by visual observation). The height of the tube above the sand surface was noted and this distance was called the critical height for movement, z_c . In these tests, the critical height above the sand surface for a more general movement of the particles (creating a small

conical mound) was noted. This height is the height for general movement of the sediment, z_g . In the second series of experiments, the scour created by a given siphon flow was measured. The siphon tube was set above the bed (up to 6.4 mm), at the soil surface, or beneath the soil surface (up to 102 mm). The maximum height inlet above the bed was selected in such a way that the pump at its maximum capacity could create measurable scour hole from that height. The maximum depth of tube inlet was so chosen that pump could create sufficient pressure head for the quick conditions to occur. The details of the experiments are given in Tables 3.1 and 3.2.

For the scour tests (the second series), where the scour hole profile created by the siphon flow was measured, the scouring process occurred in a very rapid manner and the equilibrium reached in a very short time (which was generally within a few seconds). Thus, the physical measurements of the scour hole in transient condition were not taken. Equilibrium can be described as the condition at which the scouring process ceases and there is no movement of sand grains inside the scour hole and the scour hole geometry becomes stable. Initially the tests were run for 30 min, 45 min and 1 hr to ensure the profiles did reach equilibrium. Later, the scour hole profiles were measured after each test was run for 10 to 15 min. The deviations of the scour hole radii measured in the two perpendicular directions were found within 4 % for all of the tests. Therefore the scour holes might be considered as axisymmetric and therefore the cross-sectional profiles were measured only across one direction through the center of the scour hole. The depth of scour holes relative to the original soil surface were measured by using a digital point gauge (graded to 0.01 mm). The horizontal distance of the point gauge was measured by using the scale (with 0.1 mm accuracy) attached to the horizontal traversing system.

3.2.3 Soil Sample

Only one type of cohesionless sediment was used in these tests. The soil appeared free from dust and organic matter. The grain size distribution curve (Fig. 3.3) shows that the mean size of the sand grain, D is 0.58 mm. The coefficient of uniformity is defined as the ratio of the sieve size through which 60 % of particles by weight pass to that through which 10 % of particles by weight pass (D_{60}/D_{10}) and its value for the sample is 1.9. The geometric standard deviation, $\sigma_g = \left(\frac{D_{84.1}}{D_{15.9}} \right)^{1/2}$ has been found as 1.38. From the geometric standard deviation it appears the sand is fairly uniform, although geometric standard deviation is slightly larger than the $\sigma_g=1.35$ which is considered uniform by Breusers and Raudkivi (1993). Again the ratio D_{95}/D_5 has a value of 3.5, therefore this soil sample can be considered as uniform from the hydraulic point of view (Raudkivi 1998). The particle density of the sample has been measured as 2.65. It is to be noted that, for the sake of having a clearer view of sand bed through water in some later experiments, the sand specimen was recycled from the settling basin so that the very fine particles were removed. This did not change the particle size distribution significantly and the mean diameter of the sediment sample remained almost at 0.58 mm. The hydraulic conductivity of the sample was measured according to Freeze and Cherry (1979) and its value is 2.24 mm/s.

3.3 Experimental Setup and Experiments of Mazurek and Rajaratnam

3.3.1 Experimental Setup

Mazurek and Rajaratnam (unpublished) performed a similar set of experiments as above. The sand samples were contained within a square box, 1.25 m on a side and 0.25

m deep, filled with one of two sands tested, and set within a larger cylindrical tank of 2 m diameter filled with tap water. The siphon tubes, each about 30 cm in length, were fixed to a point gauge that rested on a level bar that extended across the larger tank. Four siphon tubes were tested, with diameters d of 15, 13.7, 7.4, and 4.3 mm. The experiments were first performed using fine uniform sand with a median diameter D of 0.20 mm and a geometric standard deviation σ_g of 1.1, and then repeated using the coarse sand with a D of 0.5 mm σ_g of 1.25. The experimental setup is shown in Fig. 3.4.

The flow through the siphon was produced by a small progressing cavity pump with the flow rates ranging from 0.5 to 1.2 L/s. The height of the siphon tube inlet was also varied and was held either on the sand surface or at depths of 15 or 30 mm into the sand bed. Observations included the final scour hole profile, measured with a point gauge graduated to 0.01 mm and the time for the equilibrium scour hole profile to form. The height of the tube above the sand surface at which a few sand particles which first observed to move and at which there was a general motion of the particles was also noted. The details of the 19 experiments performed are given in Table 3.3.

Table 3.1: Details of the experiments of the scour hole geometry (Present Study).

Test No.	Q (L/s)	d (mm)	U ₀ (m/s)	z ₀ (mm)	D (mm)	T (°C)	F ₀
T2/6.35/2.06	0.310	13.86	2.06	6.35	0.58	20	21.2
T2/6.35/1.48	0.223	13.86	1.48	6.35	0.58	21	15.3
T2/6.35/1.56	0.235	13.86	1.56	6.35	0.58	21	16.1
T2/6.35/1.12	0.168	13.86	1.12	6.35	0.58	21	11.5
T1/5.08/6.41	0.461	9.57	6.41	5.08	0.58	20	66.2
T1/5.08/5.68	0.408	9.57	5.68	5.08	0.58	20	58.6
T2/5.08/1.90	0.287	13.86	1.90	5.08	0.58	20	19.6
T2/5.08/1.93	0.291	13.86	1.93	5.08	0.58	20	19.9
T1/5.08/5.31	0.382	9.57	5.31	5.08	0.58	20	54.8
T2/5.08/1.91	0.287	13.86	1.91	5.08	0.58	20	19.7
T2/5.08/1.92	0.290	13.86	1.92	5.08	0.58	20	19.8
T2/5.08/1.52	0.230	13.86	1.52	5.08	0.58	20	15.7
T2/5.08/0.94	0.141	13.86	0.94	5.08	0.58	20	9.7
T2/5.08/1.35	0.204	13.86	1.35	5.08	0.58	20	14.0
T2/5.08/1.13	0.170	13.86	1.13	5.08	0.58	20	11.7
T2/5.08/1.38	0.209	13.86	1.38	5.08	0.58	20	14.3
T2/3.81/1.77	0.267	13.86	1.77	3.81	0.58	19	18.3
T2/3.81/1.61	0.243	13.86	1.61	3.81	0.58	18	16.6
T2/3.81/1.07	0.162	13.86	1.07	3.81	0.58	18	11.1
T2/3.81/1.24	0.187	13.86	1.24	3.81	0.58	18	12.8
T2/3.81/0.90	0.135	13.86	0.90	3.81	0.58	18	9.2
T2/3.05/1.88	0.284	13.86	1.88	3.01	0.58	20	19.4
T2/3.05/1.88	0.284	13.86	1.88	3.01	0.58	19	19.4
T2/3.05/1.88	0.283	13.86	1.88	3.01	0.58	20	19.4
T1/2.54/5.60	0.403	9.57	5.60	2.54	0.58	21	57.8
T1/2.54/6.43	0.463	9.57	6.43	2.54	0.58	21	66.4
T1/2.54/5.27	0.379	9.57	5.27	2.54	0.58	19	54.4
T2/2.54/2.04	0.307	13.86	2.04	2.54	0.58	15	21.0
T2/2.54/2.01	0.303	13.86	2.01	2.54	0.58	20	20.7
T2/2.54/1.58	0.238	13.86	1.58	2.54	0.58	17	16.3
T2/2.54/1.32	0.200	13.86	1.32	2.54	0.58	21	13.7
T2/2.54/1.16	0.176	13.86	1.16	2.54	0.58	20	12.0
T2/2.54/1.39	0.210	13.86	1.39	2.54	0.58	20	14.4
T1/2.54/3.68	0.265	9.57	3.68	2.54	0.58	20	38.0
T2/2.54/1.15	0.173	13.86	1.15	2.54	0.58	20	11.9
T2/2.54/1.02	0.154	13.86	1.02	2.54	0.58	22	10.6
T2/2.54/0.81	0.123	13.86	0.81	2.54	0.58	22	8.4
T2/2.54/2.04	0.307	13.86	2.04	1.27	0.58	17	21.0
T1/1.27/3.70	0.266	9.57	3.70	1.27	0.58	21	38.2
T2/1.27/2.03	0.307	13.86	2.03	1.27	0.58	21	21.0
T2/1.27/1.49	0.226	13.86	1.49	1.27	0.58	21	15.4

Table 3.1: Cont'd...

Test No.	Q (L/s)	d (mm)	U ₀ (m/s)	z ₀ (mm)	D (mm)	T (°C)	F ₀
T2/1.27/1.43	0.216	13.86	1.43	1.27	0.58	20	14.8
T2/1.27/1.24	0.187	13.86	1.24	1.27	0.58	20	12.8
T2/1.27/1.14	0.174	13.86	1.15	1.27	0.58	20	11.9
T2/1.27/1.06	0.160	13.86	1.06	1.27	0.58	20	10.9
T2/0/0.34	0.051	13.86	0.34	0	0.58	21	3.5
T3/0/0.53	0.173	20.4	0.53	0	0.58	21	5.5
T2/0/0.64	0.096	13.86	0.64	0	0.58	21	6.6
T2/0/0.68	0.102	13.86	0.68	0	0.58	17	7.0
T2/0/0.68	0.103	13.86	0.68	0	0.58	19.5	7.0
T2/0/0.70	0.105	13.86	0.70	0	0.58	21	7.2
T1/0/0.76	0.249	20.4	0.76	0	0.58	22	7.9
T2/0/0.80	0.121	13.86	0.80	0	0.58	17	8.3
T3/0/0.86	0.281	20.4	0.86	0	0.58	21	8.9
T2/0/1.03	0.155	13.86	1.03	0	0.58	17	10.6
T2/0/1.14	0.172	13.86	1.14	0	0.58	17	11.7
T2/0/1.15	0.174	13.86	1.15	0	0.58	21	11.9
T2/0/1.20	0.181	13.86	1.20	0	0.58	19.5	12.4
T2/0/1.30	0.196	13.86	1.30	0	0.58	21	13.4
T2/0/1.34	0.203	13.86	1.34	0	0.58	19.5	13.9
T2/0/1.54	0.232	13.86	1.54	0	0.58	21	15.9
T2/0/1.55	0.234	13.86	1.55	0	0.58	23	16.0
T2/0/1.63	0.246	13.86	1.63	0	0.58	7.4	16.9
T2/0/1.78	0.268	13.86	1.78	0	0.58	22	18.3
T2/0/1.60	0.287	13.86	1.90	0	0.58	19.5	19.6
T3/0/1.95	0.142	9.65	1.95	0	0.58	21	20.1
T2/0/1.95	0.294	13.86	1.95	0	0.58	19	20.1
T2/0/1.95	0.294	13.86	1.95	0	0.58	19.5	20.1
T2/0/2.00	0.301	13.86	2.00	0	0.58	7.5	20.6
T2/0/2.18	0.329	13.86	2.18	0	0.58	22	22.5
T2/0/2.33	0.352	13.86	2.33	0	0.58	20	24.1
T1/0/2.53	0.185	9.65	2.53	0	0.58	22	26.1
T1/0/2.78	0.203	9.65	2.78	0	0.58	21	28.7
T1/0/2.87	0.210	9.65	2.87	0	0.58	21	29.6
T1/0/3.21	0.235	9.65	3.21	0	0.58	19	33.2
T1/0/3.48	0.254	9.65	3.48	0	0.58	19	35.9
T1/0/3.68	0.269	9.65	3.68	0	0.58	21	37.9
T1/0/3.87	0.283	9.65	3.87	0	0.58	18	39.9
T1/0/4.01	0.293	9.65	4.01	0	0.58	18	41.4
T1/0/4.24	0.310	9.65	4.24	0	0.58	22	43.7
T1/0/5.34	0.391	9.65	5.34	0	0.58	20	55.1
T1/0/5.48	0.401	9.65	5.48	0	0.58	21	56.6

Table 3.1: Cont'd...

Test No.	Q (L/s)	d (mm)	U ₀ (m/s)	z ₀ (mm)	D (mm)	T (°C)	F ₀
T1/0/5.560	0.410	9.65	5.60	0	0.58	18	57.8
T1/0/5.72	0.418	9.65	5.72	0	0.58	22	59.0
T1/0/5.96	0.436	9.65	5.96	0	0.58	21	61.5
T1/0/6.21	0.454	9.65	6.21	0	0.58	21	64.1
T3/-1.27/0.77	0.251	20.4	0.77	-12.7	0.58	21	7.9
T2/-1.27/1.12	0.169	13.86	1.12	-12.7	0.58	16	11.5
T2/-1.27/1.19	0.180	13.86	1.19	-12.7	0.58	16	12.3
T2/-1.27/1.20	0.181	13.86	1.20	-12.7	0.58	16	12.4
T2/-1.27/1.25	0.189	13.86	1.25	-12.7	0.58	17	12.9
T2/-1.27/1.45	0.218	13.86	1.45	-12.7	0.58	20	14.9
T2/-1.27/1.84	0.277	13.86	1.84	-12.7	0.58	21	19.0
T1/-1.27/1.88	0.137	9.65	1.88	-12.7	0.58	21	19.4
T2/-1.27/2.11	0.318	13.86	2.11	-12.7	0.58	16	21.8
T2/-1.27/2.42	0.365	13.86	2.42	-12.7	0.58	22	25.0
T1/-1.27/2.55	0.187	9.65	2.55	-12.7	0.58	22	26.3
T1/-1.27/2.94	0.215	9.65	2.94	-12.7	0.58	21	30.4
T1/-1.27/3.12	0.228	9.65	3.12	-12.7	0.58	18	32.2
T1/-1.27/3.53	0.258	9.65	3.53	-12.7	0.58	20	36.5
T1/-1.27/3.86	0.283	9.65	3.86	-12.7	0.58	20	39.9
T1/-1.27/5.85	0.428	9.65	5.85	-12.7	0.58	20	60.4
T3/-2.54/0.53	0.173	20.4	0.53	-12.7	0.58	21	5.5
T3/-2.54/0.53	0.175	20.4	0.53	-25.4	0.58	21	5.5
T3/-2.54/0.77	0.250	20.4	0.77	-25.4	0.58	21	7.9
T2/-2.54/0.97	0.147	13.86	0.97	-25.4	0.58	18	10.0
T2/-2.54/1.13	0.170	13.86	1.13	-25.4	0.58	17	11.7
T2/-2.54/1.38	0.208	13.86	1.38	-25.4	0.58	16	14.2
T2/-2.54/1.46	0.221	13.86	1.46	-25.4	0.58	20	15.1
T2/-2.54/1.84	0.278	13.86	1.84	-25.4	0.58	21	19.0
T2/-2.54/2.09	0.315	13.86	2.09	-25.4	0.58	20	21.5
T2/-2.54/2.42	0.366	13.86	2.42	-25.4	0.58	22	25.0
T1/-2.54/2.57	0.188	9.65	2.57	-25.4	0.58	22	26.5
T1/-2.54/2.84	0.208	9.65	2.84	-25.4	0.58	21	29.3
T1/-2.54/3.14	0.230	9.65	3.14	-25.4	0.58	18	32.4
T1/-2.54/3.47	0.254	9.65	3.47	-25.4	0.58	19	35.9
T1/-2.54/3.82	0.279	9.65	3.82	-25.4	0.58	18	39.4
T1/-2.54/4.22	0.309	9.65	4.22	-25.4	0.58	20	43.6
T1/-2.54/4.42	0.323	9.65	4.42	-25.4	0.58	18	45.6
T1/-2.54/4.61	0.337	9.65	4.61	-25.4	0.58	18	47.5
T1/-2.54/4.77	0.349	9.65	4.77	-25.4	0.58	20	49.3
T1/-2.54/5.23	0.383	9.65	5.23	-25.4	0.58	22	54.0
T1/-2.54/5.59	0.409	9.65	5.59	-25.4	0.58	21	57.7

Table 3.1: Cont'd...

Test No.	Q (L/s)	d (mm)	U ₀ (m/s)	z ₀ (mm)	D (mm)	T (°C)	F ₀
T3/-3.81/0.53	0.174	20.4	0.53	-38.1	0.58	22	5.5
T3/-3.81/0.77	0.252	20.4	0.77	-38.1	0.58	21	8.0
T2/-3.81/0.99	0.149	13.86	0.99	-38.1	0.58	18	10.2
T2/-3.81/1.16	0.175	13.86	1.16	-38.1	0.58	19	12.0
T2/-3.81/1.19	0.180	13.86	1.19	-38.1	0.58	17	12.3
T2/-3.81/1.35	0.204	13.86	1.35	-38.1	0.58	16	14.0
T2/-3.81/1.38	0.209	13.86	1.38	-38.1	0.58	20	14.3
T2/-3.81/1.84	0.278	13.86	1.84	-38.1	0.58	21	19.0
T2/-3.81/2.06	0.311	13.86	2.06	-38.1	0.58	20	21.3
T2/-3.81/2.33	0.352	13.86	2.33	-38.1	0.58	22	24.1
T1/-3.81/2.61	0.191	9.65	2.61	-38.1	0.58	20	27.0
T1/-3.81/3.12	0.228	9.65	3.12	-38.1	0.58	18	32.2
T1/-3.81/3.59	0.263	9.65	3.59	-38.1	0.58	22	37.1
T1/-3.81/3.79	0.277	9.65	3.79	-38.1	0.58	20	39.2
T3/-5.08/0.54	0.176	20.4	0.54	-50.8	0.58	22	5.6
T3/-5.08/0.78	0.253	20.4	0.77	-50.8	0.58	21	8.0
T2/-5.08/1.17	0.176	13.86	1.17	-50.8	0.58	17	12.0
T2/-5.08/1.22	0.184	13.86	1.22	-50.8	0.58	19	12.6
T2/-5.08/1.31	0.197	13.86	1.31	-50.8	0.58	19	13.5
T2/-5.08/1.32	0.199	13.86	1.32	-50.8	0.58	17	13.6
T2/-5.08/1.39	0.210	13.86	1.39	-50.8	0.58	19	14.4
T2/-5.08/1.85	0.280	13.86	1.85	-50.8	0.58	22	19.1
T2/-5.08/2.21	0.333	13.86	2.21	-50.8	0.58	22	22.8
T2/-5.08/2.39	0.360	13.86	2.39	-50.8	0.58	22	24.6
T1/-5.08/2.58	0.188	9.65	2.58	-50.8	0.58	20	26.6
T1/-5.08/3.12	0.228	9.65	3.12	-50.8	0.58	17	32.2
T1/-5.08/3.58	0.262	9.65	3.58	-50.8	0.58	17	36.9
T1/-5.08/3.94	0.288	9.65	3.94	-50.8	0.58	21	40.6
T1/-5.08/4.27	0.312	9.65	4.27	-50.8	0.58	22	44.1
T1/-5.08/4.35	0.318	9.65	4.35	-50.8	0.58	18	44.9
T1/-5.08/4.71	0.344	9.65	4.71	-50.8	0.58	18	48.6
T1/-5.08/5.49	0.402	9.65	5.49	-50.8	0.58	21	56.7
T1/-5.08/6.40	0.468	9.65	6.40	-50.8	0.58	22	66.1
T3/-6.35/0.54	0.175	20.4	0.54	-63.5	0.58	15	5.5
T3/-6.35/0.77	0.250	20.4	0.77	-63.5	0.58	21	7.9
T2/-6.35/1.89	0.286	13.86	1.89	-63.5	0.58	22	19.6
T2/-6.35/2.14	0.323	13.86	2.14	-63.5	0.58	21	22.1
T2/-6.35/2.36	0.356	13.86	2.36	-63.5	0.58	22	24.3
T1/-6.35/2.50	0.183	9.65	2.50	-63.5	0.58	22	25.8
T1/-6.35/3.12	0.228	9.65	3.12	-63.5	0.58	18	32.2
T1/-6.35/3.58	0.262	9.65	3.58	-63.5	0.58	17	36.9

Table 3.1: Cont'd...

Test No.	Q (L/s)	d (mm)	U ₀ (m/s)	z ₀ (mm)	D (mm)	T (°C)	F ₀
T1/-6.35/3.98	0.291	9.65	3.98	-63.5	0.58	22	41.1
T3/-7.62/0.53	0.174	20.4	0.53	-76.2	0.58	15	5.5
T3/-7.62/0.77	0.252	20.4	0.77	-76.2	0.58	21	8.0
T2/-7.62/1.13	0.171	13.86	1.13	-76.2	0.58	15	11.7
T2/-7.62/2.14	0.323	13.86	2.14	-76.2	0.58	21	22.1
T1/-7.62/2.50	0.183	9.65	2.50	-76.2	0.58	22	25.8
T1/-7.62/3.11	0.227	9.65	3.11	-76.2	0.58	18	32.1
T1/-7.62/5.44	0.398	9.65	5.44	-76.2	0.58	20	56.2
T1/-7.62/5.60	0.409	9.65	5.60	-76.2	0.58	20	57.8
T2/-10.16/1.89	0.285	13.86	1.89	-101.6	0.58	22	19.5

Code for Test No. : Tube used (T1 = 9.65 mm, T 2 = 13.86 mm and T3 = 20.40 mm tube)/ Inlet height above the bed (mm)/Velocity of fluid in the tube (m/s).

Table 3.2: Details of experiments for height of critical and general movement (present study).

Test No.	Q (L/s)	d (mm)	U ₀ (m/s)	D (mm)	Temp (°C)	F ₀
T2/1.810	0.273	13.86	1.81	0.58	7.5	18.9
T2/1.005	0.152	13.86	1.01	0.58	19.5	10.5
T2/1.178	0.178	13.86	1.18	0.58	20.0	12.3
T2/0.702	0.106	13.86	0.7	0.58	20.0	7.3
T2/1.523	0.230	13.86	1.52	0.58	20.0	15.9
T2/1.799	0.272	13.86	1.8	0.58	15.0	18.8
T2/1.624	0.245	13.86	1.62	0.58	15.0	17.0
T2/1.352	0.204	13.86	1.35	0.58	15.0	14.1
T2/1.130	0.170	13.86	1.13	0.58	15.0	11.8
T2/1.093	0.165	13.86	1.09	0.58	16.0	11.4
T2/0.950	0.143	13.86	0.95	0.58	16.0	9.9
T2/0.728	0.110	13.86	0.73	0.58	16.0	7.6
T2/0.786	0.119	13.86	0.79	0.58	16.0	8.2
T2/0.480	0.072	13.86	0.48	0.58	16.0	5.0
T2/2.139	0.323	13.86	2.14	0.58	22.0	22.3
T1/3.474	0.254	9.65	3.47	0.58	12.0	36.3
T1/3.129	0.229	9.65	3.13	0.58	12.0	32.7
T1/3.618	0.265	9.65	3.62	0.58	12.0	37.8
T1/2.242	0.164	9.65	2.24	0.58	15.0	23.4
T1/2.823	0.206	9.65	2.82	0.58	13.0	29.5
T1/2.087	0.153	9.65	2.09	0.58	21.0	21.8
T1/2.732	0.200	9.65	2.73	0.58	21.0	28.5
T1/4.733	0.340	9.57	4.73	0.58	20.0	49.4
T1/5.657	0.407	9.57	5.66	0.58	21.0	59.1
T1/6.157	0.443	9.57	6.16	0.58	21.0	64.3
T1/5.153	0.371	9.57	5.15	0.58	20.0	53.8
T1/5.967	0.429	9.57	5.97	0.58	20.0	62.3

Code for Test No.: T1= 9.57, T2 = 13.86 and T3 = 20.40 mm tube/ U₀ (m/s).

Table 3.3: Details of experiments of Mazurek and Rajaratnam (unpublished).

Test No.	Q (L/s)	d (mm)	U ₀ (m/s)	D (mm)	Temp (°C)	F ₀
1a	0.092	0.64	13.51	0.17	6.5	12.3
1b	0.092	0.64	13.51	0.17	7.5	12.3
2	0.184	1.29	13.51	0.17	8.5	24.5
3a	0.276	1.93	13.51	0.17	8.5	36.8
4a	0.316	2.20	13.51	0.17	9.0	42.0
4b	0.316	2.20	13.51	0.17	10.5	42.0
5a	0.092	0.64	13.51	0.17	10.5	12.3
5b	0.092	0.64	13.51	0.17	10.5	12.3
6c	0.184	1.29	13.51	0.17	7.5	24.5
7b	0.276	1.93	13.51	0.17	9.0	36.8
8	0.316	2.20	13.51	0.17	9.0	42.0
9	0.092	0.64	13.51	0.17	6.0	12.3
10	0.184	1.29	13.51	0.17	7.0	24.5
11	0.276	1.93	13.51	0.17	9.0	36.8
12	0.316	2.20	13.51	0.17	9.5	42.0
13	0.027	1.84	4.29	0.17	7.0	35.1
14	0.066	4.57	4.29	0.17	8.5	87.1
15a	0.027	0.61	7.44	0.17	6.5	11.7
15b	0.027	0.61	7.44	0.17	8.0	11.7
16a	0.066	1.52	7.44	0.17	8.0	29.0
16b	0.066	1.52	7.44	0.17	9.0	29.0
16c	0.066	1.52	7.44	0.17	8.5	29.0
17a	0.105	2.43	7.44	0.17	9.0	46.3
17b	0.105	2.43	7.44	0.17	9.5	46.3
17c	0.105	2.43	7.44	0.17	9.5	46.3
18a	0.132	3.03	7.44	0.17	10.0	57.8
18b	0.132	3.03	7.44	0.17	10.0	57.8
19	0.046	1.07	7.44	0.17	8.5	20.3

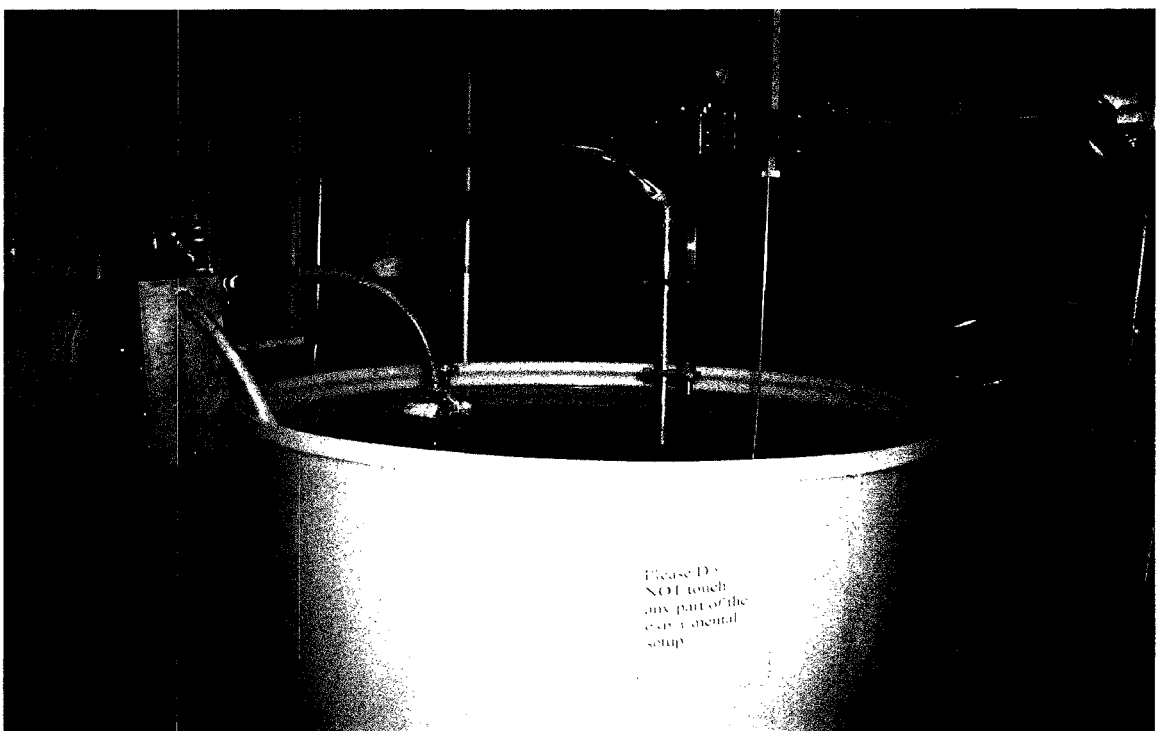


Fig. 3.1: Experimental setup of the present study.

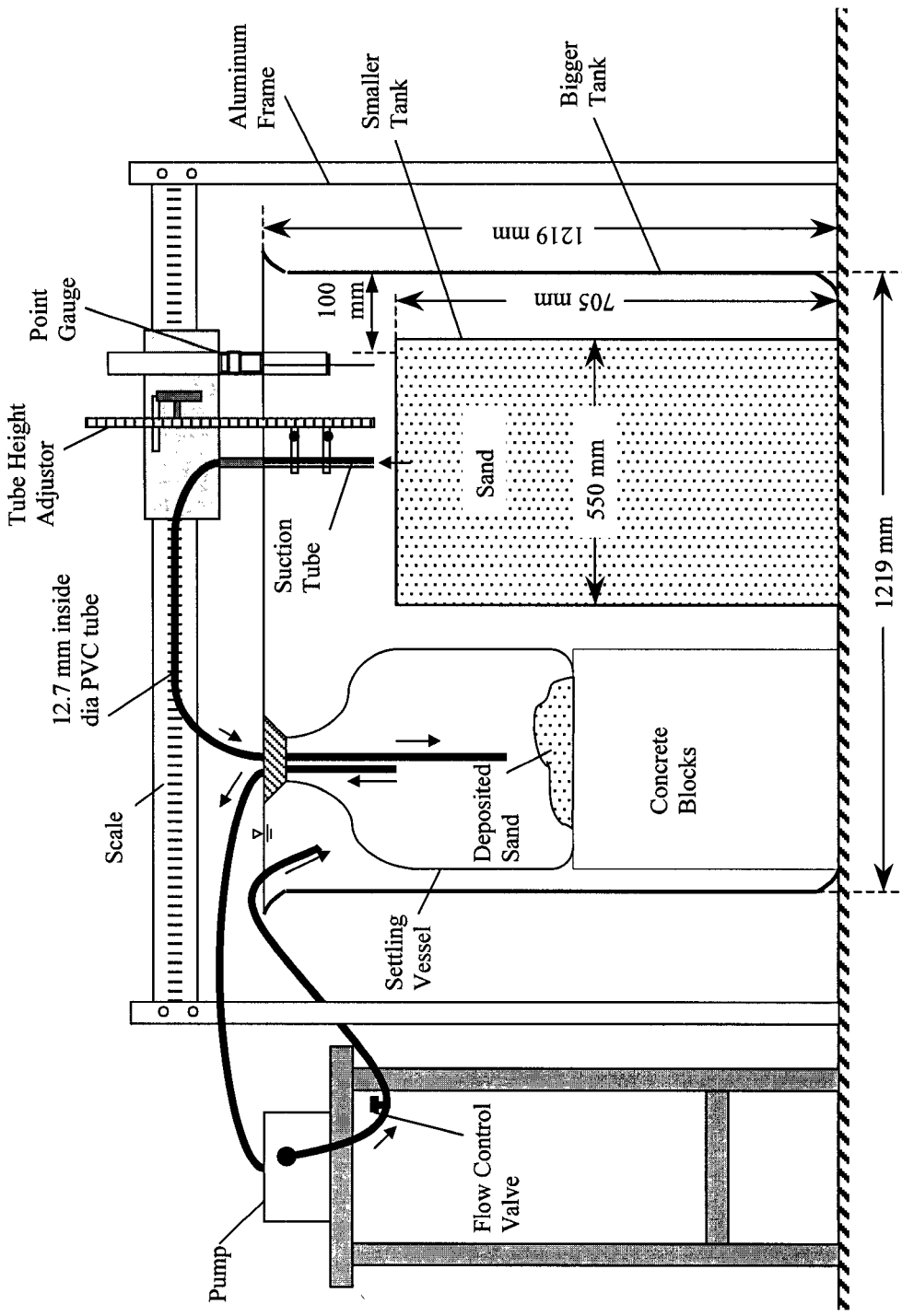


Fig. 3.2: Schematic of the experimental setup of present study.

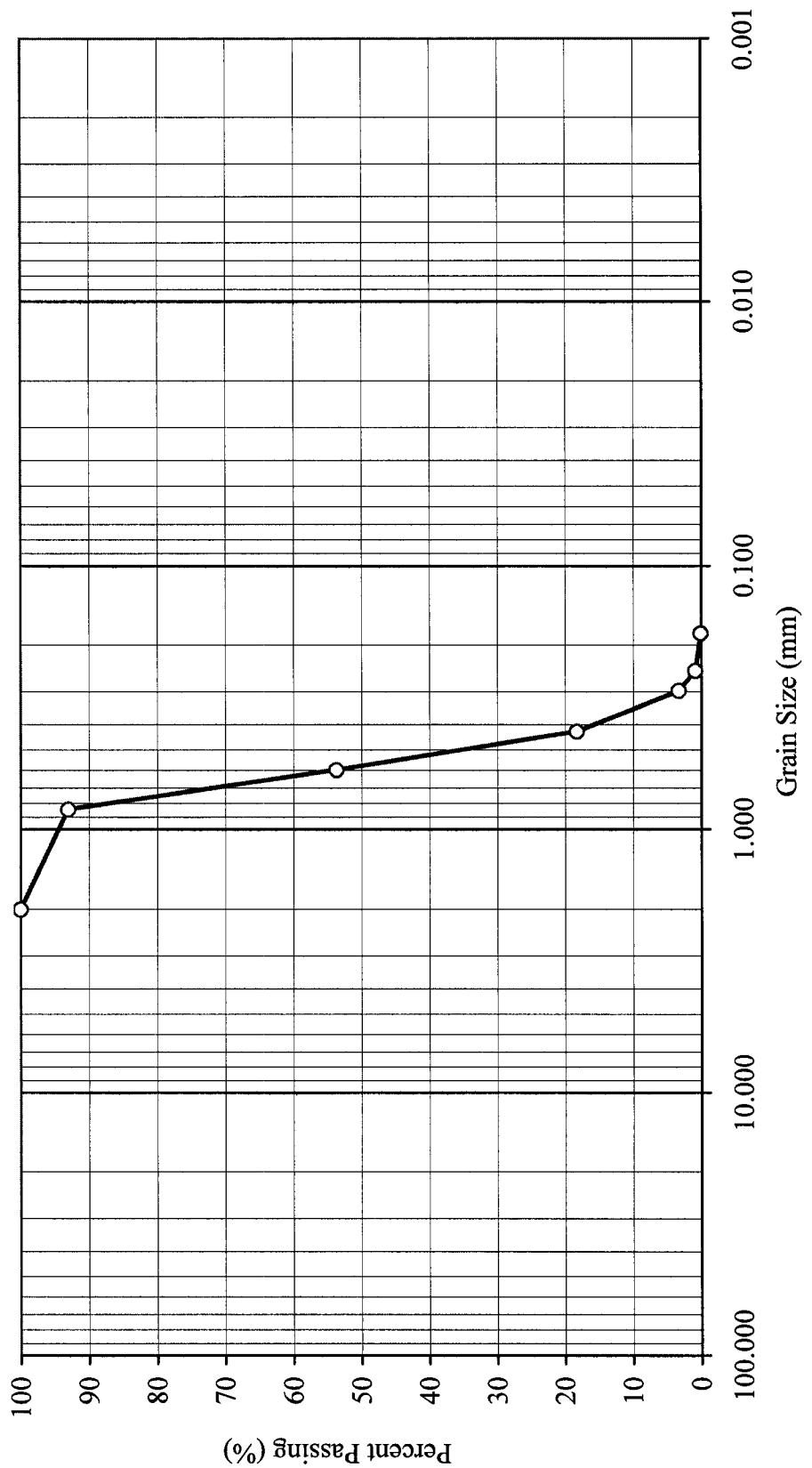


Fig. 3.3: Grain size distribution of the sand sample (present study).

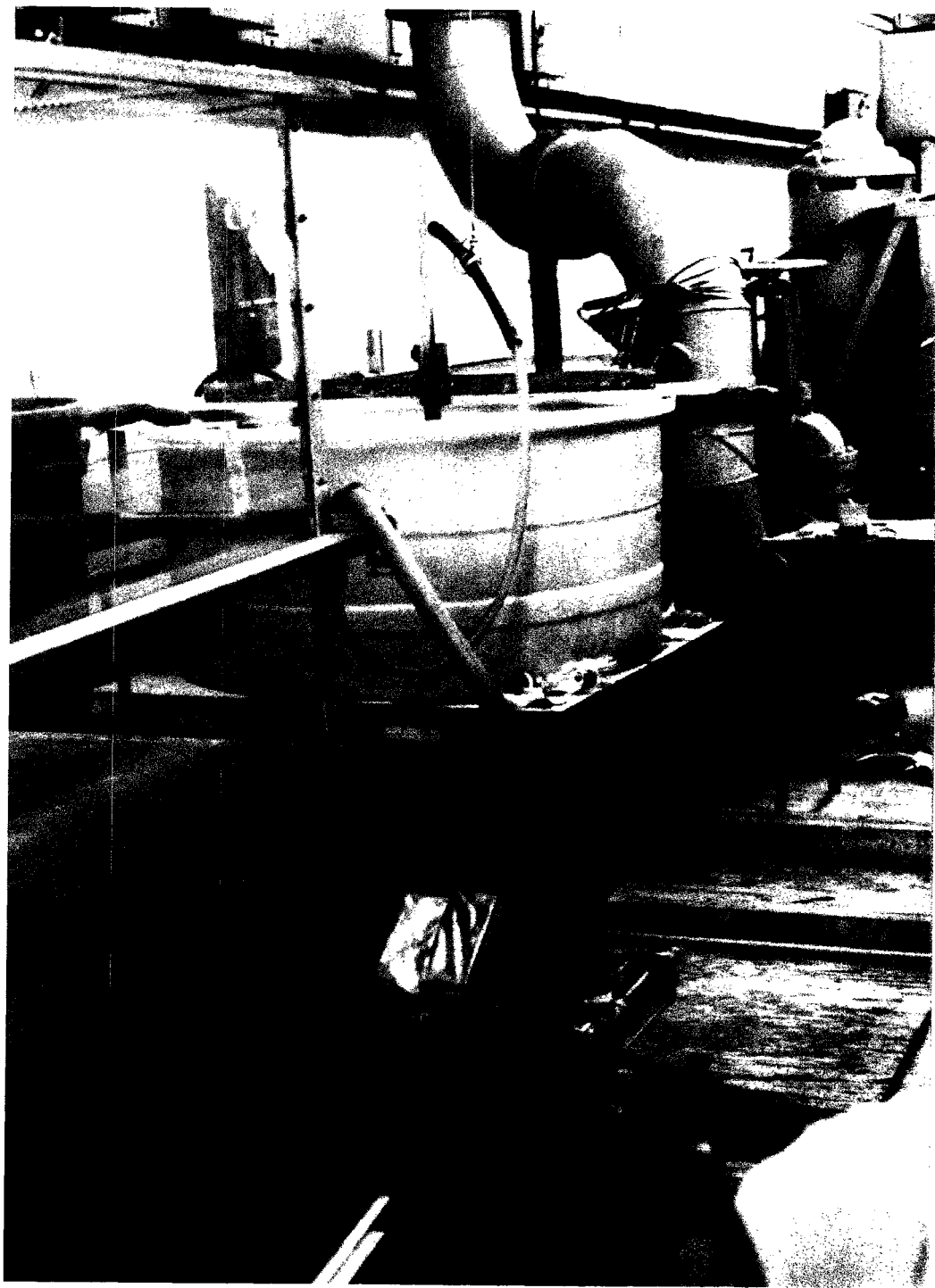


Fig. 3.4: Experimental setup of Mazurek and Rajaratnam.

CHAPTER 4: RESULTS, ANALYSIS, AND DISCUSSION

4.1 Introduction

This chapter presents details of the experimental observations and results. Dimensional analysis is used to aid in developing parameters and empirical equations that are appropriate to predict the equilibrium scour hole radius and the maximum scour hole depth and the heights of critical and general movement of particle under siphonic action. An attempt is also made to derive prediction formulae by theoretical studies and to compare these formulae with results from experiments. Data obtained from Mazurek and Rajaratnam (unpublished) and Brahme (1983) have also been used to validate these formulae. In addition, the similarity criteria of the equilibrium scour hole profiles is analyzed.

4.2 Observations

A significant part of this study concerns the analysis of the dimensions of equilibrium scour hole formed on a deeply submerged cohesionless sediment bed due to flow through a cylindrical siphon tube which was set vertically at different positions relative to the original bed level. The formation of waves or an air entraining vortex was not observed and as a result the surface of the fluid apparently has no significant effect on the scouring process.

Under a certain rate of flow through the siphon tube, when there is no movement of the sediment particles inside the scour hole, we can say that the scour hole reaches equilibrium. For tube set above sand bed ($z_0 > 0$) and on the sand bed ($z_0 = 0$), the rate of

scouring appeared to be the same in both vertical and radial direction and this rate decreased as the scour hole reached equilibrium. Typically, it took only a few seconds to remove most of the sediment. In the case where the siphon tube inserted below the bed surface ($z_0 < 0$), as the particles were being removed through the tube inlet, the sediment around the tube inlet appeared to collapse around the tube. This failure was seen at the surface of the bed as a progressive increase in radius of the scour hole until equilibrium was reached. It took normally 30 s to 1 min to complete most of the scour when the tube was below the sediment bed. The scour hole radius apparently reached equilibrium at this stage.

After most of the sediment was removed in all the three cases, sediment removal became slow and occurred intermittently. This intermittent period could be 30 s to a few minutes. A few unstable particles around the scour hole boundary would slide down towards the center and be removed immediately as they fell into the region near the maximum scour depth. The movement of these few particles occurred for a longer period (normally 10 to 15 min). At this stage, the scouring process ceased completely and there was no movement of the particle inside or outside the scour hole. For the present study, this situation is referred as equilibrium condition. The shape of the equilibrium scour hole, for every test, appeared axisymmetric and the radii measured in two perpendicular directions were found almost the same (within 4 %). Therefore, it was reasonable to measure the scour dimensions along only one direction through the center. A conical hill formed in the scour hole bed centered just below the center tube inlet. A photograph of some typical scour hole are shown in Fig. 4.1 and some typical cross-sectional profiles are shown in Fig. 4.2. It can be seen from Fig. 4.1 that the radius of the scour hole is

easily discernible. Also the maximum scour depth in three dimensions is a ring shape encircling the small conical hill at the center of the scour hole. This ring of maximum scour depth formed closer to the periphery of tube inlet in case of a bigger tube compared to that of a smaller tube.

Some tests gave unusually high scour depths and took a very long period of time to reach equilibrium. For the same setup and flow conditions, different tests would give widely varying scour depths, and take different periods to reach equilibrium (10 to 60 min). After some careful observations, it appeared that circulation in the flow around the tube inlet can cause a vortex (especially at higher siphon velocities) to form beneath the inlet. This vortex typically occurred after the major portion of the sediment was removed and some individual particles slide towards the center of the scour hole. If the circulation is prevented by some means, and the flow into the tube is only radial flow, this vortex does not form. The formation of vortex below the center of the tube inlet caused the pick up of the sediment to occur in a spiral manner (the sand was swirling) over the hill resulting in a deep scour hole. This is apparently the same behavior as the “spiral threshold pickup” as seen by Gladigau (1975). A typical scour hole profile created when the vortex was present is shown in Fig. 4.3.

In another part of this study, which was meant to determine the height of the tube above the bed for critical and general movement of the sediment particles, the observations were similar to what was described as “horizontal threshold movement” by Gladigau (1975). The distance of tube inlet from the bed at which the first grain moves is defined as the height of critical movement z_c . As the tube was lowered slowly from z_c ,

suddenly an overall movement of the sediment towards the center is observed. This smaller height is defined as the height of general movement z_g .

4.3 Results and Analysis

A total of 174 tests have been performed. Among them, there were 41 tests for $z_0 = 0$, 88 tests for $z_0 < 0$, and 45 tests $z_0 > 0$. The tube inlet position was varied from 101.6 mm below original the bed level to 6.4 mm above it. The radius at tube level, r_t , was within 19 to 35 mm, the aerial radius, r_a , was within 17 to 29 mm, and the relative maximum depth, ε_{rm} , was found within 4.4 to 14 mm. The results of these tests are given in Tables 4.1 and 4.2.

For determining the heights of critical and general movement of the particles, 26 tests were performed. The values for z_c were found within 8 to 17 mm and z_g were within 5 to 13 mm. The results are shown in Table 4.3 and 4.4. Data obtained from Mazurek and Rajaratnam (unpublished) and Brahme (1983) are also presented in Tables 4.5 to 4.9.

4.3.1 Analysis Using Dimensional Arguments

4.3.1.1 Development of a Dimensionless Length Scale

In a first attempt to analyze the scour data, an effort to develop appropriate dimensionless parameters is made by using dimensional analysis. For the present study, the significant length parameters are: r_t , the scour hole radius just at the tube level in the case where tube inlet is set on the bed ($z_0 = 0$) or below the bed level ($z_0 < 0$), r_a , the distance between the center of the tube inlet and the edge of the scour hole in the case where the tube is located above bed level ($z_0 > 0$), and ε_{rm} , the relative maximum scour hole depth (vertical distance from the tube inlet to lowest point of scour hole). The other

length parameters are the height of the inlet above the bed for threshold conditions, z_c and z_g . Let us denote all five lengths as a general length term l . It is assumed that this length is a function of

$$l = f\{U_0, \rho, g(\rho_s - \rho), v, d, D\} \quad (4.1)$$

where:

U_0	= velocity of the siphon at the tube inlet,
ρ	= density of the fluid,
ρ_s	= density of the sediment particle,
g	= acceleration due to gravity,
v	= kinematic viscosity of the fluid,
d	= inner diameter of the siphon tube,
D	= mean diameter of sediment particle.

These properties have the dimensions of length (L), mass (M), and time (T) of:

$$\begin{aligned} l &\rightarrow L \\ U_0 &\rightarrow (L/T) \\ \rho &\rightarrow (M/L^3) \\ g(\rho_s - \rho) &\rightarrow (L/T^2)(M/L^3) \rightarrow M/(L^2T) \\ v &\rightarrow L^2/T \\ d &\rightarrow L \\ D &\rightarrow L \end{aligned}$$

The functional relation in Eq. 4.1 can also be written as

$$f_1\{U_0, \rho, g(\rho_s - \rho), v, l, d, D\} = 0 \quad (4.2)$$

In this expression, we have 7 variables with a total of 3 basic units. Using Buckingham π -theorem with the repeating variables U_0 , ρ and d we will get 4 dimensionless parameters. This analysis is as follows

$$\begin{aligned}\pi_1 &= (U_0)^a (\rho)^b (d)^c l \\ \pi_1 &= (L/T)^a (M/L^3)^b (L)^c L \\ T: \quad 0 &= -a \quad a = 0 \\ M: \quad 0 &= b \quad b = 0 \\ L: \quad 0 &= a-3b+c+1 \quad c = -1 \\ \therefore \pi_1 &= \frac{l}{d}\end{aligned}$$

$$\begin{aligned}\pi_2 &= (U_0)^a (\rho)^b (d)^c v \\ \pi_2 &= (L/T)^a (M/L^3)^b (L)^c (L^2/T) \\ T: \quad 0 &= -a-1 \quad a = -1 \\ M: \quad 0 &= b \quad b = 0 \\ L: \quad 0 &= a-3b+c+1 \quad c = -1 \\ \therefore \pi_2 &= \frac{v}{U_0 d} \\ \therefore \pi_2 &= \frac{U_0 d}{v}\end{aligned}$$

$$\begin{aligned}\pi_3 &= (U_0)^a (\rho)^b (d)^c g(\rho_s - \rho) \\ \pi_3 &= (L/T)^a (M/L^3)^b (L)^c (M/(L^2 T^2)) \\ T: \quad 0 &= -a-2 \quad a = -2 \\ M: \quad 0 &= b+1 \quad b = -1 \\ L: \quad 0 &= -2+3b+c-2 \quad c = 1 \\ \therefore \pi_3 &= \frac{dg(\rho_s - \rho)}{\rho U_0^2}\end{aligned}$$

This can also be written as

$$\pi_3 = \frac{U_0}{\sqrt{g \left(\frac{\rho_s - \rho}{\rho} \right) d}}$$

$$\text{In the similar manner we can write } \pi_4 = \frac{U_0}{\sqrt{g \left(\frac{\rho_s - \rho}{\rho} \right) D}}$$

Therefore

$$\frac{l}{d} = f_2 \left\{ \frac{U_0 d}{v}, \frac{U_0}{\sqrt{g \left(\frac{\rho_s - \rho}{\rho} \right) d}}, \frac{U_0}{\sqrt{g \left(\frac{\rho_s - \rho}{\rho} \right) D}} \right\} \quad (4.3)$$

In Eq. 4.3, the term $\frac{l}{d}$ contains the independent variable l and can be referred as a dimensionless length scale. The first term is the Reynolds number of the flow through the tube, $R_0 = \frac{U_0 d}{v}$. Since water is the only fluid considered in this study and its viscosity does not change significantly, this Reynolds term might be neglected (for now).

The second term $\frac{U_0}{\sqrt{g \left(\frac{\rho_s - \rho}{\rho} \right) d}}$ is the Froude number for the flow through the siphon tube. This term will be neglected since the Froude number is not an important term for pipe flows and flows that are deeply submerged (as in the present case). If the velocity over the sediment particle on bed is assumed to be a related with the tube velocity U_0 , the last term $\frac{U_0}{\sqrt{g \left(\frac{\rho_s - \rho}{\rho} \right) D}}$ can be approximated as the ratio of the exerted force on the bed particle by the flow to its resistive force (as discussed in Chapter 2). This term here is the densimetric Froude number and is denoted by F_0 . Since it is known that erosion for cohesionless sediments typically has a strong functional relationship with F_0 , we will keep this term and therefore Eq. 4.3 can be written as

$$\frac{l}{d} = f_3 \left\{ \frac{U_0}{\sqrt{g \left(\frac{\rho_s - \rho}{\rho} \right) D}} = F_0 \right\} \quad (4.4)$$

By following the same dimensional reasoning, expressions can be written for scour hole dimensions r_t , r_a , and ε_{rm} , and tube heights for threshold condition z_c and z_g . These are as follows:

$$\frac{r_t}{d} = f_4 \{F_0\} \quad (4.5)$$

$$\frac{r_a}{d} = f_5 \{F_0\} \quad (4.6)$$

$$\frac{\varepsilon_{rm}}{d} = f_6 \{F_0\} \quad (4.7)$$

$$\frac{z_c}{d} = f_7 \{F_0\} \quad (4.8)$$

$$\frac{z_g}{d} = f_8 \{F_0\} \quad (4.9)$$

4.3.1.2 Analysis of Scour Hole Dimensions at Equilibrium

To examine the dimensionless relationships developed above, the scour hole dimensions were plotted against the densimetric Froude number, F_0 . The experimental results of Mazurek and Rajaratnam (unpublished) are also analyzed for the case when $z_0 = 0$ and $z_0 < 0$. For the case when $z_0 > 0$, the results of the scour hole radius of Brahme (1983) are used along with those of present study to test the relationship.

For the case where the tube is set on or within the bed, the equilibrium scour hole radius at the tube level, r_t , has been considered for analysis. The data of r_t , obtained from

the present study as well as from Mazurek and Rajaratnam (unpublished), are plotted with F_0 as shown in Fig. 4.4. It appears that, the two sets of experiments fall on separate curves, which can be expressed by the following equations

$$\frac{r_t}{d} = 0.635 \times F_0^{0.405} \quad (\text{Present Study}) \quad (4.10)$$

and

$$\frac{r_t}{d} = 0.664 \times F_0^{0.361} \quad (\text{Mazurek and Rajaratnam (unpublished)}) \quad (4.11)$$

with correlation coefficients R^2 of 0.95 and 0.93 respectively. These relations show that

$\frac{r_t}{d}$ increases at a decreasing rate with increasing F_0 . Also, in the present study the radius

is always larger than that found by Mazurek and Rajaratnam (unpublished).

In case when $z_0 > 0$ results from the present study as well as those from Brahme (1983) are used, as Mazurek and Rajaratnam had no experiments with the tube above the bed. For this tube position, the distance between the center of the tube inlet and edge of the scour hole or the aerial radius, r_a , are considered for analysis. This aerial radius is normalized by the tube diameter, d . From the experimental results this dimensionless aerial radius is correlated with the densimetric Froude number, F_0 , as shown in Fig. 4.5. The relationship for each data set again does not fall on one curve and each can be described separately as

$$\frac{r_a}{d} = 0.580 \times F_0^{0.389} \quad (\text{Present Study}) \quad (4.12)$$

$$\frac{r_a}{d} = 0.368 \times F_0^{0.458} \quad (\text{Brahme (1983) for fine sand}) \quad (4.13)$$

$$\frac{r_a}{d} = 0.334 \times F_0^{0.496} \quad (\text{Brahme (1983) for medium sand}) \quad (4.14)$$

$$\frac{r_a}{d} = 0.380 \times F_0^{0.434} \quad (\text{Brahme (1983) for microbeads}) \quad (4.15)$$

with respective correlation coefficient, R^2 , of 0.88, 0.93, 0.97 and 0.83. From an inspection of all of the curves (in Fig. 4.5) obtained for different materials, it is clear that

$\frac{r_a}{d}$ is increasing with F_0 in a decreasing manner in every case. The curves are almost

parallel and in case of present study the value of $\frac{r_a}{d}$ is always larger than that of Brahme (1983). It should be noted that the scale of the experiments in the present study is smaller than in Brahme (1983). Therefore, likely due to the errors in the measurements, the data of the present study shows more scatter. The scatter is more in case of lower values of the densimetric Froude number, F_0 , when the scour hole radius is smaller.

For every test of this study, the average of the two maximum relative depths formed in both sides of the centerline is taken for the reported ε_{rm} . Results obtained from Mazurek and Rajaratnam (unpublished) and the present study are used for analysis. The relations between the ε_{rm} and F_0 are shown in Fig. 4.6. It was found that the data was best fit by

$$\frac{\varepsilon_{rm}}{d} = 0.171 \times F_0^{0.491} \quad (\text{Present Study (for all three inlet positions)}) \quad (4.16)$$

$$\frac{\varepsilon_{rm}}{d} = 0.170 \times F_0^{0.432} \quad (\text{Mazurek and Rajaratnam (for } z_0 = 0, \text{ and } z_0 > 0\text{)}) \quad (4.17)$$

These relations have correlations coefficients, R^2 , of 0.93 and 0.89 respectively. The plot shows that $\frac{\varepsilon_{rm}}{d}$ increases at a decreasing rate with increasing F_0 and it is again always larger in the present study than that of Mazurek and Rajaratnam.

4.3.1.3 Analysis of Heights of Threshold Conditions

The results of the height of the tube inlet for critical and general particle movements obtained in the present study as well as those in Mazurek and Rajaratnam (unpublished) are plotted in the Fig. 4.7.and 4.8 respectively. A general relationship is found for $\frac{z_c}{d}$ data for both the studies and it is fitted with the following equation

$$\frac{z_c}{d} = 0.252 \times F_0^{0.423} \quad (4.18)$$

This equation has a correlation coefficient, R^2 , of 0.88. However, the $\frac{z_g}{d}$ data do not fall together for these studies. Two separate curves is obtained in this case which are expressed by these formula

$$\frac{z_g}{d} = 0.195 \times F_0^{0.470} \quad (\text{Present study}) \quad (4.19)$$

and

$$\frac{z_g}{d} = 0.219 \times F_0^{0.404} \quad (\text{Mazurek and Rajaratnam}) \quad (4.20)$$

The above equations fitted with correlation coefficients, R^2 , of 0.95 and 0.78 respectively. The difference between studies here may be due to difference in the judgment between the observers for the “general movement”.

From the above dimensional analysis it is apparent that, the inside tube diameter (inside diameter) is the most appropriate scale for describing the length parameters related to scour of cohesionless materials by siphon. All of the dimensions correlated fairly well with the densimetric Froude number. However, the data show slightly different trends when compared between studies where different sediment particles or

experiment scales were used. Therefore, it is apparent the densimetric Froude number alone is not adequate to describe the length parameters related to the siphon scouring. Other particle properties or flow characteristics appear have important effects and this will be explored in the following section.

4.3.2 Analysis Using Theory

As discussed above, densimetric Froude number is possibly not the only parameter important in predicting the dimensionless lengths in the scour produced by siphon flows. The following provides an attempt, from a theoretical point of view, to determine functional relationships that might be suitable to describe the equilibrium scour hole radii (r_a and r_t). These analyses are based on a comparison of the threshold shear stress of the particle and the viscous shear stress acting on the particle as the scouring reaches the equilibrium. Results from the present study, as well as from Mazurek and Rajaratnam (unpublished) and Brahme (1983) are again used to test and develop the functional relations.

4.3.2.1 Development of Functional Relationships for Equilibrium Scour Hole Radii

This first part of this section focuses on the radius of the scour hole at the tube level, r_t , for the condition $z_0 = 0$ or $z_0 < 0$, and the second part is intended to derive the aerial radius, r_a , for the scenario when $z_0 > 0$. The Shields criteria for threshold particle movement has been used for developing the theory.

A typical equilibrium scour hole profile is sketched in Fig. 4.9 for the case when $z_0 = 0$ or $z_0 < 0$. Consider the situation just before equilibrium. Part of the total flow in the tube comes from the flow above the scoured sediment bed and the other part of the

flow comes from the seepage across the sediment-fluid interface inside the scour hole.

Let us assume that the portion of flow coming from above plane AOB (Fig. 4.9) can be expressed as

$$Q_a = k_1 Q \quad (4.21)$$

where k_1 is a constant, Q_a is the portion of discharge resulting from other than seepage flow, and Q is the total flow rate through inlet. Let us consider a point A located on the boundary at the tube level. Suppose, the velocity over the boundary at point A is v_{rb} (Fig. 4.9) and it is directly proportional to the average velocity into the scour hole through the plane AOB . Then it can be written as:

$$v_{rb} = -k_2 \frac{Q_a}{\pi(r_t^2 - d^2/4)} = -k_3 \frac{Q}{\pi r_{t1}^2} \quad (4.22)$$

The negative sign in Eq. 4.22 refers that the flow is moving radially inwards. Here, k_2 and k_3 are constants, and $\left(r_t^2 - \frac{d^2}{4}\right)$ has been replaced by the term r_{t1}^2 . The term r_{t1} has no physical existence. This is a radius an imaginary circle that has the same area as the fluid enters through the plane AOB (in Fig. 4.9). Therefore, when the tube diameter is negligible, for the same flow rate, r_t represents the radius of the scour hole at tube inlet level. This by expansion also can be written as

$$r_{t1} = r_t \left[1 - \frac{1}{8} \left(\frac{d}{r_t} \right)^2 - \frac{1}{128} \left(\frac{d}{r_t} \right)^4 - \dots \right] \quad (4.23)$$

Here $0 > \frac{d}{r_t} \geq 1$. This range may be true for all practical situations (from the experimental

data of the present study, $\frac{d}{r_t}$ has been found within 0.28 to 0.94). Considering this range,

the relation in Eq. 4.23 may be reasonable to convert in a linear form with the following equation

$$r_{tl} = c_1 r_t - c_2 d \quad (4.24)$$

where c_1 and c_2 are constants. If we consider that the boundary layer at point A is laminar that the velocity distribution in boundary layer can be taken as in discussed in Chapter 2 (Eq. 2.6) (Schlichting and Gersten 2000)

$$\frac{u'}{v_{rb}} = f'(\eta) = 3 \tanh^2 \left(\frac{\eta}{\sqrt{2}} + \operatorname{arctanh} \sqrt{\frac{2}{3}} \right) - 2 \quad (4.25)$$

where v_{rb} is the velocity above the boundary layer at that point, u' is the velocity in the boundary layer at a distance z' normal to the bed, and $\eta = \frac{z'}{\delta}$ is the dimensionless distance from the bed. Here, z' is the axis normal to bed at point A , and δ is the thickness of the boundary layer which has been taken as (Schlichting and Gersten 2000)

$$\delta = \sqrt{\frac{r_{tl} v}{-v_{rb}}} \quad (4.26)$$

where, r_{tl} is the distance of point A from the center of the tube inlet when its diameter is very small, v is the kinematic viscosity of the fluid. Thus we can write

$$\eta = z' \sqrt{\frac{-v_{rb}}{r_{tl} v}} \quad (4.27)$$

At point A , the bed shear stress exerted by the fluid can be obtained from the gradient of the velocity distribution in the boundary layer. Thus, differentiating Eq. 4.25 with respect to η , and putting $\eta = 0$ for point A (since it is located on the bed) we get

$$\frac{1}{v_{rb}} \left(\frac{\partial u'}{\partial \eta} \right)_A = \frac{2}{\sqrt{3}} \quad (4.28)$$

In the practical point of view, the boundary at the point A is not a rigid and smooth. When some dye was injected into the flow near point A , there was apparently no mixing of dye by the radial flow. Thus the flow over the point A can be considered to be laminar. However, in the actual situation there is always some seepage flow at interface through the point A . For the highest flow rate (0.47 L/s), and the highest flow velocity (6.4 m/s) through the inlet, the hydraulic gradient for seepage flow over the scour hole boundary at tube level was measured. This hydraulic gradient appeared to be very small (within 5 % of the critical hydraulic gradient). Therefore, considering the boundary layer most possibly as laminar, and the effect of the seepage flow as insignificant in the scouring process, the constant in right hand side of Eq. 4.28 may need to be adjusted to some extent. Therefore, this equation can be re-written as

$$\frac{1}{v_{rb}} \left(\frac{\partial u'}{\partial \eta} \right)_A = c_3 \quad (4.29)$$

where c_3 is another constant. Again, using the value of η from Eq. 4.27 the above relation becomes

$$\frac{1}{v_{rb}} \left(\frac{\partial u'}{\partial z'} \right)_A \sqrt{\frac{r_{t1} v}{-v_{rb}}} = c_3 \quad (4.30)$$

$$\text{or, } \left(\frac{\partial u'}{\partial z'} \right)_A = c_3 \sqrt{\frac{-v_{rb}^3}{r_{t1} v}} \quad (4.31)$$

From Eq. 4.22 and 4.31 we get

$$\left(\frac{\partial u'}{\partial z'} \right)_A = c_3 \sqrt{\frac{k_3^3}{r_{t1}^7 v} \left(\frac{Q}{\pi} \right)^3} \quad (4.32)$$

Again, as discussed in Chapter 2, the bed shear stress at point A can be expressed by the Newton's law

$$\tau_A = \mu \left(\frac{\partial u'}{\partial z'} \right)_A \quad (4.33)$$

where τ_A = the shear stress at point A , and μ = the dynamic viscosity of the fluid.

The discussion so far, considers the period of scouring which is just before equilibrium is reached. At equilibrium, the particles stop sliding down from point A the bed shear stress, τ_A , reaches the critical shear stress of the particle in the inclined bed, $\tau_{c\theta s}$. Thus multiplying both sides of Eq. 4.32 by μ and using Eq. 4.33, we can write

$$\tau_{c\theta s} = \mu \left(\frac{\partial u'}{\partial z'} \right)_A = \frac{c_3 k_3^{3/2}}{\sqrt{64}} \rho \sqrt{\frac{\nu U_0^3 d^6}{r_{t1}^7}} \quad (4.34)$$

where $\tau_{c\theta s}$ is the critical shear stress of the sediment particle at point A where the bed has a slope of angle θ and seepage flow is present across the bed (Fig. 4.9). The ratio of the critical shear stress of cohesionless sediment in an inclined plane under seepage flow, $\tau_{c\theta s}$, to that in a horizontal plane without slope or seepage effect, τ_c , can be found by multiplying the terms in Eq. 2.23 with those in Eq. 2.24 as

$$\left(\frac{u_{*c\theta s}}{u_{*c}} \right)^2 = \cos \theta \left(1 - \frac{\tan \theta}{\tan \varphi} \right) \left(1 - \frac{i}{i_c} \right). \quad (4.35)$$

$$\text{or, } \frac{\tau_{c\theta s}}{\tau_c} = K'(\theta, \varphi, i) \quad (4.36)$$

where K' is a function of slope of the bed, θ , the angle of repose of the sediment particle, φ , and the hydraulic gradient, i , (since i_c has a typical value of 1 as discussed in Chapter 2). The slope of the boundary at tube level, for every equilibrium scour hole profile does not vary significantly. This will be discussed in the following section. Again, as in this experiment the hydraulic gradient for seepage flow, i , in the scour hole boundary at tube level (point A) is small compared to its critical hydraulic gradient i_c , K' could be

considered is a function of φ only. Therefore, Eq. 4.34 can be written as follows by using the relation in Eq. 4.36

$$\tau_c = \frac{\tau_{c\theta s}}{K'(\varphi)} = K''(\varphi) \rho \sqrt{\frac{v U_0^3 d^6}{r_{t1}^7}} \quad (4.37)$$

where K' and K'' are function of the angle of repose of the sediment grain. From Eq. 2.19 (which was derived from the Shields curve) we can see that the critical shear stress of cohesionless materials in a horizontal bed is a function of dimensionless particle diameter, $D^* = D \left[\frac{(\rho_s - \rho)g}{\rho v^2} \right]^{1/3}$, and the angle of repose of the particle, φ . Using this equation, Eq. 4.37 and 2.19 (when $D^* < 0.3$), the following relation can be derived.

$$\tau_c = K''(\varphi) \rho \sqrt{\frac{v U_0^3 d^6}{r_{t1}^7}} = (\rho_s - \rho) D g \times 0.5 \tan \varphi \quad (4.38)$$

After some simplifications Eq. 4.38 can be written in the following form

$$\frac{r_{t1}}{d} = \left(\frac{K''(\varphi)}{0.5 \tan \varphi} \right)^{2/7} \left(\frac{F_0^4}{R_0} \right)^{1/7} \quad (4.39)$$

where $F_0 = \frac{U_0}{\sqrt{g \left(\frac{\rho_s - \rho}{\rho} \right) D}}$ is the densimetric Froude number of the particle and

$R_0 = \frac{U_0 d}{v}$ is the Reynolds number of the flow in the tube. Again, using Eq. 4.24 and.

4.39, we get

$$\frac{r_{t1}}{d} = C_1 + [K''(\varphi)]^{2/7} \left[\frac{F_0^4}{(0.5 \tan \varphi)^2 R_0} \right]^{1/7}; \quad \text{when } D^* < 0.3. \quad (4.40)$$

The critical shear stress of the particle for other range of values of dimensionless particle size D^* , can be obtained from Eq. 2.20 to 2.22, and the following relations can be developed in the similar manner

$$\frac{r_t}{d} = C_1 + [K''(\varphi)]^{2/7} \left[\frac{F_0^{3.2} R_s^{0.8}}{(0.25 \tan \varphi)^2 R_0} \right]^{1/7}; \quad \text{when } 0.3 < D_* < 19 \quad (4.41)$$

$$\frac{r_t}{d} = C_1 + [K''(\varphi)]^{2/7} \left[\frac{F_0^{6.8}}{(0.013 \tan \varphi)^3 R_0^{1.5} R_s^{0.8}} \right]^{2/21}; \quad \text{when } 19 < D_* < 50 \quad (4.42)$$

and

$$\frac{r_t}{d} = C_1 + [K''(\varphi)]^{2/7} \left[\frac{F_0^4}{(0.06 \tan \varphi)^2 R_0} \right]^{1/7}; \quad \text{when } D_* > 50 \quad (4.43)$$

where C_1 is a constant, K'' depends on φ , $R_0 = \frac{U_0 d}{v}$ is the Reynolds number of the flow

in the tube, $F_0 = \frac{U_0}{\sqrt{g \left(\frac{\rho_s - \rho}{\rho} \right) D}}$ is the densimetric Froude number, φ is the angle of repose of the sediment grain, and $R_s = \frac{U_0 D}{v}$ is a Reynolds number of the particle on bed.

Note that these equations apply only to the cohesionless sediments since relations for τ_c have been obtained for cohesionless sediments. Appendix B provides more details of the above theory.

The above discussion was focused on the equilibrium scour hole formed when the tube is set on or below the bed. The velocity on the bed for that case was derived by using continuity equation. The following provides a theoretical analysis for the conditions when the siphon tube is set above the bed ($z_0 > 0$). In this case, the potential

flow theory will be used as an attempt to derive the radial flow velocity over the edge of the scour hole boundary.

When the ratio of the diameter of the tube inlet and its distance above the bed is very small, the center of the tube can be considered as a point sink. As discussed in the review of literature, just after start up of this configuration, the flow around the tube can be described as potential flow (Apgar and Basco (1975)). If the inlet resembles a point sink, then using Eq.2.4, the radial velocity over any point on a rigid horizontal bed becomes

$$v_r = -\frac{Q}{2\pi} \frac{r}{[z_0^2 + r^2]^{3/2}} \quad (4.44)$$

where r is the radial distance of the point, Q is the flow through the tube, and z_0 is the distance of the inlet from the bed. The negative sign in Eq. 4.44 implies the velocity is towards the centerline of the tube.

As discussed before, most of the sediment is removed in a very rapid manner in the case when $z_0 > 0$. A sketch of a typical scour hole formed at this instant is shown in Fig. 4.10, where A is any point on the edge of the scour hole near bed level. Below the tube inlet, the bed is no longer horizontal and also the seepage flow is now included in the total flow, Q . As a result, the velocity over point A should differ to some extent from v_r , which has been described in Eq. 4.44. Suppose, just before equilibrium, the component of the radial velocity over point A is v_{rb} . Then it may be reasonable to assume that

$$v_{rb} = g_1(\theta, i)v_r \quad (4.45)$$

where g_1 accounts for the slope effect and the seepage flow and should depend on the slope at point A , θ , and hydraulic gradient of the seepage flow at point A , i . Just before the equilibrium, it may be reasonable to assume that the streamlines are parallel to the bed surface, over the point A and seepage has a negligible effect on further scouring. Therefore, at this stage, the parameter, $g_1(\theta, i)$, described in Eq. 4.45 may be considered primarily as a function of the bed slope, θ . Since the flow around the tube inlet is likely to be laminar, the velocity distribution can be expressed by the similar equation as Eq. 4.27. In this case, the dimensionless distance from the bed is

$$\eta = z' \sqrt{\frac{-v_{rb}}{(z_0^2 + r^2)^{1/2} v}} \quad (4.46)$$

In a similar manner as in Eq. 4.31, we get

$$\left(\frac{\partial u'}{\partial z'} \right)_A = \frac{2}{\sqrt{3}} \sqrt{\frac{-v_{rb}^3}{(z_0^2 + r^2)^{1/2} v}} = \frac{2}{\sqrt{3}} \sqrt{\frac{-v_{rb}^3}{r_{a0} v}} \quad (4.47)$$

where $r_{a0} = \sqrt{(z_0^2 + r^2)}$ the aerial distance of the point A (the distance between the inlet center and the edge of the scour hole boundary) when the inlet is considered as a point sink, and r its radial distance from the centerline, and z_0 is the height of the point sink above the bed level and using Equation 4.45, 4.46 and 4.47 we get (More details are given in Appendix B)

$$\left(\frac{\partial u'}{\partial z'} \right)_A = \frac{1}{\sqrt{384}} \sqrt{\frac{[g_1(\theta)]^3 U_0^3 d^6 r^3}{v r_{a0}^{10}}} \quad (4.48)$$

The scouring process ceases, as the bed shear stress at point A reduces to its critical value $\tau_{c\theta s}$. Multiplying both sides of Eq. 4.48 by μ , similarly as in Eq. 4.34, we get

$$\tau_{c\theta s} = \frac{[g_1(\theta)]^{3/2}}{19.6} \rho \sqrt{\frac{v U_0^3 d^6 r^3}{r_{a0}^{10}}} \quad (4.49)$$

where $\tau_{c\theta s}$ = the critical shear stress of the sediment particle when a bed slope and seepage flow is present. At equilibrium there is no particle movement inside the scour hole and the radius at the bed level is now increased to r_b which be expressed as (Fig. 4.10)

$$r_b = r_{a0} \sin \psi \quad (4.50)$$

where ψ is the angle between the tube centerline and aerial radius, r_{a0} . Hence, Eq. 4.49 becomes

$$\tau_{c\theta s} = \frac{[g_1(\theta)]^{3/2}}{19.6} \rho \sqrt{\frac{v U_0^3 d^6 \sin^3 \psi}{r_{a0}^7}} \quad (4.51)$$

From the experiments, it has been observed that, for the case $z_0 > 0$, at the edge of the equilibrium scour hole (point A in Fig. 4.10), the slope θ is not the same. Therefore, using Eq. 4.36 and 4.51, the critical shear stress at horizontal bed can be expressed as

$$\tau_c = \frac{[g_1(\theta)]^{3/2}}{19.6 K'(\theta, \varphi, i)} \rho \sqrt{\frac{v U_0^3 d^6 \sin^3 \psi}{r_{a0}^7}} \quad (4.52)$$

where $K'(\theta, \varphi, i)$ = the ratio of the critical shear stress in the inclined sediment bed to that in the horizontal bed of a cohesionless material (Eq. 4.36). In this case, if the hydraulic gradient for seepage flow is very less compared to its critical hydraulic gradient, K' should be the function of θ and φ . Therefore, Eq. 4.52 can also be written in the following form

$$\tau_c = [K''(\theta, \varphi) \sin^{3/2} \psi] \rho \sqrt{\frac{v U_0^3 d^6}{r_{a0}^7}} \quad (4.53)$$

where K''' is a parameter that depends on the bed slope, θ , and the angle of repose of the particle, ϕ . If the dimensionless particle size $D_* < 0.3$, the following expression can be derived in a similar manner as in Eq. 4.39

$$\frac{r_{a0}}{d} = \left(\frac{[K'''(\theta, \phi) \sin^{3/2} \psi]}{0.5 \tan \phi} \right)^{2/7} \left(\frac{F_0^4}{R_0} \right)^{1/7} \quad (4.54)$$

Eq. 4.54 has been derived for the scour hole formed by a point flow located above a cohesionless sediment bed. In the actual situation, we used siphon tubes of different diameters. The diameter has some influence on sink strength along the radial direction as well as the resulting scour radius. If the diameter of siphon is bigger, the flow converges at some radial distance away from the center which is in case of pipe negligible diameter converges at closer to tube center. This effect has been depicted in Fig. 4.11. Therefore we can expect greater scour radius and thus greater aerial distance in the actual situation and this might be reasonably assumed as

$$r_a = r_{a0} + C_2 d \quad (4.55)$$

where r_a = the scour hole radius formed when tube inlet has a diameter d , and C_2 is another constant. Hence Eq. 4.54 becomes

$$\frac{r_a}{d} = C_2 + [K'''(\theta, \phi)]^{2/7} \left[\frac{F_0^4 \sin^3 \psi}{(0.5 \tan \phi)^2 R_0} \right]^{1/7}; \text{ when } D_* < 0.3 \quad (4.56)$$

Similarly using Eq. 4.53, and the value for τ_c (from Eq. 2.20 to 2.22) for other ranges of values of D_* , we get

$$\frac{r_a}{d} = C_2 + [K'''(\theta, \phi)]^{2/7} \left[\frac{F_0^{3.2} R_s^{0.8} \sin^3 \psi}{(0.25 \tan \phi)^2 R_0} \right]^{1/7}; \text{ when } 0.3 < D_* < 19 \quad (4.57)$$

$$\frac{r_a}{d} = C_2 + [K''(\theta, \varphi)]^{2/7} \left[\frac{F_0^{6.8} \sin^3 \psi}{(0.013 \tan \varphi)^3 R_0^{1.5} R_s^{0.8}} \right]^{2/21}; \text{ when } 19 < D_* < 50 \quad (4.58)$$

and

$$\frac{r_a}{d} = C_2 + [K''(\theta, \varphi)]^{2/7} \left[\frac{F_0^4 \sin^3 \psi}{(0.06 \tan \varphi)^2 R_0} \right]^{1/7}; \text{ when } D_* > 50 \quad (4.59)$$

Note that the above equations should apply only for cohesionless materials.

4.3.2.2 Validation of the Theory using Experimental Data

The theory developed in the previous discussion will now be evaluated using the experimental data of the equilibrium scour hole radii, r_t and r_a . This validation can enable us to find the prediction formula for the length parameters that incorporates the theoretical functions. First, the data of equilibrium scour hole radius at tube level r_t , from the present study as well as those from Mazurek and Rajaratnam (unpublished) are used for the case $z_0 = 0$ and $z_0 < 0$. Later, for the case $z_0 > 0$, the aerial radius r_a of the equilibrium scour hole obtained from the present study and from Brahme (1983) are tested to validate these functions. Table 4.10 shows the values of the dimensionless particle diameter D_* of the cohesionless materials used in the present studies as well as in Mazurek and Rajaratnam and Brahme (1983). The angle of repose, φ , at submerged condition used was (from Simons, 1957) as nearly 30° for all the materials. Therefore, for all of the materials used in different studies, the dimensionless particle diameters are found within the range of $0.3 < D_* < 19$ (Table 4.10).

For the equilibrium scour radius at tube level, we will use the functional relation described in Eq. 4.41. Fig. 4.12 shows a plot of r_t data from this study and Mazurek and

Rajaratnam (unpublished) have been related by a single straight line with the theoretical function. This relation can be expressed by the following equation

$$\frac{r_t}{d} = 0.320 + 0.450 \times \left[\frac{F_0^{3.2} R_s^{0.8}}{(0.25 \tan \varphi)^2 R_0} \right]^{1/7} \quad (4.60)$$

where, F_0 = the densimetric Froude number, R_s = the particle Reynolds number, R_0 = Reynolds number of the flow in the tube, and φ is the angle of repose of the sediments. This equation has a correlation coefficient, R^2 , of 0.95. This equation is an improvement over Eq. 4.10 and 4.11 since a general relation is obtained for the two different experiments. Comparing Eq. 4.41 and 4.60 we can see that, $C_I = 0.32$ and $K''(\varphi)$ has a constant value of 0.06.

For the aerial radius, r_a , of the equilibrium scour hole, data from the present and that from Brahme (1983) are used as before. Brahme used three different cohesionless materials of different mean diameters, whereas in the present study only one sand is used. The dimensionless particle sizes for different materials are shown in Table 4.10. Since all the particle fall within the range of $0.3 < D_* < 19$, we must use the function described in Eq. 4.57. Fig. 4.13 shows the plot of dimensionless aerial radius r_a with the theoretical function. The relation is fitted with a straight line having the following equation

$$\frac{r_a}{d} = 0.240 + 0.463 \times \left[\frac{F_0^{3.2} R_s^{0.8} \sin^3 \psi}{(0.25 \tan \varphi)^2 R_0} \right]^{1/7} \quad (4.61)$$

This equation has a value of correlation coefficient, R^2 of 0.93. It is evident that, Eq. 4.61 has a general applicability since both the experiments were used in different scales with a variety of cohesionless materials, where using only the densimetric Froude number, we obtained separate relations for each sediment material (Eq. 4.12 to 4.15 and

Fig. 4.5). By comparing the coefficients in Eq. 4.57 and 4.61, it can be noted that,

$K''(\theta, \phi)$ in Eq. 4.57 appears to have a very weak correlation with $\frac{r_a}{d}$ and may be taken

as a constant. The value of K'' here is 0.07.

In both of these equation (Eq. 4.60 and 4.61), we can see that the constants C_1 and C_2 has value of 0.32 and 0.24 respectively. This implies that the tube diameter has an added effect on the equilibrium scour hole radii.

4.3.2.3 Applying the Theory for Predicting the Equilibrium Scour Hole Depth

The functional relationships developed above were for the equilibrium scour hole radii. The following provides an attempt to correlate the maximum depth with the scour hole radius at the tube level that might help to find a prediction formula for this depth, as it appears that Reynolds number should be included in the relations.

The maximum scour depth is measured from the inlet and plotted with the radius at tube inlet (Fig. 4.14). They can be related by the following formula

$$\frac{\varepsilon_{rm}}{d} = 0.410 \times \frac{r_t}{d} - 0.13 \quad (4.62)$$

This equation has a coefficient of correlation, R^2 , of 0.95. From Eq. 4.60 and 4.62, it is evident that, $\frac{\varepsilon_{rm}}{d}$ also has a relationship with the previously developed function (Eq. 4.41). Using the experimental results of the relative maximum scour hole depth at equilibrium, ε_{rm} , and corresponding values of the theoretical function are plotted in Fig. 4.15. This plot is fitted with a straightline which also has the equation as

$$\frac{\varepsilon_{rm}}{d} = 0.205 \times \left[\frac{F_0^{3.2} R_s^{0.8}}{(0.25 \tan \phi)^2 R_0} \right]^{1/7} \quad (4.63)$$

This equation fit the data with an $R^2 = 0.90$. Unlike the formula for predicting r_t (Eq. 4.60), the straight line in this case goes through the origin. Therefore it can be said that diameter of the tube inlet possibly have no additional effect in predicting the maximum scour hole depth, ε_{rm} .

4.3.2.4 Applying the Theory for Predicting the Threshold Heights

For threshold heights the shear stress at bed cannot be explained the theory that discussed above. This is because the velocity of the flowing fluid is approaching towards the center loses its radial component (the flow becomes vertical as it moves through the tube). Therefore transfer of momentum to the bed and thereby bed shear stress is reduced to zero as the fluid particle closes to the center. The location and the magnitude of the maximum bed shear stress for different inlet heights are yet to determine to obtain any theory for predicting the threshold heights. The present study does not include this analysis. However, the functional relationship derived for the scour hole radius at tube level, r_t , here has been used to examine their correlations. Data from the present study and those from Mazurek and Rajaratnam has been used for this purpose. Fig 4.16 and 4.17 show plots of the threshold heights for critical and general movements of the particles fitted with the theoretical function (as specified in Eq. 4.41, 4.60, 4.63). These has been (Fig. 4.16 and 4.17) and related with the following equations

$$\frac{z_c}{d} = 0.240 \times \left[\frac{F_0^{3.2} R_s^{0.8}}{(0.25 \tan \phi)^2 R_0} \right]^{1/7} \quad (4.64)$$

$$\frac{z_g}{d} = 0.213 \times \left[\frac{F_0^{3.2} R_s^{0.8}}{(0.25 \tan \phi)^2 R_0} \right]^{1/7} \quad (4.65)$$

Eq. 4.64 and Eq. 4.65 are fitted with a coefficient of correlation, R^2 , of 0.89 and 0.91 respectively. The equation for the critical height (Eq. 4.64) shows a better correlation than what obtained with the densimetric Froude number (Eq. 4.18). Again, Eq. 4.65 is a general form for both the experiments thus an improvement over the previous equations as described in Eq. 4.19 and 4.20. It is noted that the equations for dimensionless height of general movement (Eq. 4.65) and dimensionless maximum scour hole depth (Eq. 4.63) contain almost same coefficient for the theoretical function. This shows that the maximum depth below the tube is almost the same as the tube inlet for general movement, z_g , which would intuitively be the case.

4.6 The Scour Hole Profiles at Equilibrium State

As discussed in Chapter 3, due to its axisymmetric pattern, scour hole profiles were measured only one diametric direction. Appendix A gives the complete data for the scour hole profile measurements. In the case when $z_0 = 0$ or $z_0 < 0$, several different scales were tried to nondimensionalize the scour hole profile data. These include the scour hole radius at bed level and the radial distance at half of the maximum scour hole depth for the scale for radial distance r , but yielded no good correlation. Again, the maximum scour hole measured from the bed level also tried as a scale for depth (or axial direction). This also did not work well to collapse all the data. A similarity in the scour hole profiles have been found when the scour hole profiles are normalized with the radius of the scour hole at inlet level, r_t , as the scale for the radial distance; and the maximum scour depth from the tube inlet level, ε_{rm} , as the scale for scour depth. The data of the present study are used for the dimensionless profile. Fig. 4.18 and Fig 4.19 shows the plots of the normalized scour hole profiles of different tests for tube set -2.54, 5.08, 7.62

and 10.16 cm below the bed and on the bed respectively. All of the profiles fall within the same curve. The origin of this nondimensionalized profile is the center of the tube inlet. The equation of the dimensionless scour hole profile below the tube level can be expressed as follows

$$\frac{\varepsilon_r}{\varepsilon_{rm}} = -1.32 \times \left(\frac{r}{r_t} \right)^3 + 3.83 \times \left(\frac{r}{r_t} \right)^2 - 1.72 \times \left(\frac{r}{r_t} \right) - 0.79; \quad (\text{when } 0 \leq \frac{r}{r_t} \leq 1) \quad (4.66)$$

This relationship fit with data with an $R^2 = 0.95$. Using Eq. 4.66, we can find that the maximum scour depth occurs at a radial distance of $0.26r_t$. Again, when $\frac{r}{r_t}$ is greater

than 1, and $\frac{\varepsilon_r}{\varepsilon_{rm}}$ is positive, a linear relation has been found which is shown in Fig. 4.18.

This can be expressed by the equation

$$\frac{\varepsilon_r}{\varepsilon_{rm}} = 2.147 \times \left(\frac{r}{r_t} - 1 \right); \quad (\text{when } \frac{r}{r_t} \geq 1) \quad (4.67)$$

For this part, a correlation coefficient $R^2 = 0.99$ has been found.

By using Eq. 4.62 and 4.67, we can get a relation between scour hole measured from the original bed and the radial distance. This can be expressed by the following equation

$$\varepsilon_r = \left(0.88 - 0.314 \times \frac{d}{r_t} \right) (r - r_t); \quad (\text{when } \frac{r}{r_t} \geq 1) \quad (4.68)$$

From the experimental result, $\frac{d}{r_t}$ has been found within the range of 0.28 to 0.94. Using

these values, the scour hole boundary above the tube level has a slope within 35° to 40° . This range of values of slope is somewhat greater than the angle of repose in the two-dimensional case which is about 30° . The increase in the angle of repose might be

expected since the particles are more stable because of dynamic flow conditions and the conical shape in the scour hole around the tube axis.

In the case when tube is set above the bed level ($z_0 > 0$) the scour hole radius at bed level was checked as a scale for radial direction and found inappropriate. Again, no r_t data can be obtained from the experiments when tube is above the bed level. Therefore, for each test, the imaginary radius r_t at tube level is obtained by putting the value of the function $\frac{F_0^{3.2} R_s^{0.8}}{(0.25 \tan \phi)^2 R_0}$ in Eq. 4.60. Now the radial distance of the scour hole profiles are normalized by r_t values. The depth is normalized as before by the relative scour depth ε_{rm} . Only data from the present study has been used for this purpose which is plotted in Fig. 4.20. This relation fits with the following equation

$$\frac{\varepsilon_r}{\varepsilon_{rm}} = -1.59 \times \left(\frac{r}{r_t} \right)^3 + 3.94 \times \left(\frac{r}{r_t} \right)^2 - 1.73 \times \left(\frac{r}{r_t} \right) - 0.79; \quad (\text{when } 0 \leq \frac{r}{r_t} \leq 1) \quad (4.69)$$

This equation fitted with the profile with a correlation coefficient, R^2 , of 0.89. The correlation in this case is not as good as in previous cases since a small setup is used in the experiment which might have led observation errors.

4.7 Analysis of Errors

The following provides estimates of the errors in measured and derived quantities in the present study. The calculations used in estimating these errors are based on Topping (1957). The errors given are the maximum errors and thus represent the worst case.

The flow was measured using a bucket of known volume and stop watch. For the same pump configuration and experimental setup, flow rate differs 2.0 % from the mean

value thus an error of 2.0 % is estimated. The tube diameter has an estimated error in measurement of 0.1 mm which was the precision of the digital calipers used for the tube measurements. This gives an error of 1.0 % for 9.67 mm tube, 0.70 % for 13.86 mm tube and 0.5 % for 20.4 mm tube. The maximum errors in the velocity measurement for each tube are obtained as 4.0 %, 2.4 % and 2.0 % respectively. The measurement of mean grain diameter has a largest possible error possible error of 3.5 %. Using these errors, the

error in the densimetric Froude number, $F_0 = \frac{U_0}{\sqrt{g\left(\frac{\rho_s - \rho}{\rho}\right)D}}$, can be calculated estimated

5.6 % for 9.67 mm tube, 4.2 % for 13.86 mm tube and 3.8 % for 20.4 mm tube.

The maximum possible errors in determining tube Reynolds number, R_0 , are 5 % for 9.67 mm tube, 3.1 % for 13.86 mm tube and 2.5 % for 20.4 mm tube. The particle Reynolds number, R_s , is calculated with the maximum errors of 7.5 % for 9.67 tube, 5.9 % for 13.86 mm tube and 5.5 % for 20.4 mm tube.

Therefore, the maximum error the calculated value of theoretical function $\left[\frac{F_0^{3.2} R_s^{0.8}}{(0.25 \tan \phi)^2 R_0} \right]^{1/7}$ can be approximated as: 6.7 % for 9.67 mm tube, 6.9 % for 13.86 mm tube and 4.1 % for 20.4 mm tube.

The tube position was calculated with a Vernier scale having a precision of 0.254 mm. The minimum tube inlet position was 1.27 mm for all the tubes. This gives the maximum percentage of error 20 %. The error in the measurement of the tube inlet height iz_0 estimated as 2.5 %. The same scale was used for determining the heights for critical and general movement, z_c and z_g . The lowest value found for these lengths are 7.62 and 5.53 mm and therefore the maximum percent error of 3.3 % and 4.5 %

respectively. Again the scour depth was measured by a digital point gauge with a precision of 0.01 mm. However due to error in observation this error can be as high as 10 %. This estimation was made by the deviation from the mean value of several readings of the same scour hole depth. Therefore relative maximum scour depth, $\varepsilon_{rm} = \varepsilon - z_0$, has the most probable maximum error of 10 %. The minimum equilibrium scour hole depth at tube inlet level, r_t , is 19.0 mm. The possible maximum error in all the derived and measured quantities is shown in Table 4.11.

4.8 Discussion

The siphon tube diameter has been found to be the best scale for normalizing all the length parameters. The relations obtained from dimensional analysis give reasonably good results for the length parameters when particular sediment is taken into consideration. However, they show quite distinct curves when compared with those obtained for other sediment particles used in different experiments. It appears that besides the densimetric Froude number, F_0 , other sediment characteristics and its behavior in the flow have important effects on the equilibrium scour hole dimensions and the threshold heights. All the length parameters were fitted by power curves with the densimetric Froude number of the particle.

Theoretical analysis was based on comparing the viscous shear stress exerted on the particle at equilibrium and its threshold shear stress. An effort has been made to determine the functional relationship for the equilibrium scour hole radii. It has been found from the analysis that these scour hole radii are related to a dimensionless term that includes the tube Reynolds number; and densimetric Froude number, Reynolds number and dimensionless diameter of the cohesionless sediment particle. Experimental data

from the present study and studies by Mazurek and Rajaratnam (unpublished); and Brahme (1983) were used to validate the theory. Both the dimensionless scour hole radii, ($\frac{r_t}{d}$ and $\frac{r_a}{d}$), well fitted by common straightlines for all the experiments. Again, the function also showed a general relation when the maximum scour hole was fitted with it. It has been noticed that, the flow towards the inlet can be considered as a sink flow if the maximum depth is taken into account. For the scour hole radii, the size of the tube has an incremental effect.

The threshold heights for particle movement showed better relations with the theoretical function. Both $\frac{z_c}{d}$ and $\frac{z_g}{d}$ are fitted with general straightlines, when the data of the present study as well as those of Mazurek and Rajaratnam (unpublished) are plotted together.

The scour hole profiles for all the case were found similar when normalized with the relative maximum scour depth as depth scale and radius of the scour hole at tube level. These profiles were fitted with a common equation for the condition $z_0 = 0$ and $z_0 < 0$. However for the case when $z_0 > 0$ the profile show a slightly different relation. The slope of the scour hole above the tube inlet level for all tests has been found to be almost same which is approximately 35° to 40° above the horizontal direction. The radial distance of the maximum scour hole depth was obtained about $0.26r_t$ from the centerline.

Table 4.1: The maximum relative scour hole depth and scour hole radius at equilibrium for the tube set on or below the bed level (Present Study).

Test No.	Q	d	U_0	z_0	D	T	F_0	R_0	R_s	ϵ_m	ϵ_{m0}/d	r_t	(mm)	r_t/d	$\left[\frac{F_0^{3.2} R_s^{0.8}}{(0.25 \tan \phi)^2 R_0} \right]^{1/7}$
T2/0/0.34	0.051	13.86	0.34	0.00	0.58	21.0	3.47	4747	199	-4.37	0.32	19.00	1.37	1.68	
T3/0/0.53	0.173	20.40	0.53	0.00	0.58	21.0	5.47	11036	314	-6.24	0.31	24.00	1.18	1.93	
T2/0/0.64	0.096	13.86	0.64	0.00	0.58	21.0	6.57	9002	377	-5.82	0.42	20.50	1.48	2.21	
T2/0/0.68	0.102	13.86	0.68	0.00	0.58	17.0	7.00	8700	364	-5.77	0.42	19.00	1.37	2.27	
T2/0/0.68	0.103	13.86	0.68	0.00	0.58	19.5	7.03	9114	381	-6.90	0.50	21.50	1.55	2.27	
T2/0/0.70	0.105	13.86	0.70	0.00	0.58	21.0	7.18	9839	412	-7.81	0.56	22.00	1.59	2.29	
T1/0/0.76	0.249	20.40	0.76	0.00	0.58	22.0	7.87	16286	463	-8.42	0.41	27.00	1.32	2.25	
T2/0/0.80	0.121	13.86	0.80	0.00	0.58	17.0	8.26	10263	429	-6.22	0.45	21.00	1.52	2.44	
T3/0/0.86	0.281	20.40	0.86	0.00	0.58	21.0	8.88	17913	509	-9.35	0.46	27.50	1.35	2.37	
T2/0/1.03	0.155	13.86	1.03	0.00	0.58	17.0	10.60	13176	551	-7.21	0.52	23.50	1.70	2.71	
T2/0/1.14	0.172	13.86	1.14	0.00	0.58	17.0	11.74	14598	611	-7.74	0.56	24.00	1.73	2.84	
T2/0/1.15	0.174	13.86	1.15	0.00	0.58	21.0	11.92	16335	684	-7.19	0.52	24.00	1.73	2.85	
T2/0/1.20	0.181	13.86	1.20	0.00	0.58	19.5	12.36	16028	671	-8.55	0.62	25.50	1.84	2.90	
T2/0/1.30	0.196	13.86	1.30	0.00	0.58	21.0	13.42	18390	770	-8.01	0.58	23.50	1.70	2.99	
T2/0/1.34	0.203	13.86	1.34	0.00	0.58	19.5	13.88	18000	753	-9.71	0.70	26.50	1.91	3.04	
T2/0/1.54	0.232	13.86	1.54	0.00	0.58	21.0	15.87	21739	910	-10.56	0.76	26.50	1.91	3.22	
T2/0/1.55	0.234	13.86	1.55	0.00	0.58	23.0	16.04	23027	964	-8.19	0.59	24.50	1.77	3.23	
T2/0/1.63	0.246	13.86	1.63	0.00	0.58	7.4	16.85	16164	676	-10.53	0.76	26.50	1.91	3.34	
T2/0/1.78	0.268	13.86	1.78	0.00	0.58	22.0	18.33	25777	1079	-10.10	0.73	27.00	1.95	3.42	
T2/0/1.80	0.287	13.86	1.90	0.00	0.58	19.5	19.61	25441	1065	-10.32	0.74	28.50	2.06	3.53	
T3/0/1.95	0.142	9.65	1.95	0.00	0.58	21.0	20.11	19184	1153	-7.68	0.80	19.50	2.02	3.75	
T2/0/1.95	0.294	13.86	1.95	0.00	0.58	19.0	20.12	26936	1127	-10.88	0.79	31.00	2.24	3.56	
T2/0/1.95	0.294	13.86	1.95	0.00	0.58	19.5	20.12	26104	1092	-10.38	0.75	29.00	2.09	3.57	
T2/0/2.00	0.301	13.86	2.00	0.00	0.58	7.5	20.62	19776	828	-10.45	0.75	30.50	2.20	3.64	
T2/0/2.18	0.329	13.86	2.18	0.00	0.58	22.0	22.54	31688	1326	-10.46	0.75	29.50	2.13	3.74	
T2/0/2.33	0.352	13.86	2.33	0.00	0.58	20.0	24.05	32194	1347	-10.93	0.79	30.50	2.20	3.85	
T1/0/2.53	0.185	9.65	2.53	0.00	0.58	22.0	26.13	25579	1537	-7.75	0.80	23.00	2.38	4.19	
T1/0/2.78	0.203	9.65	2.78	0.00	0.58	21.0	28.65	27331	1643	-8.09	0.84	22.50	2.33	4.37	
T1/0/2.87	0.210	9.65	2.87	0.00	0.58	21.0	29.64	28276	1700	-8.39	0.87	23.00	2.38	4.43	
T1/0/3.21	0.235	9.65	3.21	0.00	0.58	19.0	33.15	30897	1857	-9.09	0.94	25.50	2.64	4.65	
T1/0/3.48	0.254	9.65	3.48	0.00	0.58	19.0	35.92	33474	2012	-9.83	1.02	27.00	2.80	4.81	
T1/0/3.68	0.269	9.65	3.68	0.00	0.58	21.0	37.95	36199	2176	-10.16	1.05	25.50	2.64	4.92	
T1/0/3.87	0.283	9.65	3.87	0.00	0.58	18.0	39.95	35396	2127	-10.69	1.11	29.00	3.01	5.04	
T1/0/4.01	0.293	9.65	4.01	0.00	0.58	18.0	41.36	36647	2203	-10.48	1.09	27.50	2.85	5.12	

Table 4.1: cont'd...

Test No.	Q	d	U ₀	z ₀	D	T	F ₀	R ₀	R _t	ε _m	ε _{m/d}	r _t	(mm)	r _{t/d}	$\left[\frac{F_0}{(0.25 \tan \phi)^2 R_0} \right]^{1/7}$
T1/0/4.24	0.310	9.65	4.24	0.00	0.58	22.0	43.74	42811	2573	-9.78	1.01	27.50	2.85	5.23	
T1/0/5.34	0.391	9.65	5.34	0.00	0.58	20.0	55.13	51578	3088	-11.92	1.23	30.50	3.16	5.78	
T1/0/5.48	0.401	9.65	5.48	0.00	0.58	21.0	56.59	53979	3244	-11.28	1.17	30.00	3.11	5.84	
T1/0/5.560	0.410	9.65	5.60	0.00	0.58	18.0	57.84	51252	3080	-11.36	1.18	30.00	3.11	5.91	
T1/0/5.72	0.418	9.65	5.72	0.00	0.58	22.0	59.02	57776	3473	-12.05	1.25	32.50	3.37	5.95	
T1/0/5.96	0.436	9.65	5.96	0.00	0.58	21.0	61.53	58690	3527	-11.41	1.18	31.50	3.26	6.06	
T1/0/6.21	0.454	9.65	6.21	0.00	0.58	21.0	64.14	61181	3677	-11.54	1.20	30.50	3.16	6.17	
T3/-1.27/0.77	0.251	20.40	0.77	-12.70	0.58	21.0	7.91	15960	454	-21.21	0.42	27.17	1.33	2.26	
T2/-1.27/1.12	0.169	13.86	1.12	-12.70	0.58	16.0	11.53	13947	584	-20.24	0.54	22.99	1.66	2.82	
T2/-1.27/1.19	0.180	13.86	1.19	-12.70	0.58	16.0	12.30	14877	623	-20.99	0.60	25.26	1.82	2.90	
T2/-1.27/1.20	0.181	13.86	1.20	-12.70	0.58	16.0	12.40	14994	627	-21.69	0.65	25.55	1.84	2.90	
T2/-1.27/1.25	0.189	13.86	1.25	-12.70	0.58	17.0	12.92	16058	672	-21.24	0.62	23.90	1.72	2.95	
T2/-1.27/1.45	0.218	13.86	1.45	-12.70	0.58	20.0	14.94	19993	837	-22.17	0.68	25.62	1.85	3.14	
T2/-1.27/1.84	0.277	13.86	1.84	-12.70	0.58	21.0	18.96	25980	1087	-24.24	0.83	29.39	2.12	3.47	
T1/-1.27/1.88	0.137	9.65	1.88	-12.70	0.58	21.0	19.38	18483	1111	-19.45	0.70	19.50	2.02	3.69	
T2/-1.27/2.11	0.318	13.86	2.11	-12.70	0.58	16.0	21.78	26340	1102	-23.98	0.81	28.25	2.04	3.70	
T2/-1.27/2.42	0.365	13.86	2.42	-12.70	0.58	22.0	24.95	35082	1468	-25.23	0.90	32.04	2.31	3.90	
T1/-1.27/2.55	0.187	9.65	2.55	-12.70	0.58	22.0	26.33	25775	1549	-20.46	0.80	21.03	2.18	4.21	
T1/-1.27/2.94	0.215	9.65	2.94	-12.70	0.58	21.0	30.40	28995	1743	-21.54	0.92	22.24	2.30	4.48	
T1/-1.27/3.12	0.228	9.65	3.12	-12.70	0.58	18.0	32.21	28545	1716	-21.22	0.88	22.33	2.31	4.60	
T1/-1.27/3.53	0.258	9.65	3.53	-12.70	0.58	20.0	36.48	34002	2044	-22.40	1.00	26.17	2.71	4.84	
T1/-1.27/3.86	0.283	9.65	3.86	-12.70	0.58	20.0	39.89	37176	2234	-22.65	1.03	27.16	2.81	5.03	
T1/-1.27/5.85	0.428	9.65	5.85	-12.70	0.58	20.0	60.35	56252	3381	-24.84	1.26	32.76	3.39	6.01	
T3/-2.54/0.53	0.173	20.40	0.53	-12.70	0.58	21.0	5.47	11026	313	-19.26	0.32	21.58	1.06	1.93	
T3/-2.54/0.53	0.175	20.40	0.53	-25.40	0.58	21.0	5.51	11117	316	-33.58	0.40	25.19	1.24	1.94	
T3/-2.54/0.77	0.250	20.40	0.77	-25.40	0.58	21.0	7.91	15948	453	-34.93	0.47	29.56	1.45	2.26	
T2/-2.54/0.97	0.147	13.86	0.97	-25.40	0.58	18.0	10.04	12784	535	-33.09	0.55	21.84	1.58	2.65	
T2/-2.54/1.13	0.170	13.86	1.13	-25.40	0.58	17.0	11.66	14491	606	-32.87	0.54	23.22	1.68	2.83	
T2/-2.54/1.38	0.208	13.86	1.38	-25.40	0.58	16.0	14.22	17202	720	-33.64	0.59	25.04	1.81	3.08	
T2/-2.54/1.46	0.221	13.86	1.46	-25.40	0.58	20.0	15.10	20208	846	-34.97	0.69	27.10	1.96	3.15	
T2/-2.54/1.84	0.278	13.86	1.84	-25.40	0.58	21.0	19.03	26077	1091	-35.59	0.74	28.99	2.03	3.48	
T2/-2.54/2.09	0.315	13.86	2.09	-25.40	0.58	20.0	21.53	28825	1206	-36.43	0.80	29.78	2.15	3.67	
T2/-2.54/2.42	0.366	13.86	2.42	-25.40	0.58	22.0	25.02	35181	1472	-37.64	0.88	32.86	2.37	3.91	
T1/-2.54/2.57	0.188	9.65	2.57	-25.40	0.58	22.0	26.48	25925	1558	-33.10	0.80	22.39	2.32	4.22	
T1/-2.54/2.84	0.208	9.65	2.84	-25.40	0.58	21.0	29.30	27949	1680	-34.03	0.89	24.97	2.59	4.41	

Table 4.1: cont'd...

Test No.	Q	d	U ₀	z ₀	D	T	F ₀	R ₀	R _t	ε _m	ε _{mt/d}	r _t	(mm)	r _{t/d}	$\left[\frac{F_0^{3.2} R_s^{0.8}}{(0.25 \tan \varphi)^2 R_0} \right]^{1/7}$
T1/-2.54/3.14	0.230	9.65	3.14	-25.40	0.58	18.0	32.43	28738	1727	-32.72	0.76	21.79	2.26	4.61	4.81
T1/-2.54/3.47	0.254	9.65	3.47	-25.40	0.58	19.0	35.86	33419	2009	-36.12	1.11	28.70	2.97	5.02	5.23
T1/-2.54/3.82	0.279	9.65	3.82	-25.40	0.58	18.0	39.42	34934	2100	-35.86	1.08	25.33	2.63	5.23	5.34
T1/-2.54/4.22	0.309	9.65	4.22	-25.40	0.58	20.0	43.59	40627	2442	-34.57	0.95	28.04	2.91	5.34	5.43
T1/-2.54/4.42	0.323	9.65	4.42	-25.40	0.58	18.0	45.64	40444	2431	-37.97	1.30	32.69	3.39	5.43	5.51
T1/-2.54/4.61	0.337	9.65	4.61	-25.40	0.58	18.0	47.55	42129	2532	-37.25	1.23	31.37	3.25	5.51	5.72
T1/-2.54/4.77	0.349	9.65	4.77	-25.40	0.58	20.0	49.25	45905	2759	-36.87	1.19	30.87	3.20	5.72	5.89
T1/-2.54/5.23	0.383	9.65	5.23	-25.40	0.58	22.0	54.00	52863	3177	-36.86	1.19	31.56	3.27	5.89	5.99
T1/-2.54/5.59	0.409	9.65	5.59	-25.40	0.58	21.0	57.73	55067	3310	-36.46	1.15	32.25	3.34	5.99	6.14
T3/-3.81/0.53	0.174	20.40	0.53	-38.10	0.58	22.0	5.50	11383	324	-46.48	0.41	27.28	1.34	1.93	2.27
T3/-3.81/0.77	0.252	20.40	0.77	-38.10	0.58	21.0	7.97	16065	457	-47.51	0.46	28.89	1.42	2.67	2.86
T2/-3.81/0.99	0.149	13.86	0.99	-38.10	0.58	18.0	10.17	12946	542	-45.86	0.56	22.27	1.61	2.67	2.86
T2/-3.81/1.16	0.175	13.86	1.16	-38.10	0.58	19.0	11.99	16056	672	-45.98	0.57	24.64	1.78	2.90	3.06
T2/-3.81/1.19	0.180	13.86	1.19	-38.10	0.58	17.0	12.32	15319	641	-46.72	0.62	26.04	1.88	2.90	3.06
T2/-3.81/1.35	0.204	13.86	1.35	-38.10	0.58	16.0	13.97	16901	707	-47.31	0.66	26.87	1.94	3.06	3.27
T2/-3.81/1.38	0.209	13.86	1.38	-38.10	0.58	20.0	14.27	19102	799	-46.75	0.62	25.90	1.87	3.08	3.27
T2/-3.81/1.84	0.278	13.86	1.84	-38.10	0.58	21.0	19.00	26036	1090	-48.82	0.77	29.81	2.15	3.48	3.65
T2/-3.81/2.06	0.311	13.86	2.06	-38.10	0.58	20.0	21.29	28495	1192	-49.49	0.82	31.14	2.25	3.48	3.65
T2/-3.81/2.33	0.352	13.86	2.33	-38.10	0.58	22.0	24.09	33864	1417	-49.15	0.80	31.57	2.28	3.48	3.65
T1/-3.81/2.61	0.191	9.65	2.61	-38.10	0.58	20.0	26.97	25137	1511	-47.40	0.96	24.88	2.58	4.26	4.60
T1/-3.81/3.12	0.228	9.65	3.12	-38.10	0.58	18.0	32.21	28536	1715	-46.25	0.84	23.94	2.48	4.26	4.60
T1/-3.81/3.59	0.263	9.65	3.59	-38.10	0.58	22.0	37.11	36324	2183	-49.21	1.15	27.52	2.85	4.87	5.02
T1/-3.81/3.79	0.277	9.65	3.79	-38.10	0.58	20.0	39.16	36302	2194	-48.26	1.05	27.32	2.83	4.99	5.14
T3/-5.08/0.54	0.176	20.40	0.54	-50.80	0.58	22.0	5.56	11513	327	-58.69	0.39	26.86	1.32	1.94	2.27
T3/-5.08/0.78	0.253	20.40	0.77	-50.80	0.58	21.0	7.98	16091	457	-59.17	0.41	28.19	1.38	2.27	2.53
T2/-5.08/1.17	0.176	13.86	1.17	-50.80	0.58	17.0	12.05	14980	627	-60.26	0.68	26.61	1.92	2.87	3.08
T2/-5.08/1.22	0.184	13.86	1.22	-50.80	0.58	19.0	12.56	16814	704	-56.64	0.42	21.19	1.53	2.91	3.48
T2/-5.08/1.31	0.197	13.86	1.31	-50.80	0.58	19.0	13.51	18083	757	-60.06	0.67	27.11	1.96	3.01	3.55
T2/-5.08/1.32	0.199	13.86	1.32	-50.80	0.58	17.0	13.64	16953	709	-61.20	0.75	27.60	1.99	3.02	3.55
T2/-5.08/1.39	0.210	13.86	1.39	-50.80	0.58	19.0	14.36	19222	804	-60.02	0.67	26.76	1.93	3.08	3.55
T2/-5.08/1.85	0.280	13.86	1.85	-50.80	0.58	22.0	19.13	26689	1125	-61.25	0.75	29.69	2.14	3.48	3.88
T2/-5.08/2.21	0.333	13.86	2.21	-50.80	0.58	22.0	22.79	32040	1341	-62.14	0.82	32.32	2.33	3.75	4.23
T2/-5.08/2.39	0.360	13.86	2.39	-50.80	0.58	22.0	24.63	34628	1449	-63.40	0.91	35.07	2.53	3.88	4.23
T1/-5.08/2.58	0.188	9.65	2.58	-50.80	0.58	20.0	26.60	24789	1490	-59.31	0.88	24.33	2.52	2.59	3.02
T1/-5.08/3.12	0.228	9.65	3.12	-50.80	0.58	17.0	32.20	27870	1675	-60.06	0.96	25.02	2.59	4.60	5.02

Table 4.1: cont'd...

Test No.	Q	d	U ₀	z ₀	D	T	F ₀	R ₀	R _t	ε _m	ε _{m/d}	r _t	(mm)	r _{t/d}	$\left[\frac{F_0}{(0.25 \tan \varphi)^2} R_s \right]^{1/7}$
T1/-5.08/3.58	0.262	9.65	3.58	-50.80	0.58	17.0	36.92	31960	1921	-59.50	0.90	25.00	2.59	4.88	
T1/-5.08/3.94	0.288	9.65	3.94	-50.80	0.58	21.0	40.63	38754	2329	-61.43	1.10	27.19	2.82	5.07	
T1/-5.08/4.27	0.312	9.65	4.27	-50.80	0.58	22.0	44.09	43158	2394	-61.04	1.06	28.93	3.00	5.25	
T1/-5.08/4.35	0.318	9.65	4.35	-50.80	0.58	18.0	44.88	39766	2390	-61.74	1.13	30.69	3.18	5.30	
T1/-5.08/4.71	0.344	9.65	4.71	-50.80	0.58	18.0	48.60	43064	2588	-62.07	1.17	31.01	3.21	5.49	
T1/-5.08/5.49	0.402	9.65	5.49	-50.80	0.58	21.0	56.69	54073	3250	-62.91	1.25	31.69	3.28	5.85	
T1/-5.08/6.40	0.468	9.65	6.40	-50.80	0.58	22.0	66.06	64663	3887	-62.28	1.19	31.95	3.31	6.24	
T3/-6.35/0.54	0.175	20.40	0.54	-63.50	0.58	15.0	5.53	9587	273	-71.12	0.37	25.92	1.27	1.95	
T3/-6.35/0.77	0.250	20.40	0.77	-63.50	0.58	21.0	7.90	15927	453	-71.50	0.39	27.85	1.37	2.26	
T2/-6.35/1.89	0.286	13.86	1.89	-63.50	0.58	22.0	19.56	27501	1151	-73.50	0.72	29.40	2.12	3.52	
T2/-6.35/2.14	0.323	13.86	2.14	-63.50	0.58	21.0	22.11	30297	1268	-74.94	0.83	31.44	2.27	3.71	
T2/-6.35/2.36	0.356	13.86	2.36	-63.50	0.58	22.0	24.34	34223	1432	-75.29	0.85	32.14	2.32	3.86	
T1/-6.35/2.50	0.183	9.65	2.50	-63.50	0.58	22.0	25.80	25259	1518	-73.17	1.00	25.75	2.67	4.17	
T1/-6.35/3.12	0.228	9.65	3.12	-63.50	0.58	18.0	32.21	28539	1715	-71.53	0.83	25.72	2.67	4.60	
T1/-6.35/3.58	0.262	9.65	3.58	-63.50	0.58	17.0	36.94	31978	1922	-72.72	0.95	26.68	2.76	4.88	
T1/-6.35/3.98	0.291	9.65	3.98	-63.50	0.58	22.0	41.09	40224	2418	-75.01	1.19	29.56	3.06	5.09	
T3/-7.62/0.53	0.174	20.40	0.53	-76.20	0.58	15.0	5.50	9535	271	-84.32	0.40	25.42	1.25	1.94	
T3/-7.62/0.77	0.252	20.40	0.77	-76.20	0.58	21.0	7.97	16077	457	-84.95	0.43	28.84	1.41	2.27	
T2/-7.62/1.13	0.171	13.86	1.13	-76.20	0.58	15.0	11.70	13785	577	-85.94	0.70	26.90	1.94	2.84	
T2/-7.62/2.14	0.323	13.86	2.14	-76.20	0.58	21.0	22.13	30319	1269	-90.31	1.02	33.99	2.45	3.71	
T1/-7.62/2.50	0.183	9.65	2.50	-76.20	0.58	22.0	25.82	25271	1519	-83.46	0.75	21.43	2.22	4.17	
T1/-7.62/3.11	0.227	9.65	3.11	-76.20	0.58	18.0	32.10	28444	1710	-84.40	0.85	25.39	2.63	4.59	
T1/-7.62/5.44	0.398	9.65	5.44	-76.20	0.58	20.0	56.19	52372	3148	-89.66	1.40	34.03	3.53	5.83	
T1/-7.62/5.60	0.409	9.65	5.60	-76.20	0.58	20.0	57.76	53833	3236	-89.03	1.33	33.72	3.49	5.90	
T2/-10.16/1.89	0.285	13.86	1.89	-101.60	0.58	22.0	19.50	27416	1147	-111.10	0.69	26.77	1.93	3.51	

Code for Test No.: Tube used (T1 = 9.65 mm, T2 = 13.86 mm and T3 = 20.40 mm tube)/ inlet height above the bed (mm)/Velocity of fluid in the tube (m/s).

Table 4.2: The maximum relative scour hole depth and scour hole radius at equilibrium for the tube set above the bed level (Present Study).

Test No.	Q (L/s)	d (mm)	U ₀ (m/s)	Z ₀ (mm)	D (mm)	T (°C)	F ₀ (mm)	R ₀ (mm)	R _s (mm)	ε _m (mm)	ε _{rm/d} (mm)	r ₀ (mm)	ψ (rad)	r _a (mm)	r _{s/d} [$\frac{F_0^{3.2} R_s^{0.8}}{(0.25 \tan \phi)^2 R_0}$] ^{1/7}	$\left[\frac{F_0^{3.2} R_s^{0.8} \sin^3 \psi}{(0.25 \tan \phi)^2 R_0} \right]^{1/7}$	
T2/6.35/2.0	0.310	13.86	2.06	6.35	0.58	20	21.23	28420	1189	-4.51	0.78	22.5	1.53	23.4	1.69	3.65	3.59
T2/6.35/1.4	0.223	13.86	1.48	6.35	0.58	21	15.25	20895	874	-4.66	0.79	22.5	1.53	23.4	1.69	3.16	3.11
T2/6.35/1.5	0.235	13.86	1.56	6.35	0.58	21	16.10	22058	923	-3.60	0.72	20.0	1.52	21.0	1.51	3.24	3.17
T2/6.35/1.1	0.168	13.86	1.12	6.35	0.58	21	11.51	15771	660	-1.43	0.56	15.5	1.51	16.8	1.21	2.80	2.71
T1/5.08/6.4	0.461	9.65	6.31	5.08	0.58	20	65.12	60698	3648	-7.12	1.26	27.0	1.53	27.5	2.85	6.21	6.16
T1/5.08/5.6	0.408	9.65	5.58	5.08	0.58	20	57.64	53720	3229	-6.89	1.24	25.0	1.53	25.5	2.64	5.89	5.84
T2/5.08/1.9	0.287	13.86	1.90	5.08	0.58	20	19.61	26253	1099	-6.77	0.85	27.0	1.53	27.5	1.98	3.53	3.50
T2/5.08/1.9	0.291	13.86	1.93	5.08	0.58	20	19.90	26636	1115	-6.29	0.82	25.5	1.53	26.0	1.88	3.55	3.52
T1/5.08/5.3	0.382	9.65	5.22	5.08	0.58	20	53.90	50234	3019	-5.98	1.15	25.5	1.53	26.0	2.69	5.73	5.68
T2/5.08/1.9	0.287	13.86	1.91	5.08	0.58	20	19.67	26325	1102	-5.66	0.77	26.5	1.53	27.0	1.95	3.53	3.50
T2/5.08/1.9	0.290	13.86	1.92	5.08	0.58	20	19.82	26536	1110	-5.32	0.75	25.0	1.53	25.5	1.84	3.54	3.51
T2/5.08/1.5	0.230	13.86	1.52	5.08	0.58	20	15.73	21057	881	-3.64	0.63	19.5	1.52	20.2	1.45	3.21	3.16
T2/5.08/0.9	0.141	13.86	0.94	5.08	0.58	20	9.66	12926	541	-3.25	0.60	20.0	1.52	20.6	1.49	2.60	2.57
T2/5.08/1.3	0.204	13.86	1.35	5.08	0.58	20	13.97	18703	783	-2.82	0.57	21.5	1.52	22.1	1.59	3.05	3.01
T2/5.08/1.1	0.170	13.86	1.13	5.08	0.58	20	11.66	15603	653	-2.74	0.56	18.5	1.52	19.2	1.38	2.82	2.78
T2/5.08/1.3	0.209	13.86	1.38	5.08	0.58	20	14.27	19098	799	-2.41	0.54	20.5	1.52	21.1	1.52	3.08	3.04
T2/3.81/1.7	0.267	13.86	1.77	3.81	0.58	19	18.29	24489	1025	-6.63	0.75	24.5	1.53	24.8	1.79	3.42	3.40
T2/3.81/1.6	0.243	13.86	1.61	3.81	0.58	18	16.65	21188	887	-5.28	0.66	21.0	1.52	21.3	1.54	3.29	3.27
T2/3.81/1.0	0.162	13.86	1.07	3.81	0.58	18	11.07	14092	590	-4.88	0.63	19.0	1.52	19.4	1.40	2.76	2.74
T2/3.81/1.2	0.187	13.86	1.24	3.81	0.58	18	12.81	16308	682	-3.63	0.54	20.0	1.52	20.4	1.47	2.94	2.92
T2/3.81/0.9	0.135	13.86	0.90	3.81	0.58	18	9.25	11766	492	-3.39	0.52	19.5	1.52	19.9	1.43	2.56	2.54
T2/3.05/1.8	0.284	13.86	1.88	3.05	0.58	20	19.41	25986	1087	-5.95	0.65	22.0	1.53	22.2	1.60	3.51	3.50
T2/3.05/1.8	0.284	13.86	1.88	3.05	0.58	19	19.41	25986	1087	-5.83	0.64	23.0	1.53	23.2	1.67	3.51	3.50
T2/3.05/1.8	0.283	13.86	1.88	3.05	0.58	20	19.36	25919	1085	-5.83	0.64	24.5	1.53	24.7	1.78	3.51	3.49
T1/2.54/5.6	0.403	9.65	5.50	2.54	0.58	21	56.82	54196	3257	-9.36	1.23	29.0	1.54	29.1	3.02	5.85	5.84
T1/2.54/6.4	0.463	9.65	6.33	2.54	0.58	21	65.29	62284	3743	-8.96	1.19	29.0	1.54	29.1	3.02	6.21	6.20
T1/2.54/5.2	0.379	9.65	5.18	2.54	0.58	19	53.47	49839	2996	-8.66	1.16	28.0	1.54	28.1	2.91	5.71	5.70
T2/2.54/2.0	0.307	13.86	2.04	2.54	0.58	15	21.01	24742	1035	-8.09	0.77	27.0	1.53	27.1	1.96	3.64	3.64
T2/2.54/2.0	0.303	13.86	2.01	2.54	0.58	20	20.72	27731	1160	-7.86	0.75	26.5	1.53	26.6	1.92	3.61	3.60

Table 4.2: cont'd...

Test No.	Q	d	U ₀	z ₀	D	F ₀	T	R ₀	R _s	ε_m	$\varepsilon_{m/d}$	r ₀	ψ	r _{a/d}	$\left[\frac{F_0^{3.2} R_s^{0.8}}{(0.25 \tan \varphi)^2 R_0} \right]^{1/7}$		
	(L/s)	(mm)	(m/s)	(mm)	(mm)	(°C)				(mm)	(mm)	(rad)	(mm)				
T2/2.54/1.5	0.238	13.86	1.58	2.54	0.58	17	16.32	20286	849	-7.08	0.69	24.0	1.53	24.1	1.74	3.27	3.26
T2/2.54/1.3	0.200	13.86	1.32	2.54	0.58	21	13.65	18707	783	-6.68	0.67	22.5	1.53	22.6	1.63	3.02	3.01
T2/2.54/1.1	0.176	13.86	1.16	2.54	0.58	20	12.01	16079	673	-6.56	0.66	22.0	1.53	22.1	1.60	2.86	2.85
T2/2.54/1.3	0.210	13.86	1.39	2.54	0.58	20	14.39	19257	806	-6.40	0.65	23.0	1.53	23.1	1.67	3.09	3.08
T1/2.54/3.6	0.265	9.65	3.62	2.54	0.58	20	37.34	34800	2092	-6.25	0.91	24.0	1.53	24.1	2.50	4.89	4.88
T2/2.54/1.1	0.173	13.86	1.15	2.54	0.58	20	11.87	15884	665	-5.78	0.60	23.5	1.53	23.6	1.71	2.84	2.84
T2/2.54/1.0	0.154	13.86	1.02	2.54	0.58	22	10.56	14841	621	-5.03	0.55	20.5	1.52	20.7	1.49	2.70	2.69
T2/2.54/0.8	0.123	13.86	0.81	2.54	0.58	22	8.40	11810	494	-4.31	0.49	20.0	1.52	20.2	1.45	2.45	2.44
T2/2.54/2.0	0.307	13.86	2.04	1.27	0.58	17	21.01	26117	1093	-10.19	0.83	29.0	1.54	29.0	2.09	3.64	3.64
T1/1.27/3.7	0.266	9.65	3.64	1.27	0.58	21	37.53	35796	2151	-8.51	1.01	24.0	1.53	24.0	2.49	4.90	4.90
T2/1.27/2.0	0.307	13.86	2.03	1.27	0.58	21	21.00	28778	1204	-8.28	0.69	26.0	1.53	26.0	1.88	3.63	3.63
T2/1.27/1.4	0.226	13.86	1.49	1.27	0.58	21	15.43	21139	885	-8.08	0.67	25.5	1.53	25.5	1.84	3.18	3.18
T2/1.27/1.4	0.216	13.86	1.43	1.27	0.58	20	14.77	19766	827	-7.28	0.62	24.0	1.53	24.0	1.73	3.12	3.12
T2/1.27/1.2	0.187	13.86	1.24	1.27	0.58	20	12.82	17156	718	-6.68	0.57	22.0	1.53	22.0	1.59	2.94	2.94
T2/1.27/1.1	0.174	13.86	1.15	1.27	0.58	20	11.89	15921	666	-7.13	0.61	23.5	1.53	23.5	1.70	2.85	2.84
T2/1.27/1.0	0.160	13.86	1.06	1.27	0.58	20	10.92	14624	612	-6.57	0.57	24.0	1.53	24.0	1.73	2.74	2.74

Table 4.3: Height for critical movement (Present Study).

Test No.	Q	U_0	d	D	T	F_0	R_0	R_s	z_c	z_c/d	$\left[\frac{F_0^{3/2} R_s}{(0.25 \tan \phi)^2 R_0} \right]^{1/7}$
T2/1.81	0.273	1.81	13.86	0.58	7.5	18.7	17924	750	11.94	0.86	3.49
T2/1.01	0.152	1.01	13.86	0.58	19.5	10.4	13463	563	9.40	0.68	2.69
T2/1.18	0.178	1.18	13.86	0.58	20.0	12.2	16274	681	8.64	0.62	2.87
T2/0.70	0.106	0.70	13.86	0.58	20.0	7.2	9695	406	9.14	0.66	2.30
T2/1.52	0.230	1.52	13.86	0.58	20.0	15.7	21052	881	11.18	0.81	3.21
T2/1.80	0.271	1.80	13.86	0.58	15.0	18.6	21877	915	11.18	0.81	3.46
T2/1.62	0.245	1.62	13.86	0.58	15.0	16.8	19747	826	9.65	0.70	3.31
T2/1.35	0.204	1.35	13.86	0.58	15.0	14.0	16443	688	10.92	0.79	3.06
T2/1.13	0.170	1.13	13.86	0.58	15.0	11.7	13735	575	10.16	0.73	2.83
T2/1.09	0.165	1.09	13.86	0.58	16.0	11.3	13643	571	10.92	0.79	2.79
T2/0.95	0.143	0.95	13.86	0.58	16.0	9.8	11863	496	8.38	0.60	2.63
T2/0.73	0.110	0.73	13.86	0.58	16.0	7.5	9090	380	8.13	0.59	2.34
T2/0.79	0.119	0.79	13.86	0.58	16.0	8.1	9811	411	8.64	0.62	2.42
T2/0.48	0.072	0.48	13.86	0.58	16.0	4.9	5987	251	7.62	0.55	1.96
T1/3.47	0.254	3.47	9.65	0.58	12.0	35.9	27034	1625	11.94	1.24	4.84
T1/3.13	0.229	3.13	9.65	0.58	12.0	32.3	24354	1464	11.18	1.16	4.63
T1/3.62	0.265	3.62	9.65	0.58	12.0	37.3	28155	1692	11.68	1.21	4.92
T1/2.24	0.164	2.24	9.65	0.58	15.0	23.1	18978	1141	10.16	1.05	4.00
T1/2.82	0.206	2.82	9.65	0.58	13.0	29.1	22698	1364	10.67	1.11	4.42
T1/2.09	0.153	2.09	9.65	0.58	21.0	21.5	20552	1235	8.38	0.87	3.86
T1/2.73	0.200	2.73	9.65	0.58	21.0	28.2	26898	1617	9.65	1.00	4.34
T1/4.73	0.340	4.73	9.57	0.58	20.0	48.9	45159	2737	15.24	1.59	5.50
T1/5.66	0.407	5.66	9.57	0.58	21.0	58.4	55246	3348	13.72	1.43	5.93
T1/6.16	0.443	6.16	9.57	0.58	21.0	63.6	60128	3644	16.76	1.75	6.15
T1/5.15	0.371	5.15	9.57	0.58	20.0	53.2	43256	2622	13.97	1.46	5.72
T1/5.97	0.429	5.97	9.57	0.58	20.0	61.6	50093	3036	12.70	1.33	6.09

Code for Test No. : Tube used (T1 = 9.65 mm, T2 = 13.86 mm and T3 = 20.40 mm tube) / Velocity of fluid in the tube (m/s).

Table 4.4: Height for general movement (Present Study).

Test No.	Q	U_0	d	D	T	F_0	R_0	R_s	z_g	z_g/d	$\left[\frac{F_0^{3/2} R_s^{0.8}}{(0.25 \tan \phi)^2 R_0} \right]^{1/7}$
	(L/s)	(m/s)	(mm)	(mm)	(°C)				(mm)		
T2/1.83	0.276	1.83	13.86	0.58	7.5	18.9	18125	758	11.18	0.81	3.50
T2/1.01	0.152	1.01	13.86	0.58	19.5	10.4	13524	566	8.64	0.62	2.69
T2/1.14	0.172	1.14	13.86	0.58	20.0	11.8	15740	659	8.13	0.59	2.83
T2/0.70	0.106	0.70	13.86	0.58	20.0	7.2	9695	406	5.84	0.42	2.30
T2/1.53	0.231	1.53	13.86	0.58	20.0	15.8	21186	887	10.92	0.79	3.22
T2/1.78	0.269	1.78	13.86	0.58	20.0	18.4	21685	907	10.67	0.77	3.44
T2/1.63	0.245	1.63	13.86	0.58	20.0	16.8	19781	828	10.16	0.73	3.31
T2/1.30	0.196	1.30	13.86	0.58	20.0	13.4	15762	660	9.40	0.68	3.00
T2/1.14	0.172	1.14	13.86	0.58	20.0	11.8	13872	581	9.14	0.66	2.84
T2/1.10	0.166	1.10	13.86	0.58	20.0	11.4	13747	575	8.89	0.64	2.80
T2/0.92	0.139	0.92	13.86	0.58	15.0	9.5	11511	482	7.37	0.53	2.59
T2/0.73	0.110	0.73	13.86	0.58	16.0	7.5	9082	380	7.62	0.55	2.34
T2/0.76	0.115	0.76	13.86	0.58	16.0	7.9	9519	398	7.11	0.51	2.39
T2/0.47	0.072	0.47	13.86	0.58	16.0	4.9	5929	248	5.33	0.38	1.95
T1/3.47	0.254	3.47	9.65	0.58	12.0	35.9	27034	1625	11.18	1.16	4.84
T1/3.13	0.229	3.13	9.65	0.58	12.0	32.3	24354	1464	10.67	1.11	4.63
T1/3.62	0.265	3.62	9.65	0.58	12.0	37.3	28155	1692	10.60	1.10	4.92
T1/2.24	0.164	2.24	9.65	0.58	15.0	23.1	18978	1141	9.40	0.97	4.00
T1/2.82	0.206	2.82	9.65	0.58	13.0	29.1	22698	1364	8.93	0.93	4.42
T1/2.09	0.153	2.09	9.65	0.58	21.0	21.5	20552	1235	7.11	0.74	3.86
T1/2.73	0.200	2.73	9.65	0.58	21.0	28.2	26898	1617	8.38	0.87	4.34
T1/4.73	0.340	4.73	9.57	0.58	20.0	48.9	45159	2737	10.69	1.12	5.50
T1/5.66	0.407	5.66	9.57	0.58	21.0	58.4	55246	3348	12.70	1.33	5.93
T1/6.16	0.443	6.16	9.57	0.58	21.0	63.6	60128	3644	13.21	1.38	6.15
T1/5.15	0.371	5.15	9.57	0.58	20.0	53.2	43256	2622	11.18	1.17	5.72
T1/5.97	0.429	5.97	9.57	0.58	20.0	61.6	50093	3036	12.19	1.27	6.09

Table 4.5 : The maximum relative scour hole depth and the scour hole radius at equilibrium for the tube set on or below the bed of fine sand from Mazurek and Rajaratnam (unpublished).

Test No.	Q (L/s)	d (mm)	U ₀ (m/s)	z ₀ (mm)	D ₅₀ (mm)	T (°C)	F ₀	R ₀	R _s	ε _{rm} (mm)	ε _{rm/d}	r _t (mm)	r _{t,d} $\left[\frac{F_0^{3/2} R_s^{0.8}}{(0.25 \tan \phi)^2 R_0} \right]^{1/7}$
1	0.092	13.51	0.64	0.0	0.17	7.5	12.28	6159	78	7.3	0.54	2.1	1.57
2	0.184	13.51	1.29	0.0	0.17	8.5	24.53	12675	159	9.4	0.70	2.9	2.15
3	0.276	13.51	1.93	0.0	0.17	8.5	36.77	19002	239	11.0	0.81	3.1	2.31
4	0.316	13.51	2.20	0.0	0.17	10.5	42.02	23059	290	12.3	0.91	3.4	2.52
5	0.092	13.51	0.64	-30.5	0.17	10.5	12.28	6741	85	7.3	0.54	2.3	1.67
6	0.184	13.51	1.29	-30.5	0.17	7.5	24.53	12298	155	8.8	0.65	2.7	2.02
7	0.276	13.51	1.93	-30.5	0.17	9.0	36.77	19298	243	10.7	0.79	3.1	2.29
8	0.316	13.51	2.20	-30.5	0.17	9.0	42.02	22052	277	13.2	0.98	3.2	2.38
9	0.092	13.51	0.64	-15.2	0.17	6.0	12.28	5892	74	7.1	0.52	2.2	1.65
10	0.184	13.51	1.29	-15.2	0.17	7.0	24.53	12110	152	8.5	0.63	2.6	1.95
11	0.276	13.51	1.93	-15.2	0.17	9.0	36.77	19298	243	10.3	0.76	3.2	2.34
12	0.316	13.51	2.20	-15.2	0.17	9.5	42.02	22400	282	13.2	0.97	3.6	2.70
13	0.027	4.29	1.84	0.0	0.17	7.0	35.09	5502	218	3.4	0.79	1.2	2.68
14	0.066	4.29	4.57	0.0	0.17	8.5	87.12	14298	567	4.7	1.10	1.5	3.50
15	0.027	7.44	0.61	0.0	0.17	8.0	11.67	32275	75	3.4	0.46	1.0	1.76
16	0.066	7.44	1.52	0.0	0.17	6.5	28.97	7763	177	5.1	0.69	1.7	2.28
17	0.105	7.44	2.43	0.0	0.17	9.5	46.27	13584	310	5.8	0.78	1.9	2.74
18	0.132	7.44	3.03	0.0	0.17	10.0	57.80	17243	394	8.0	1.08	2.3	3.02
19	0.046	7.44	1.07	0.0	0.17	8.5	20.32	5782	132	4.1	0.55	1.5	1.95

Table 4.6: Critical and general movement heights from Mazurek and Rajaratnam (unpublished).

Test No.	Q	U_0	d	D	T	F_0	R_0	R_s	z_c	z_g	z_d/d	z_g/d	$\left[\frac{F_0^{3/2} R_s^{0.8}}{(0.25 \tan \phi)^2 R_0} \right]^{1/7}$
	(L/sec)	(m/s)	(mm)	(mm)	(°C)				(mm)	(mm)			
1a	0.092	0.64	13.51	0.17	6.5	12.3	5977	75 ^a	7.03 ^a	0.52	2.59
1b	0.092	0.64	13.51	0.17	7.5	12.3	6159	78	8.86 ^a	0.66 ^a	2.59
2	0.184	1.29	13.51	0.17	8.5	24.5	12675	159	13.76	11.62	1.02	0.86	3.48
3a	0.276	1.93	13.51	0.17	8.5	36.8	19002	239	17.78	12.58	1.32	0.93	4.13
4a	0.316	2.20	13.51	0.17	9.0	42.0	22052	277	13.76	12.54	1.02	0.93	4.38
4b	0.316	2.20	13.51	0.17	10.5	42.0	23059	290	15.60	12.54	1.15	0.93	4.37
5a	0.092	0.64	13.51	0.17	10.5	12.3	6741	85	9.79	8.26	0.72	0.61	2.58
5b	0.092	0.64	13.51	0.17	10.5	12.3	6741	85	7.95	7.34	0.59	0.54	2.58
6c	0.184	1.29	13.51	0.17	7.5	24.5	12298	155	11.62	10.39	0.86	0.77	3.48
7b	0.276	1.93	13.51	0.17	9.0	36.8	19298	243	15.76	12.54	1.17	0.93	4.13
8	0.316	2.20	13.51	0.17	9.0	42.0	22052	277	14.05	13.46	1.04	1.00	4.38
9	0.092	0.64	13.51	0.17	6.0	12.3	5892	74	9.48	7.65	0.70	0.57	2.59
10	0.184	1.29	13.51	0.17	7.0	24.5	12110	152 ^a	10.40 ^a	0.77	3.48
11	0.276	1.93	13.51	0.17	9.0	36.8	19298	243 ^a	12.54 ^a	0.93	4.13
12	0.316	2.20	13.51	0.17	9.5	42.0	22400	282 ^a	12.84 ^a	0.95	4.37
13	0.027	1.84	4.29	0.17	7.0	35.1	5502	218	4.59	3.67	1.07	0.86	4.78
14	0.066	4.57	4.29	0.17	8.5	87.1	14298	567	7.34	6.73	1.71	1.57	7.05
15a	0.027	0.61	7.44	0.17	6.5	11.7	3127	71 ^a	3.98 ^a	0.53	2.76
15b	0.027	0.61	7.44	0.17	8.0	11.7	3275	75	7.34	7.34	0.99	0.99	2.75
16a	0.066	1.52	7.44	0.17	8.0	29.0	8132	186 ^a	6.42 ^a	0.86	4.07
16b	0.066	1.52	7.44	0.17	9.0	29.0	8373	191	7.64	6.42	1.03	0.86	4.06
16c	0.066	1.52	7.44	0.17	8.5	29.0	8244	188	7.34	6.73	0.99	0.90	4.06
17a	0.105	2.43	7.44	0.17	9.0	46.3	13373	306	8.87	7.95	1.19	1.07	4.97
17b	0.105	2.43	7.44	0.17	9.5	46.3	13584	310 ^a	7.64 ^a	1.03	4.96
17c	0.105	2.43	7.44	0.17	9.5	46.3	13584	310 ^a	7.03 ^a	0.94	4.96
18a	0.132	3.03	7.44	0.17	10.0	57.8	17243	394 ^a	8.56 ^a	1.15	5.46
18b	0.132	3.03	7.44	0.17	10.0	57.8	17243	394 ^a	8.56 ^a	1.15	5.46
19	0.046	1.07	7.44	0.17	8.5	20.3	5782	132 ^a	5.20 ^a	0.70	3.49

^aNot available.

Table 4.7: The maximum relative scour hole depth and the aerial scour hole radius at equilibrium for the tube set above the bed of fine sand
Brahme (1983).

Test No.	Q (L/s)	d (mm)	U ₀ (m/s)	z ₀ (mm)	D ₅₀ (mm)	T (°C)	F ₀	R ₀	R _s	r ₀ (mm)	r _a (mm)	r _{a/d}	$\left[\frac{F_0^{3/2} R_s^{0.8} \sin^3 \psi}{(0.25 \tan \phi)^2 R_0} \right]^{1/7}$
1	3.15	27.9	5.15	31.8	0.22	33.5	86.0	193431	1523	70.0	76.9	2.75	5.41
2	2.52	27.9	4.12	31.8	0.22	30.5	68.8	145642	1147	57.5	65.7	2.35	4.92
3	3.15	27.9	5.15	22.9	0.22	31.5	86.0	186439	1468	75.0	78.4	2.81	5.41
4	2.52	27.9	4.12	22.9	0.22	33.5	68.8	154745	1219	65.0	68.9	2.47	4.91
5	3.15	27.9	5.15	12.7	0.22	33.5	86.0	193431	1523	82.5	83.5	2.99	5.41
6	2.52	27.9	4.12	12.7	0.22	31.5	68.8	149151	1175	72.5	73.6	2.63	4.92
7	3.53	41.1	2.66	31.8	0.22	32.5	44.4	145313	777	80.0	86.1	2.09	3.86
8	3.03	41.1	2.28	31.8	0.22	33.0	38.0	124471	665	70.0	76.9	1.87	3.61
9	2.52	41.1	1.90	31.8	0.22	30.0	31.7	97736	523	57.5	65.7	1.60	3.34
10	3.53	41.1	2.66	22.9	0.22	31.5	44.4	141812	758	84.7	87.7	2.13	3.86
11	3.03	41.1	2.28	22.9	0.22	34.0	38.0	126027	674	77.5	80.8	1.96	3.61
12	2.52	41.1	1.90	22.9	0.22	32.0	31.7	102503	548	67.5	71.2	1.73	3.34
13	3.53	41.1	2.66	12.7	0.22	32.0	44.4	143541	767	92.5	93.4	2.27	3.86
14	3.03	41.1	2.28	12.7	0.22	33.0	38.0	124471	665	85.0	85.9	2.09	3.61
15	2.52	41.1	1.90	12.7	0.22	33.5	31.7	105066	562	75.0	76.1	1.85	3.34
16	3.53	50.8	1.74	31.8	0.22	32.5	29.1	117680	510	80.0	86.1	1.69	3.12
17	3.03	50.8	1.49	31.8	0.22	33.0	24.9	100802	436	70.0	76.9	1.51	2.92
18	2.52	50.8	1.24	31.8	0.22	32.5	20.8	84036	364	60.0	67.9	1.34	2.70
19	3.53	50.8	1.74	22.9	0.22	32.0	29.1	116245	503	85.0	88.0	1.73	3.12
20	3.03	50.8	1.49	22.9	0.22	33.5	24.9	102062	442	77.5	80.8	1.59	2.92
21	2.52	50.8	1.24	22.9	0.22	30.0	20.8	79150	343	70.0	73.7	1.45	2.71
22	3.53	50.8	1.74	12.7	0.22	31.0	29.1	113478	491	95.0	95.8	1.89	3.13
23	3.03	50.8	1.49	12.7	0.22	33.0	24.9	100802	436	87.5	88.4	1.74	2.92
24	2.52	50.8	1.24	12.7	0.22	32.0	20.8	83011	359	80.0	81.0	1.59	2.70

Table 4.8: The maximum relative scour hole depth and the aerial scour hole radius at equilibrium for the tube set above the bed of medium sand
Brahme (1983).

Test No.	Q (L/s)	d (mm)	U ₀ (m/s)	z ₀ (mm)	D ₅₀ (mm)	T (°C)	F ₀	R ₀	R _s	r ₀ (mm)	r _a (mm)	r _{a/d} $\left[\frac{F_0^{3/2} R_s^{0.8} \sin^3 \psi}{(0.25 \tan \varphi)^2 R_0} \right]^{1/7}$
1	3.03	27.9	4.94	31.8	0.42	32.5	60.1	183326	2756	60.0	67.9	2.43
2	2.52	27.9	4.12	31.8	0.42	33.0	50.1	152834	2298	52.4	61.3	2.19
3	3.03	27.9	4.94	22.9	0.42	31.0	60.1	176778	2658	67.4	71.1	2.55
4	2.52	27.9	4.12	22.9	0.42	31.0	50.1	147376	2216	60.0	64.3	2.30
5	3.03	27.9	4.94	12.7	0.42	33.0	60.1	183326	2756	75.0	76.0	2.72
6	2.52	27.9	4.12	12.7	0.42	33.0	50.1	152834	2298	64.9	66.2	2.37
7	3.53	41.1	2.66	31.8	0.42	32.5	32.3	145313	1483	70.1	77.0	1.87
8	3.03	41.1	2.28	31.8	0.42	32.0	27.7	122953	1255	60.0	67.9	1.65
9	3.53	41.1	2.66	22.9	0.42	30.0	32.3	136865	1397	75.0	78.4	1.91
10	3.03	41.1	2.28	22.9	0.42	32.0	27.7	122953	1255	64.9	68.8	1.67
11	3.53	41.1	2.66	12.7	0.42	33.0	32.3	145313	1483	79.9	80.9	1.97
12	3.03	41.1	2.28	12.7	0.42	32.0	27.7	122953	1255	70.1	71.2	1.73
13	3.53	50.8	1.74	31.8	0.42	32.5	21.2	117680	973	70.1	77.0	1.51
14	3.03	50.8	1.49	31.8	0.42	33.0	18.2	100802	833	60.0	67.9	1.34
15	3.53	50.8	1.74	22.9	0.42	32.5	21.2	117680	973	75.0	78.4	1.54
16	3.03	50.8	1.49	22.9	0.42	31.0	18.2	97201	803	64.9	68.8	1.35
17	3.53	50.8	1.74	12.7	0.42	32.0	21.2	116245	961	82.5	83.5	1.64
18	3.03	50.8	1.49	12.7	0.42	31.0	18.2	97201	803	72.5	73.6	1.45
												2.72

Table 4.9: The maximum relative scour hole depth and scour hole radius at equilibrium for the tube set above the bed of microbeads
Brahme (1983).

Test	Q	d	U_0	z_0	D_{50}	T	F_0	R_0	R_s	r_0	r_a	r_a/d	$\left[\frac{F_0^{3/2} R_s^{0.8} \sin^3 \psi}{(0.25 \tan \varphi)^2 R_0} \right]^{1/7}$
No.	(L/s)	(mm)	(m/s)	(mm)	(mm)	(°C)				(mm)			
1	3.15	27.9	5.15	31.8	0.10	32.0	136.4	188713	675	75.0	81.5	2.92	6.11
2	2.52	27.9	4.12	31.8	0.10	31.0	109.1	147376	528	70.0	76.9	2.75	5.55
3	3.15	27.9	5.15	22.9	0.10	33.0	136.4	191043	684	82.5	85.6	3.06	6.10
4	2.52	27.9	4.12	22.9	0.10	32.0	109.1	150970	540	72.5	76.0	2.72	5.55
5	3.15	27.9	5.15	12.7	0.10	34.0	136.4	193431	692	92.5	93.4	3.34	6.10
6	2.52	27.9	4.12	12.7	0.10	31.0	109.1	147376	528	82.5	83.5	2.99	5.55
7	3.53	41.1	2.66	31.8	0.10	32.0	70.4	143541	349	102.6	107.4	2.61	4.35
8	3.03	41.1	2.28	31.8	0.10	33.0	60.3	124471	302	82.5	88.4	2.15	4.07
9	2.52	41.1	1.90	31.8	0.10	30.5	50.3	98885	240	67.5	74.6	1.81	3.77
10	3.53	41.1	2.66	22.9	0.10	32.5	70.4	145313	353	107.5	109.9	2.67	4.35
11	3.03	41.1	2.28	22.9	0.10	30.5	60.3	118614	288	85.0	88.0	2.14	4.08
12	2.52	41.1	1.90	22.9	0.10	32.0	50.3	102503	249	75.0	78.4	1.91	3.77
13	3.53	41.1	2.66	12.7	0.10	30.0	70.4	136865	333	122.5	123.2	2.99	4.36
14	3.03	41.1	2.28	12.7	0.10	33.0	60.3	124471	302	100.0	100.8	2.45	4.07
15	2.52	41.1	1.90	12.7	0.10	31.5	50.3	101268	246	92.5	93.4	2.27	3.77
16	3.53	50.8	1.74	31.8	0.10	32.5	46.2	117680	232	90.0	95.4	1.88	3.52
17	3.03	50.8	1.49	31.8	0.10	31.0	39.6	97201	191	82.5	88.4	1.74	3.30
18	2.52	50.8	1.24	31.8	0.10	31.0	33.0	81035	159	70.0	76.9	1.51	3.05
19	3.53	50.8	1.74	22.9	0.10	31.5	46.2	114845	226	100.0	102.6	2.02	3.53
20	3.03	50.8	1.49	22.9	0.10	28.5	39.6	92783	183	87.5	90.4	1.78	3.31
21	2.52	50.8	1.24	22.9	0.10	31.0	33.0	81035	159	82.5	85.6	1.69	3.05
22	3.53	50.8	1.74	12.7	0.10	32.0	46.2	116245	229	117.5	118.2	2.33	3.53
23	3.03	50.8	1.49	12.7	0.10	31.0	39.6	97201	191	100.0	100.8	1.98	3.30
24	2.52	50.8	1.24	12.7	0.10	30.5	33.0	80081	158	95.0	95.8	1.89	3.05

Table 4.10: Calculation for dimensionless particle diameter (D_*) for different studies.

Study/Material	D_{50} (mm)	ϕ	D_{50} (mm)	$\frac{\rho_s - \rho}{\rho}$	D_*
Present Study	0.58	30°	0.58	2.65	14.64
Mazurek and Rajaratnam	0.19	30°	0.19	2.65	4.81
Brahme (1983) Fine Sand	0.22	30°	0.22	2.66	5.58
Brahme (1983) Medium Sand	0.40	30°	0.40	2.64	10.10
Brahme (1983) Microbeads	0.10	30°	0.10	2.45	2.43

Table 4.11: Maximum errors in measured and derived quantities.

Quantity	Maximum Error	Notes
Q	up to 2 % of flow rate 1.0 % for 9.67 mm tube 0.7 % for 13.86 mm tube 0.5 % for 20.4 mm tube	From deviation from the mean value
d	4.0 % for 9.67 mm tube 2.4 % for 13.86 mm tube 2.0 % for 20.4 mm tube	
U_0	5.6 % for 9.67 mm tube 4.2 % for 13.86 mm tube 3.8 % for 20.4 mm tube	
F_0	5.0 % for 9.67 mm tube 3.1 % for 13.86 mm tube 2.5 % for 20.4 mm tube	
R_s	7.5 % for 9.67 mm tube 5.9 % for 13.86 mm tube 5.5 % for 20.4 mm tube	
φ	10 %	
$\left[\frac{F_0^{3.2} R_s^{0.8}}{(0.25 \tan \varphi)^2 R_0} \right]^{1/7}$	6.7 % for 9.67 mm tube 6.9 % for 13.86 mm tube 4.1 % for 20.4 mm tube	
z_0	20 %	
ε	10 %	
ε_r	22.4 %	
r	0.1 %	estimated
r_t	0.1%	estimated
z_c	20%	
z_g	20%	
$\frac{r_t}{d}, \frac{r_a}{d}$	1.1 %	
$\frac{\varepsilon_{rm}}{d}$	23.4 % for 9.67 mm tube 23.1% for 13.86 mm tube 22.9 % for 20.4 mm tube	
$\frac{z_c}{d}, \frac{z_g}{d}$	20.1% for 9.67 mm tube 20.7% for 13.86 mm tube 20.5 % for 20.4 mm tube	

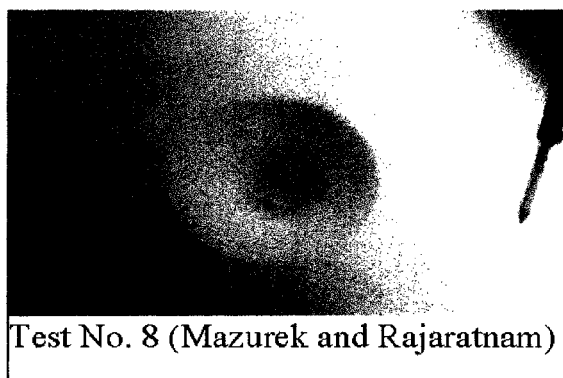
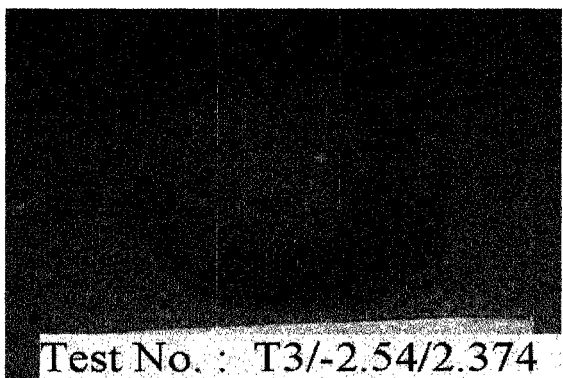
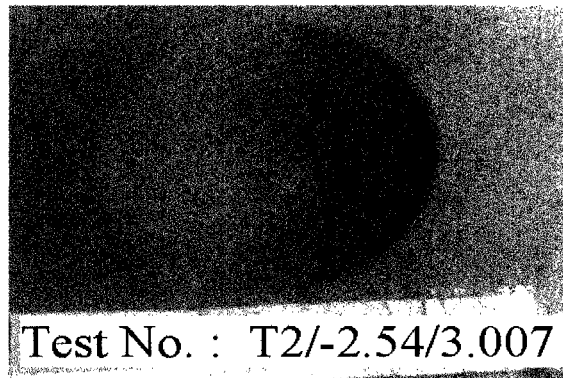
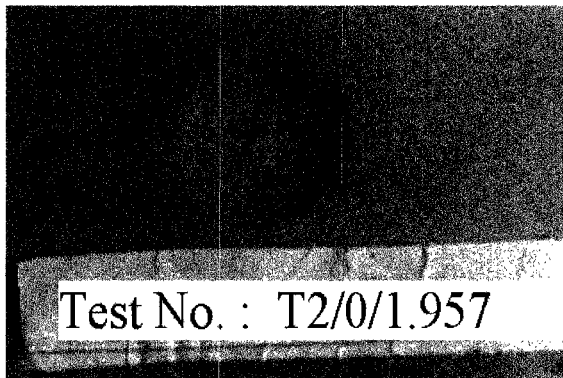
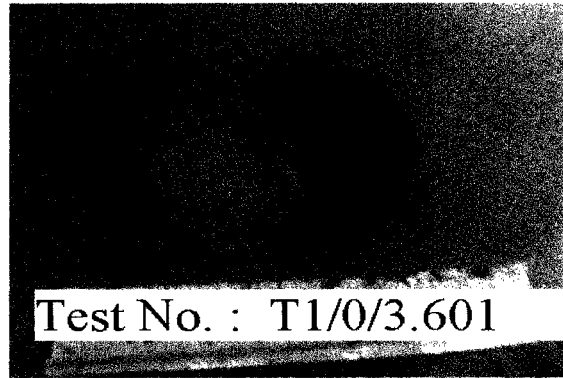
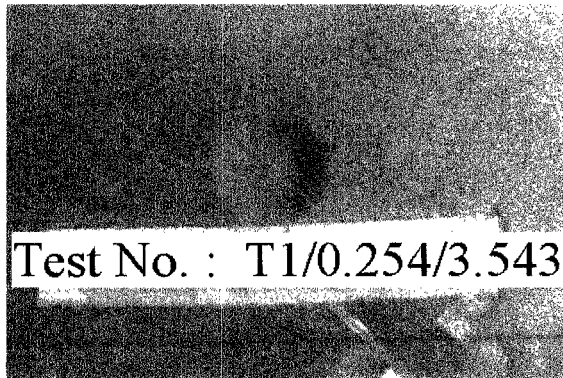


Fig. 4.1: Photograph of the some typical scour holes at equilibrium.

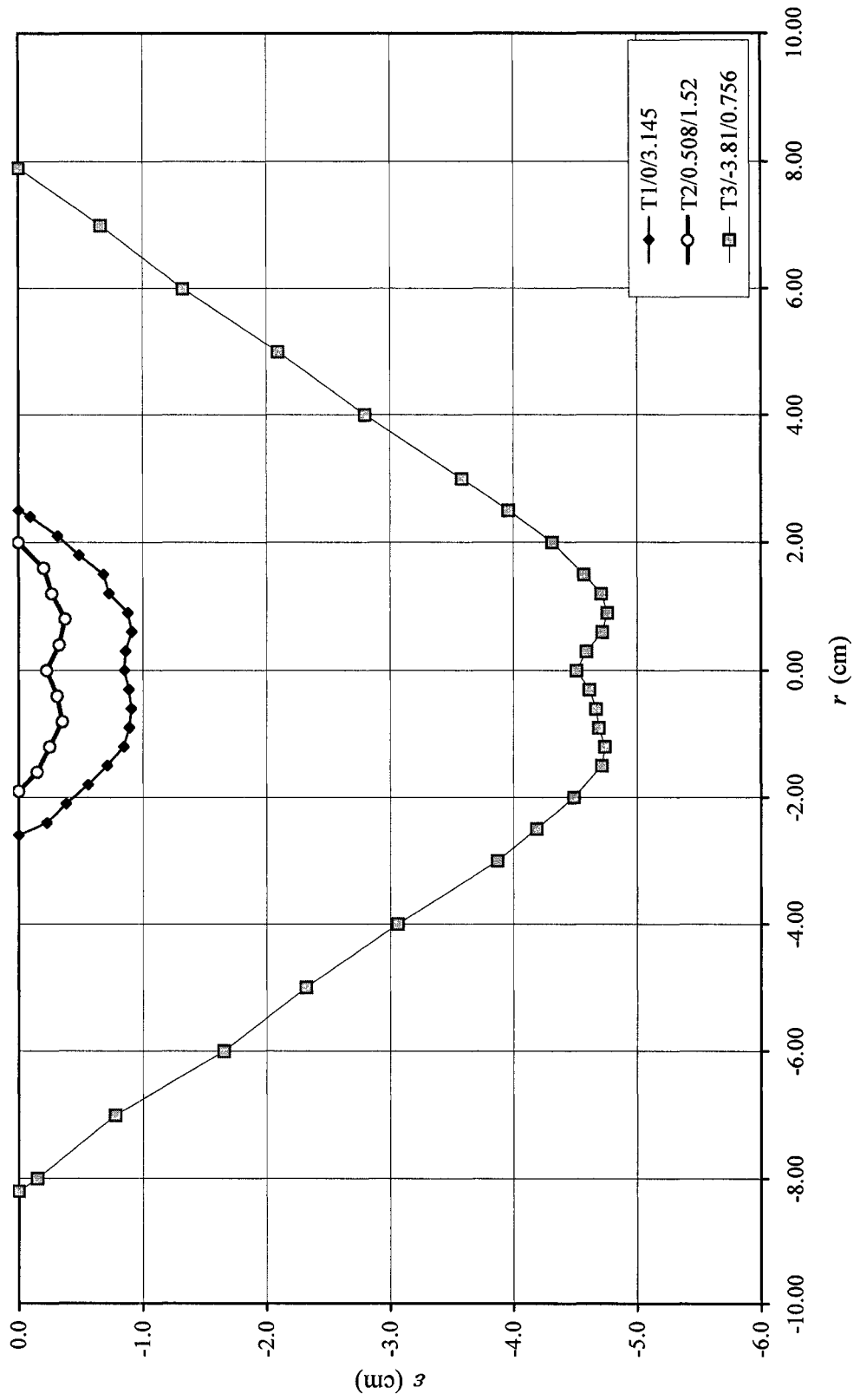


Fig. 4.2: Typical scour hole profiles for three different inlet heights.

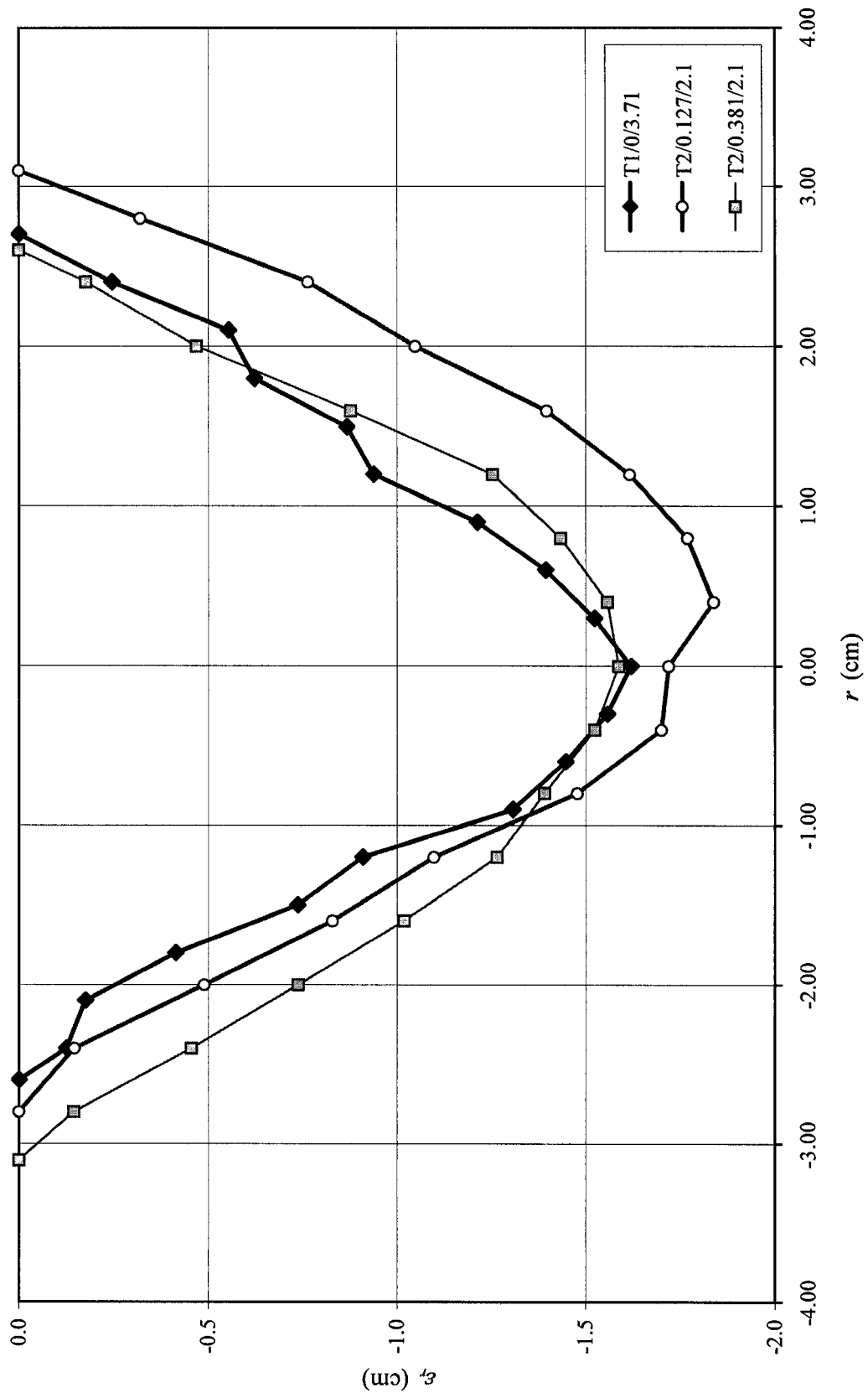


Fig. 4.3: Typical scour hole profiles when vortex was generated below tube inlet.

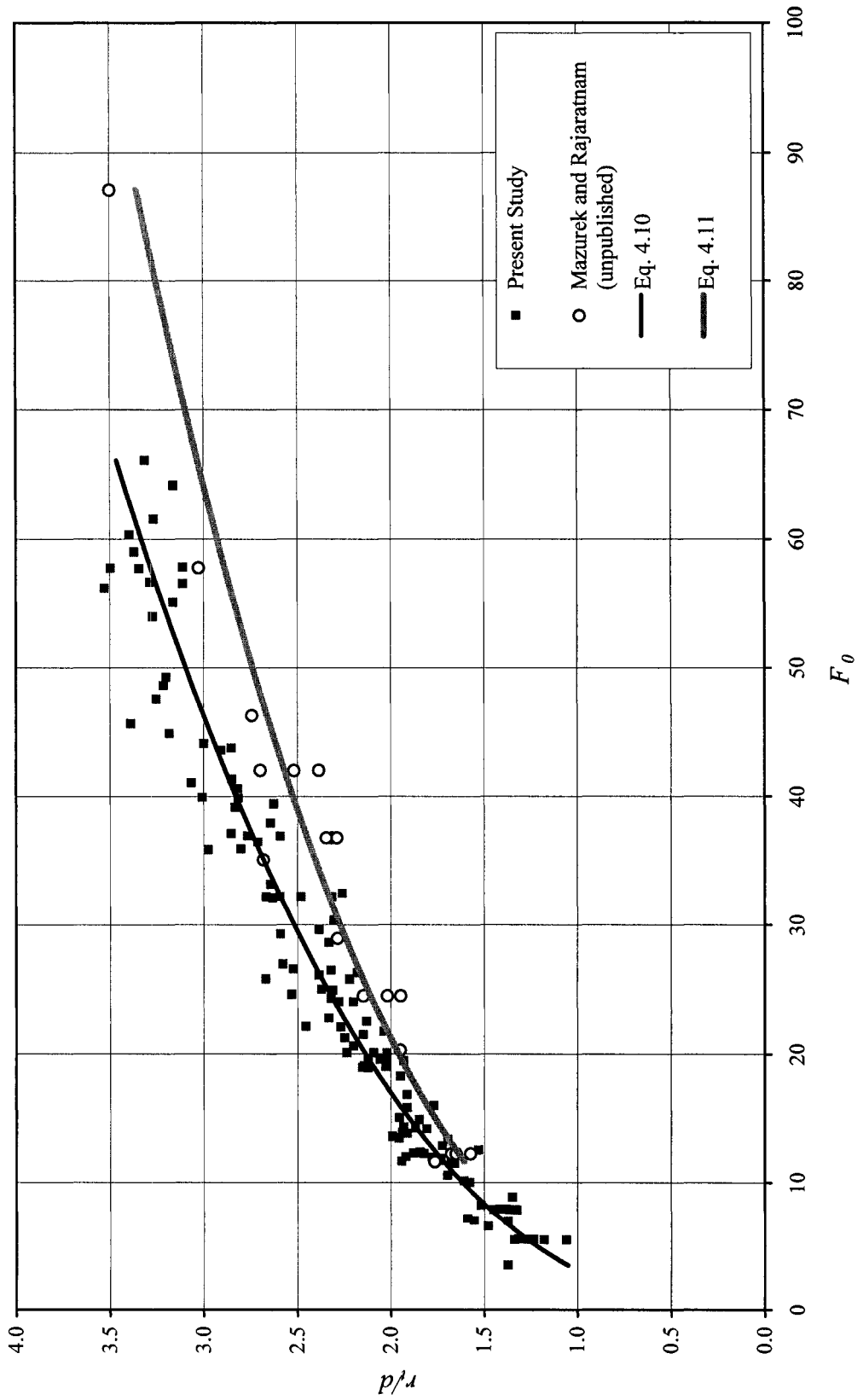


Fig. 4.4: The dimensionless equilibrium scour radius at the tube level with the dimensionless Froude number for the cases where the tube is set on or below the bed level.

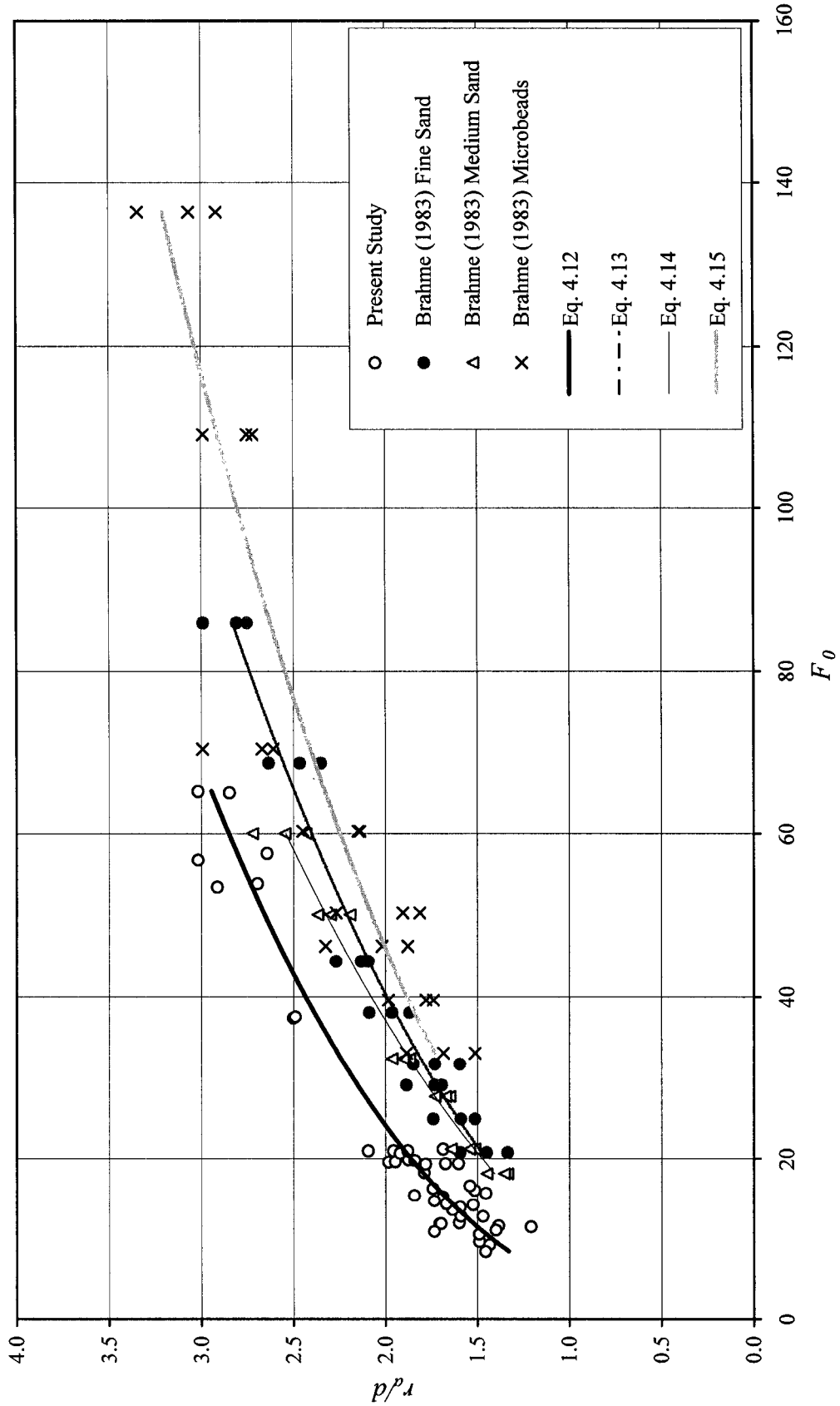


Fig. 4.5: The dimensionless equilibrium aerial scour radius with the densimetric Froude number for the case where the tube is set above the bed level.

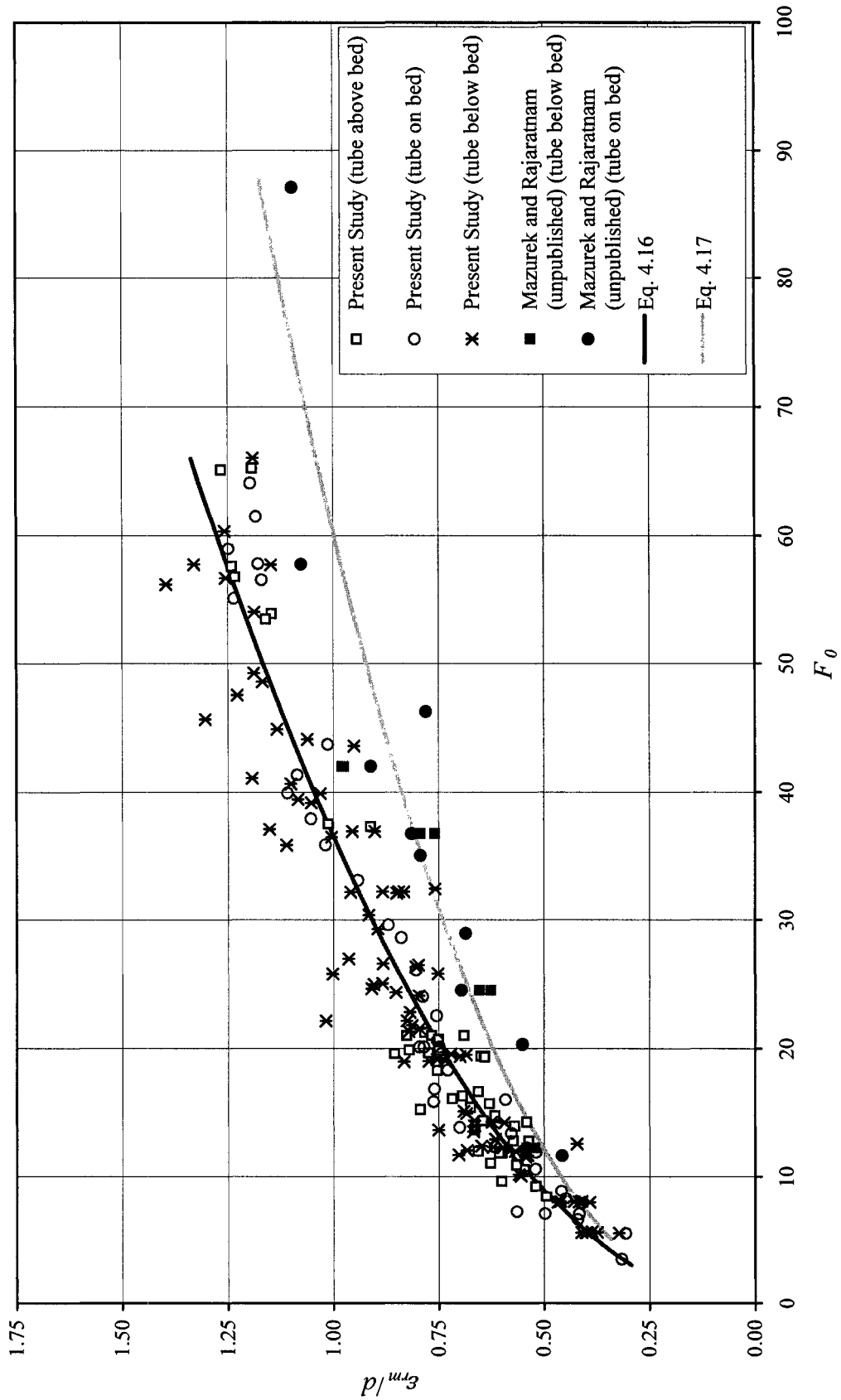


Fig. 4.6: The dimensionless equilibrium scour depth measured from the tube inlet level with densimetric Froude number.

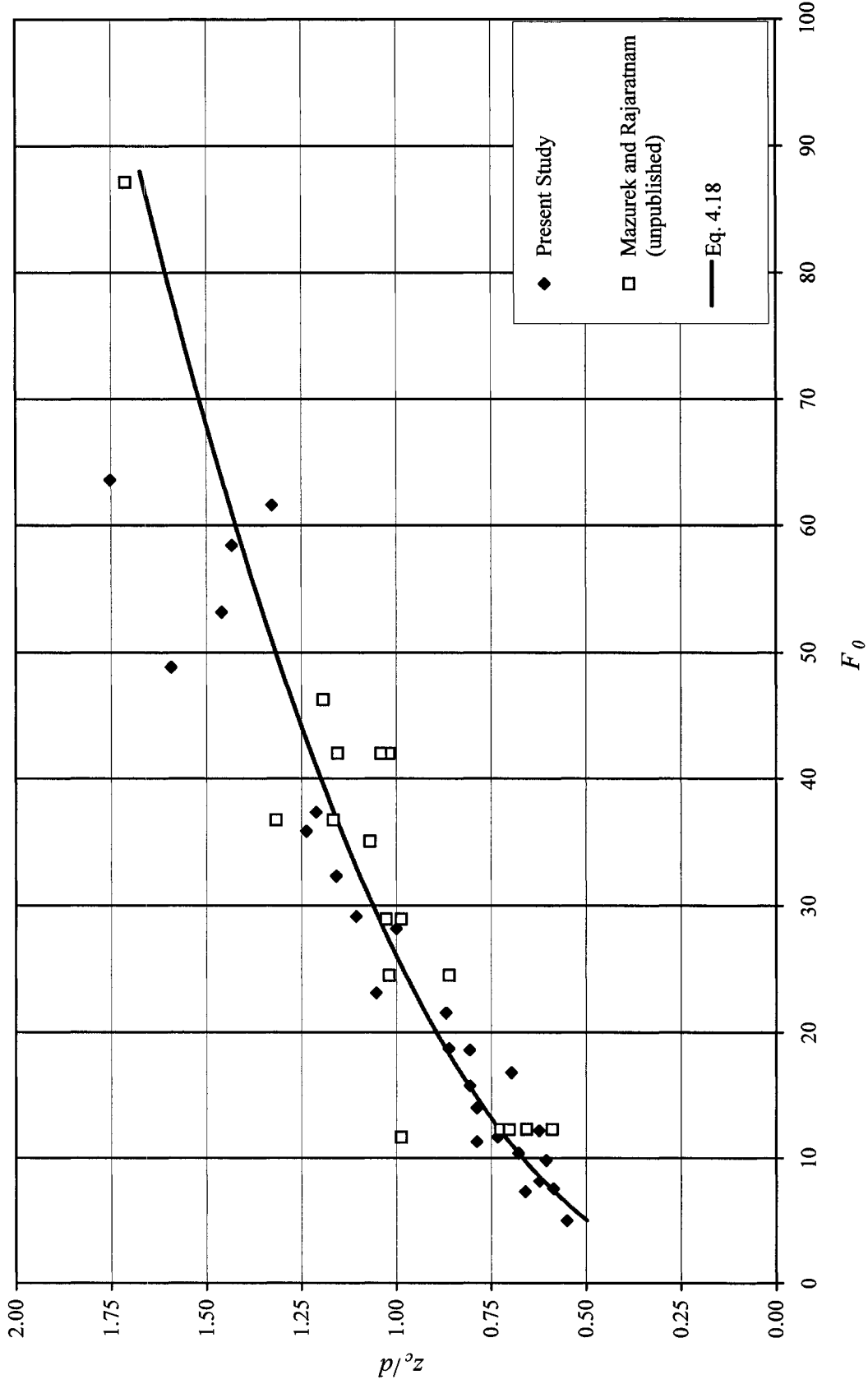


Fig. 4.7: The dimensionless height for critical movement with the densimetric Froude number.



Fig. 4.8: The dimensionless height for general movement with the densimetric Froude number.

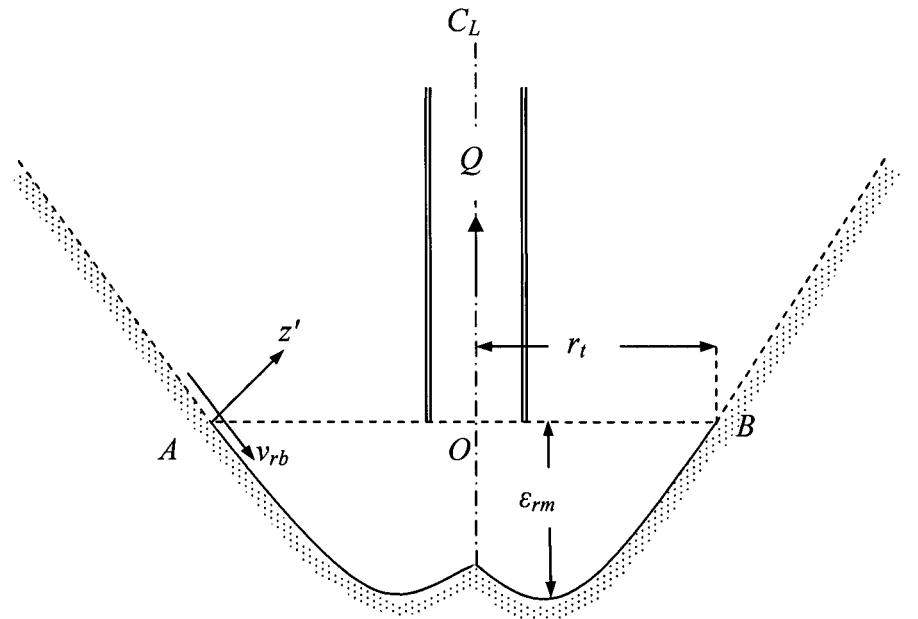


Fig. 4.9: Typical scour hole profile for the case when tube is set on or below bed level.

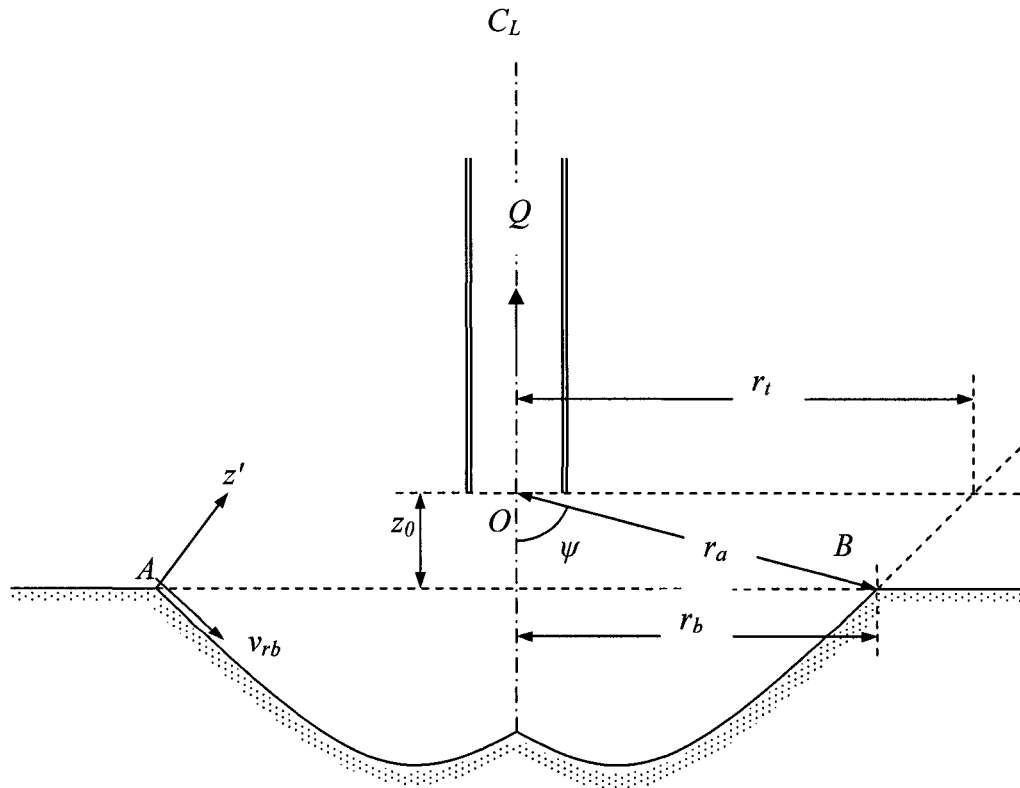


Fig.4.10: Typical scour hole profile for the case when tube is set above the bed.

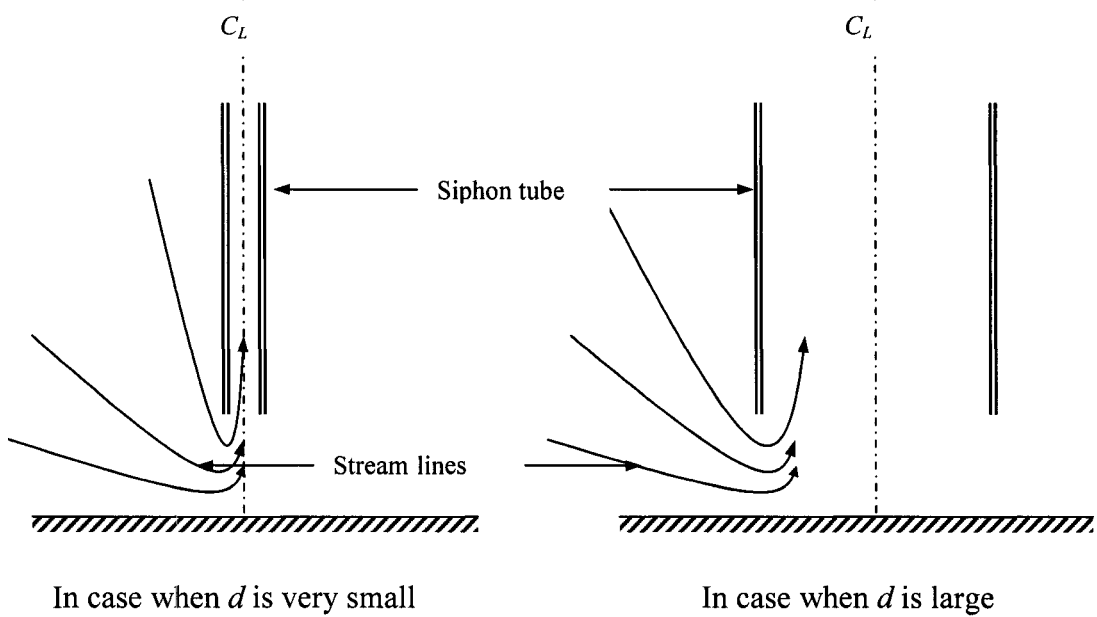


Fig. 4.11: Possible effect of tube diameter on flow convergence at bed.

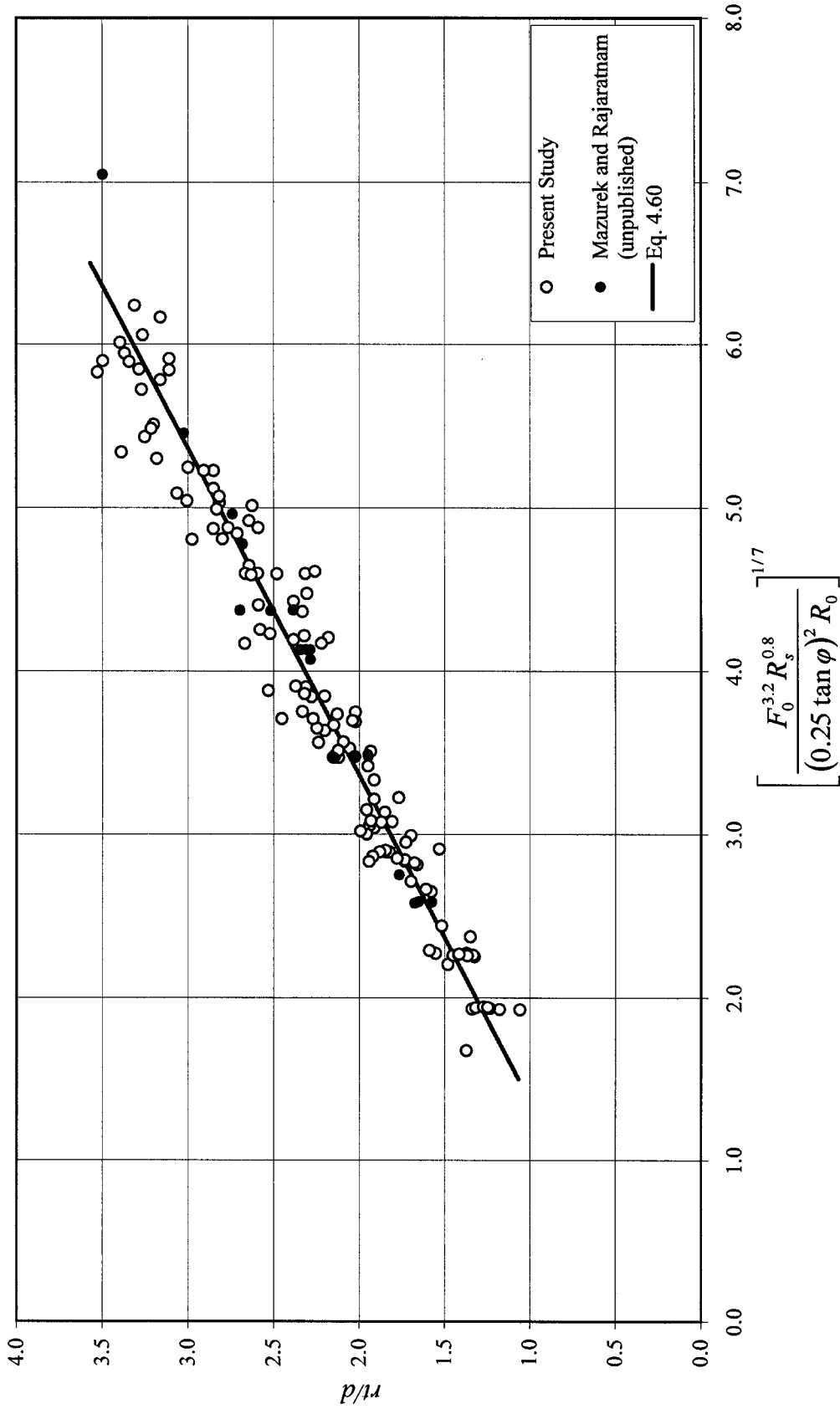


Fig. 4.12: The dimensionless equilibrium scour radius at inlet level with the theoretical function for the case where the tube is set on or below bed.

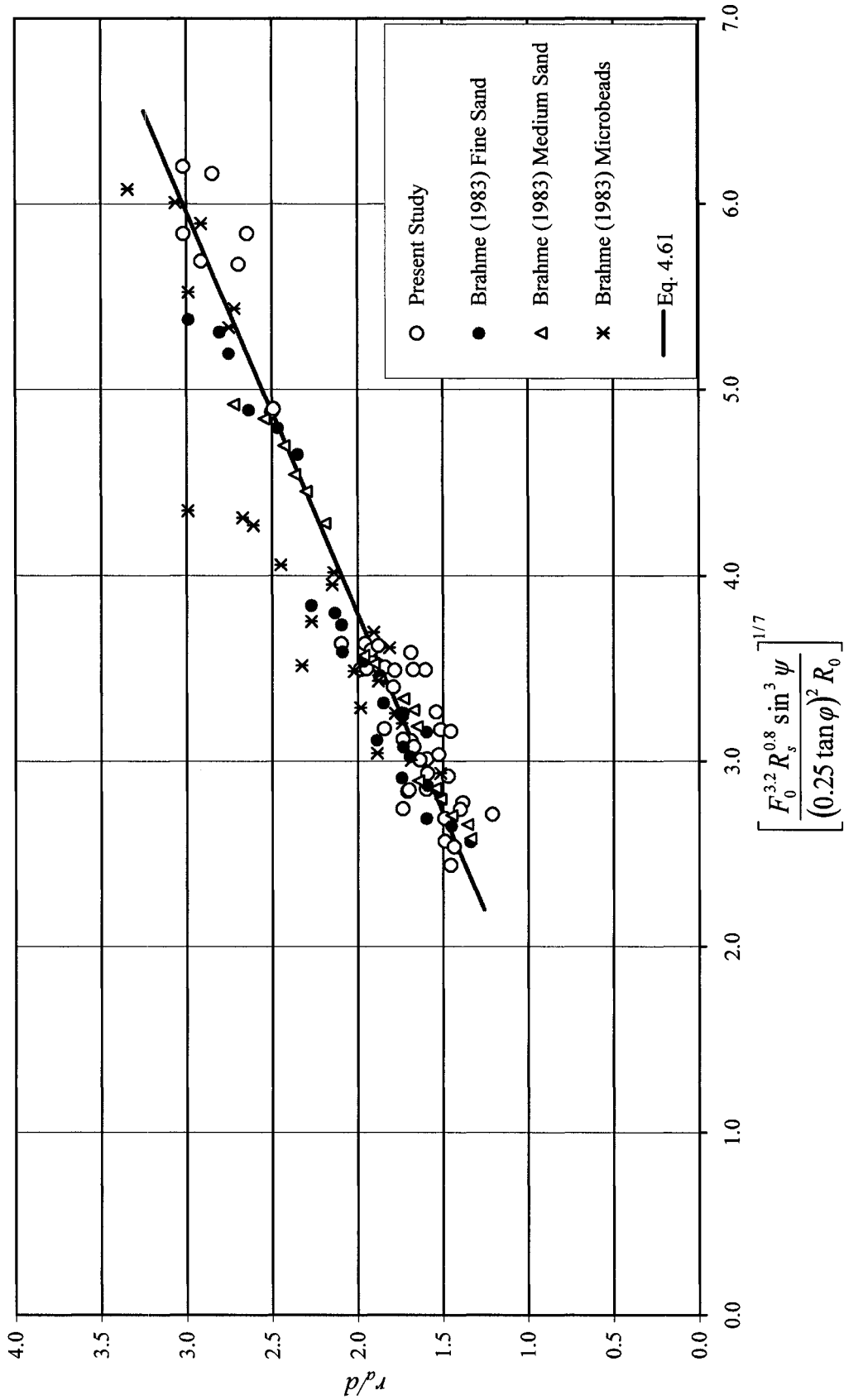


Fig.4.13: The dimensionless aerial scour radius at equilibrium with the theoretical function for the case where the tube is set above the bed.

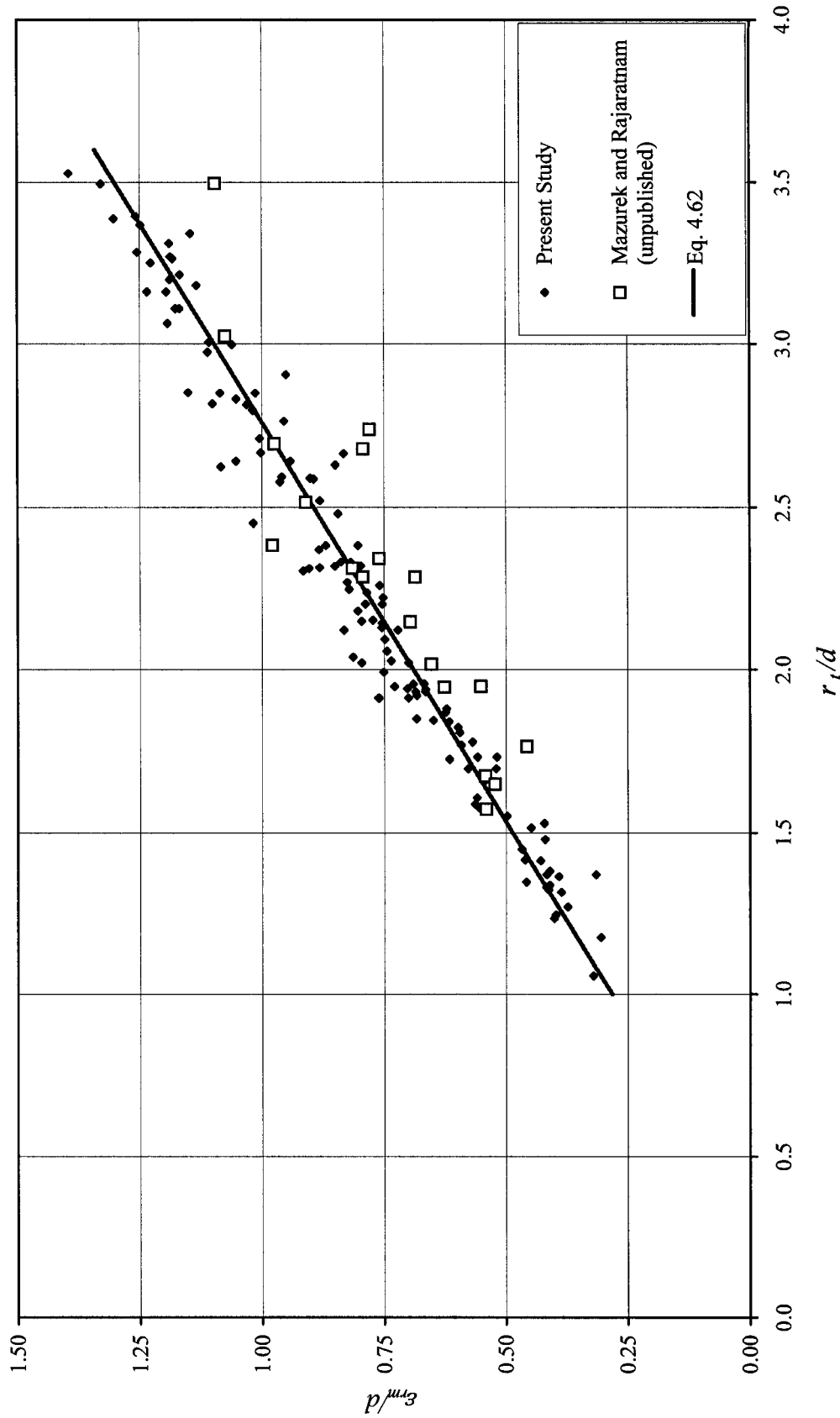


Fig. 4.14: The dimensionless relative maximum scour depth with the dimensionless scour radius measured at tube level at equilibrium.

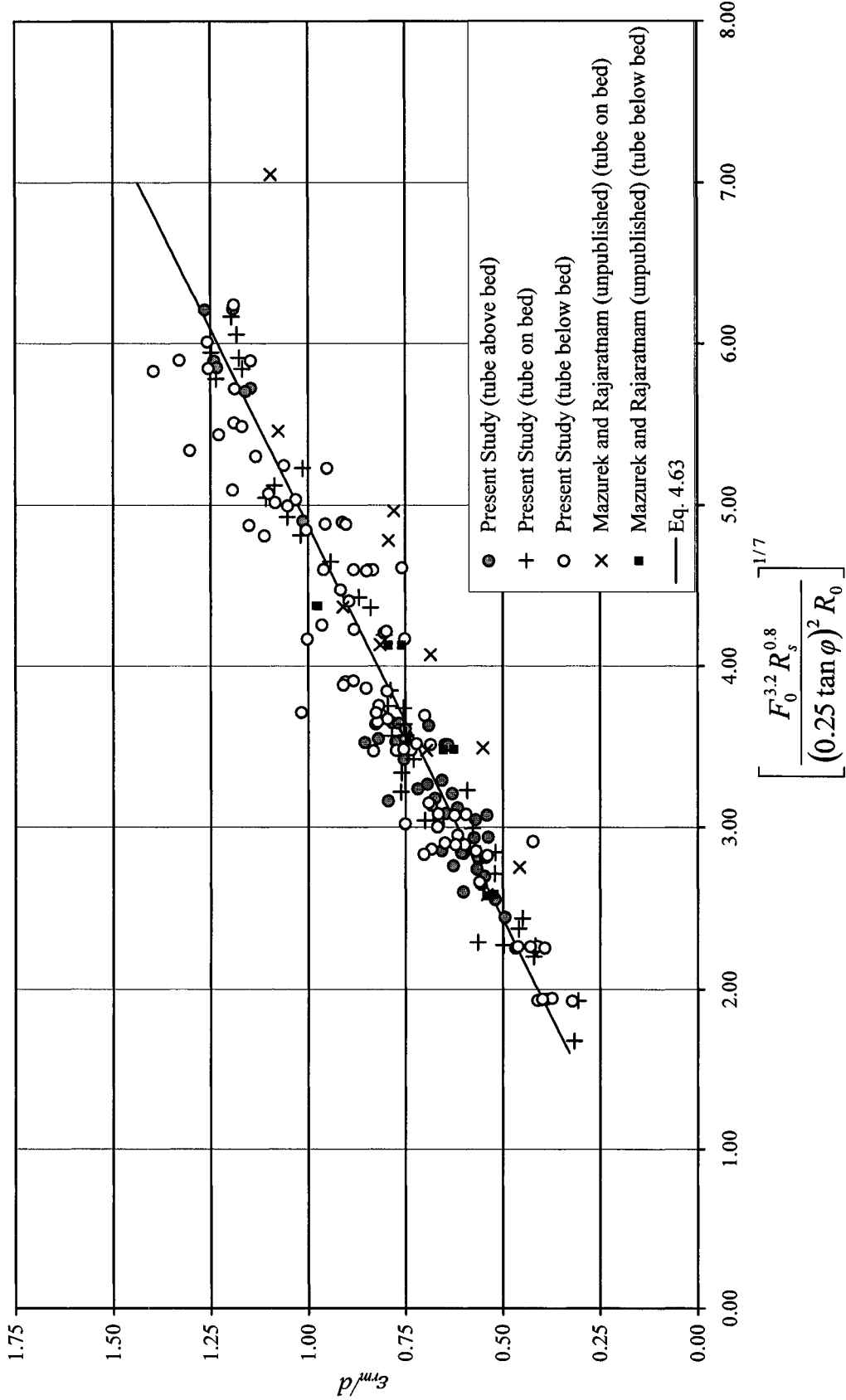


Fig.4.15: The dimensionless equilibrium maximum scour depth measured the tube inlet with the theoretical function.

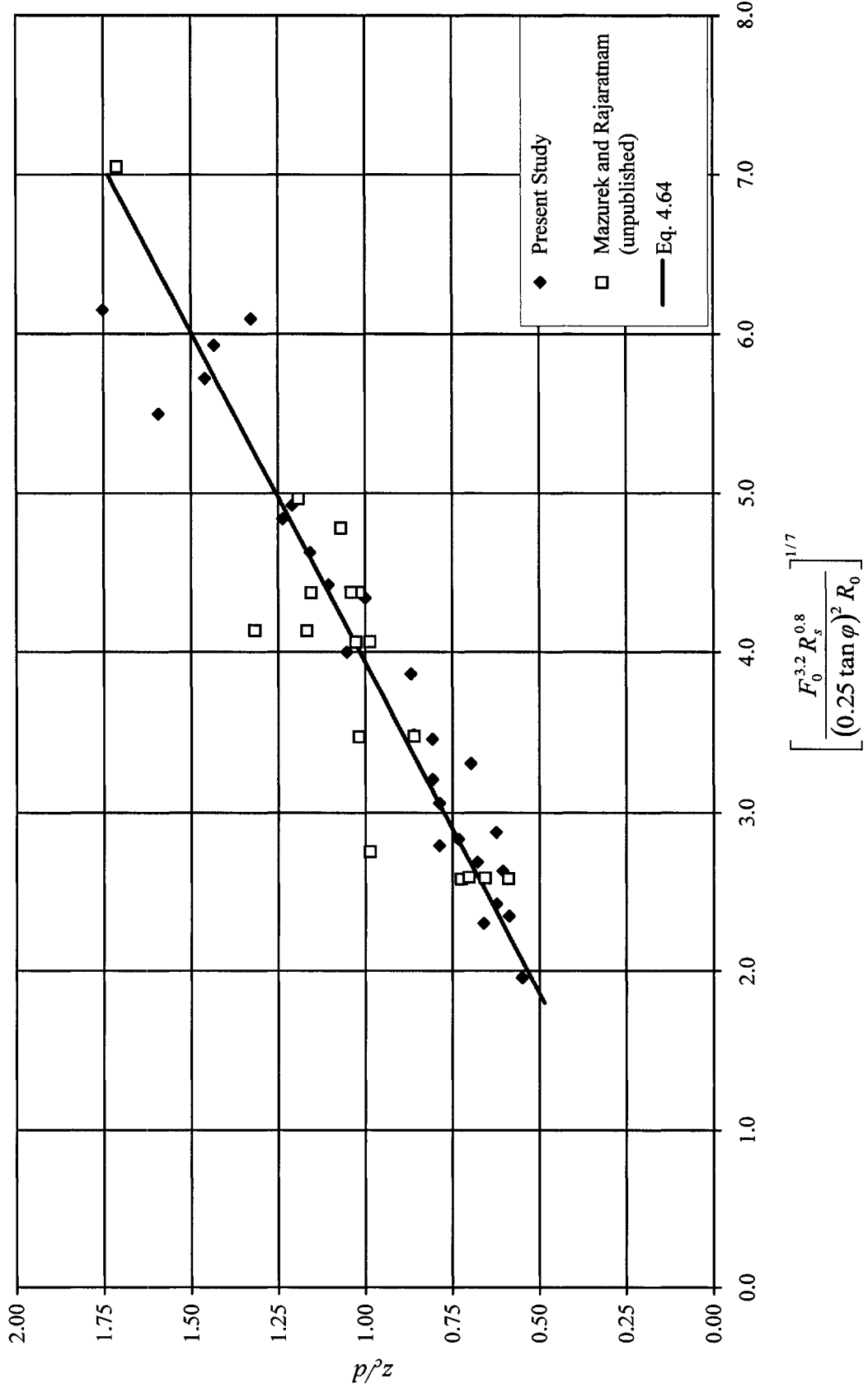


Fig.4.16: The dimensionless height for the critical movement with the theoretical function.

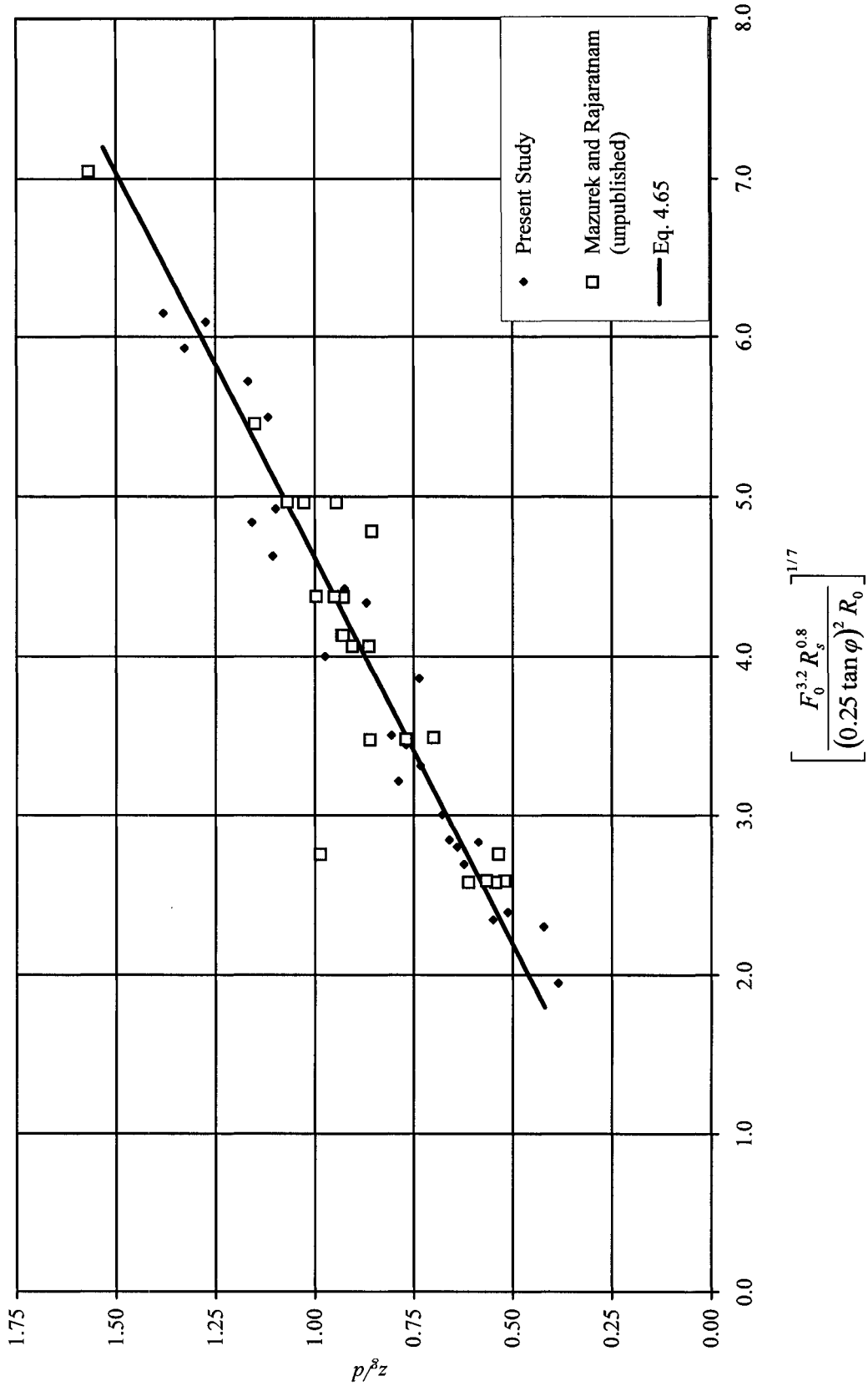


Fig.4.17: The dimensionless height for general movement with the theoretical function.

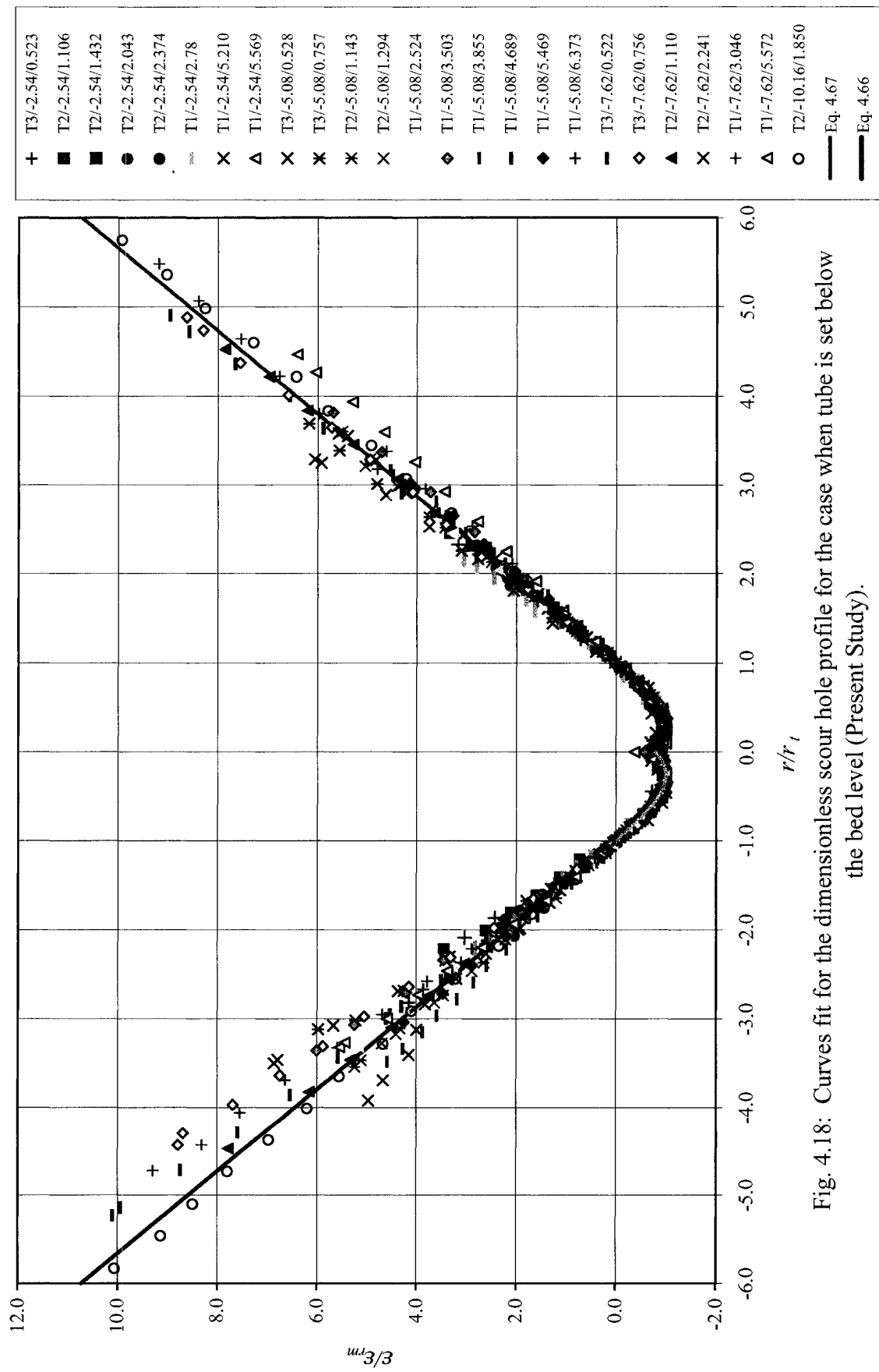


Fig. 4.18: Curves fit for the dimensionless scour hole profile for the case when tube is set below the bed level (Present Study).

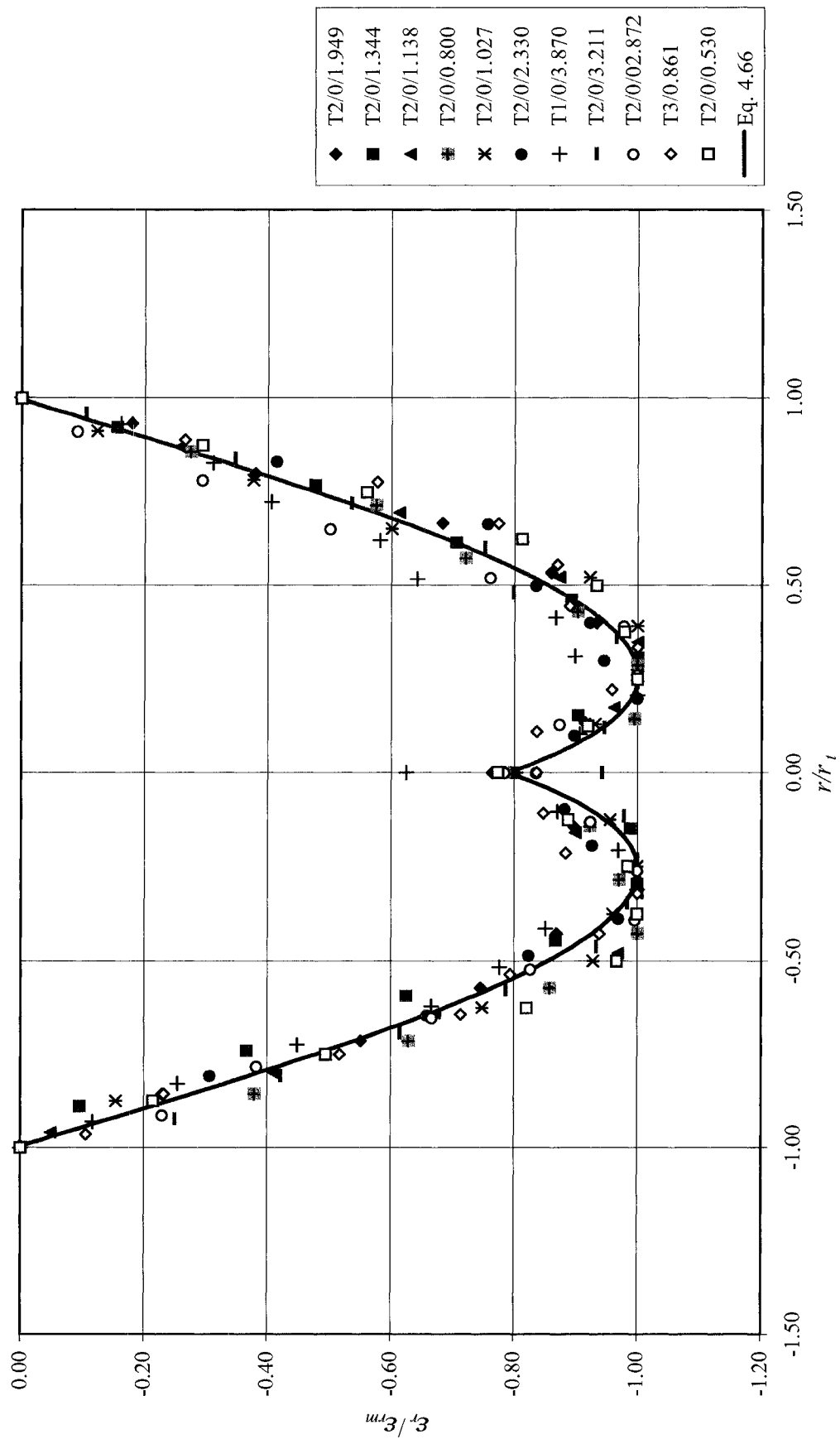


Fig. 4.19: Curve fits for the dimensionless scour hole profile for the case when tube is set on the bed level (Present Study).

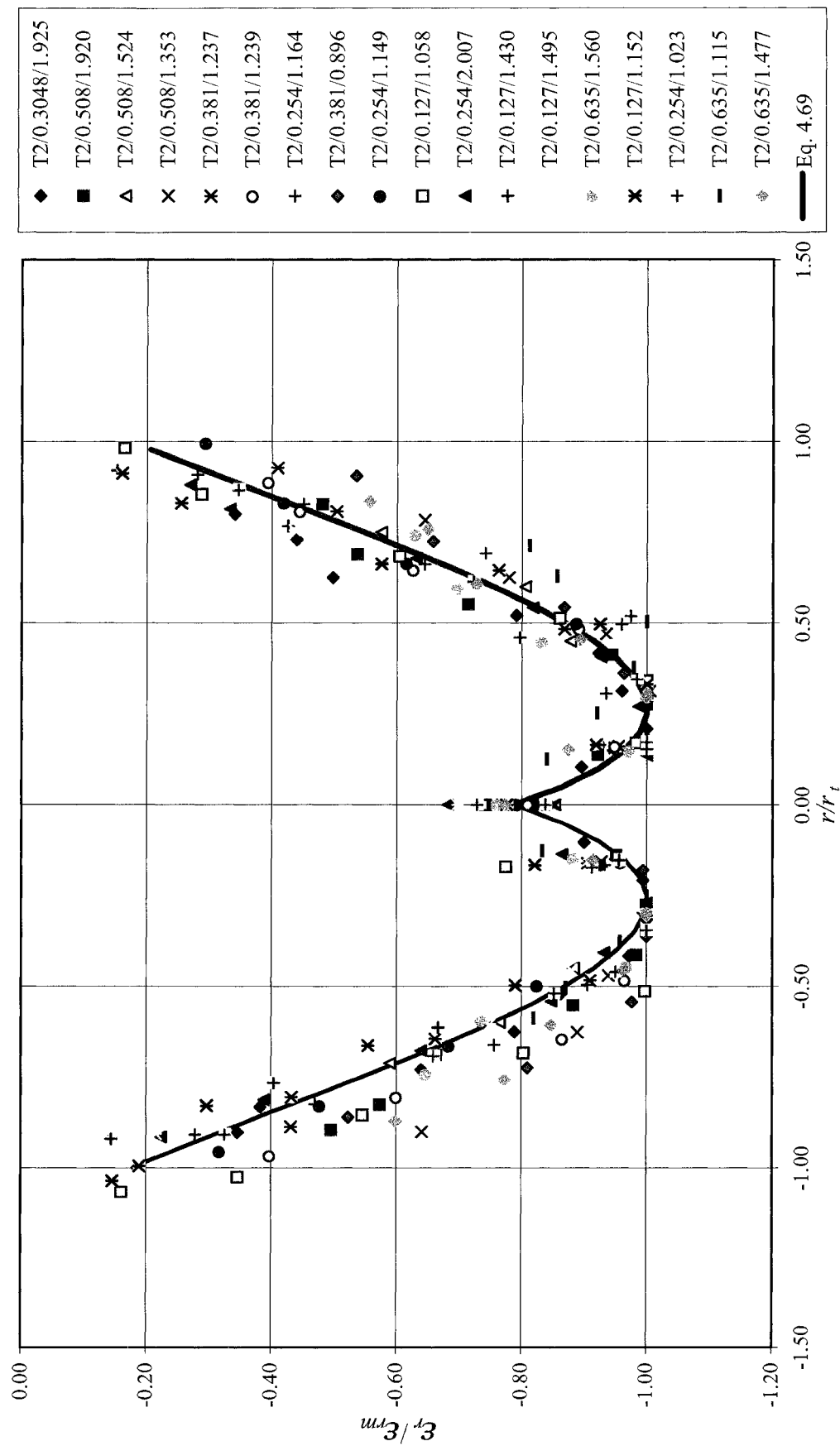


Fig. 4.20: Curve fits for the dimensionless scour hole profile for the case when tube is set above the bed level (Present Study).

CHAPTER 5: CONCLUSIONS

5.1 Summary of Observations

A review of literature showed that scouring by siphon has received a little attention and studies were mainly empirical in nature. The present study contributes a comprehensive investigation of the equilibrium scour hole geometry and the threshold criteria for removal of cohesionless sediments by a siphon flow. The siphon tube selected was cylindrical in shape and set vertically on, above, or within the sediment bed. Initially, dimensional analysis was used to find prediction formulae for the scour hole dimensions and heights for critical movement.

Later, an attempt was made using a theoretical analysis to find dimensionless functions that affect the length parameters related to siphon scour. The following significant observations were drawn from this study:

1. Most of the scouring occurred very rapidly and normally within a minute, for all the tube positions. After removal of most of the sediment, the scouring occurred intermittently and continued for a few minutes (normally 10 to 15 minutes). In this period, a single or few particles around the boundary of the scour hole have slide down towards the center and then immediately removed into the siphon tube. After this intermittent scouring the scour hole reached equilibrium and there was no movement of particles on or outside the scour hole.
2. The equilibrium scour holes were axisymmetric and looked similar in shape. The radius of the scour hole could easily visible in every test. The maximum scour hole depth occurred at some radial distance away from the center, and encircles a small

conical hill located at the center. This distance to this maximum depth was found to be 0.26 times the radius of the equilibrium scour hole at the tube level.

3. The dimensionless analysis yielded a general relation of the dimensionless length parameters and the densimetric Froude number. All of the length parameters related to siphon scour have been normalized by the inside tube diameter and fitted by power curves with the densimetric Froude number. These length parameters found increased at a decreasing rate with an increase in the densimetric Froude number. For a particular type of sediment, they showed good correlations with the densimetric Froude number. However, the relations were quite distinct when compared with the same length parameters where different sediment particle were used in the experiments. This indicates that the densimetric Froude number alone is not enough to describe the length parameters related to siphon scour.
4. An approach from theoretical point of view resulted in general semi-empirical relationships for the equilibrium scour hole radii, (r_t and r_a). These functions have been derived by comparing the threshold criteria for sediment movement and the viscous shear stress on the particle at equilibrium. For both the equilibrium scour hole radii, the function differed with different ranges of value of the dimensionless particle diameter, D^* . These theoretical functions implied that, although the densimetric Froude number has an important effect, other particle and flow properties (such as the Reynolds number of the flow through the tube, the angle of repose, and the Reynolds number of the sediment particle) have also some influence on the equilibrium scour hole radii, r_t and r_a . Experimental data of the scour hole radii, r_t and r_a , obtained from this study as well as from other studies have been used for

validation and general linear relationships have been found for each of the radius. Thus, it may be concluded that the function has a general applicability regardless of the size of the cohesionless sediment and the scale of the experiment.

5. The straightlines for the dimensionless scour hole radii, $\frac{r_t}{d}$ and $\frac{r_a}{d}$, and the theoretical functions found to cross the positive Y-axis at 0.32 and 0.24 respectively. This indicated an incremental effect of the inside tube diameter on the scour hole radii.
6. The experimental data of the dimensionless scour hole radius at the tube level, $\frac{r_t}{d}$ varies linearly with the dimensionless maximum depth of equilibrium scour hole, $\frac{\varepsilon_{rm}}{d}$.
7. A general relationship has been found with $\frac{\varepsilon_{rm}}{d}$ and the theoretical function. This relation was a straightline passing through the origin. Therefore it could be suggested that there is no additional effect of tube inlet diameter on the maximum scour hole depth.
8. The height for critical and general movement also showed general linear relationships with the theoretical function.
9. The straightlines for the maximum depth of equilibrium scour hole and the height for the general movement were almost the same. This might imply that the hydraulic conditions below the tube inlet are the same for both the cases.
10. A similarity could be found when the scour hole profiles were made dimensionless by using the maximum scour depth from the tube inlet as scale for the scour depths and the radius of the equilibrium scour hole at tube level for the radial distance. The

origin of the profile was the tube inlet. The lower part of the profile was fitted with a cubic formula whereas the upper portion was fitted with a straightline. The slope of the scour hole was almost the same and it is within 35° to 40° above the horizontal.

5.2 Conclusions

The main conclusions of this study are as follows:

1. Besides, the densiometric Froude number; the Reynolds number of the particle as well as of the flow through tube are needed to obtain proper scale.
2. The maximum scour hole dimensions (depth and radius) at equilibrium, can be predicted if the tube diameter, flow rate, fluid properties (kinematic viscosity and density); and the particle properties (particle mean diameter, density and the angle of repose) are known.
3. The scour hole profiles are similar in shape and they are fitted with common equations. Therefore, using these equations, the actual scour hole profile can be obtained if the maximum dimensions (depth and radius) at equilibrium are known.

5.3 Recommendations for Future Research

The theoretical derivation assumes the velocity distribution in the boundary layer to be the same as in case of line sink located on the rigid bed. This should be measured with proper accuracy to get the actual shear stress on the sediment bed. The theory for determining the heights for the threshold movement should be studied. The location of the maximum shear stress around the centerline might be necessary to know in order to derive the theory. Bigger experiment scale, and different types of soil and fluid should be used for this purpose.

Although this study covers analyses for the uniform cohesionless sediment materials; investigation should be carried out on other type of soil such as the non-uniform cohesionless sediment and cohesive soils. The role of seepage flow in predicting the equilibrium scour hole dimensions should also be examined. The present study considers the tube inlet which is deeply submerged. The effect of lower submergence of the tube inlet on the scouring should be studied. A similar experiment should be carried out where a stream flow is added perpendicular to the tube axis. Again, the transient nature of the scour hole dimensions should be studied. The generation of the vortex below the tube inlet caused excessive removal of sediment and random values for the scour depth. The present study has not elaborated on this phenomenon. This should be studied further.

REFERENCES

- Apgar, W.J., and Basco, D.R. (1973). "An Experimental and Theoretical Study of Flow Field Surrounding a Pipe Inlet", *TAMU-SG-74-203*, Sea Grant Office, Texas A&M University, College Station, Texas.
- Brahme, S.B. (1983). "Environmental Aspects of Suction Cutterheads", PhD Thesis, Texas A&M University, Texas, USA.
- Breusers, H.N.C., and Raudkivi, A.J. (1991). "Scouring", *Hydraulic Structures Design Manual 2*, International Association for Hydraulic Research, A.A. Balkema, Rotterdam.
- Cheng, N.S., and Chiew, Y.M. (1999). "Incipient Sediment Motion with Upward Seepage", *Journal of Hydraulic Research*, IAHR, Vol. 37, No. 5, pp. 665-681.
- Chiew, Y.M., and Parker, G. (1994). "Incipient Sediment Motion on Non-Horizontal Slopes", *Journal of Hydraulic Research*, IAHR, Vol. 32, No. 5, pp. 649-660.
- Das, B.M. (2002). *Principles of Geotechnical Engineering*, 5th ed., Thomson Learning Inc., USA.
- Epskamp, R.J.C., and Nedam, B. (1995). "Environmental of Dredging Activities", Sediment Remediation '95, an international exchange of experience in the remediation of contaminated sediments, Windsor, Canada, May 8-10, 1995.
- Freeze, R.A, and Cherry, J. A. (1979). *Groundwater*, Prentice Hall, N.J., pp. 604.
- Gladigau, L.N. (1975). "Interactions Between Sand and Water", *Proceedings of the Sixth World Dredging Conference*, WODCON VI, Taipei, Taiwan, pp. 261-294.
- Herbich, J.B. (2000). *Handbook of Dredging Engineering*, 2nd Edition, McGraw-Hill Book Company, New York, USA.
- Herbich, J.B., and Brahme, S.B. (1991). "Literature Review and Technical Evaluation of Sediment Resuspension During Dredging", Center for Dredging Studies, Civil Engineering Department, Texas A & M University, January, 1991, p. 41.
- International Joint Commission (IJC). (1985). "Report on Great Lakes Water Quality", Great Lakes Water Quality Board, Kingston, Ontario, Canada, p. 212.
- Julien, P.Y. (1998). *Erosion and Sedimentation*, First paperback edition, Cambridge University Press, NY, USA, pp 112-117.

- Kramer, H. (1935). "Sand mixture and Sand Movement in Fluvial Model", *Trans.*, ASCE, Vol. 100, pp. 798-988.
- Mih, W.C., and Kabir, J. (1983). "Impingement of Water Jets on Nonuniform Streambed", *Journal of Hydraulic Engineering*, ASCE, Vol. 109, No. 4, pp 536-548.
- Parthasarathy, S.P. (1969). "The Transient Boundary Layer Produced by a Sink on a Plane Wall", PhD. Thesis, California Institute of Technology, Pasadena, California, USA.
- Raudkivi, A.J. (1998). *Loose Boundary Hydraulics*, A.A. Balkema, Rotterdam, Netherlands.
- Rehbinder, G. (1994). "Sediment Removal with a Siphon at Critical Flux", *Journal of Hydraulic Research*, IAHR, Vol. 132, No. 6, pp. 845-860.
- Salzmann, H. (1977). "A Laboratory Study of Fluid and Soil Mechanics Process During Hydraulic Design", Translated by Adam, G.M. and Edited by Basco, D.R., TAMU-SG-77-204, CDS Report No. 184. Texas A & M University, Texas, USA.
- Schlichting, H., and Gersten, K. (2000). *Boundary-Layer Theory*, 8th ed., Springer-Verlag Berlin Heidelberg New York, Germany.
- Shields, A. (1936). "Application of Similarity Principles, and Turbulence Research to Bed-Load Movement", California Institute of Technology, Pasadena (translated from German).
- Simons, D.B. (1957), "Theory and design of stable channels in alluvial material", P.hD. dissertation, Colorado State University, USA.
- Slotta, L.S. (1968). "Flow Visualization Techniques Used in Dredge Cutterhead Evaluation", *Proceeding of the 1968 World Dredging Conference*, WODCON II, Rotterdam, Holland, pp. 56-77.
- Topping, J. (1957). *Errors of Observation and Their Treatment*, The Institute of Physics, London.
- US Environmental Protection Agency (USEPA). (1994). "Assessment and Remediation of Contaminated Sediments (ARCS) Program", *EPA/905/R-94/003*, Great Lakes National Program Office, Chicago, Illinois.
- Vallentine, H.R. (1959). *Applied Hydromechanics*, First edition, Butterworths & Co. (Publishers) Limited, London.

- Vanoni, V.A. and Brooks, N.H. (1975). "Sedimentation engineering", *Manuals and Reports on Engineering*, Practice No. 54, ASCE, New York.
- White, C.M. (1940), "The Equilibrium of Grains on the Bed of Stream", *Proceedings of the Royal Society, Series A*, Vol. 174, London, pp. 322-334.
- Yang, C.T. (1996). *Sediment Transport: Theory and Practice*, The Mc-Graw Hill Companies, Inc. New York.

APPENDIX A
Experimental Results

The variables used for all tests

Sand Size, D (mm)	0.6
Depth of water, Z (cm)	23
Bucket volume (L)	11.56

Test No. T2/01.95

	z_0 (cm)	r (cm)	Depth reading (mm)	ε (cm)	Horizontal position (cm)	r (cm)	Depth reading (mm)	ε (cm)
Test No. T2/01.95	0.00	r_b (cm)+ve	3.00	0.00	z_0 (cm)	1.39	r_b (cm)+ve	3.00
d (cm)	1.39	r_b (cm)-ve	3.10	d (cm)	20.00	r_b (cm)-ve	2.80	
Time to Equilibrium (min)	20.00	r_b (cm)-ve	3.05	Time to Equilibrium (min)	20.00	r_b (cm)-ve	2.80	
Water temp (°C)	19.50	average r_b (cm)	3.05	Water temp (°C)	19.50	average r_b (cm)	2.90	
Tube position (cm)	86.80	ε_m (cm)+ve	-1.02	Tube position (cm)	87.50	ε_m (cm)+ve	-1.01	
Time to fill (s)	39.32	ε_m (cm)-ve	-1.07	Time to fill (s)	39.32	ε_m (cm)-ve	-1.07	
Q (L/s)	0.29	average ε_m (cm)	-1.04	Q (L/s)	0.29	average ε_m (cm)	-1.04	
Test No. T2/01.95								
Horizontal position (cm)	r (cm)	Depth reading (mm)	ε (cm)		Horizontal position (cm)	r (cm)	Depth reading (mm)	ε (cm)
83.70	-3.10	0.00	0.00		84.70	-2.80	0.00	0.00
84.00	-2.80	1.56	-0.16		85.10	-2.40	2.44	-0.24
84.40	-2.40	5.08	-0.51		85.50	-2.00	5.87	-0.59
84.80	-2.00	8.08	-0.81		85.90	-1.60	7.94	-0.79
85.20	-1.60	9.12	-0.91		86.30	-1.20	9.26	-0.93
85.60	-1.20	10.38	-1.04		86.70	-0.80	10.65	-1.07
86.00	-0.80	10.65	-1.07		87.10	-0.40	9.54	-0.95
86.40	-0.40	9.87	-0.99		87.50	0.00	8.14	-0.81
86.80	0.00	8.22	-0.82		87.90	0.40	9.23	-0.92
87.20	0.40	9.77	-0.98		88.30	0.80	10.10	-1.01
87.60	0.80	10.24	-1.02		88.70	1.20	9.42	-0.94
88.00	1.20	9.72	-0.97		89.10	1.60	8.68	-0.87
88.40	1.60	8.12	-0.81		89.50	2.00	6.90	-0.69
88.80	2.00	5.62	-0.56		89.90	2.40	3.83	-0.38
89.20	2.40	3.24	-0.32		90.30	2.80	1.81	-0.18
89.60	2.80	0.20	-0.02		90.50	3.00	0.00	0.00
89.80	3.00	0.00	0.00					

Test No. T2/01.90

z_0 (cm)	0.00	r_b (cm)+ve	2.90	z_0 (cm)	0.00	r_b (cm)+ve	2.60
d (cm)	1.39	r_b (cm)-ve	2.80	d (cm)	1.39	r_b (cm)-ve	2.70
Time to Equilibrium (min)	20.00	average r_b (cm)	2.85	Time to Equilibrium (min)	20.00	average r_b (cm)	2.65
Water temp (°C)	19.50	ε_m (cm)+ve	-1.05	Water temp (°C)	19.50	ε_m (cm)+ve	-0.99
Tube position (cm)	87.60	ε_m (cm)-ve	-1.16	Tube position (cm)	87.70	ε_m (cm)-ve	-0.95
Time to fill (s)	40.34	average ε_m (cm)	-1.11	Time to fill (s)	57.02	ε_m (cm)-ve	-0.95
Q (L/s)	0.29			Q (L/s)	0.20	average ε_m (cm)	-0.97
Horizontal position (cm)	r (cm)	Depth reading (mm)	ε (cm)	Horizontal position (cm)	r (cm)	Depth reading (mm)	ε (cm)
84.80	-2.80	0.00	0.00	85.00	-2.70	0.00	0.00
85.20	-2.40	2.72	-0.27	85.30	-2.40	0.91	-0.09
85.60	-2.00	6.30	-0.63	85.70	-2.00	3.49	-0.35
86.00	-1.60	9.17	-0.92	86.10	-1.60	5.96	-0.60
86.40	-1.20	10.35	-1.04	86.50	-1.20	8.26	-0.83
86.80	-0.80	11.62	-1.16	86.90	-0.80	9.53	-0.95
87.20	-0.40	10.80	-1.08	87.30	-0.40	9.42	-0.94
87.60	0.00	8.52	-0.85	87.70	0.00	7.60	-0.76
88.00	0.40	9.72	-0.97	88.10	0.40	8.92	-0.89
88.40	0.80	10.49	-1.05	88.50	0.80	9.88	-0.99
88.80	1.20	10.22	-1.02	88.90	1.20	8.81	-0.88
89.20	1.60	8.91	-0.89	89.30	1.60	6.97	-0.70
89.60	2.00	6.26	-0.63	89.70	2.00	4.71	-0.47
90.00	2.40	4.05	-0.41	90.10	2.40	1.53	-0.15
90.40	2.80	1.08	-0.11	90.30	2.60	0.00	0.00
90.50	2.90	0.00	0.00				

Test No. T2/01.34

z_0 (cm)	0.00	r_b (cm)+ve	2.60	z_0 (cm)	0.00	r_b (cm)-ve	2.70
d (cm)	1.39	r_b (cm)-ve	2.70	d (cm)	1.39	r_b (cm)-ve	2.70
Time to Equilibrium (min)	20.00	average r_b (cm)	2.65	Time to Equilibrium (min)	20.00	average r_b (cm)	2.65
Water temp (°C)	19.50	ε_m (cm)+ve	-0.99	Water temp (°C)	19.50	ε_m (cm)+ve	-0.99
Tube position (cm)	87.60	ε_m (cm)-ve	-0.95	Tube position (cm)	87.70	ε_m (cm)-ve	-0.95
Time to fill (s)	40.34	average ε_m (cm)	-0.95	Time to fill (s)	57.02	ε_m (cm)-ve	-0.95
Q (L/s)	0.29		-0.97	Q (L/s)	0.20	average ε_m (cm)	-0.97
Horizontal position (cm)	r (cm)	Depth reading (mm)	ε (cm)	Horizontal position (cm)	r (cm)	Depth reading (mm)	ε (cm)
84.80	-2.80	0.00	0.00	85.00	-2.70	0.00	0.00
85.20	-2.40	2.72	-0.27	85.30	-2.40	0.91	-0.09
85.60	-2.00	6.30	-0.63	85.70	-2.00	3.49	-0.35
86.00	-1.60	9.17	-0.92	86.10	-1.60	5.96	-0.60
86.40	-1.20	10.35	-1.04	86.50	-1.20	8.26	-0.83
86.80	-0.80	11.62	-1.16	86.90	-0.80	9.53	-0.95
87.20	-0.40	10.80	-1.08	87.30	-0.40	9.42	-0.94
87.60	0.00	8.52	-0.85	87.70	0.00	7.60	-0.76
88.00	0.40	9.72	-0.97	88.10	0.40	8.92	-0.89
88.40	0.80	10.49	-1.05	88.50	0.80	9.88	-0.99
88.80	1.20	10.22	-1.02	88.90	1.20	8.81	-0.88
89.20	1.60	8.91	-0.89	89.30	1.60	6.97	-0.70
89.60	2.00	6.26	-0.63	89.70	2.00	4.71	-0.47
90.00	2.40	4.05	-0.41	90.10	2.40	1.53	-0.15
90.40	2.80	1.08	-0.11	90.30	2.60	0.00	0.00
90.50	2.90	0.00	0.00				

Test No. T2/0/1.20

Horizontal position (cm)	<i>r</i> (cm)	Depth reading (mm)	<i>ε</i> (cm)
85.20	-2.60	0.00	0.00
85.40	-2.40	0.38	-0.04
85.80	-2.00	3.24	-0.32
86.20	-1.60	5.55	-0.56
86.60	-1.20	7.69	-0.77
87.00	-0.80	8.64	-0.86
87.40	-0.40	7.86	-0.79
87.80	0.00	6.33	-0.63
88.20	0.40	7.55	-0.76
88.60	0.80	8.46	-0.85
89.00	1.20	7.84	-0.78
89.40	1.60	6.14	-0.61
89.80	2.00	2.76	-0.28
90.20	2.40	0.16	-0.02
90.30	2.50	0.00	0.00

Test No. T2/0/1.95

<i>z</i> ₀ (cm)	<i>r</i> _b (cm)+ve	2.50	0.00	<i>r</i> _b (cm)+ve	3.00
<i>d</i> (cm)	<i>r</i> _b (cm)-ve	2.60	<i>d</i> (cm)	<i>r</i> _b (cm)-ve	3.20
Time to Equilibrium (min)	20.00	average <i>r</i> _b (cm)	2.55	Time to Equilibrium (min)	120.00
Water temp (°C)	19.50	<i>ε</i> _m (cm)+ve	-0.85	Water temp (°C)	19.00
Tube position (cm)	87.80	<i>ε</i> _m (cm)-ve	-0.86	Tube position (cm)	87.80
Time to fill (s)	64.03	average <i>ε</i> _m (cm)	-0.86	Time to fill (s)	39.32
<i>Q</i> (L/s)	0.18	<i>Q</i> (L/s)	-0.86	<i>Q</i> (L/s)	0.29
				average <i>ε</i> _m (cm)	-1.09

Test No. T2/0/1.14

Horizontal position (cm)	<i>r</i> (cm)	Depth reading (mm)	<i>ε</i> (cm)
77.40	-2.50	-0.90	0.00
77.50	-2.40	-0.50	-0.04
77.90	-2.00	2.37	-0.31
78.30	-1.60	4.49	-0.51
78.70	-1.20	6.87	-0.74
79.10	-0.80	7.23	-0.76
79.50	-0.40	6.58	-0.68
79.90	0.00	5.74	-0.59
80.30	0.40	7.54	-0.76
80.70	0.80	7.96	-0.79
81.10	1.20	7.08	-0.69
81.50	1.60	5.16	-0.48
81.90	2.00	2.48	-0.20
82.20	2.30	0.55	0.00

Test No. T2/0/0.80

	<i>z₀</i> (cm)	<i>r_b</i> (cm)+ve	<i>r_b</i> (cm)-ve	<i>d</i> (cm)	<i>z₀</i> (cm)	<i>r_b</i> (cm)+ve	<i>r_b</i> (cm)-ve	<i>d</i> (cm)
<i>d</i> (cm)	1.39			2.30		1.39		2.10
Time to Equilibrium (min)	10.00	<i>r_b</i> (cm)-ve		2.50	Time to Equilibrium (min)	10.00	<i>r_b</i> (cm)-ve	2.10
Water temp (°C)	17.00	average <i>r_b</i> (cm)		2.40	Water temp (°C)	17.00	average <i>r_b</i> (cm)	2.10
Tube position (cm)	79.90	<i>ε_m</i> (cm)+ve		-0.79	Tube position (cm)	79.70	<i>ε_m</i> (cm)+ve	-0.60
Time to fill (s)	67.37	<i>ε_m</i> (cm)-ve		-0.76	Time to fill (s)	95.83	<i>ε_m</i> (cm)-ve	-0.65
<i>Q</i> (L/s)	0.17	average <i>ε_m</i> (cm)		-0.77	<i>Q</i> (L/s)	0.12	average <i>ε_m</i> (cm)	-0.62
					Horizontal position (cm)	<i>r</i> (cm)	Depth reading (mm)	<i>ε</i> (cm)

Test No. T2/0/0.68

Horizontal position (cm)	<i>r</i> (cm)	Depth reading (mm)	<i>ε</i> (cm)
77.70	-2.00	-0.95	0.00
77.90	-1.80	0.41	-0.13
78.20	-1.50	1.47	-0.23
78.50	-1.20	4.03	-0.49
78.80	-0.90	4.72	-0.55
79.10	-0.60	4.97	-0.57
79.40	-0.30	4.65	-0.53
79.70	0.00	4.04	-0.47
80.00	0.30	4.60	-0.52
80.30	0.60	5.29	-0.58
80.60	0.90	4.72	-0.52
80.90	1.20	3.00	-0.35
81.20	1.50	1.36	-0.18
81.50	1.80	-0.37	0.00

Test No. T2/0/1.03

Test No. T2/0/1.03	
<i>z</i> ₀ (cm)	0.00
<i>d</i> (cm)	1.39
Time to Equilibrium (min)	10.00
Water temp (°C)	17.00
Tube position (cm)	79.70
Time to fill (s)	113.05
<i>Q</i> (L/s)	0.10
<i>z</i> ₀ (cm)	0.00
<i>d</i> (cm)	1.39
Time to Equilibrium (min)	10.00
Water temp (°C)	17.00
Tube position (cm)	79.90
Time to fill (s)	74.64
<i>Q</i> (L/s)	0.15
<i>r</i> _b (cm)+ve	1.39
<i>r</i> _b (cm)-ve	10.00
average <i>r</i> _b (cm)	17.00
<i>ε</i> _m (cm)+ve	17.00
<i>ε</i> _m (cm)-ve	79.90
average <i>ε</i> _m (cm)	74.64
<i>r</i> (cm)	0.15
Depth reading (mm)	0.15
<i>ε</i> (cm)	0.00

Test No. T2/0/1.16

Horizontal position (cm)	<i>r</i> (cm)	Depth reading (mm)	<i>ε</i> (cm)
78.00	-2.40	-1.56	0.00
78.30	-2.10	-0.31	-0.12
78.60	-1.80	2.12	-0.35
78.90	-1.50	3.56	-0.48
79.20	-1.20	5.06	-0.63
79.50	-0.90	5.92	-0.70
79.80	-0.60	6.45	-0.75
80.10	-0.30	6.11	-0.70
80.40	0.00	4.74	-0.56
80.70	0.30	4.98	-0.57
81.00	0.60	6.00	-0.66
81.30	0.90	6.36	-0.69
81.60	1.20	6.06	-0.65
81.90	1.50	4.58	-0.50
82.20	1.80	3.45	-0.37
82.50	2.10	1.24	-0.14
82.80	2.40	-0.10	0.00

Test No. T2/0/0.64

	<i>z₀</i> (cm)	<i>r_b</i> (cm)+ve	<i>r_b</i> (cm)-ve	<i>d</i> (cm)	<i>z₀</i> (cm)	<i>r_b</i> (cm)+ve	<i>r_b</i> (cm)-ve	<i>d</i> (cm)
<i>d</i> (cm)	1.39	<i>r_b</i> (cm)+ve	<i>r_b</i> (cm)-ve	2.40	0.00	1.39	<i>r_b</i> (cm)+ve	2.10
Time to Equilibrium (min)	10.00	<i>r_b</i> (cm)-ve	average <i>r_b</i> (cm)	2.40	<i>d</i> (cm)	10.00	<i>r_b</i> (cm)-ve	1.90
Water temp (°C)	21.00	average <i>r_b</i> (cm)	2.40	Time to Equilibrium (min)	10.00	average <i>r_b</i> (cm)	21.00	2.00
Tube position (cm)	80.40	<i>ε_m</i> (cm)+ve	-0.69	Water temp (°C)	21.00	<i>ε_m</i> (cm)+ve	80.40	-0.44
Time to fill (s)	66.36	<i>ε_m</i> (cm)-ve	-0.75	Tube position (cm)	21.00	<i>ε_m</i> (cm)-ve	120.41	-0.45
<i>Q</i> (L/s)	0.17	average <i>ε_m</i> (cm)	-0.72	Time to fill (s)	120.41	average <i>ε_m</i> (cm)	0.10	-0.44
				<i>Q</i> (L/s)		average <i>ε_m</i> (cm)		

Test No. T2/0/0.34

Horizontal position (cm)	<i>r</i> (cm)	Depth reading (mm)	<i>ε</i> (cm)
78.40	-2.00	-0.85	0.00
78.60	-1.80	0.21	-0.10
78.90	-1.50	2.33	-0.31
79.20	-1.20	3.87	-0.46
79.50	-0.90	4.83	-0.56
79.80	-0.60	5.25	-0.60
80.10	-0.30	4.45	-0.52
80.40	0.00	3.75	-0.44
80.70	0.30	4.64	-0.53
81.00	0.60	5.24	-0.59
81.30	0.90	5.19	-0.58
81.60	1.20	4.13	-0.47
81.90	1.50	2.58	-0.31
82.20	1.80	1.79	-0.23
82.50	2.10	-0.49	0.00

Test No. T2/0/1.55

	<i>z₀</i> (cm)	<i>d</i> (cm)	<i>r_b</i> (cm)+ve	<i>r_b</i> (cm)-ve	<i>r_b</i> (cm)+ve	<i>r_b</i> (cm)-ve	<i>r_b</i> (cm)+ve	<i>r_b</i> (cm)-ve	<i>r_b</i> (cm)+ve	<i>r_b</i> (cm)-ve	<i>r_b</i> (cm)+ve	<i>r_b</i> (cm)-ve
<i>z₀</i> (cm)	0.00				0.00				0.00			
<i>d</i> (cm)	1.39		<i>r_b</i> (cm)+ve	2.10		<i>r_b</i> (cm)-ve	1.39		<i>r_b</i> (cm)+ve	2.40		
Time to Equilibrium (min)	1.00		<i>r_b</i> (cm)-ve	2.00		Time to Equilibrium (min)	10.00		<i>r_b</i> (cm)-ve	2.50		
Water temp (°C)	21.00		average <i>r_b</i> (cm)	2.05		Water temp (°C)	24.00		average <i>r_b</i> (cm)	2.45		
Tube position (cm)	80.40		<i>ε_m</i> (cm)+ve	-0.59		Tube position (cm)	80.40		<i>ε_m</i> (cm)+ve	-0.81		
Time to fill (s)	228.31		<i>ε_m</i> (cm)-ve	-0.60		Time to fill (s)	49.34		<i>ε_m</i> (cm)-ve	-0.83		
<i>Q</i> (L/s)	0.05		average <i>ε_m</i> (cm)	-0.59		<i>Q</i> (L/s)	0.23		average <i>ε_m</i> (cm)	-0.82		
	<i>z₀</i> (cm)	<i>d</i> (cm)	<i>r</i> (cm)	Depth reading (mm)	<i>ε</i> (cm)	Horizontal position (cm)	<i>r</i> (cm)	Depth reading (mm)	<i>r</i> (cm)	Depth reading (mm)	<i>r</i> (cm)	Depth reading (mm)

Test No. T2/0/0.68

Horizontal position (cm)	<i>r</i> (cm)	Depth reading (mm)	<i>ε</i> (cm)
73.3	-2.00	51.86	0.00
73.7	-1.60	53.67	-0.17
74.1	-1.20	56.76	-0.48
74.5	-0.80	58.42	-0.63
74.9	-0.40	59.02	-0.69
75.3	0.00	57.87	-0.56
75.7	0.40	59.24	-0.69
76.1	0.80	59.18	-0.68
76.5	1.20	58.54	-0.61
76.9	1.60	56.19	-0.37
77.3	2.00	53.30	-0.07
77.6	2.30	52.66	0.00

Test No. T2/0/1.63

	<i>z₀</i> (cm)	<i>z₀</i> (cm)	<i>r_b</i> (cm)+ve	<i>d</i> (cm)	<i>d</i> (cm)	<i>r_b</i> (cm)+ve	<i>r_b</i> (cm)-ve	<i>r_b</i> (cm)-ve	<i>r_b</i> (cm)+ve	<i>r_b</i> (cm)-ve	<i>r_b</i> (cm)+ve
<i>d</i> (cm)	0.00	1.39	<i>r_b</i> (cm)+ve	2.30	2.00	1.39	1.39	0.00	2.80	2.50	2.50
Time to Equilibrium (min)	10.00	10.00	<i>r_b</i> (cm)-ve			10.00	10.00				
Water temp (°C)	19.50	average <i>r_b</i> (cm)		2.15		Time to Equilibrium (min)					
Tube position (cm)	75.30	<i>ε_m</i> (cm)+ve		-0.69		Water temp (°C)	7.40	average <i>r_b</i> (cm)	2.65		
Time to fill (s)	112.61	<i>ε_m</i> (cm)-ve		-0.69		Tube position (cm)	73.90	<i>ε_m</i> (cm)+ve	-1.02		
<i>Q</i> (L/s)	0.10	average <i>ε_m</i> (cm)		-0.69		Time to fill (s)	46.94	<i>ε_m</i> (cm)-ve	-1.08		
						<i>Q</i> (L/s)	0.25	average <i>ε_m</i> (cm)	-1.05		

Test No. T2/01.54

Horizontal position (cm)	<i>r</i> (cm)	Depth reading (mm)	<i>ε</i> (cm)	Horizontal position (cm)	<i>r</i> (cm)	Depth reading (mm)	<i>ε</i> (cm)
72.0	-2.80	49.24	0.00	71.5	-2.40	50.22	0.00
72.4	-2.40	51.42	-0.21	71.9	-2.00	52.88	-0.27
72.8	-2.00	55.72	-0.63	72.3	-1.60	55.64	-0.55
73.2	-1.60	58.49	-0.89	72.7	-1.20	57.69	-0.75
73.6	-1.20	59.98	-1.03	73.1	-0.80	58.46	-0.83
74.0	-0.80	60.96	-1.11	73.5	-0.40	58.06	-0.79
74.4	-0.40	60.14	-1.02	73.9	0.00	56.35	-0.62
74.8	0.00	58.06	-0.80	74.3	0.40	57.81	-0.77
75.2	0.40	59.47	-0.93	74.7	0.80	57.72	-0.76
75.6	0.80	60.24	-1.00	75.1	1.20	56.81	-0.67
76.0	1.20	59.43	-0.90	75.5	1.60	55.81	-0.58
76.4	1.60	56.84	-0.63	75.9	2.00	52.07	-0.20
76.8	2.00	54.05	-0.34	76.2	2.30	50.02	0.00
77.2	2.40	52.25	-0.15				
77.3	2.50	50.76	0.00				

Test No. T2/01.30

<i>z</i> ₀ (cm)	<i>z</i> ₀ (cm)	<i>d</i> (cm)	<i>d</i> (cm)	<i>r</i> _b (cm)+ve	<i>r</i> _b (cm)-ve	Time to Equilibrium (min)	Time to Equilibrium (min)	Water temp (°C)	average <i>r</i> _b (cm)	average <i>r</i> _b (cm)	Tube position (cm)	Tube position (cm)	Time to fill (s)	Time to fill (s)	<i>Q</i> (L/s)	average <i>ε</i> _m (cm)	average <i>ε</i> _m (cm)	average <i>ε</i> _m (cm)
0.00	0.00	1.39	2.50	1.39	2.30	10.00	10.00	21.00	1.39	2.30	73.90	73.90	58.94	58.94	0.20	0.20	0.20	0.20
<i>d</i> (cm)	<i>d</i> (cm)	10.00	2.80	<i>r</i> _b (cm)-ve	2.40													
Time to Equilibrium (min)	Time to Equilibrium (min)	21.00	2.65	average <i>r</i> _b (cm)	2.35													
Water temp (°C)	Water temp (°C)	74.80	-1.00	<i>ε</i> _m (cm)+ve	-0.77													
Tube position (cm)	Tube position (cm)	49.86	-1.11	<i>ε</i> _m (cm)-ve	-0.83													
Time to fill (s)	Time to fill (s)	0.23	-1.06	average <i>ε</i> _m (cm)	-0.80													
<i>Q</i> (L/s)	<i>Q</i> (L/s)																	

Test No. T2/0/0.70

Horizontal position (cm)	<i>r</i> (cm)	Depth reading (mm)	<i>ε</i> (cm)
70.9	-2.20	0.20	0.00
71.1	-2.00	1.95	-0.18
71.5	-1.60	4.56	-0.44
71.9	-1.20	7.15	-0.70
72.3	-0.80	7.86	-0.77
72.7	-0.40	7.21	-0.71
73.1	0.00	6.47	-0.63
73.5	0.40	7.58	-0.75
73.9	0.80	8.01	-0.79
74.3	1.20	7.25	-0.72
74.7	1.60	4.78	-0.47
75.1	2.00	1.28	-0.12
75.3	2.20	0.05	0.00

Test No. T2/0/2.18

	<i>z₀</i> (cm)	<i>r_b</i> (cm)+ve	<i>d</i> (cm)	<i>r_b</i> (cm)-ve	<i>Time to Equilibrium (min)</i>	<i>d</i> (cm)	<i>r_b</i> (cm)+ve	<i>r_b</i> (cm)-ve	<i>Time to Equilibrium (min)</i>	<i>Water temp (°C)</i>	<i>Tube position (cm)</i>	<i>average r_b</i> (cm)	<i>ε_m</i> (cm)+ve	<i>ε_m</i> (cm)-ve	<i>Time to fill (s)</i>	<i>Q</i> (L/s)	<i>average ε_m</i> (cm)	<i>average ε_m</i> (cm)	<i>Depth reading (mm)</i>	<i>ε</i> (cm)
	0.00	1.39	2.20	2.20	10.00	1.39	10.00	10.00	22.00	22.00	average <i>r_b</i> (cm)	22.00	22.00	22.00	35.10	0.33	0.33	0.33	-1.05	
<i>d</i> (cm)	0.00	1.39	2.20	2.20	10.00	1.39	10.00	10.00	22.00	22.00	average <i>r_b</i> (cm)	22.00	22.00	22.00	35.10	0.33	0.33	0.33	-1.05	
Time to Equilibrium (min)	10.00	<i>r_b</i> (cm)-ve	2.20	average <i>r_b</i> (cm)	2.20	average <i>r_b</i> (cm)	2.20	average <i>r_b</i> (cm)	2.20	average <i>r_b</i> (cm)	35.10	0.33	0.33	0.33	-1.05					
Water temp (°C)	21.00	average <i>r_b</i> (cm)	2.20	average <i>r_b</i> (cm)	2.20	average <i>r_b</i> (cm)	2.20	average <i>r_b</i> (cm)	2.20	average <i>r_b</i> (cm)	35.10	0.33	0.33	0.33	-1.05					
Tube position (cm)	73.10	<i>ε_m</i> (cm)+ve	-0.79	<i>ε_m</i> (cm)-ve	-0.77	<i>ε_m</i> (cm)-ve	-0.77	<i>ε_m</i> (cm)-ve	-0.77	<i>ε_m</i> (cm)-ve	35.10	0.33	0.33	0.33	-1.05					
Time to fill (s)	110.16	<i>ε_m</i> (cm)-ve	-0.77	average <i>ε_m</i> (cm)	-0.78	average <i>ε_m</i> (cm)	-0.78	average <i>ε_m</i> (cm)	-0.78	average <i>ε_m</i> (cm)	35.10	0.33	0.33	0.33	-1.05					
<i>Q</i> (L/s)	0.10	average <i>ε_m</i> (cm)	-0.78	average <i>ε_m</i> (cm)	-0.78	average <i>ε_m</i> (cm)	-0.78	average <i>ε_m</i> (cm)	-0.78	average <i>ε_m</i> (cm)	35.10	0.33	0.33	0.33	-1.05					

Test No. T2/0/2.33

Horizontal position (cm)	<i>r</i> (cm)	Depth reading (mm)	<i>ε</i> (cm)
76.90	-3.10	-1.39	0.00
77.50	-2.50	2.17	-0.35
78.00	-2.00	6.21	-0.74
78.50	-1.50	8.16	-0.93
78.80	-1.20	9.84	-1.09
79.10	-0.90	10.24	-1.12
79.40	-0.60	9.48	-1.04
79.70	-0.30	9.03	-0.99
80.00	0.00	8.56	-0.94
80.30	0.30	8.75	-0.95
80.60	0.60	9.89	-1.06
80.90	0.90	9.37	-1.00
81.20	1.20	9.18	-0.98
81.50	1.50	8.31	-0.89
82.00	2.00	7.57	-0.80
82.50	2.50	4.02	-0.44
83.00	3.00	-0.28	0.00

Test No. T1/0/3.87

	<i>z₀</i> (cm)	<i>r_b</i> (cm)+ve	<i>r_b</i> (cm)-ve	<i>d</i> (cm)	<i>z₀</i> (cm)	<i>d</i> (cm)	<i>r_b</i> (cm)+ve	<i>r_b</i> (cm)-ve	Time to Equilibrium (min)	Time to Equilibrium (min)	<i>r_b</i> (cm)+ve	<i>r_b</i> (cm)-ve	Water temp (°C)	Tube position (cm)	average <i>r_b</i> (cm)	<i>ε_m</i> (cm)+ve	<i>ε_m</i> (cm)-ve	Time to fill (s)	Time to fill (s)	<i>ε_m</i> (cm)+ve	<i>ε_m</i> (cm)-ve	Q (L/s)	average <i>z_m</i> (cm)	average <i>z_m</i> (cm)	<i>ε</i> (cm)
	0.00	1.39	10.00	3.00	0.00	3.10	10.00	10.00	18.00	18.00	0.97	0.97	2.90	2.90	2.90	78.00	78.00	40.86	40.86	0.28	0.28	0.00	0.00	0.00	
Time to Equilibrium (min)	22.00	average <i>r_b</i> (cm)	8.00	3.05	22.00	average <i>r_b</i> (cm)	8.00	8.00	18.00	18.00	0.97	0.97	2.90	2.90	2.90	78.00	78.00	40.86	40.86	0.28	0.28	0.00	0.00	0.00	
Water temp (°C)	80.00	<i>ε_m</i> (cm)+ve	32.90	-1.06	80.00	<i>ε_m</i> (cm)+ve	32.90	-1.06	18.00	18.00	0.97	0.97	2.90	2.90	2.90	78.00	78.00	40.86	40.86	0.28	0.28	0.00	0.00	0.00	
Tube position (cm)	32.90	<i>ε_m</i> (cm)-ve	0.35	-1.12	32.90	<i>ε_m</i> (cm)-ve	0.35	-1.12	18.00	18.00	0.97	0.97	2.90	2.90	2.90	78.00	78.00	40.86	40.86	0.28	0.28	0.00	0.00	0.00	
Time to fill (s)																									
<i>Q</i> (L/s)																									

Test No. T1/03.48

Horizontal position (cm)	<i>r</i> (cm)	Depth reading (mm)	<i>ε</i> (cm)
75.60	-2.80	-0.63	0.00
75.70	-2.70	0.00	-0.06
76.00	-2.40	1.50	-0.21
76.30	-2.10	3.97	-0.45
76.60	-1.80	5.84	-0.64
76.90	-1.50	8.35	-0.88
77.20	-1.20	9.11	-0.96
77.50	-0.90	9.97	-1.04
77.80	-0.60	10.08	-1.05
78.10	-0.30	8.98	-0.93
78.40	0.00	7.03	-0.73
78.70	0.30	8.49	-0.88
79.00	0.60	8.98	-0.92
79.30	0.90	8.52	-0.87
79.60	1.20	7.19	-0.74
79.90	1.50	6.64	-0.68
80.20	1.80	4.39	-0.45
80.50	2.10	2.22	-0.23
80.80	2.40	1.30	-0.13
81.00	2.60	0.00	0.00

Test No. T1/03.21

	<i>z₀</i> (cm)	<i>d</i> (cm)	<i>r_b</i> (cm)+ve	<i>r_b</i> (cm)-ve	<i>d</i> (cm)	<i>r_b</i> (cm)+ve	<i>r_b</i> (cm)-ve	Time to Equilibrium (min)	Water temp (°C)	Tube position (cm)	average <i>r_b</i> (cm)	<i>ε_m</i> (cm)+ve	<i>ε_m</i> (cm)-ve	Time to fill (s)	<i>Q</i> (L/s)	average <i>ε_m</i> (cm)	<i>ε</i> (cm)
	0.00	0.97	2.60	0.97	0.97	2.50											
	1.00	1.00	2.80	10.00	10.00	2.60											
Time to Equilibrium (min)	18.00	average <i>r_b</i> (cm)	2.70	18.00	average <i>r_b</i> (cm)	2.55											
Water temp (°C)	78.40	<i>ε_m</i> (cm)+ve	-0.92	78.30	<i>ε_m</i> (cm)+ve	-0.91											
Tube position (cm)	45.44	<i>ε_m</i> (cm)-ve	-1.05	49.23	<i>ε_m</i> (cm)-ve	-0.91											
Time to fill (s)	0.25	average <i>ε_m</i> (cm)	-0.98	0.23	average <i>ε_m</i> (cm)	-0.91											
<i>Q</i> (L/s)																	

Test No. T1/0/2.53

Horizontal position (cm)	<i>r</i> (cm)	Depth reading (mm)	<i>ε</i> (cm)
76.00	-2.40	0.00	0.00
76.30	-2.10	0.31	-0.03
76.60	-1.80	2.46	-0.25
76.90	-1.50	5.03	-0.50
77.20	-1.20	6.54	-0.65
77.50	-0.90	6.96	-0.70
77.80	-0.60	7.67	-0.77
78.10	-0.30	6.86	-0.69
78.40	0.00	6.13	-0.61
78.70	0.30	7.18	-0.72
79.00	0.60	7.38	-0.74
79.30	0.90	7.83	-0.78
79.60	1.20	5.62	-0.56
79.90	1.50	4.15	-0.42
80.20	1.80	3.10	-0.31
80.50	2.10	0.23	-0.02
80.60	2.20	0.00	0.00

Test No. T1/0/1.95

	<i>z₀</i> (cm)	<i>r_b</i> (cm)+ve	<i>r_b</i> (cm)-ve	<i>d</i> (cm)	<i>z₀</i> (cm)	<i>r_b</i> (cm)+ve	<i>r_b</i> (cm)-ve	<i>d</i> (cm)	<i>z₀</i> (cm)	<i>r_b</i> (cm)+ve	<i>r_b</i> (cm)-ve	<i>d</i> (cm)
<i>d</i> (cm)	0.97	<i>r_b</i> (cm)+ve	<i>r_b</i> (cm)-ve	2.20	0.00	0.97	<i>r_b</i> (cm)+ve	2.00	0.00	0.97	<i>r_b</i> (cm)+ve	2.00
Time to Equilibrium (min)	10.00	<i>r_b</i> (cm)-ve	average <i>r_b</i> (cm)	2.40	Time to Equilibrium (min)	10.00	<i>r_b</i> (cm)-ve	1.90	Time to Equilibrium (min)	10.00	<i>r_b</i> (cm)-ve	1.90
Water temp (°C)	22.00	average <i>r_b</i> (cm)	2.30	Water temp (°C)	21.00	average <i>r_b</i> (cm)	1.95	Water temp (°C)	21.00	average <i>r_b</i> (cm)	1.95	Water temp (°C)
Tube position (cm)	78.40	<i>ε_m</i> (cm)+ve	-0.78	Tube position (cm)	78.50	<i>ε_m</i> (cm)+ve	-0.76	Tube position (cm)	78.50	<i>ε_m</i> (cm)+ve	-0.76	Tube position (cm)
Time to fill (s)	62.46	<i>ε_m</i> (cm)-ve	-0.77	Time to fill (s)	81.15	<i>ε_m</i> (cm)-ve	-0.78	Time to fill (s)	81.15	<i>ε_m</i> (cm)-ve	-0.78	Time to fill (s)
<i>Q</i> (L/s)	0.19	average <i>ε_m</i> (cm)	-0.78	<i>Q</i> (L/s)	0.14	average <i>ε_m</i> (cm)	-0.77	<i>Q</i> (L/s)	0.14	average <i>ε_m</i> (cm)	-0.77	<i>Q</i> (L/s)

Test No. T1/0/2.87

Horizontal position (cm)	<i>r</i> (cm)	Depth reading (mm)	<i>ε</i> (cm)
76.00	-2.30	-0.32	0.00
76.20	-2.10	1.69	-0.20
76.50	-1.80	3.04	-0.33
76.80	-1.50	5.52	-0.57
77.10	-1.20	6.94	-0.71
77.40	-0.90	8.44	-0.85
77.70	-0.60	8.52	-0.86
78.00	-0.30	7.92	-0.79
78.30	0.00	6.77	-0.67
78.60	0.30	7.28	-0.72
78.90	0.60	8.36	-0.82
79.20	0.90	8.23	-0.80
79.50	1.20	6.50	-0.63
79.80	1.50	4.41	-0.41
80.10	1.80	2.75	-0.24
80.40	2.10	1.13	-0.07
80.60	2.30	0.42	0.00

Test No. T1/0/2.78

	<i>z</i> ₀ (cm)	<i>r</i> _b (cm)+ve	<i>d</i> (cm)	<i>r</i> _b (cm)-ve	<i>d</i> (cm)	<i>r</i> _b (cm)+ve	<i>r</i> _b (cm)-ve	<i>r</i> _b (cm)+ve	<i>r</i> _b (cm)-ve	<i>r</i> _b (cm)+ve	<i>r</i> _b (cm)-ve
<i>d</i> (cm)	0.97	<i>r</i> _b (cm)+ve	2.30	<i>r</i> _b (cm)-ve	2.30	<i>r</i> _b (cm)+ve	<i>r</i> _b (cm)-ve	0.97	<i>r</i> _b (cm)+ve	0.97	<i>r</i> _b (cm)-ve
Time to Equilibrium (min)	10.00	<i>r</i> _b (cm)-ve	2.30	average <i>r</i> _b (cm)	2.30	Time to Equilibrium (min)	10.00	<i>r</i> _b (cm)-ve	10.00	<i>r</i> _b (cm)-ve	2.40
Water temp (°C)	21.00	average <i>r</i> _b (cm)	2.30	Water temp (°C)	21.00	average <i>r</i> _b (cm)	21.00	average <i>r</i> _b (cm)	21.00	average <i>r</i> _b (cm)	2.25
Tube position (cm)	78.30	<i>ε</i> _m (cm)+ve	-0.82	Tube position (cm)	78.30	<i>ε</i> _m (cm)+ve	78.30	<i>ε</i> _m (cm)+ve	78.30	<i>ε</i> _m (cm)+ve	-0.80
Time to fill (s)	55.06	<i>ε</i> _m (cm)-ve	-0.86	Time to fill (s)	56.96	<i>ε</i> _m (cm)-ve	56.96	<i>ε</i> _m (cm)-ve	56.96	<i>ε</i> _m (cm)-ve	-0.82
<i>Q</i> (L/s)	0.21	average <i>ε</i> _m (cm)	-0.84	<i>Q</i> (L/s)	0.20	average <i>ε</i> _m (cm)	0.20	average <i>ε</i> _m (cm)	0.20	average <i>ε</i> _m (cm)	-0.81

Test No. T1/0/3.68

Horizontal position (cm)	<i>r</i> (cm)	Depth reading (mm)	<i>ε</i> (cm)
75.80	-2.50	0.19	0.00
75.90	-2.40	1.09	-0.09
76.20	-2.10	3.74	-0.35
76.50	-1.80	5.83	-0.56
76.80	-1.50	7.29	-0.71
77.10	-1.20	9.84	-0.96
77.40	-0.90	10.00	-0.98
77.70	-0.60	10.37	-1.02
78.00	-0.30	9.88	-0.97
78.30	0.00	9.74	-0.95
78.60	0.30	9.96	-0.97
78.90	0.60	10.41	-1.02
79.20	0.90	9.67	-0.94
79.50	1.20	9.34	-0.91
79.80	1.50	7.24	-0.70
80.10	1.80	6.25	-0.60
80.40	2.10	3.66	-0.34
80.70	2.40	1.69	-0.14
80.90	2.60	0.27	0.00

Test No. T3/0/0.86

	<i>z₀</i> (cm)	<i>d</i> (cm)	<i>r_b</i> (cm)+ve	<i>r_b</i> (cm)-ve	<i>d</i> (cm)	<i>z₀</i> (cm)	<i>r_b</i> (cm)+ve	<i>r_b</i> (cm)-ve	<i>d</i> (cm)	<i>z₀</i> (cm)	<i>r_b</i> (cm)+ve	<i>r_b</i> (cm)-ve	<i>d</i> (cm)	<i>Time to Equilibrium (min)</i>	<i>Time to Equilibrium (min)</i>	<i>Water temp (°C)</i>	<i>Tube position (cm)</i>	<i>average r_b</i> (cm)	<i>average r_b</i> (cm)	<i>Water temp (°C)</i>	<i>Tube position (cm)</i>	<i>average r_b</i> (cm)	<i>average r_b</i> (cm)	<i>Water temp (°C)</i>	<i>Tube position (cm)</i>	<i>average r_b</i> (cm)	<i>average r_b</i> (cm)	
Time to Equilibrium (min)	10.00	0.97	2.60	2.50	10.00	0.00	2.04	2.04	10.00	0.00	2.04	2.04	10.00	21.00	21.00	21.00	78.30	78.30	78.30	78.30	41.11	41.11	41.11	41.11	2.75	2.75	2.75	2.75
Water temp (°C)	21.00	10.00	average <i>r_b</i> (cm)																									
Tube position (cm)	78.30	78.30	<i>ε_m</i> (cm)+ve	<i>ε_m</i> (cm)-ve	-1.02	-1.02	-1.02	-1.02	-1.02	-1.02	-1.02	-1.02	-1.02	-1.02	-1.02	-1.02	-1.02	-1.02	-1.02	-1.02	-1.02	-1.02	-1.02	-1.02	-1.02	-1.02		
Time to fill (s)	43.01	43.01	<i>ε_m</i> (cm)-ve	<i>ε_m</i> (cm)-ve	-1.02	-1.02	-1.02	-1.02	-1.02	-1.02	-1.02	-1.02	-1.02	-1.02	-1.02	-1.02	-1.02	-1.02	-1.02	-1.02	-1.02	-1.02	-1.02	-1.02	-1.02	-1.02	-1.02	
<i>Q</i> (L/s)	0.27	0.27	average <i>ε_m</i> (cm)	average <i>ε_m</i> (cm)	-1.02	-1.02	-1.02	-1.02	-1.02	-1.02	-1.02	-1.02	-1.02	-1.02	-1.02	-1.02	-1.02	-1.02	-1.02	-1.02	-1.02	-1.02	-1.02	-1.02	-1.02	-1.02	-1.02	
			<i>Q</i> (L/s)	<i>Q</i> (L/s)	0.28	0.28	average <i>ε_m</i> (cm)																					

Test No. T3/0/0.53

Horizontal position (cm)	<i>r</i> (cm)	Depth reading (mm)	<i>ε</i> (cm)
73.80	-2.40	0.17	0.00
74.10	-2.10	1.55	-0.14
74.40	-1.80	3.35	-0.32
74.70	-1.50	5.44	-0.52
75.00	-1.20	6.38	-0.62
75.30	-0.90	6.60	-0.64
75.60	-0.60	6.51	-0.63
75.90	-0.30	5.89	-0.57
76.20	0.00	5.17	-0.49
76.50	0.30	5.71	-0.55
76.80	0.60	6.20	-0.60
77.10	0.90	6.08	-0.58
77.40	1.20	5.82	-0.56
77.70	1.50	5.10	-0.48
78.00	1.80	3.61	-0.33
78.30	2.10	2.02	-0.17
78.60	2.40	0.28	0.00

Test No. T3/0/0.76

	<i>z₀</i> (cm)	<i>z₀</i> (cm)
<i>d</i> (cm)	0.00	0.00
Time to Equilibrium (min)	2.04	2.40
Water temp (°C)	10.00	2.40
Tube position (cm)	21.00	average <i>r_b</i> (cm)
Time to fill (s)	76.20	<i>ε_m</i> (cm)+ve
<i>Q</i> (L/s)	66.73	<i>ε_m</i> (cm)-ve
	0.17	average <i>ε_m</i> (cm)
	<i>d</i> (cm)	<i>d</i> (cm)
		Time to Equilibrium (min)
		Water temp (°C)
		Tube position (cm)
		Time to fill (s)
		<i>Q</i> (L/s)
	<i>r_b</i> (cm)+ve	<i>r_b</i> (cm)-ve
	<i>r_b</i> (cm)-ve	
	average <i>r_b</i> (cm)	average <i>r_b</i> (cm)
		<i>ε_m</i> (cm)+ve
		<i>ε_m</i> (cm)-ve
		average <i>ε_m</i> (cm)
	<i>ε</i> (cm)	<i>ε</i> (cm)
		Depth reading (mm)
		<i>r</i> (cm)
		Horizontal position (cm)

Test No. T1/0/4.31

Horizontal position (cm)	<i>r</i> (cm)	Depth reading (mm)	<i>ε</i> (cm)
73.40	-2.70	0.14	0.00
73.70	-2.40	1.71	-0.15
74.00	-2.10	4.73	-0.45
74.30	-1.80	7.05	-0.68
74.60	-1.50	8.58	-0.83
74.90	-1.20	9.62	-0.94
75.20	-0.90	9.85	-0.96
75.50	-0.60	9.91	-0.96
75.80	-0.30	10.12	-0.98
76.10	0.00	8.89	-0.85
76.40	0.30	9.86	-0.95
76.70	0.60	9.88	-0.95
77.00	0.90	10.20	-0.98
77.30	1.20	9.90	-0.94
77.60	1.50	8.27	-0.78
77.90	1.80	6.42	-0.59
78.20	2.10	4.59	-0.41
78.50	2.40	2.12	-0.16
78.80	2.70	0.87	-0.03
78.90	2.80	0.58	0.00

Test No. T1/0/5.81

	<i>z₀</i> (cm)	<i>z₀</i> (cm)	<i>d</i> (cm)	<i>d</i> (cm)	<i>r_b</i> (cm)+ve	<i>r_b</i> (cm)-ve	Time to Equilibrium (min)	Time to Equilibrium (min)	<i>r_b</i> (cm)+ve	<i>r_b</i> (cm)-ve	<i>ε_m</i> (cm)+ve	<i>ε_m</i> (cm)-ve	Water temp (°C)	Tube position (cm)	average <i>r_b</i> (cm)	average <i>r_b</i> (cm)	<i>ε_m</i> (cm)+ve	<i>ε_m</i> (cm)-ve	Time to fill (s)	Time to fill (s)	<i>Q</i> (L/s)	<i>Q</i> (L/s)	average <i>ε_m</i> (cm)	average <i>ε_m</i> (cm)	<i>Q</i> (L/s)	<i>Q</i> (L/s)	average <i>ε_m</i> (cm)	average <i>ε_m</i> (cm)
	0.00	0.97	<i>r_b</i> (cm)+ve	2.80			0.00	0.97	<i>r_b</i> (cm)+ve	3.20																		
<i>d</i> (cm)	0.97	10.00	<i>r_b</i> (cm)-ve	2.70			10.00	10.00	<i>r_b</i> (cm)-ve	3.30																		
Time to Equilibrium (min)	10.00		average <i>r_b</i> (cm)	2.75				22.00		average <i>r_b</i> (cm)	3.25																	
Water temp (°C)	20.00		<i>ε_m</i> (cm)+ve	-0.98				78.50		<i>ε_m</i> (cm)+ve	-1.21																	
Tube position (cm)	76.10		<i>ε_m</i> (cm)-ve	-0.98				27.65		<i>ε_m</i> (cm)-ve	-1.20																	
Time to fill (s)	37.32		average <i>ε_m</i> (cm)	-0.98				0.42		average <i>ε_m</i> (cm)	-1.20																	
<i>Q</i> (L/s)	0.31		<i>Q</i> (L/s)	-0.98																								

Test No. T1/0/6.32

Horizontal position (cm)	r (cm)	Depth reading (mm)	ε (cm)
73.10	-3.20	0.11	0.00
73.30	-3.00	1.23	-0.11
73.60	-2.70	3.10	-0.30
73.90	-2.40	5.26	-0.52
74.20	-2.10	7.52	-0.74
74.50	-1.80	8.39	-0.83
74.80	-1.50	10.38	-1.03
75.10	-1.20	10.67	-1.06
75.40	-0.90	11.75	-1.17
75.70	-0.60	11.42	-1.14
76.00	-0.30	10.74	-1.07
76.30	0.00	10.21	-1.02
76.60	0.30	10.78	-1.08
76.90	0.60	11.34	-1.13
77.20	0.90	11.38	-1.14
77.50	1.20	10.75	-1.08
77.80	1.50	9.90	-0.99
78.10	1.80	8.41	-0.84
78.40	2.10	6.51	-0.65
78.70	2.40	4.12	-0.42
79.00	2.70	1.84	-0.19
79.20	2.90	-0.05	0.00

Test No. T1/0/6.06

z_o (cm)	r_b (cm)+ve	0.00	r_b (cm)-ve	3.10
d (cm)	r_b (cm)-ve	0.97	r_b (cm)+ve	3.20
Water temp (°C)	average r_b (cm)	3.05	Water temp (°C)	3.15
Tube position (cm)	76.30	ε_m (cm)+ve	-1.14	Tube position (cm)
Time to fill (s)	25.45	ε_m (cm)-ve	-1.17	Time to fill (s)
Q (L/s)	0.45	average ε_m (cm)	-1.15	Q (L/s)
			0.44	average ε_m (cm)
				-1.14
				Depth reading (mm)
				ε (cm)
				Horizontal position (cm)
				r (cm)
				z_o (cm)
				d (cm)

Test No. T1/0/5.459

Horizontal position (cm)	<i>r</i> (cm)	Depth reading (mm)	<i>ε</i> (cm)
75.20	-3.10	0.61	0.00
75.30	-3.00	1.14	-0.05
75.60	-2.70	2.66	-0.20
75.90	-2.40	5.34	-0.47
76.20	-2.10	7.32	-0.67
76.50	-1.80	9.28	-0.87
76.80	-1.50	10.22	-0.96
77.10	-1.20	11.33	-1.07
77.40	-0.90	11.91	-1.13
77.70	-0.60	11.31	-1.07
78.00	-0.30	10.92	-1.03
78.30	0.00	10.03	-0.94
78.60	0.30	11.39	-1.07
78.90	0.60	11.93	-1.13
79.20	0.90	11.56	-1.09
79.50	1.20	10.83	-1.02
79.80	1.50	9.14	-0.85
80.10	1.80	7.57	-0.69
80.40	2.10	6.03	-0.54
80.70	2.40	2.84	-0.22
81.00	2.70	1.05	-0.04
81.20	2.90	0.68	0.00

Test No. T1/0/5.318

z ₀ (cm)	<i>r</i> (cm)+ve	0.00	0.97	<i>r_b</i> (cm)+ve	3.10
<i>d</i> (cm)	<i>r_b</i> (cm)-ve	2.90	<i>d</i> (cm)	<i>r_b</i> (cm)-ve	3.00
Time to Equilibrium (min)	average <i>r_b</i> (cm)	3.10	Time to Equilibrium (min)	10.00	3.05
Water temp (°C)		3.00	Water temp (°C)	20.00	average <i>r_b</i> (cm)
Tube position (cm)	<i>ε_m</i> (cm)+ve	-1.13	Tube position (cm)	76.50	<i>ε_m</i> (cm)+ve
Time to fill (s)	<i>ε_m</i> (cm)-ve	-1.13	Time to fill (s)	29.61	<i>ε_m</i> (cm)-ve
<i>Q</i> (L/s)	average <i>ε_m</i> (cm)	-1.13	<i>Q</i> (L/s)	0.00	average <i>ε_m</i> (cm)
Horizontal position (cm)			Horizontal position (cm)	<i>r</i> (cm)	Depth reading (mm)
					<i>ε</i> (cm)

Test No. T1/0/3.99

z_0 (cm)	0.00	r_b (cm)+ve	2.70	ε (cm)	0.00	Horizontal position (cm)	r (cm)	Depth reading (mm)	ε (cm)
d (cm)	0.97	r_b (cm)-ve	2.80			77.00	-2.80	0.38	0.00
Time to Equilibrium (min)	10.00	r_b (cm)-ve	2.75			77.10	-2.70	0.70	-0.03
Water temp (°C)	18.00	average r_b (cm)	2.75			77.40	-2.40	3.16	-0.27
Tube position (cm)	79.80	ε_m (cm)+ve	-1.05			77.70	-2.10	5.71	-0.52
Time to fill (s)	39.46	ε_m (cm)-ve	-1.05			78.00	-1.80	8.12	-0.76
Q (L/s)	0.00	average ε_m (cm)	-1.05			78.30	-1.50	9.13	-0.86

Test No. T1/0/5.580

z_0 (cm)	0.00	d (cm)	0.97	r_b (cm)+ve	0.00	Horizontal position (cm)	r (cm)	Depth reading (mm)	ε (cm)
d (cm)	0.97	r_b (cm)-ve	2.80	Time to Equilibrium (min)	10.00	r_b (cm)-ve	0.97	r_b (cm)+ve	3.00
Time to Equilibrium (min)	10.00	average r_b (cm)	2.75	Water temp (°C)	18.00	average r_b (cm)	0.97	r_b (cm)-ve	3.00
Water temp (°C)	18.00			Tube position (cm)	79.60	ε_m (cm)+ve	0.97	r_b (cm)+ve	3.00
Tube position (cm)	79.80	ε_m (cm)+ve	-1.05	Time to fill (s)	28.22	ε_m (cm)-ve	0.97	r_b (cm)-ve	3.00
Time to fill (s)	39.46	ε_m (cm)-ve	-1.05	Q (L/s)	0.00	average ε_m (cm)	0.97	r_b (cm)+ve	3.00
Q (L/s)	0.00	average ε_m (cm)	-1.05						

Test No. 0.6-1.27/1.25

z_0 (cm)	-1.27	r_i (cm)+ve	4.10	z_0 (cm)	-1.27
d (cm)	1.39	r_i (cm)-ve	4.40	d (cm)	1.39
Time to Equilibrium (min)	21.00	r_i (cm)-ve	4.40	Time to Equilibrium (min)	21.00
Water temp (°C)	17.00	average r_i (cm)	4.25	Water temp (°C)	17.00
Tube position (cm)	78.40	ε_m (cm)+ve	-2.10	Tube position (cm)	76.50
Time to fill (s)	61.25	ε_m (cm)-ve	-2.14	Time to fill (s)	63.82
Q (L/s)	0.19	average ε_m (cm)	-2.12	Q (L/s)	0.18
Horizontal position (cm)	r (cm)	Depth reading (mm)	ε (cm)	Horizontal position (cm)	r (cm)
74.00	-4.40	-2.29	0.00	72.00	-4.50
74.40	-4.00	0.29	-0.25	72.50	-4.00
74.90	-3.50	3.27	-0.53	73.00	-3.50
75.40	-3.00	6.81	-0.87	73.50	-3.00
75.90	-2.50	10.50	-1.22	74.00	-2.50
76.40	-2.00	13.88	-1.55	74.50	-2.00
76.90	-1.50	17.82	-1.93	75.00	-1.50
77.20	-1.20	18.83	-2.02	75.30	-1.20
77.50	-0.90	20.17	-2.14	75.60	-0.90
77.80	-0.60	19.89	-2.11	75.90	-0.60
78.10	-0.30	19.27	-2.04	76.20	-0.30
78.40	0.00	18.12	-1.91	76.50	0.00
78.70	0.30	19.12	-2.00	76.80	0.30
79.00	0.60	20.21	-2.10	77.10	0.60
79.30	0.90	20.20	-2.09	77.40	0.90
79.60	1.20	19.46	-2.01	77.70	1.20
79.90	1.50	18.16	-1.87	78.00	1.50
80.40	2.00	15.44	-1.59	78.50	2.00
80.90	2.50	11.03	-1.13	79.00	2.50
81.40	3.00	8.05	-0.82	79.50	3.00
81.90	3.50	3.41	-0.34	80.00	3.50
82.40	4.00	0.61	-0.04	80.50	4.00
82.50	4.10	0.20	0.00		0.57

Test No. 0.6/-1.27/1.20

z_0 (cm)	d (cm)	r_i (cm)+ve	4.00	r_i (cm)-ve	4.50
d (cm)	d (cm)	r_i (cm)-ve	4.25	average r_i (cm)	4.25
Time to Equilibrium (min)	21.00	r_i (cm)-ve	4.40	Time to Equilibrium (min)	21.00
Water temp (°C)	17.00	average r_i (cm)	4.25	Water temp (°C)	17.00
Tube position (cm)	78.40	ε_m (cm)+ve	-2.10	Tube position (cm)	76.50
Time to fill (s)	61.25	ε_m (cm)-ve	-2.14	Time to fill (s)	63.82
Q (L/s)	0.19	average ε_m (cm)	-2.12	Q (L/s)	0.18
Horizontal position (cm)	r (cm)	Depth reading (mm)	ε (cm)	Horizontal position (cm)	r (cm)
74.00	-4.40	-2.29	0.00	72.00	-4.50
74.40	-4.00	0.29	-0.25	72.50	-4.00
74.90	-3.50	3.27	-0.53	73.00	-3.50
75.40	-3.00	6.81	-0.87	73.50	-3.00
75.90	-2.50	10.50	-1.22	74.00	-2.50
76.40	-2.00	13.88	-1.55	74.50	-2.00
76.90	-1.50	17.82	-1.93	75.00	-1.50
77.20	-1.20	18.83	-2.02	75.30	-1.20
77.50	-0.90	20.17	-2.14	75.60	-0.90
77.80	-0.60	19.89	-2.11	75.90	-0.60
78.10	-0.30	19.27	-2.04	76.20	-0.30
78.40	0.00	18.12	-1.91	76.50	0.00
78.70	0.30	19.12	-2.00	76.80	0.30
79.00	0.60	20.21	-2.10	77.10	0.60
79.30	0.90	20.20	-2.09	77.40	0.90
79.60	1.20	19.46	-2.01	77.70	1.20
79.90	1.50	18.16	-1.87	78.00	1.50
80.40	2.00	15.44	-1.59	78.50	2.00
80.90	2.50	11.03	-1.13	79.00	2.50
81.40	3.00	8.05	-0.82	79.50	3.00
81.90	3.50	3.41	-0.34	80.00	3.50
82.40	4.00	0.61	-0.04	80.50	4.00
82.50	4.10	0.20	0.00		0.57

Test No. 0.6/-1.27/1.19

z_0 (cm)	-1.27	r_t (cm)+ve	2.57	d (cm)	-1.27	r_t (cm)+ve	2.07
d (cm)	1.39	r_t (cm)-ve	2.48	Time to Equilibrium (min)	21.00	r_t (cm)-ve	2.53
Time to Equilibrium (min)	21.00	r_t (cm)-ve	2.48	Water temp (°C)	16.00	average r_t (cm)	2.30
Water temp (°C)	16.00	average r_t (cm)	2.53	Tube position (cm)	2.06	Tube position (cm)	2.03
Tube position (cm)	78.40	ε_m (cm)+ve	-2.06	Time to fill (s)	80.30	ε_m (cm)+ve	-2.03
Time to fill (s)	64.33	ε_m (cm)-ve	-2.14	Q (L/s)	68.62	ε_m (cm)-ve	-2.01
Q (L/s)	0.18	average ε_m (cm)	-2.10		0.17	average ε_m (cm)	-2.02
Horizontal position (cm)	r (cm)	Depth reading (mm)	ε (cm)	Horizontal position (cm)	r (cm)	Depth reading (mm)	ε (cm)
74.00	-4.40	-2.92	0.00	76.00	-4.30	-1.47	0.00
74.40	-4.00	-0.56	-0.22	76.30	-4.00	0.68	-0.21
74.80	-3.60	2.36	-0.50	76.70	-3.60	3.82	-0.52
75.20	-3.20	5.33	-0.78	77.10	-3.20	7.02	-0.83
75.60	-2.80	8.22	-1.06	77.50	-2.80	10.09	-1.13
76.00	-2.40	11.02	-1.32	77.90	-2.40	12.24	-1.34
76.40	-2.00	13.63	-1.57	78.30	-2.00	15.03	-1.61
76.80	-1.60	16.20	-1.81	78.70	-1.60	17.13	-1.81
77.20	-1.20	18.28	-2.01	79.10	-1.20	18.71	-1.96
77.50	-0.90	19.69	-2.14	79.50	-0.80	19.31	-2.01
77.80	-0.60	19.67	-2.12	79.90	-0.40	18.61	-1.94
78.10	-0.30	18.56	-2.00	80.30	0.00	17.91	-1.86
78.40	0.00	17.66	-1.90	80.70	0.40	19.49	-2.01
78.70	0.30	18.46	-1.97	81.10	0.80	19.81	-2.03
79.00	0.60	19.39	-2.05	81.50	1.20	18.42	-1.89
79.30	0.90	19.60	-2.06	81.90	1.60	16.37	-1.67
79.60	1.20	19.06	-2.00	82.30	2.00	12.89	-1.32
80.00	1.60	17.52	-1.83	82.70	2.40	10.21	-1.04
80.40	2.00	15.46	-1.61	83.10	2.80	7.09	-0.72
80.80	2.40	13.46	-1.39	83.50	3.20	4.71	-0.48
81.20	2.80	10.72	-1.11	83.90	3.60	1.45	-0.15
81.60	3.20	6.50	-0.67	84.20	3.90	0.05	0.00
82.00	3.60	3.18	-0.32				
82.40	4.00	0.09	0.00				

Test No. 0.6/-1.27/1.12

z_0 (cm)	-1.27	r_t (cm)	1.39	r_t (cm)+ve	2.07
d (cm)	2.57	d (cm)	-1.27	r_t (cm)-ve	2.53
Time to Equilibrium (min)	21.00	r_t (cm)-ve	21.00	r_t (cm)-ve	2.53
Water temp (°C)	16.00	average r_t (cm)	16.00	average r_t (cm)	2.30
Tube position (cm)	78.40	ε_m (cm)+ve	80.30	ε_m (cm)+ve	2.03
Time to fill (s)	64.33	ε_m (cm)-ve	68.62	ε_m (cm)-ve	-2.01
Q (L/s)	0.18	average ε_m (cm)	0.17	average ε_m (cm)	-2.02
Horizontal position (cm)	r (cm)	Depth reading (mm)	r (cm)	Depth reading (mm)	ε (cm)
74.00	-4.40	-2.92	76.00	-4.30	-1.47
74.40	-4.00	-0.56	76.30	-4.00	0.68
74.80	-3.60	2.36	76.70	-3.60	3.82
75.20	-3.20	5.33	77.10	-3.20	7.02
75.60	-2.80	8.22	77.50	-2.80	10.09
76.00	-2.40	11.02	77.90	-2.40	12.24
76.40	-2.00	13.63	78.30	-2.00	15.03
76.80	-1.60	16.20	78.70	-1.60	17.13
77.20	-1.20	18.28	79.10	-1.20	18.71
77.50	-0.90	19.69	79.50	-0.80	19.31
77.80	-0.60	19.67	79.90	-0.40	18.61
78.10	-0.30	18.56	80.30	0.00	17.91
78.40	0.00	17.66	80.70	0.40	19.49
78.70	0.30	18.46	81.10	0.80	19.81
79.00	0.60	19.39	81.50	1.20	18.42
79.30	0.90	19.60	81.90	1.60	16.37
79.60	1.20	19.06	82.30	2.00	12.89
80.00	1.60	17.52	82.70	2.40	10.21
80.40	2.00	15.46	83.10	2.80	7.09
80.80	2.40	13.46	83.50	3.20	4.71
81.20	2.80	10.72	83.90	3.60	1.45
81.60	3.20	6.50	84.20	3.90	0.05
82.00	3.60	3.18			0.00
82.40	4.00	0.09			

Test No. 0.6/-3.81/0.99

Horizontal position (cm)	<i>r</i> (cm)	Depth reading (mm)	<i>ε</i> (cm)
70.80	-7.30	-4.95	0.00
71.60	-6.50	1.21	-0.59
72.60	-5.50	9.77	-1.42
73.60	-4.50	16.74	-2.09
74.10	-4.00	20.63	-2.46
74.60	-3.50	24.94	-2.88
75.10	-3.00	29.75	-3.34
75.60	-2.50	33.59	-3.71
76.10	-2.00	36.63	-4.00
76.60	-1.50	39.82	-4.30
76.90	-1.20	41.69	-4.48
77.20	-0.90	42.70	-4.57
77.50	-0.60	42.59	-4.55
77.80	-0.30	42.27	-4.51
78.10	0.00	40.78	-4.35
78.40	0.30	42.44	-4.51
78.70	0.60	43.38	-4.60
79.00	0.90	42.76	-4.53
79.30	1.20	41.53	-4.39
79.60	1.50	40.31	-4.26
80.10	2.00	36.72	-3.89
80.60	2.50	33.73	-3.58
81.10	3.00	30.04	-3.19

Test No. 0.6/-2.54/1.13

z ₀ (cm)	<i>r</i> _t (cm)+ve	z ₀ (cm)	d (cm)	<i>r</i> _t (cm)+ve	2.16		
1.39	<i>r</i> _t (cm)-ve	2.13	d (cm)	<i>r</i> _t (cm)-ve	2.48		
21.00	average <i>r</i> _t (cm)	2.33	Time to Equilibrium (min)	21.00	average <i>r</i> _t (cm)		
19.00	average <i>r</i> _t (cm)	2.23	Water temp (°C)	17.00	2.32		
78.10	<i>ε_m</i> (cm)+ve	-4.60	Tube position (cm)	80.10	<i>ε_m</i> (cm)+ve		
77.77	<i>ε_m</i> (cm)-ve	-4.57	Time to fill (s)	67.87	<i>ε_m</i> (cm)-ve		
0.15	average <i>ε_m</i> (cm)	-4.59	<i>Q</i> (L/s)	0.17	average <i>ε_m</i> (cm)		
Horizontal position (cm)	<i>r</i> (cm)	Depth reading (mm)	<i>ε</i> (cm)	Horizontal position (cm)	<i>r</i> (cm)	Depth reading (mm)	<i>ε</i> (cm)
74.60	74.60	-5.50	-0.65	74.60	74.60	-5.50	0.00
75.10	75.10	-5.00	4.45	75.60	75.60	-4.50	-0.51
76.10	76.10	-4.50	8.58	76.60	76.60	-4.00	-0.91
76.60	76.60	-4.00	13.16	77.10	77.10	-3.50	-1.37
77.10	77.10	-3.00	16.64	77.60	77.60	-2.50	-1.71
77.60	77.60	-2.50	19.61	78.10	78.10	-2.00	-2.00
78.10	78.10	-2.00	24.93	78.60	78.60	-1.50	-2.53
78.60	78.60	-1.50	28.10	79.50	79.50	-1.00	-2.84
79.50	79.50	-0.90	30.65	79.80	79.80	-0.50	-3.09
79.80	79.80	-0.90	31.68	80.10	80.10	-0.30	-3.19
80.10	80.10	0.00	32.52	80.40	80.40	0.30	-3.27
80.40	80.40	0.30	32.35	81.60	81.60	0.60	-3.26
81.60	81.60	0.60	31.56	81.30	81.30	-0.30	-3.17
81.30	81.30	0.00	30.70	81.00	81.00	0.00	-3.08
81.00	81.00	0.30	32.07	81.30	81.30	0.30	-3.22
81.30	81.30	0.60	32.91	81.60	81.60	0.60	-3.30
81.60	81.60	0.90	32.44	81.30	81.30	0.90	-3.25
81.30	81.30	1.20	30.46	81.00	81.00	1.20	-3.05
81.00	81.00	1.50	29.94	81.30	81.30	1.50	-2.99
81.30	81.30	2.00	26.83	81.60	81.60	2.00	-2.68
81.60	81.60	2.50	22.51	82.60	82.60	2.50	-2.24
82.60	82.60	3.00	19.16	83.10	83.10	3.00	-1.90
83.10	83.10	3.50	15.19	83.60	83.60	3.50	-1.50

Horizontal position (cm)	<i>r</i> (cm)	Depth reading (mm)	<i>ε</i> (cm)
81.60	3.50	26.37	-2.81
82.10	4.00	22.63	-2.42
83.10	5.00	14.72	-1.60
84.10	6.00	7.14	-0.81
85.10	7.00	-0.68	0.00

Test No. 0.6/-3.81/1.19

<i>z</i> ₀ (cm)	<i>r</i> _t (cm)+ve	2.49	<i>d</i> (cm)	-3.81
<i>d</i> (cm)	<i>r</i> _t (cm)-ve	2.72	Time to Equilibrium (min)	21.00
Time to Equilibrium (min)	21.00	average <i>r</i> _t (cm)	Water temp (°C)	17.00
Water temp (°C)	17.00	2.60	Tube position (cm)	78.40
Tube position (cm)	80.00	<i>ε</i> _m (cm)+ve	Time to fill (s)	56.62
Time to fill (s)	64.21	<i>ε</i> _m (cm)-ve	<i>Q</i> (L/s)	0.20
<i>Q</i> (L/s)	0.18	average <i>ε</i> _m (cm)		average <i>ε</i> _m (cm)

Test No. 0.6/-3.81/1.35

<i>z</i> ₀ (cm)	<i>d</i> (cm)	1.39	<i>r</i> _t (cm)+ve	2.69
<i>d</i> (cm)	<i>r</i> _t (cm)-ve	2.72	<i>r</i> _t (cm)-ve	2.69
Time to Equilibrium (min)	21.00	average <i>r</i> _t (cm)	average <i>r</i> _t (cm)	2.69
Water temp (°C)	17.00	2.60	Tube position (cm)	78.40
Tube position (cm)	80.00	<i>ε</i> _m (cm)+ve	Time to fill (s)	56.62
Time to fill (s)	64.21	<i>ε</i> _m (cm)-ve	<i>Q</i> (L/s)	0.20
<i>Q</i> (L/s)	0.18	average <i>ε</i> _m (cm)		average <i>ε</i> _m (cm)

Horizontal position (cm)	<i>r</i> (cm)	Depth reading (mm)	<i>ε</i> (cm)	Horizontal position (cm)	<i>r</i> (cm)	Depth reading (mm)	<i>ε</i> (cm)
72.80	-7.20	-3.60	0.00	70.70	-7.70	-5.42	0.00
73.20	-6.80	0.17	-0.37	70.90	-7.50	-4.24	-0.11
73.70	-6.30	6.03	-0.94	71.40	-7.00	-0.18	-0.50
74.20	-5.80	10.34	-1.35	71.90	-6.50	3.37	-0.84
74.70	-5.30	14.91	-1.80	72.40	-6.00	7.94	-1.27
75.20	-4.80	18.49	-2.14	72.90	-5.50	12.67	-1.73
75.70	-4.30	23.22	-2.60	73.40	-5.00	15.66	-2.01
76.20	-3.80	28.11	-3.07	73.90	-4.50	19.40	-2.37
76.70	-3.30	30.94	-3.34	74.40	-4.00	23.91	-2.80
77.20	-2.80	35.35	-3.77	74.90	-3.50	28.17	-3.21
77.70	-2.30	38.25	-4.04	75.40	-3.00	32.63	-3.63
78.20	-1.80	41.47	-4.35	75.90	-2.50	35.66	-3.92
78.50	-1.50	43.65	-4.56	76.40	-2.00	39.08	-4.24
78.80	-1.20	44.54	-4.64	76.90	-1.50	42.31	-4.55
79.10	-0.90	45.17	-4.69	77.20	-1.20	43.41	-4.65
79.40	-0.60	44.82	-4.65	77.50	-0.90	44.15	-4.71

Horizontal position (cm)	<i>r</i> (cm)	Depth reading (mm)	ε (cm)	Horizontal position (cm)	<i>r</i> (cm)	Depth reading (mm)	ε (cm)
79.70	-0.30	44.12	-4.57	77.80	-0.60	44.82	-4.76
80.00	0.00	43.61	-4.51	78.10	-0.30	43.55	-4.63
80.30	0.30	44.54	-4.59	78.40	0.00	42.76	-4.54
80.60	0.60	45.08	-4.64	78.70	0.30	44.19	-4.67
80.90	0.90	45.27	-4.65	79.00	0.60	44.51	-4.69
81.20	1.20	44.49	-4.56	79.30	0.90	44.78	-4.71
81.50	1.50	43.74	-4.48	79.60	1.20	44.20	-4.64
81.80	1.80	41.04	-4.20	79.90	1.50	42.59	-4.46
82.30	2.30	39.21	-4.00	80.40	2.00	40.81	-4.27
82.80	2.80	34.21	-3.49	80.90	2.50	38.19	-3.99
83.30	3.30	30.59	-3.11	81.40	3.00	33.56	-3.51
83.80	3.80	26.88	-2.73	81.90	3.50	28.74	-3.01
84.80	4.80	19.48	-1.96	82.90	4.50	21.17	-2.21
85.30	5.30	15.39	-1.53	83.40	5.00	18.10	-1.89
85.80	5.80	12.10	-1.19	83.90	5.50	13.86	-1.45
86.30	6.30	6.28	-0.59	84.40	6.00	10.96	-1.14
86.80	6.80	2.35	-0.19	84.90	6.50	6.57	-0.68
87.00	7.00	0.55	0.00	85.40	7.00	1.69	-0.17
				85.80	7.40	0.10	0.00

Test No. 0.6/-5.08/1.32

z_0 (cm)	-5.08	z_0 (cm)	-5.08
d (cm)	1.39	r_i (cm)+ve	1.39
Time to Equilibrium (min)	21.00	r_i (cm)-ve	21.00
Water temp (°C)	17.00	average r_i (cm)	average r_i (cm)
Tube position (cm)	78.40	ε_m (cm)+ve	r_i (cm)+ve
Time to fill (s)	58.02	ε_m (cm)-ve	r_i (cm)-ve
Q (L/s)	0.20	average ε_m (cm)	average ε_m (cm)

Test No. 0.6/-5.08/1.17

z_0 (cm)	2.68	r_i (cm)+ve	2.58
d (cm)	2.84	r_i (cm)-ve	2.74
Time to Equilibrium (min)			
Water temp (°C)			
Tube position (cm)	76.50	ε_m (cm)+ve	-6.00
Time to fill (s)	65.66	ε_m (cm)-ve	-6.05
Q (L/s)	0.18	average ε_m (cm)	-6.03

Horizontal position (cm)	<i>r</i> (cm)	Depth reading (mm)	<i>ε</i> (cm)
69.10	-9.30	-6.92	0.00
69.40	-9.00	-3.75	-0.31
70.40	-8.00	4.95	-1.14
72.40	-6.00	21.16	-2.69
73.40	-5.00	27.08	-3.24
74.40	-4.00	36.98	-4.19
74.90	-3.50	40.35	-4.51
75.40	-3.00	45.16	-4.97
75.90	-2.50	48.65	-5.30
76.40	-2.00	52.82	-5.70
76.90	-1.50	55.18	-5.92
77.20	-1.20	57.43	-6.13
77.50	-0.90	57.81	-6.16
77.80	-0.60	57.49	-6.12
78.10	-0.30	56.64	-6.02
78.40	0.00	55.78	-5.92
78.70	0.30	56.11	-5.95
79.00	0.60	57.32	-6.06
79.60	1.20	57.32	-6.03
79.90	1.50	56.11	-5.90
80.40	2.00	53.67	-5.64
80.90	2.50	49.23	-5.18
81.40	3.00	46.75	-4.91
81.90	3.50	41.91	-4.41
82.40	4.00	38.55	-4.05
83.40	5.00	31.24	-3.28
84.40	6.00	23.28	-2.45
85.40	7.00	16.09	-1.70
86.40	8.00	5.98	-0.65
87.00	8.60	-0.27	0.00

Horizontal position (cm)	<i>r</i> (cm)	Depth reading (mm)	<i>ε</i> (cm)	Horizontal position (cm)	<i>r</i> (cm)	Depth reading (mm)	<i>ε</i> (cm)
66.80	-9.70	-5.28	0.00	67.00	-9.50	-3.97	-0.12
68.00	-8.50	3.93	-0.88	70.00	-6.50	20.90	-2.51
71.00	-5.50	28.00	-3.18	72.00	-4.50	35.62	-3.91
73.00	-3.50	42.26	-4.54	73.00	-3.00	46.09	-4.91
74.00	-2.50	49.55	-5.24	74.00	-2.00	53.45	-5.61
75.00	-1.50	56.70	-5.92	75.00	-1.20	57.78	-6.02
75.30	-1.20	57.78	-6.02	75.60	-0.90	58.20	-6.05
75.90	-0.90	58.20	-6.05	75.90	-0.60	58.01	-6.02
76.20	-0.60	56.77	-5.88	76.20	-0.30	56.03	-5.80
76.50	-0.30	56.03	-5.80	76.50	0.00	56.03	-5.80
76.80	0.30	57.55	-5.94	76.80	0.30	57.55	-5.94
77.10	0.60	58.26	-6.00	77.10	0.60	58.26	-6.00
77.70	1.20	57.12	-5.87	77.70	1.20	57.12	-5.87
78.00	1.50	56.68	-5.81	78.00	1.50	56.68	-5.81
78.50	2.00	53.78	-5.51	78.50	2.00	53.78	-5.51
79.00	2.50	50.33	-5.14	79.00	2.50	50.33	-5.14
79.50	3.00	46.58	-4.75	79.50	3.00	46.58	-4.75
80.00	3.50	42.66	-4.34	80.00	3.50	42.66	-4.34
80.50	4.00	35.19	-3.56	81.00	4.50	35.19	-3.56
81.00	5.00	27.55	-2.76	82.00	5.50	27.55	-2.76
81.50	6.00	19.35	-1.91	83.00	6.50	19.35	-1.91
82.00	7.00	12.39	-1.18	84.00	7.50	12.39	-1.18
82.50	8.00	6.07	-0.51	85.00	8.50	6.07	-0.51
83.00	8.60	0.00	0.00	85.80	9.30	1.20	0.00

Test No. 0.6/-2.54/0.97

Horizontal position (cm)	<i>r</i> (cm)	Depth reading (mm)	<i>ε</i> (cm)
72.50	-5.70	-3.71	0.00
72.70	-5.50	-0.95	-0.27
73.20	-5.00	1.63	-0.51
73.70	-4.50	5.65	-0.90
74.20	-4.00	10.21	-1.34
74.70	-3.50	14.99	-1.80
75.20	-3.00	17.64	-2.05
75.70	-2.50	20.78	-2.34
76.20	-2.00	25.41	-2.79
76.70	-1.50	28.66	-3.10
77.00	-1.20	30.14	-3.24
77.30	-0.90	31.11	-3.32
77.60	-0.60	30.88	-3.29
77.90	-0.30	30.29	-3.22
78.50	0.30	30.56	-3.23
78.80	0.60	31.29	-3.29
79.10	0.90	30.83	-3.24
79.40	1.20	29.19	-3.06
79.70	1.50	27.82	-2.92
80.20	2.00	25.17	-2.64
80.70	2.50	19.91	-2.09
81.20	3.00	15.89	-1.67
81.70	3.50	13.89	-1.46
82.20	4.00	8.81	-0.93

Test No. 0.6/-3.81/0.99

<i>z</i> ₀ (cm)	<i>d</i> (cm)	<i>r</i> _t (cm)+ve	2.09	-3.81	<i>r</i> _t (cm)+ve	2.13
<i>d</i> (cm)	<i>r</i> _t (cm)-ve	2.28	Time to Equilibrium (min)	21.00	<i>r</i> _t (cm)-ve	2.33
Time to Equilibrium (min)	average <i>r</i> _t (cm)	2.18	Water temp (°C)	19.00	average <i>r</i> _t (cm)	2.23
Water temp (°C)	<i>ε</i> _m (cm)+ve	3.29	Tube position (cm)	78.10	<i>ε</i> _m (cm)+ve	4.60
Tube position (cm)	<i>ε</i> _m (cm)-ve	-3.32	Time to fill (s)	77.77	<i>ε</i> _m (cm)-ve	-4.57
Time to fill (s)	<i>Q</i> (L/s)	-3.31	<i>Q</i> (L/s)	0.15	average <i>ε</i> _m (cm)	-4.59
72.50	-5.70	-3.71	70.80	-7.30	-4.95	0.00
72.70	-5.50	-0.95	71.60	-6.50	1.21	-0.59
73.20	-5.00	1.63	72.60	-5.50	9.77	-1.42
73.70	-4.50	5.65	73.60	-4.50	16.74	-2.09
74.20	-4.00	10.21	74.10	-4.00	20.63	-2.46
74.70	-3.50	14.99	74.60	-3.50	24.94	-2.88
75.20	-3.00	17.64	75.10	-3.00	29.75	-3.34
75.70	-2.50	20.78	75.60	-2.50	33.59	-3.71
76.20	-2.00	25.41	76.10	-2.00	36.63	-4.00
76.70	-1.50	28.66	76.60	-1.50	39.82	-4.30
77.00	-1.20	30.14	76.90	-1.20	41.69	-4.48
77.30	-0.90	31.11	77.20	-0.90	42.70	-4.57
77.60	-0.60	30.88	77.50	-0.60	42.59	-4.55
77.90	-0.30	30.29	77.80	-0.30	42.27	-4.51
78.50	0.30	30.56	78.40	0.30	42.44	-4.51
78.80	0.60	31.29	78.70	0.60	43.38	-4.60
79.10	0.90	30.83	79.00	0.90	42.76	-4.53
79.40	1.20	29.19	79.30	1.20	41.53	-4.39
79.70	1.50	27.82	79.60	1.50	40.31	-4.26
80.20	2.00	25.17	80.10	2.00	36.72	-3.89
80.70	2.50	19.91	80.60	2.50	33.73	-3.58
81.20	3.00	15.89	81.10	3.00	30.04	-3.19
81.70	3.50	13.89	81.60	3.50	26.37	-2.81
82.20	4.00	8.81	82.10	4.00	22.63	-2.42

Horizontal position (cm)	<i>r</i> (cm)	Depth reading (mm)	ε (cm)
82.70	4.50	5.46	-0.58
83.20	5.00	1.87	-0.21
83.60	5.40	-0.07	0.00
<hr/>			
Test No. 0.6/-2.54/1.38			
z_0 (cm)	-2.54		
d (cm)	1.39	r_t (cm)+ve	2.48
Time to Equilibrium (min)	21.00	r_t (cm)-ve	2.54
Water temp (°C)	17.00	average r_t (cm)	2.51
Tube position (cm)	78.40	ε_m (cm)+ve	-3.33
Time to fill (s)	55.63	ε_m (cm)-ve	-3.40
Q (L/s)	0.21	average ε_m (cm)	-3.36
<hr/>			
Horizontal position (cm)	<i>r</i> (cm)	Depth reading (mm)	ε (cm)
72.20	-6.20	-2.72	0.00
72.40	-6.00	-1.95	-0.07
72.90	-5.50	0.93	-0.35
73.40	-5.00	4.59	-0.70
73.90	-4.50	7.37	-0.96
74.40	-4.00	10.38	-1.25
74.90	-3.50	15.16	-1.71
75.40	-3.00	18.67	-2.05
75.90	-2.50	24.15	-2.59
76.40	-2.00	27.59	-2.92
76.90	-1.50	30.45	-3.19
77.20	-1.20	31.96	-3.33
77.80	-0.60	32.44	-3.36
78.10	-0.30	31.71	-3.28
78.40	0.00	30.61	-3.16
78.70	0.30	32.05	-3.30
79.00	0.60	32.45	-3.33

Horizontal position (cm)	<i>r</i> (cm)	Depth reading (mm)	ε (cm)
83.10		5.00	14.72
84.10		6.00	7.14
85.10		7.00	-0.68
<hr/>			
Test No. 0.6/-5.08/1.22			
z_0 (cm)	-5.08		
d (cm)	1.39	r_t (cm)+ve	1.88
Time to Equilibrium (min)	21.00	r_t (cm)-ve	2.27
Water temp (°C)	19.00	average r_t (cm)	2.08
Tube position (cm)	78.50	ε_m (cm)+ve	-5.65
Time to fill (s)	62.99	ε_m (cm)-ve	-5.69
Q (L/s)	0.18	average ε_m (cm)	-5.67
<hr/>			
Horizontal position (cm)	<i>r</i> (cm)	Depth reading (mm)	ε (cm)
69.30		-9.20	-2.58
70.00		-8.50	4.07
71.00		-7.50	11.01
72.00		-6.50	19.04
73.00		-5.50	26.05
74.00		-4.50	31.88
74.50		-4.00	35.86
75.00		-3.50	40.36
75.50		-3.00	44.55
76.00		-2.50	48.21
76.50		-2.00	50.67
77.00		-1.50	53.66
77.60		-0.90	55.59
77.90		-0.60	55.42
78.20		-0.30	55.07
78.50		0.00	53.71
78.80		0.30	54.89
<hr/>			

Horizontal position (cm)	<i>r</i> (cm)	Depth reading (mm)	<i>ε</i> (cm)	Horizontal position (cm)	<i>r</i> (cm)	Depth reading (mm)	<i>ε</i> (cm)
79.30	0.90	32.43	-3.32	79.10	0.60	55.45	-5.65
79.60	1.20	31.42	-3.21	79.40	0.90	55.18	-5.62
79.90	1.50	30.28	-3.09	79.70	1.20	53.80	-5.47
80.40	2.00	27.92	-2.84	80.00	1.50	52.25	-5.31
80.90	2.50	24.92	-2.53	80.50	2.00	49.27	-5.01
81.40	3.00	20.87	-2.11	81.00	2.50	46.76	-4.75
81.90	3.50	16.72	-1.68	81.50	3.00	43.04	-4.37
82.40	4.00	13.46	-1.34	82.00	3.50	40.35	-4.09
82.90	4.50	9.36	-0.92	82.50	4.00	36.42	-3.69
83.40	5.00	6.06	-0.57	83.50	5.00	29.59	-2.99
83.90	5.50	1.27	-0.08	84.50	6.00	22.73	-2.29
84.00	5.60	0.50	0.00	85.50	7.00	15.37	-1.54
				86.50	8.00	8.27	-0.81
				87.40	8.90	0.30	0.00

Test No. 0.6-5.08/1.31							Test No. 0.6-5.08/1.39
z_0 (cm)	-5.08	r_t (cm)+ve	2.27	z_0 (cm)	70.40		
d (cm)	1.39	r_t (cm)-ve	3.15	d (cm)	71.00		
Time to Equilibrium (min)	21.00	average r_t (cm)	2.71	Time to Equilibrium (min)	72.00		
Water temp (°C)	19.00	ε_m (cm)+ve	-5.93	Water temp (°C)	73.00		
Tube position (cm)	78.70	ε_m (cm)-ve	-6.08	Tube position (cm)	74.00		
Time to fill (s)	58.57	average ε_m (cm)	-6.01	Time to fill (s)	75.00		
Q (L/s)	0.20	Q (L/s)		Horizontal position (cm)			
Horizontal position (cm)	r (cm)	Depth reading (mm)	ε (cm)	Horizontal position (cm)			
68.70	-10.00	-7.59	0.00	68.70			
69.20	-9.50	-3.77	-0.36	69.20			
70.20	-8.50	3.78	-1.08	70.20			
71.20	-7.50	13.14	-1.98	71.20			
72.20	-6.50	21.77	-2.81	72.20			
73.20	-5.50	28.25	-3.42	73.20			

Horizontal position (cm)	<i>r</i> (cm)	Depth reading (mm)	<i>ε</i> (cm)	Horizontal position (cm)	<i>r</i> (cm)	Depth reading (mm)	<i>ε</i> (cm)
74.20	-4.50	35.16	-4.08	75.50	-4.00	36.81	-4.12
75.20	-3.50	43.01	-4.83	76.00	-3.50	40.60	-4.48
75.70	-3.00	46.84	-5.19	76.50	-3.00	44.94	-4.90
76.20	-2.50	50.32	-5.52	77.00	-2.50	48.10	-5.20
76.70	-2.00	53.50	-5.82	77.50	-2.00	51.93	-5.57
77.20	-1.50	55.53	-6.01	78.00	-1.50	54.89	-5.85
77.50	-1.20	56.36	-6.08	78.30	-1.20	55.43	-5.90
77.80	-0.90	56.46	-6.08	78.60	-0.90	56.68	-6.02
78.10	-0.60	56.57	-6.08	78.90	-0.60	57.01	-6.04
78.40	-0.30	55.55	-5.96	79.20	-0.30	56.46	-5.98
78.70	0.00	54.34	-5.83	79.50	0.00	55.33	-5.86
79.00	0.30	55.03	-5.89	79.80	0.30	55.95	-5.91
79.30	0.60	55.58	-5.93	80.10	0.60	56.41	-5.95
79.60	0.90	54.73	-5.84	80.40	0.90	56.65	-5.96
79.90	1.20	53.38	-5.69	80.70	1.20	55.62	-5.85
80.20	1.50	52.79	-5.62	81.00	1.50	55.09	-5.79
80.70	2.00	49.21	-5.25	81.50	2.00	52.70	-5.54
81.20	2.50	46.31	-4.94	82.00	2.50	49.45	-5.20
81.70	3.00	41.18	-4.41	82.50	3.00	45.60	-4.80
82.20	3.50	37.37	-4.01	83.00	3.50	42.23	-4.45
82.70	4.00	33.45	-3.60	83.50	4.00	38.45	-4.06
83.70	5.00	26.37	-2.85	84.00	4.50	34.94	-3.69
84.70	6.00	20.56	-2.24	85.00	5.50	25.91	-2.76
85.70	7.00	10.91	-1.24	86.00	6.50	19.71	-2.12
86.70	8.00	3.40	-0.45	87.00	7.50	11.26	-1.24
87.20	8.50	-0.91	0.00	88.00	8.50	3.86	-0.47
					9.00	-0.75	0.00
					88.50		

Test No. 0.6/-3.81/1.38

Horizontal position (cm)	<i>r</i> (cm)	Depth reading (mm)	<i>ε</i> (cm)	Horizontal position (cm)	<i>r</i> (cm)	Depth reading (mm)	<i>ε</i> (cm)
70.70	-7.80	-5.32	0.00	71.50	-8.40	-5.88	0.00
71.00	-7.50	-2.70	-0.25	72.40	-7.50	0.83	-0.64
72.00	-6.50	4.29	-0.92	73.40	-6.50	8.77	-1.40
73.00	-5.50	12.61	-1.71	74.40	-5.50	16.00	-2.08
74.00	-4.50	20.32	-2.45	75.40	-4.50	24.21	-2.87
74.50	-4.00	24.14	-2.81	75.90	-4.00	27.73	-3.20
75.00	-3.50	27.82	-3.16	76.40	-3.50	30.99	-3.51
75.50	-3.00	33.06	-3.67	76.90	-3.00	34.29	-3.82
76.00	-2.50	36.20	-3.97	77.40	-2.50	39.37	-4.31
76.50	-2.00	39.20	-4.25	77.90	-2.00	42.59	-4.62
77.00	-1.50	42.00	-4.51	78.40	-1.50	44.46	-4.79
77.30	-1.20	42.71	-4.57	78.70	-1.20	45.76	-4.91
77.60	-0.90	44.03	-4.69	79.00	-0.90	46.74	-4.99
77.90	-0.60	43.92	-4.67	79.30	-0.60	46.61	-4.97
78.20	-0.30	42.95	-4.56	79.60	-0.30	45.58	-4.86
78.50	0.00	42.25	-4.48	79.90	0.00	44.63	-4.75
78.80	0.30	42.85	-4.53	80.20	0.30	46.29	-4.91
79.10	0.60	44.18	-4.66	80.50	0.60	46.94	-4.96
79.40	0.90	43.62	-4.59	80.80	0.90	47.23	-4.98
79.70	1.20	43.06	-4.52	81.10	1.20	46.97	-4.94
80.00	1.50	41.56	-4.36	81.40	1.50	46.00	-4.84
80.50	2.00	39.34	-4.12	81.90	2.00	44.03	-4.62
81.00	2.50	35.76	-3.75	82.40	2.50	41.07	-4.31
81.50	3.00	31.56	-3.31	82.90	3.00	38.94	-4.08

Test No. 0.6/-3.81/2.33

	<i>z₀</i> (cm)	<i>r_i</i> (cm)+ve	<i>d</i> (cm)	<i>z₀</i> (cm)	<i>r_i</i> (cm)+ve	<i>d</i> (cm)	<i>z₀</i> (cm)
<i>d</i> (cm)	1.39	<i>r_i</i> (cm)+ve	2.42	2.76	Time to Equilibrium (min)	10.00	<i>r_i</i> (cm)-ve
Time to Equilibrium (min)	21.00	<i>r_i</i> (cm)-ve	2.76	Water temp (°C)	22.00	average <i>r_i</i> (cm)	3.29
Water temp (°C)	20.00	average <i>r_i</i> (cm)	2.59	Tube position (cm)	79.90	<i>ε_m</i> (cm)+ve	3.02
Tube position (cm)	78.50	<i>ε_m</i> (cm)+ve	4.66	Time to fill (s)	32.85	<i>ε_m</i> (cm)-ve	3.16
Time to fill (s)	55.44	<i>ε_m</i> (cm)-ve	4.69	<i>Q</i> (L/s)	0.35	average <i>ε_m</i> (cm)	4.98
<i>Q</i> (L/s)	0.21	average <i>ε_m</i> (cm)	4.67				-4.99

Horizontal position (cm)	<i>r</i> (cm)	Depth reading (mm)	ε (cm)	Horizontal position (cm)	<i>r</i> (cm)	Depth reading (mm)	ε (cm)
82.00	3.50	29.41	-3.08	83.40	3.50	34.54	-3.62
82.50	4.00	25.14	-2.63	83.90	4.00	31.19	-3.27
83.00	4.50	20.38	-2.14	84.40	4.50	26.54	-2.78
84.00	5.50	12.73	-1.34	85.40	5.50	20.51	-2.14
85.00	6.50	5.68	-0.60	86.40	6.50	12.58	-1.32
85.90	7.40	0.00	0.00	87.40	7.50	5.35	-0.56
			88.00		8.10	0.00	0.00
Test No. 0.6/-7.62/2.29							
z_0 (cm)	-7.62			z_0 (cm)	-7.62		
<i>d</i> (cm)	1.39	r_i (cm)+ve	3.63	<i>d</i> (cm)	1.39	r_i (cm)+ve	2.61
Time to Equilibrium (min)	10.00	r_i (cm)-ve	3.52	Time to Equilibrium (min)	21.00	r_i (cm)-ve	2.77
Water temp (°C)	22.00	average r_i (cm)	3.58	Water temp (°C)	15.00	average r_i (cm)	2.69
Tube position (cm)	80.20	ε_m (cm)+ve	-8.98	Tube position (cm)	78.40	ε_m (cm)+ve	-8.59
Time to fill (s)	33.50	ε_m (cm)-ve	-9.15	Time to fill (s)	67.60	ε_m (cm)-ve	-8.60
Q (L/s)	0.35	average ε_m (cm)	-9.07	Q (L/s)	0.17	average ε_m (cm)	-8.59
Test No. 0.6/-7.62/1.13							
z_0 (cm)				z_0 (cm)			
<i>d</i> (cm)				<i>d</i> (cm)			
Time to Equilibrium (min)				Time to Equilibrium (min)			
Water temp (°C)				Water temp (°C)			
Tube position (cm)				Tube position (cm)			
Time to fill (s)				Time to fill (s)			
Q (L/s)				Q (L/s)			
Horizontal position (cm)	<i>r</i> (cm)	Depth reading (mm)	ε (cm)	Horizontal position (cm)	<i>r</i> (cm)	Depth reading (mm)	ε (cm)
66.40	-13.80	-10.05	0.00	66.00	-12.40	-7.85	0.00
67.20	-13.00	-5.25	-0.46	67.80	-10.60	8.74	-1.60
68.20	-12.00	2.92	-1.25	68.80	-9.60	17.12	-2.41
69.20	-11.00	5.55	-1.48	69.80	-8.60	25.54	-3.21
70.20	-10.00	8.44	-1.74	70.80	-7.60	33.15	-3.94
71.20	-9.00	18.24	-2.69	71.30	-7.10	37.06	-4.32
72.20	-8.00	27.73	-3.61	71.80	-6.60	40.46	-4.64
73.20	-7.00	38.57	-4.67	72.30	-6.10	45.04	-5.08
74.20	-6.00	47.98	-5.58	72.80	-5.60	48.29	-5.39
75.20	-5.00	56.27	-6.38	73.30	-5.10	52.78	-5.82
76.20	-4.00	65.70	-7.30	73.80	-4.60	56.15	-6.14
76.70	-3.50	69.20	-7.64	74.30	-4.10	60.54	-6.57
77.20	-3.00	73.47	-8.05	74.80	-3.60	64.96	-6.99
77.70	-2.50	77.68	-8.46	75.30	-3.10	68.76	-7.36

Horizontal position (cm)	<i>r</i> (cm)	Depth reading (mm)	ε (cm)	Horizontal position (cm)	<i>r</i> (cm)	Depth reading (mm)	ε (cm)
78.20	-2.00	81.42	-8.82	75.80	-2.60	72.95	-7.76
78.70	-1.50	83.13	-8.97	76.30	-2.10	76.46	-8.09
79.00	-1.20	84.71	-9.12	76.60	-1.80	78.15	-8.25
79.30	-0.90	85.12	-9.15	76.90	-1.50	79.96	-8.42
79.60	-0.60	84.23	-9.06	77.20	-1.20	81.31	-8.55
79.90	-0.30	83.88	-9.01	77.50	-0.90	81.90	-8.60
80.20	0.00	82.30	-8.85	77.80	-0.60	81.45	-8.54
80.50	0.30	82.71	-8.88	78.10	-0.30	80.88	-8.48
80.80	0.60	83.42	-8.94	78.40	0.00	79.88	-8.37
81.10	0.90	83.92	-8.98	78.70	0.30	81.45	-8.51
81.60	1.40	82.91	-8.87	79.00	0.60	82.01	-8.56
82.10	1.90	81.42	-8.71	79.30	0.90	82.40	-8.59
82.60	2.40	79.17	-8.47	79.60	1.20	81.60	-8.50
83.10	2.90	76.60	-8.20	79.90	1.50	79.53	-8.28
83.60	3.40	72.42	-7.76	80.40	2.00	76.90	-8.00
84.10	3.90	69.50	-7.46	80.90	2.50	74.28	-7.72
85.10	4.90	61.62	-6.64	81.40	3.00	69.61	-7.24
86.10	5.90	54.19	-5.87	81.90	3.50	66.64	-6.93
87.10	6.90	46.49	-5.07	82.40	4.00	62.18	-6.47
88.10	7.90	39.20	-4.32	82.90	4.50	58.46	-6.08
89.10	8.90	31.00	-3.47	83.40	5.00	54.59	-5.67
90.10	9.90	22.34	-2.57	84.40	6.00	47.44	-4.93
91.10	10.90	13.83	-1.69	85.40	7.00	39.26	-4.08
92.10	11.90	7.46	-1.03	86.40	8.00	32.45	-3.36
93.10	12.90	0.05	-0.26	87.40	9.00	24.15	-2.50
93.20	13.00	-2.52	0.00	88.40	10.00	15.55	-1.61

Test No. 0.6/-6.35/2.36

Horizontal position (cm)	<i>r</i> (cm)	Depth reading (mm)	<i>ε</i> (cm)
68.00	-11.90	-8.53	0.00
68.90	-11.00	-1.36	-0.69
69.90	-10.00	7.20	-1.51
70.90	-9.00	15.80	-2.33
71.90	-8.00	22.90	-3.01
72.90	-7.00	30.96	-3.78
73.90	-6.00	37.03	-4.36
74.90	-5.00	44.29	-5.05
75.90	-4.00	52.05	-5.79
76.40	-3.50	55.17	-6.08
76.90	-3.00	58.82	-6.43
77.40	-2.50	63.47	-6.88
77.90	-2.00	66.05	-7.12
78.40	-1.50	68.80	-7.38
78.70	-1.20	70.27	-7.52
79.00	-0.90	70.63	-7.54
79.30	-0.60	70.54	-7.52
79.60	-0.30	69.77	-7.44
79.90	0.00	68.53	-7.30
80.20	0.30	69.72	-7.41
80.50	0.60	70.33	-7.46
80.80	0.90	71.00	-7.52
81.10	1.20	70.23	-7.43
81.40	1.50	69.76	-7.37

Test No. 0.6/-5.08/2.39

	<i>z₀</i> (cm)	<i>r_t</i> (cm)+ve	<i>z₀</i> (cm)	-5.08
	<i>d</i> (cm)	<i>r_t</i> (cm)-ve	<i>d</i> (cm)	1.39
	Time to Equilibrium (min)	10.00	Time to Equilibrium (min)	<i>r_t</i> (cm)+ve
Water temp (°C)	22.00	average <i>r_t</i> (cm)	3.12	3.50
Tube position (cm)	79.90	<i>ε_m</i> (cm)+ve	3.21	3.51
Time to fill (s)	32.50	<i>ε_m</i> (cm)-ve	-7.52	-6.31
<i>Q</i> (L/s)	0.36	average <i>ε_m</i> (cm)	-7.54	-6.37
			0.36	average <i>ε_m</i> (cm)

	<i>Horizontal position (cm)</i>	<i>r</i> (cm)	Horizontal position (cm)	<i>r</i> (cm)	Depth reading (mm)	<i>ε</i> (cm)
	69.90	-10.00	69.90	-10.00	-6.52	0.00
	70.40	-9.50	70.40	-9.50	-1.13	-0.53
	71.40	-8.50	71.40	-8.50	6.65	-1.28
	72.40	-7.50	72.40	-7.50	15.15	-2.11
	73.40	-6.50	73.40	-6.50	22.31	-2.80
	74.40	-5.50	74.40	-5.50	30.19	-3.57
	75.40	-4.50	75.40	-4.50	37.80	-4.31
	75.90	-4.00	75.90	-4.00	41.91	-4.71
	76.40	-3.50	76.40	-3.50	45.76	-5.08
	76.90	-3.00	76.90	-3.00	49.33	-5.43
	77.40	-2.50	77.40	-2.50	51.94	-5.68
	77.90	-2.00	77.90	-2.00	56.20	-6.09
	78.40	-1.50	78.40	-1.50	57.56	-6.22
	78.70	-1.20	78.70	-1.20	59.09	-6.36
	79.00	-0.90	79.00	-0.90	59.22	-6.37
	79.30	-0.60	79.30	-0.60	59.00	-6.34
	79.60	-0.30	79.60	-0.30	57.73	-6.21
	79.90	0.00	79.90	0.00	56.98	-6.12
	80.20	0.30	80.20	0.30	58.05	-6.22
	80.50	0.60	80.50	0.60	58.97	-6.31
	80.80	0.90	80.80	0.90	59.07	-6.31
	81.10	1.20	81.10	1.20	58.43	-6.24
	81.40	1.50	81.40	1.50	58.21	-6.21
					56.31	-6.01

Horizontal position (cm)	<i>r</i> (cm)	Depth reading (mm)	ε (cm)
81.90	2.00	67.72	-7.15
82.40	2.50	66.11	-6.97
82.90	3.00	62.24	-6.57
83.40	3.50	58.87	-6.22
84.40	4.50	52.04	-5.50
85.40	5.50	44.08	-4.67
86.40	6.50	37.73	-4.00
87.40	7.50	26.69	-2.86
88.40	8.50	22.96	-2.45
89.40	9.50	15.72	-1.70
90.40	10.50	6.86	-0.78
91.40	11.50	-0.56	0.00

Test No. 0.6/1.27/1.45

z_0 (cm)	z_0 (cm)
<i>d</i> (cm)	<i>d</i> (cm)
1.27	-1.27
1.39	1.39
<i>r</i> , (cm)+ve	<i>r</i> , (cm)+ve
21.00	21.00
<i>r</i> , (cm)-ve	<i>r</i> , (cm)-ve
average <i>r</i> , (cm)	average <i>r</i> , (cm)
15.00	15.00
ε_m (cm)+ve	ε_m (cm)+ve
78.50	79.90
ε_m (cm)-ve	ε_m (cm)-ve
52.97	31.71
0.22	0.36
average ε_m (cm)	average ε_m (cm)
-2.22	-2.52

Horizontal position (cm)	<i>r</i> (cm)	Depth reading (mm)	ε (cm)	Horizontal position (cm)	<i>r</i> (cm)	Depth reading (mm)	ε (cm)
74.40	4.10	-1.85	0.00	75.40	-4.50	-2.25	0.00
74.50	-4.00	-1.01	-0.08	75.90	-4.00	2.14	-0.43
75.00	-3.50	3.78	-0.55	76.40	-3.50	6.18	-0.82
75.50	-3.00	8.31	-0.99	76.90	-3.00	10.10	-1.19
76.00	-2.50	12.53	-1.40	77.40	-2.50	14.67	-1.64
76.50	-2.00	16.12	-1.75	77.90	-2.00	19.04	-2.06
77.00	-1.50	19.32	-2.06	78.40	-1.50	21.90	-2.33
77.30	-1.20	20.26	-2.14	78.70	-1.20	22.98	-2.43

Test No. 0.6/1.27/2.42

z_0 (cm)	z_0 (cm)
<i>d</i> (cm)	<i>d</i> (cm)
1.27	-1.27
1.39	1.39
<i>r</i> , (cm)+ve	<i>r</i> , (cm)+ve
10.00	10.00
<i>r</i> , (cm)-ve	<i>r</i> , (cm)-ve
average <i>r</i> , (cm)	average <i>r</i> , (cm)
21.00	21.00
Water temp (°C)	Water temp (°C)
Tube position (cm)	Tube position (cm)
Time to fill (s)	Time to fill (s)
Q (L/s)	Q (L/s)

Horizontal position (cm)	<i>r</i> (cm)	Depth reading (mm)	<i>ε</i> (cm)	Horizontal position (cm)	<i>r</i> (cm)	Depth reading (mm)	<i>ε</i> (cm)
77.60	-0.90	21.48	-2.26	79.00	-0.90	23.74	-2.50
77.90	-0.60	21.07	-2.21	79.30	-0.60	24.39	-2.56
78.20	-0.30	20.24	-2.12	79.60	-0.30	22.75	-2.39
78.50	0.00	19.47	-2.04	79.90	0.00	21.65	-2.27
78.80	0.30	20.60	-2.14	80.20	0.30	22.40	-2.33
79.10	0.60	20.69	-2.14	80.50	0.60	23.90	-2.48
79.40	0.90	21.09	-2.18	80.80	0.90	24.07	-2.49
79.70	1.20	19.48	-2.01	81.10	1.20	24.16	-2.49
80.00	1.50	18.20	-1.87	81.40	1.50	24.01	-2.46
80.50	2.00	15.38	-1.58	81.90	2.00	21.96	-2.25
81.00	2.50	12.16	-1.25	82.40	2.50	18.74	-1.91
81.50	3.00	8.45	-0.86	82.90	3.00	15.98	-1.62
82.00	3.50	3.88	-0.40	83.40	3.50	12.56	-1.26
82.30	3.80	0.00	0.00	83.90	4.00	7.14	-0.71
				84.50	4.60	0.21	0.00

Test No. 0.6/-1.27/3.86		Test No. 0.6/-1.27/2.11	
<i>z</i> ₀ (cm)	-1.27	<i>z</i> ₀ (cm)	-1.27
<i>d</i> (cm)	0.97	<i>r</i> _t (cm)+ve	1.39
Time to Equilibrium (min)	10.00	<i>r</i> _t (cm)-ve	<i>r</i> _t (cm)+ve
Water temp (°C)	20.00	average <i>r</i> _t (cm)	10.00
Tube position (cm)	78.10	<i>ε</i> _m (cm)+ve	average <i>r</i> _t (cm)
Time to fill (s)	40.92	<i>ε</i> _m (cm)-ve	16.00
<i>Q</i> (L/s)	0.28	average <i>ε</i> _m (cm)	80.30
			<i>ε</i> _m (cm)+ve
			<i>ε</i> _m (cm)-ve
			36.33
			0.32
			average <i>ε</i> _m (cm)
			-2.37
			-2.43
			-2.40

	Horizontal position (cm)	<i>r</i> (cm)	Depth reading (mm)	ε (cm)	Horizontal position (cm)	<i>r</i> (cm)	Depth reading (mm)	ε (cm)
73.90	-4.20	-1.28	0.00		76.10	-4.20	-1.79	0.00
74.20	-3.90	2.45	-0.37		76.40	-3.90	1.86	-0.36
74.50	-3.60	4.94	-0.61		76.70	-3.60	5.01	-0.67
74.80	-3.30	7.37	-0.84		77.00	-3.30	7.73	-0.93
75.10	-3.00	10.87	-1.18		77.30	-3.00	10.31	-1.19
75.40	-2.70	12.90	-1.38		77.60	-2.70	12.93	-1.44
75.70	-2.40	14.95	-1.58		77.90	-2.40	15.06	-1.65
76.00	-2.10	16.80	-1.75		78.20	-2.10	17.98	-1.94
76.30	-1.80	18.72	-1.94		78.50	-1.80	19.62	-2.09
76.60	-1.50	20.84	-2.14		78.80	-1.50	20.76	-2.20
76.90	-1.20	21.71	-2.22		79.10	-1.20	22.05	-2.33
77.20	-0.90	22.66	-2.31		79.40	-0.90	23.15	-2.43
77.50	-0.60	22.14	-2.25		79.70	-0.60	22.66	-2.38
77.80	-0.30	20.47	-2.07		80.00	-0.30	21.81	-2.28
78.10	0.00	19.67	-1.99		80.30	0.00	20.91	-2.19
78.40	0.30	20.79	-2.09		80.60	0.30	21.63	-2.25
78.70	0.60	22.17	-2.22		80.90	0.60	22.08	-2.29
79.00	0.90	21.35	-2.13		81.20	0.90	22.85	-2.37
79.30	1.20	21.32	-2.12		81.50	1.20	22.33	-2.31
79.60	1.50	20.65	-2.05		81.80	1.50	20.95	-2.16
79.90	1.80	17.87	-1.76		82.10	1.80	19.10	-1.97
80.20	2.10	16.27	-1.59		82.40	2.10	16.96	-1.75
80.50	2.40	14.43	-1.40		82.70	2.40	15.79	-1.63
80.80	2.70	12.13	-1.16		83.00	2.70	12.67	-1.31
81.10	3.00	9.30	-0.87		83.30	3.00	10.09	-1.05
81.40	3.30	7.83	-0.72		83.60	3.30	7.66	-0.80
81.70	3.60	4.23	-0.35		83.90	3.60	5.37	-0.56
82.00	3.90	2.45	-0.16		84.40	4.10	0.18	0.00
82.30	4.20	0.89	0.00					

	Horizontal position (cm)	<i>r</i> (cm)	Depth reading (mm)	ε (cm)	Horizontal position (cm)	<i>r</i> (cm)	Depth reading (mm)	ε (cm)
73.90	-4.20	-1.28	0.00		76.10	-4.20	-1.79	0.00
74.20	-3.90	2.45	-0.37		76.40	-3.90	1.86	-0.36
74.50	-3.60	4.94	-0.61		76.70	-3.60	5.01	-0.67
74.80	-3.30	7.37	-0.84		77.00	-3.30	7.73	-0.93
75.10	-3.00	10.87	-1.18		77.30	-3.00	10.31	-1.19
75.40	-2.70	12.90	-1.38		77.60	-2.70	12.93	-1.44
75.70	-2.40	14.95	-1.58		77.90	-2.40	15.06	-1.65
76.00	-2.10	16.80	-1.75		78.20	-2.10	17.98	-1.94
76.30	-1.80	18.72	-1.94		78.50	-1.80	19.62	-2.09
76.60	-1.50	20.84	-2.14		78.80	-1.50	20.76	-2.20
76.90	-1.20	21.71	-2.22		79.10	-1.20	22.05	-2.33
77.20	-0.90	22.66	-2.31		79.40	-0.90	23.15	-2.43
77.50	-0.60	22.14	-2.25		79.70	-0.60	22.66	-2.38
77.80	-0.30	20.47	-2.07		80.00	-0.30	21.81	-2.28
78.10	0.00	19.67	-1.99		80.30	0.00	20.91	-2.19
78.40	0.30	20.79	-2.09		80.60	0.30	21.63	-2.25
78.70	0.60	22.17	-2.22		80.90	0.60	22.08	-2.29
79.00	0.90	21.35	-2.13		81.20	0.90	22.85	-2.37
79.30	1.20	21.32	-2.12		81.50	1.20	22.33	-2.31
79.60	1.50	20.65	-2.05		81.80	1.50	20.95	-2.16
79.90	1.80	17.87	-1.76		82.10	1.80	19.10	-1.97
80.20	2.10	16.27	-1.59		82.40	2.10	16.96	-1.75
80.50	2.40	14.43	-1.40		82.70	2.40	15.79	-1.63
80.80	2.70	12.13	-1.16		83.00	2.70	12.67	-1.31
81.10	3.00	9.30	-0.87		83.30	3.00	10.09	-1.05
81.40	3.30	7.83	-0.72		83.60	3.30	7.66	-0.80
81.70	3.60	4.23	-0.35		83.90	3.60	5.37	-0.56
82.00	3.90	2.45	-0.16		84.40	4.10	0.18	0.00
82.30	4.20	0.89	0.00					

Test No. 0.6/-2.54/2.09

z_0 (cm)	-2.54	r_i (cm)+ve	2.76	z_0 (cm)	-5.08
d (cm)	1.39	r_i (cm)+ve	2.76	d (cm)	0.97
Time to Equilibrium (min)	10.00	r_i (cm)-ve	3.19	Time to Equilibrium (min)	10.00
Water temp (°C)	20.00	average r_i (cm)	2.98	Water temp (°C)	21.00
Tube position (cm)	80.20	ε_m (cm)+ve	-3.60	Tube position (cm)	80.20
Time to fill (s)	36.74	ε_m (cm)-ve	-3.69	Time to fill (s)	40.17
Q (L/s)	0.31	average ε_m (cm)	-3.64	Q (L/s)	0.29
Horizontal position (cm)	r (cm)	Depth reading (mm)	ε (cm)	Horizontal position (cm)	r (cm)
74.20	-6.00	-3.31	0.00	70.80	-9.40
74.50	-5.70	0.13	-0.34	71.20	-9.00
74.80	-5.40	2.60	-0.57	71.70	-8.50
75.10	-5.10	5.47	-0.85	72.20	-8.00
75.40	-4.80	9.07	-1.20	72.70	-7.50
75.70	-4.50	11.15	-1.40	73.20	-7.00
76.00	-4.20	14.31	-1.71	73.70	-6.50
76.30	-3.90	16.83	-1.96	74.20	-6.00
76.60	-3.60	19.37	-2.20	74.70	-5.50
76.90	-3.30	22.00	-2.46	75.20	-5.00
77.20	-3.00	24.46	-2.69	75.70	-4.50
77.50	-2.70	26.45	-2.88	76.20	-4.00
77.80	-2.40	28.39	-3.07	76.70	-3.50
78.10	-2.10	30.53	-3.28	77.20	-3.00
78.40	-1.80	32.66	-3.48	77.70	-2.50
78.70	-1.50	33.96	-3.60	78.20	-2.00
79.00	-1.20	34.36	-3.63	78.70	-1.50
79.30	-0.90	35.00	-3.69	79.00	-1.20
79.60	-0.60	34.73	-3.65	79.30	-0.90
79.90	-0.30	33.88	-3.56	79.60	-0.60
80.20	0.00	32.01	-3.37	79.90	-0.30
80.50	0.30	33.58	-3.51	80.20	0.00
80.80	0.60	34.29	-3.58	80.50	0.30
81.10	0.90	34.59	-3.60	80.80	0.60

Test No. 0.6/-5.08/3.94

z_0 (cm)	2.76	r_i (cm)+ve	0.97
d (cm)	3.19	r_i (cm)-ve	2.70
Time to Equilibrium (min)	20.00	average r_i (cm)	2.77
Water temp (°C)	2.98	Tube position (cm)	6.20
Tube position (cm)	3.60	Time to fill (s)	-6.19
Time to fill (s)	3.69	Q (L/s)	-6.19
Q (L/s)	3.64	average ε_m (cm)	-6.19
Horizontal position (cm)	r (cm)	Depth reading (mm)	ε (cm)
70.80		-9.40	-1.70
71.20		-9.00	1.78
71.70		-8.50	6.26
72.20		-8.00	9.57
72.70		-7.50	14.14
73.20		-7.00	17.98
73.70		-6.50	21.00
74.20		-6.00	25.51
74.70		-5.50	27.89
75.20		-5.00	32.71
75.70		-4.50	35.35
76.20		-4.00	40.58
76.70		-3.50	44.07
77.20		-3.00	47.44
77.70		-2.50	52.88
78.20		-2.00	57.01
78.70		-1.50	59.37
79.00		-1.20	60.63
79.30		-0.90	61.04
79.60		-0.60	62.34
79.90		-0.30	61.23
80.20		0.00	60.00
80.50		0.30	61.55
80.80		0.60	62.19
81.10		0.90	62.14

Horizontal position (cm)	<i>r</i> (cm)	Depth reading (mm)	<i>ε</i> (cm)	Horizontal position (cm)	<i>r</i> (cm)	Depth reading (mm)	<i>ε</i> (cm)
81.70	1.50	32.11	-3.33	81.40	1.20	61.60	-6.07
82.00	1.80	30.90	-3.20	81.70	1.50	61.15	-6.02
82.30	2.10	29.71	-3.08	82.20	2.00	58.44	-5.74
82.60	2.40	26.48	-2.74	82.70	2.50	55.21	-5.40
82.90	2.70	24.81	-2.57	83.20	3.00	50.72	-4.94
83.20	3.00	23.45	-2.43	83.70	3.50	47.71	-4.63
83.50	3.30	21.04	-2.18	84.20	4.00	44.55	-4.30
83.80	3.60	17.65	-1.83	84.70	4.50	41.45	-3.98
84.10	3.90	16.03	-1.66	85.20	5.00	37.14	-3.53
84.40	4.20	12.46	-1.29	85.70	5.50	32.59	-3.06
84.70	4.50	10.91	-1.13	86.20	6.00	27.78	-2.57
85.00	4.80	8.61	-0.89	86.70	6.50	23.16	-2.10
85.30	5.10	5.14	-0.54	87.20	7.00	19.21	-1.69
85.60	5.40	2.25	-0.24	87.70	7.50	15.69	-1.33
85.90	5.70	-0.05	0.00	88.20	8.00	12.75	-1.02
				88.70	8.50	5.69	-0.30
				89.20	9.00	2.80	0.00

Test No. 0.6/-3.81/2.06

<i>z</i> ₀ (cm)	-3.81	<i>r</i> _t (cm)+ve	2.89	<i>z</i> ₀ (cm)	-7.62
<i>d</i> (cm)	1.39	<i>r</i> _t (cm)-ve	2.89	<i>d</i> (cm)	0.97
Time to Equilibrium (min)	10.00	<i>r</i> _t (cm)-ve	3.34	Time to Equilibrium (min)	10.00
Water temp (°C)	20.00	average <i>r</i> _t (cm)	3.11	Water temp (°C)	21.00
Tube position (cm)	78.20	<i>ε</i> _m (cm)+ve	-4.90	Tube position (cm)	78.40
Time to fill (s)	37.17	<i>ε</i> _m (cm)-ve	-5.00	Time to fill (s)	50.84
<i>Q</i> (L/s)	0.31	average <i>ε</i> _m (cm)	-4.95	<i>Q</i> (L/s)	0.23
				average <i>ε</i> _m (cm)	-8.44

Test No. 0.6/-7.62/3.11

<i>z</i> ₀ (cm)	-7.62
<i>d</i> (cm)	0.97
Time to Equilibrium (min)	10.00
Water temp (°C)	21.00
Tube position (cm)	78.40
Time to fill (s)	50.84
<i>Q</i> (L/s)	0.23
	average <i>ε</i> _m (cm)

Horizontal position (cm)	<i>r</i> (cm)	Depth reading (mm)	<i>ε</i> (cm)	Horizontal position (cm)	<i>r</i> (cm)	Depth reading (mm)	<i>ε</i> (cm)
69.90	-8.30	-6.46	0.00	65.60	-12.80	-0.48	0.00
70.20	-8.00	-3.94	-0.24	66.40	-12.00	7.57	-0.80
70.70	-7.50	0.58	-0.67	67.40	-11.00	13.85	-1.43
71.20	-7.00	4.77	-1.07	68.40	-10.00	21.40	-2.18
71.70	-6.50	8.20	-1.40	69.40	-9.00	30.00	-3.04
72.20	-6.00	12.85	-1.84	70.40	-8.00	37.36	-3.78
72.70	-5.50	16.70	-2.21	71.40	-7.00	44.79	-4.52
73.20	-5.00	21.04	-2.62	72.40	-6.00	52.07	-5.25
73.70	-4.50	24.90	-2.99	73.40	-5.00	60.80	-6.12
74.20	-4.00	28.40	-3.32	74.40	-4.00	65.97	-6.63
74.70	-3.50	32.38	-3.69	75.40	-3.00	73.36	-7.37
75.20	-3.00	36.22	-4.06	75.90	-2.50	77.65	-7.80
75.70	-2.50	40.03	-4.42	76.40	-2.00	80.82	-8.12
76.20	-2.00	42.85	-4.68	76.90	-1.50	83.39	-8.37
76.70	-1.50	45.11	-4.89	77.20	-1.20	84.00	-8.43
77.00	-1.20	45.82	-4.95	77.50	-0.90	84.05	-8.44
77.30	-0.90	46.44	-5.00	77.80	-0.60	84.17	-8.45
77.60	-0.60	46.15	-4.96	78.10	-0.30	83.98	-8.43
77.90	-0.30	44.96	-4.83	78.40	0.00	83.03	-8.33
78.20	0.00	44.25	-4.74	78.70	0.30	83.81	-8.41
78.50	0.30	45.33	-4.84	79.00	0.60	84.00	-8.43
78.80	0.60	45.77	-4.87	79.30	0.90	83.71	-8.40
79.10	0.90	46.16	-4.90	79.60	1.20	82.74	-8.30
79.40	1.20	45.27	-4.80	79.90	1.50	81.29	-8.16
79.70	1.50	44.08	-4.67	80.40	2.00	78.84	-7.91
80.20	2.00	42.10	-4.45	80.90	2.50	74.88	-7.52
80.70	2.50	38.65	-4.09	81.40	3.00	71.05	-7.13
81.20	3.00	35.29	-3.73	82.40	4.00	62.85	-6.31
81.70	3.50	31.52	-3.33	83.40	5.00	58.65	-5.89
82.20	4.00	28.54	-3.01	84.40	6.00	52.00	-5.22
82.70	4.50	24.37	-2.58	85.40	7.00	44.20	-4.44
83.20	5.00	20.09	-2.13	86.40	8.00	37.73	-3.79

Horizontal position (cm)	<i>r</i> (cm)	Depth reading (mm)	ε (cm)
83.70	5.50	17.87	-1.89
84.20	6.00	14.24	-1.51
84.70	6.50	10.53	-1.12
85.20	7.00	6.23	-0.67
85.70	7.50	2.68	-0.29
86.10	7.90	-0.07	0.00

Test No. 0.6/-6.35/2.14

z_0 (cm)	<i>r</i> (cm)+ve	2.85	-6.35
<i>d</i> (cm)	1.39	<i>r</i> (cm)-ve	2.85
Time to Equilibrium (min)	10.00	<i>r</i> (cm)-ve	3.44
Water temp (°C)	21.00	average <i>r</i> , (cm)	3.14
Tube position (cm)	78.30	ε_m (cm)+ve	-7.47
Time to fill (s)	35.78	ε_m (cm)-ve	-7.51
\underline{Q} (L/s)	0.32	average ε_m , (cm)	-7.49
Horizontal position (cm)	<i>r</i> (cm)	Depth reading (mm)	ε (cm)
66.90	-11.40	-7.10	0.00
67.80	-10.50	3.71	-1.05
68.80	-9.50	10.65	-1.71
69.80	-8.50	18.62	-2.48
70.80	-7.50	27.08	-3.29
71.80	-6.50	34.43	-3.99
72.80	-5.50	43.42	-4.86
73.80	-4.50	52.19	-5.70
74.80	-3.50	58.54	-6.30
75.30	-3.00	62.40	-6.67
75.80	-2.50	66.15	-7.03
76.30	-2.00	68.63	-7.26
76.80	-1.50	70.79	-7.46
Horizontal position (cm)	<i>r</i> (cm)	Depth reading (mm)	ε (cm)
66.90	66.90	-11.40	-7.10
67.80	67.80	-10.50	3.71
68.80	68.80	-9.50	-10.65
69.80	69.80	-8.50	18.62
70.80	70.80	-7.50	-27.08
71.80	71.80	-6.50	34.43
72.80	72.80	-5.50	-43.42
73.80	73.80	-4.50	52.19
74.80	74.80	-3.50	-58.54
75.30	75.30	-3.00	62.40
75.80	75.80	-2.50	66.15
76.30	76.30	-2.00	68.63
76.80	76.80	-1.50	70.79

Test No. 0.6/-6.35/2.14

z_0 (cm)	<i>d</i> (cm)	r_t (cm)+ve	r_t (cm)-ve	average r_t , (cm)	ε_m (cm)+ve	ε_m (cm)-ve	average ε_m , (cm)	ε (cm)
Time to Equilibrium (min)	10.00	r_t (cm)-ve	3.44	10.00	r_t (cm)-ve	3.44	10.00	3.44
Water temp (°C)	21.00	average <i>r</i> , (cm)	3.14	21.00	average r_t , (cm)	3.14	21.00	3.14
Tube position (cm)	78.30	ε_m (cm)+ve	-7.47	78.30	ε_m (cm)+ve	-7.47	78.30	-7.47
Time to fill (s)	35.78	ε_m (cm)-ve	-7.51	35.78	ε_m (cm)-ve	-7.51	35.78	-7.51
\underline{Q} (L/s)	0.32	average ε_m , (cm)	-7.49	0.32	average ε_m , (cm)	-7.49	0.32	-7.49

Horizontal position (cm)	<i>r</i> (cm)	Depth reading (mm)	<i>ε</i> (cm)	Horizontal position (cm)	<i>r</i> (cm)	Depth reading (mm)	<i>ε</i> (cm)
77.10	-1.20	71.03	-7.48	77.10	-1.20	71.03	-7.48
77.40	-0.90	71.51	-7.51	77.40	-0.90	71.51	-7.51
77.70	-0.60	70.50	-7.40	77.70	-0.60	70.50	-7.40
78.00	-0.30	69.75	-7.32	78.00	-0.30	69.75	-7.32
78.30	0.00	69.12	-7.24	78.30	0.00	69.12	-7.24
78.60	0.30	70.00	-7.32	78.60	0.30	70.00	-7.32
78.90	0.60	71.34	-7.45	78.90	0.60	71.34	-7.45
79.20	0.90	71.72	-7.47	79.20	0.90	71.72	-7.47
79.50	1.20	70.60	-7.35	79.50	1.20	70.60	-7.35
79.80	1.50	69.13	-7.20	79.80	1.50	69.13	-7.20
80.30	2.00	66.17	-6.88	80.30	2.00	66.17	-6.88
80.80	2.50	63.78	-6.63	80.80	2.50	63.78	-6.63
81.30	3.00	60.00	-6.23	81.30	3.00	60.00	-6.23
81.80	3.50	56.41	-5.86	81.80	3.50	56.41	-5.86
82.30	4.00	52.44	-5.44	82.30	4.00	52.44	-5.44
82.80	4.50	49.14	-5.10	82.80	4.50	49.14	-5.10
83.30	5.00	45.23	-4.69	83.30	5.00	45.23	-4.69
83.80	5.50	42.82	-4.43	83.80	5.50	42.82	-4.43
84.30	6.00	38.40	-3.97	84.30	6.00	38.40	-3.97
84.80	6.50	33.90	-3.51	84.80	6.50	33.90	-3.51
85.30	7.00	32.30	-3.33	85.30	7.00	32.30	-3.33
85.80	7.50	29.22	-3.01	85.80	7.50	29.22	-3.01
86.30	8.00	25.96	-2.66	86.30	8.00	25.96	-2.66
86.80	8.50	20.81	-2.13	86.80	8.50	20.81	-2.13
87.30	9.00	18.32	-1.87	87.30	9.00	18.32	-1.87
87.80	9.50	15.08	-1.53	87.80	9.50	15.08	-1.53
88.30	10.00	9.78	-0.98	88.30	10.00	9.78	-0.98
88.80	10.50	6.81	-0.67	88.80	10.50	6.81	-0.67
89.30	11.00	3.30	-0.30	89.30	11.00	3.30	-0.30
89.80	11.50	0.48	0.00	89.80	11.50	0.48	0.00

Test No. 0.6/-2.54/3.82

z_0 (cm)	-2.54	r_i (cm)+ve	2.59	z_0 (cm)	-7.62
d (cm)	0.97	r_i (cm)-ve	2.48	d (cm)	2.04
Time to Equilibrium (min)	10.00	r_i (cm)-ve	2.53	Time to Equilibrium (min)	10.00
Water temp (°C)	18.00	average r_i (cm)	2.58	Water temp (°C)	15.00
Tube position (cm)	80.10	ε_m (cm)+ve	-3.58	Tube position (cm)	73.90
Time to fill (s)	41.40	ε_m (cm)-ve	-3.60	Time to fill (s)	66.39
Q (L/s)	0.28	average ε_m (cm)	-3.59	Q (L/s)	0.17

Test No. 0.6/-7.62/0.53

Horizontal position (cm)	r (cm)	Depth reading (mm)	ε (cm)	Horizontal position (cm)	r (cm)	Depth reading (mm)	ε (cm)
74.60	-5.50	-0.90	0.00	61.70	-12.20	8.10	0.00
74.70	-5.40	1.30	-0.22	61.90	-12.00	9.32	-0.12
75.00	-5.10	2.80	-0.37	62.90	-11.00	18.44	-1.03
75.30	-4.80	5.02	-0.59	63.90	-10.00	27.17	-1.90
75.60	-4.50	7.71	-0.85	64.90	-9.00	35.18	-2.69
75.90	-4.20	8.83	-0.96	65.90	-8.00	42.45	-3.42
76.20	-3.90	11.70	-1.25	66.90	-7.00	49.79	-4.14
76.50	-3.60	13.69	-1.44	67.90	-6.00	58.12	-4.97
76.80	-3.30	17.57	-1.83	68.90	-5.00	65.01	-5.66
77.10	-3.00	20.04	-2.07	69.90	-4.00	73.02	-6.45
77.40	-2.70	21.33	-2.20	70.90	-3.00	80.14	-7.16
77.70	-2.40	25.90	-2.66	71.40	-2.50	83.15	-7.46
78.00	-2.10	26.40	-2.70	71.90	-2.00	87.96	-7.94
78.30	-1.80	28.81	-2.94	72.40	-1.50	90.86	-8.23
78.60	-1.50	29.59	-3.02	72.70	-1.20	92.36	-8.37
78.90	-1.20	32.14	-3.27	73.00	-0.90	91.75	-8.31
79.20	-0.90	33.77	-3.43	73.30	-0.60	91.32	-8.27
79.50	-0.60	35.46	-3.60	73.60	-0.30	91.27	-8.26
79.80	-0.30	34.88	-3.54	73.90	0.00	90.15	-8.15
80.10	0.00	33.72	-3.42	74.20	0.30	91.00	-8.23
80.40	0.30	34.01	-3.44	74.50	0.60	91.97	-8.33
81.90	1.80	30.70	-3.10	76.40	2.50	87.21	-7.84
82.20	2.10	29.24	-2.95	76.90	3.00	82.85	-7.40

Horizontal position (cm)	<i>r</i> (cm)	Depth reading (mm)	<i>ε</i> (cm)
82.50	2.40	26.82	-2.71
82.80	2.70	24.19	-2.44
83.10	3.00	23.58	-2.38
83.40	3.30	22.22	-2.24
83.70	3.60	18.96	-1.91
84.00	3.90	15.14	-1.53
84.30	4.20	14.05	-1.42
84.60	4.50	10.90	-1.10
84.90	4.80	9.02	-0.91
85.20	5.10	5.07	-0.51
85.50	5.40	3.58	-0.36
85.80	5.70	0.00	0.00

Test No. 0.6/-2.54/0.53

Horizontal position (cm)	<i>r</i> (cm)	Depth reading (mm)	<i>ε</i> (cm)	Horizontal position (cm)	<i>r</i> (cm)	Depth reading (mm)	<i>ε</i> (cm)
70.70	-5.60	-0.70	0.00	73.40	-6.50	-3.11	0.00
71.30	-5.00	4.54	-0.51	74.40	-5.50	4.65	-0.75
72.30	-4.00	14.70	-1.50	75.40	-4.50	12.61	-1.53
73.30	-3.00	23.24	-2.33	76.40	-3.50	20.88	-2.33
73.80	-2.50	26.55	-2.65	76.90	-3.00	23.91	-2.62
74.30	-2.00	30.36	-3.02	77.40	-2.50	27.61	-2.98
74.80	-1.50	31.65	-3.14	77.90	-2.00	31.41	-3.35
75.10	-1.20	31.75	-3.14	78.40	-1.50	34.12	-3.61

Test No. 0.6/-2.54/2.42

<i>z</i> ₀ (cm)	<i>d</i> (cm)	<i>r</i> _t (cm)+ve	<i>d</i> (cm)	<i>r</i> _t (cm)-ve	<i>r</i> _t (cm)+ve
		2.04	2.36	1.39	3.43
Time to Equilibrium (min)	10.00	<i>r</i> _t (cm)-ve	2.68	10.00	3.14
Water temp (°C)	21.00	average <i>r</i> _t (cm)	2.52	average <i>r</i> _t (cm)	3.29
Tube position (cm)	76.30	<i>ε</i> _m (cm)+ve	-3.34	79.90	<i>ε</i> _m (cm)+ve
Time to fill (s)	66.24	<i>ε</i> _m (cm)-ve	-3.38	31.62	<i>ε</i> _m (cm)-ve
<i>Q</i> (L/s)	0.17	average <i>ε</i> _m (cm)	-3.36	0.37	average <i>ε</i> _m (cm)

Horizontal position (cm)	<i>r</i> (cm)	Depth reading (mm)	<i>ε</i> (cm)
75.40	-0.90	34.16	-3.38
75.70	-0.60	33.15	-3.27
76.00	-0.30	32.22	-3.17
76.30	0.00	30.91	-3.03
76.60	0.30	32.18	-3.15
76.90	0.60	33.97	-3.32
77.20	0.90	34.23	-3.34
77.50	1.20	32.52	-3.16
77.80	1.50	31.18	-3.02
78.30	2.00	29.00	-2.79
78.80	2.50	25.66	-2.45
79.30	3.00	21.03	-1.97
79.80	3.50	18.04	-1.66
80.80	4.50	10.16	-0.85
81.80	5.50	1.91	0.00
		86.30	86.30

Horizontal position (cm)	<i>r</i> (cm)	Depth reading (mm)	<i>ε</i> (cm)	Horizontal position (cm)	<i>r</i> (cm)	Depth reading (mm)	<i>ε</i> (cm)
78.70				78.70	-1.20	35.19	-3.71
				79.00	-0.90	35.75	-3.76
				79.30	-0.60	36.09	-3.79
				79.60	-0.30	35.19	-3.69
				79.90	0.00	33.62	-3.53
				80.20	0.30	34.79	-3.64
				80.50	0.60	35.85	-3.74
				80.80	0.90	35.67	-3.71
				81.10	1.20	34.80	-3.62
				81.40	1.50	34.35	-3.57
				81.90	2.00	33.01	-3.42
				82.40	2.50	29.82	-3.09
				83.40	3.50	24.07	-2.50
				84.40	4.50	17.06	-1.77
				85.40	5.50	9.65	-1.01
				86.30	6.40	-0.25	0.00

Test No. 0.6/-6.35/3.98

<i>z</i> ₀ (cm)	-6.35	<i>z</i> ₀ (cm)	-7.62
<i>d</i> (cm)	0.97	<i>r</i> _t (cm)+ve	0.97
Time to Equilibrium (min)	10.00	<i>r</i> _t (cm)-ve	10.00
Water temp (°C)	22.00	average <i>r</i> _t (cm)	18.00
Tube position (cm)	78.20	<i>ε</i> _m (cm)+ve	80.20
Time to fill (s)	39.72	<i>ε</i> _m (cm)-ve	40.91
<i>Q</i> (L/s)	0.29	average <i>ε</i> _m (cm)	0.28

Test No. 0.6/-7.62/3.86

<i>z</i> ₀ (cm)		<i>r</i> _t (cm)+ve	3.40
<i>d</i> (cm)		<i>r</i> _t (cm)-ve	2.81
Time to Equilibrium (min)		average <i>r</i> _t (cm)	3.11
Water temp (°C)		Tube position (cm)	-8.92
Tube position (cm)		Time to fill (s)	-8.93
Time to fill (s)		<i>Q</i> (L/s)	-8.92
<i>Q</i> (L/s)		average <i>ε</i> _m (cm)	-8.92

Horizontal position (cm)	<i>r</i> (cm)	Depth reading (mm)	ε (cm)	Horizontal position (cm)	<i>r</i> (cm)	Depth reading (mm)	ε (cm)
67.40	-10.80	-2.48	0.00	67.30	-12.90	-1.10	0.00
67.70	-10.50	0.78	-0.32	67.70	-12.50	-0.47	-0.06
68.70	-9.50	9.21	-1.15	68.70	-11.50	9.60	-1.07
69.70	-8.50	17.98	-2.01	69.70	-10.50	17.42	-1.85
70.70	-7.50	25.17	-2.72	70.70	-9.50	27.47	-2.85
71.70	-6.50	34.67	-3.65	71.70	-8.50	35.31	-3.64
72.70	-5.50	42.32	-4.40	72.70	-7.50	41.62	-4.27
73.70	-4.50	49.88	-5.15	73.70	-6.50	49.70	-5.07
74.70	-3.50	57.41	-5.88	74.70	-5.50	57.76	-5.88
75.70	-2.50	65.33	-6.66	75.70	-4.50	63.86	-6.49
76.70	-1.50	71.65	-7.28	76.70	-3.50	68.36	-6.94
77.00	-1.20	72.35	-7.35	77.70	-2.50	78.31	-7.93
77.30	-0.90	72.54	-7.36	78.70	-1.50	84.41	-8.54
77.60	-0.60	73.84	-7.49	79.00	-1.20	86.06	-8.71
77.90	-0.30	73.54	-7.45	79.30	-0.90	88.25	-8.93
78.20	0.00	73.30	-7.42	79.60	-0.60	87.85	-8.88
78.50	0.30	73.55	-7.44	79.90	-0.30	86.51	-8.75
78.80	0.60	73.90	-7.47	80.20	0.00	85.38	-8.64
79.10	0.90	74.36	-7.52	80.50	0.30	86.74	-8.77
79.40	1.20	72.65	-7.34	80.80	0.60	88.26	-8.92
79.70	1.50	72.27	-7.30	81.10	0.90	86.83	-8.78
80.20	2.00	69.82	-7.05	81.40	1.20	86.15	-8.71
80.70	2.50	66.76	-6.73	81.70	1.50	85.45	-8.64
81.20	3.00	63.05	-6.36	82.70	2.50	81.77	-8.27
81.70	3.50	60.73	-6.12	83.70	3.50	74.53	-7.55
82.70	4.50	52.53	-5.28	84.70	4.50	66.72	-6.77
83.70	5.50	45.49	-4.56	85.70	5.50	60.00	-6.09
84.70	6.50	38.92	-3.89	86.70	6.50	51.92	-5.29
85.70	7.50	32.22	-3.21	87.70	7.50	45.87	-4.68
86.70	8.50	23.74	-2.35	88.70	8.50	38.33	-3.93
87.70	9.50	16.45	-1.60	89.70	9.50	31.59	-3.25

Horizontal position (cm)	<i>r</i> (cm)	Depth reading (mm)	ε (cm)
88.70	10.50	8.06	-0.75
89.40	11.20	0.67	0.00

Test No. 0.6/-2.54/2.84

z_0 (cm)	-2.54	z_0 (cm)	-7.62
<i>d</i> (cm)	0.97	r_t (cm)+ve	1.39
Time to Equilibrium (min)	10.00	r_t (cm)-ve	r_t (cm)+ve
Water temp (°C)	21.00	average r_t (cm)	r_t (cm)-ve
Tube position (cm)	80.40	ε_m (cm)+ve	average r_t (cm)
Time to fill (s)	55.70	ε_m (cm)-ve	average r_t (cm)
Q (L/s)	0.21	average ε_m (cm)	average r_t (cm)

Test No. 0.6/-7.62/2.14

z_0 (cm)	d (cm)	z_0 (cm)	d (cm)
Time to Equilibrium (min)	10.00	r_t (cm)-ve	1.39
Water temp (°C)	21.00	average r_t (cm)	r_t (cm)+ve
Tube position (cm)	80.40	ε_m (cm)+ve	average r_t (cm)
Time to fill (s)	55.70	ε_m (cm)-ve	average r_t (cm)
Q (L/s)	0.21	average ε_m (cm)	average r_t (cm)

Horizontal position (cm)	<i>r</i> (cm)	Depth reading (mm)	ε (cm)	Horizontal position (cm)	<i>r</i> (cm)	Depth reading (mm)	ε (cm)
74.80	-5.60	-3.21	0.00	66.60	-13.40	-5.30	0.00
75.00	-5.40	-0.40	-0.27	67.00	-13.00	1.76	-0.70
75.30	-5.10	1.97	-0.50	68.00	-12.00	10.01	-1.51
75.60	-4.80	4.23	-0.72	69.00	-11.00	17.68	-2.26
75.90	-4.50	6.66	-0.95	70.00	-10.00	26.00	-3.07
76.20	-4.20	8.98	-1.17	71.00	-9.00	33.52	-3.81
76.50	-3.90	12.10	-1.47	72.00	-8.00	40.76	-4.51
76.80	-3.60	13.34	-1.58	73.00	-7.00	48.94	-5.31
77.10	-3.30	15.96	-1.83	74.00	-6.00	54.48	-5.85
77.40	-3.00	18.60	-2.09	75.00	-5.00	61.85	-6.57
77.70	-2.70	22.12	-2.43	76.00	-4.00	70.37	-7.40
78.00	-2.40	24.21	-2.63	77.00	-3.00	77.10	-8.06
78.30	-2.10	25.35	-2.73	77.50	-2.50	80.64	-8.41
78.60	-1.80	27.96	-2.98	78.00	-2.00	84.13	-8.75
78.90	-1.50	30.22	-3.20	78.50	-1.50	85.51	-8.88

Horizontal position (cm)	<i>r</i> (cm)	Depth reading (mm)	<i>ε</i> (cm)	Horizontal position (cm)	<i>r</i> (cm)	Depth reading (mm)	<i>ε</i> (cm)
79.20	-1.20	30.71	-3.23	78.80	-1.20	86.68	-8.99
79.50	-0.90	31.63	-3.31	79.10	-0.90	87.14	-9.03
79.80	-0.60	32.97	-3.44	79.40	-0.60	87.01	-9.01
80.10	-0.30	32.34	-3.36	79.70	-0.30	85.99	-8.90
80.40	0.00	31.43	-3.26	80.00	0.00	84.65	-8.76
80.70	0.30	32.34	-3.34	80.30	0.30	85.74	-8.87
81.00	0.60	32.51	-3.35	80.60	0.60	87.44	-9.03
81.30	0.90	32.81	-3.37	80.90	0.90	86.64	-8.95
81.60	1.20	31.27	-3.20	81.20	1.20	86.13	-8.89
81.90	1.50	29.25	-2.99	81.50	1.50	84.77	-8.75
82.20	1.80	28.67	-2.92	82.00	2.00	81.66	-8.43
82.50	2.10	26.13	-2.66	82.50	2.50	78.20	-8.08
82.80	2.40	25.37	-2.57	83.00	3.00	74.53	-7.70
83.10	2.70	24.03	-2.43	84.00	4.00	68.33	-7.06
83.40	3.00	20.77	-2.09	85.00	5.00	60.57	-6.27
83.70	3.30	18.66	-1.87	86.00	6.00	53.70	-5.57
84.00	3.60	15.86	-1.58	87.00	7.00	46.65	-4.84
84.30	3.90	12.07	-1.19	88.00	8.00	40.82	-4.24
84.60	4.20	10.67	-1.04	89.00	9.00	30.69	-3.21
84.90	4.50	8.58	-0.82	90.00	10.00	24.33	-2.56
85.20	4.80	5.57	-0.50	91.00	11.00	12.69	-1.38
85.50	5.10	2.83	-0.22	92.00	12.00	5.40	-0.63
85.70	5.30	0.71	0.00	92.70	12.70	-0.80	0.00

Test No. 0.6/-1.27/3.53				Test No. 0.6/-2.54/3.14			
<i>z</i> ₀ (cm)	-1.27	<i>r</i> _t (cm)+ve	2.48	<i>z</i> ₀ (cm)	-2.54	<i>r</i> _t (cm)+ve	2.21
<i>d</i> (cm)	0.97	<i>r</i> _t (cm)-ve	2.76	<i>d</i> (cm)	0.97	<i>r</i> _t (cm)-ve	2.15
Time to Equilibrium (min)	10.00	<i>r</i> _t (cm)-ve	2.76	Time to Equilibrium (min)	10.00	average <i>r</i> _t (cm)	2.18
Water temp (°C)	20.00	average <i>r</i> _t (cm)	2.62	Water temp (°C)	18.00	<i>r</i> _t (cm)-ve	2.23
Tube position (cm)	78.40	<i>ε</i> _m (cm)+ve	-2.25	Tube position (cm)	78.30	<i>ε</i> _m (cm)+ve	-3.31
Time to fill (s)	44.74	<i>ε</i> _m (cm)-ve	-2.30	Time to fill (s)	50.32	<i>ε</i> _m (cm)-ve	-3.27
<i>Q</i> (L/s)	0.26	average <i>ε</i> _m (cm)	-2.27	<i>Q</i> (L/s)	0.23	average <i>ε</i> _m (cm)	-3.27

	Horizontal position (cm)	<i>r</i> (cm)	Depth reading (mm)	ε (cm)	Horizontal position (cm)	<i>r</i> (cm)	Depth reading (mm)	ε (cm)
74.20	-4.20	-1.36	0.00	72.90	-5.40	0.78	0.00	0.00
74.50	-3.90	1.48	-0.28	73.30	-5.00	3.74	-0.30	-0.30
74.80	-3.60	3.98	-0.52	73.80	-4.50	6.63	-0.59	-0.59
75.10	-3.30	7.31	-0.85	74.30	-4.00	11.15	-1.05	-1.05
75.40	-3.00	10.37	-1.15	74.80	-3.50	14.96	-1.43	-1.43
75.70	-2.70	12.82	-1.39	75.30	-3.00	20.06	-1.95	-1.95
76.00	-2.40	14.60	-1.57	75.80	-2.50	23.35	-2.28	-2.28
76.30	-2.10	17.15	-1.82	76.30	-2.00	27.06	-2.66	-2.66
76.60	-1.80	18.65	-1.96	76.80	-1.50	30.86	-3.04	-3.04
76.90	-1.50	20.71	-2.16	77.10	-1.20	32.18	-3.17	-3.17
77.20	-1.20	21.84	-2.27	77.40	-0.90	33.12	-3.27	-3.27
77.50	-0.90	22.15	-2.30	77.70	-0.60	33.52	-3.31	-3.31
77.80	-0.60	21.58	-2.23	78.00	-0.30	32.31	-3.19	-3.19
78.10	-0.30	21.48	-2.22	78.30	0.00	31.18	-3.08	-3.08
78.40	0.00	19.27	-1.99	78.60	0.30	31.35	-3.10	-3.10
78.70	0.30	21.14	-2.18	78.90	0.60	32.40	-3.21	-3.21
79.00	0.60	21.94	-2.25	79.20	0.90	32.59	-3.23	-3.23
79.30	0.90	21.57	-2.21	79.50	1.20	32.00	-3.17	-3.17
79.60	1.20	20.90	-2.14	79.80	1.50	30.07	-2.98	-2.98
79.90	1.50	19.79	-2.02	80.30	2.00	27.17	-2.70	-2.70
80.20	1.80	18.26	-1.86	80.80	2.50	23.27	-2.31	-2.31
80.50	2.10	15.05	-1.54	81.30	3.00	19.71	-1.96	-1.96
80.80	2.40	13.13	-1.34	81.80	3.50	15.70	-1.56	-1.56
81.10	2.70	10.50	-1.07	82.30	4.00	12.17	-1.21	-1.21
81.40	3.00	8.33	-0.85	82.80	4.50	7.56	-0.76	-0.76
81.70	3.30	5.06	-0.52	83.30	5.00	2.00	-0.21	-0.21
82.00	3.60	2.15	-0.22	83.50	5.20	0.00	0.00	0.00
82.40	4.00	0.00	0.00					

Test No. 0.6/-3.81/3.12

z_0 (cm)	-3.81	r_t (cm)+ve	2.29	d (cm)	0.97	r_t (cm)+ve	2.75
d (cm)	0.97	r_t (cm)-ve	2.50	Time to Equilibrium (min)	10.00	r_t (cm)-ve	2.75
Time to Equilibrium (min)	10.00	average r_t (cm)	2.39	Water temp (°C)	22.00	average r_t (cm)	2.75
Water temp (°C)	18.00	ε_m (cm)+ve	-4.61	Tube position (cm)	78.50	ε_m (cm)+ve	-4.91
Tube position (cm)	78.30	ε_m (cm)-ve	-4.64	Time to fill (s)	43.98	ε_m (cm)-ve	-4.93
Time to fill (s)	50.68	average ε_m (cm)	-4.62	Q (L/s)	0.26	average ε_m (cm)	-4.92
Horizontal position (cm)	r (cm)	Depth reading (mm)	ε (cm)	Horizontal position (cm)	r (cm)	Depth reading (mm)	ε (cm)
71.10	-7.20	-0.40	0.00	71.00	-7.50	-3.15	0.00
71.30	-7.00	1.33	-0.17	71.50	-7.00	-0.44	-0.26
71.80	-6.50	5.12	-0.54	72.00	-6.50	5.44	-0.83
72.30	-6.00	9.48	-0.98	72.50	-6.00	8.70	-1.15
72.80	-5.50	13.45	-1.37	73.00	-5.50	12.69	-1.54
73.30	-5.00	17.15	-1.73	73.50	-5.00	15.15	-1.77
73.80	-4.50	21.97	-2.21	74.00	-4.50	23.65	-2.61
74.30	-4.00	26.27	-2.63	74.50	-4.00	27.35	-2.96
74.80	-3.50	30.64	-3.06	75.00	-3.50	30.17	-3.23
75.30	-3.00	23.29	-2.32	75.50	-3.00	33.57	-3.56
75.80	-2.50	38.27	-3.82	76.00	-2.50	38.71	-4.06
76.30	-2.00	41.62	-4.15	76.50	-2.00	41.95	-4.38
76.80	-1.50	43.97	-4.38	77.00	-1.50	44.71	-4.64
77.10	-1.20	45.74	-4.55	77.30	-1.20	46.93	-4.85
77.40	-0.90	46.42	-4.61	77.60	-0.90	47.41	-4.90
77.70	-0.60	46.69	-4.64	77.90	-0.60	47.82	-4.93
78.00	-0.30	45.07	-4.47	78.20	-0.30	47.28	-4.87
78.30	0.00	43.84	-4.35	78.50	0.00	46.06	-4.74
78.60	0.30	45.58	-4.52	78.80	0.30	47.44	-4.87
78.90	0.60	46.55	-4.61	79.10	0.60	47.94	-4.91
79.20	0.90	45.70	-4.52	79.40	0.90	47.85	-4.90
79.50	1.20	44.94	-4.44	79.70	1.20	45.75	-4.68
79.80	1.50	44.01	-4.35	80.00	1.50	45.05	-4.60
80.30	2.00	41.18	-4.06	80.50	2.00	43.35	-4.42

Test No. 0.6/-3.81/3.59

z_0 (cm)	-3.81	d (cm)	0.97	r_t (cm)+ve	2.75		
d (cm)	0.97	r_t (cm)-ve	2.50	Time to Equilibrium (min)	10.00		
Time to Equilibrium (min)	10.00	average r_t (cm)	2.39	Water temp (°C)	22.00		
Water temp (°C)	18.00	ε_m (cm)+ve	-4.61	Tube position (cm)	78.50		
Tube position (cm)	78.30	ε_m (cm)-ve	-4.64	Time to fill (s)	43.98		
Time to fill (s)	50.68	average ε_m (cm)	-4.62	Q (L/s)	0.26		
Horizontal position (cm)	r (cm)	Depth reading (mm)	ε (cm)	Horizontal position (cm)	r (cm)	Depth reading (mm)	ε (cm)
71.10	-7.20	-0.40	0.00	71.00	-7.50	-3.15	0.00
71.30	-7.00	1.33	-0.17	71.50	-7.00	-0.44	-0.26
71.80	-6.50	5.12	-0.54	72.00	-6.50	5.44	-0.83
72.30	-6.00	9.48	-0.98	72.50	-6.00	8.70	-1.15
72.80	-5.50	13.45	-1.37	73.00	-5.50	12.69	-1.54
73.30	-5.00	17.15	-1.73	73.50	-5.00	15.15	-1.77
73.80	-4.50	21.97	-2.21	74.00	-4.50	23.65	-2.61
74.30	-4.00	26.27	-2.63	74.50	-4.00	27.35	-2.96
74.80	-3.50	30.64	-3.06	75.00	-3.50	30.17	-3.23
75.30	-3.00	23.29	-2.32	75.50	-3.00	33.57	-3.56
75.80	-2.50	38.27	-3.82	76.00	-2.50	38.71	-4.06
76.30	-2.00	41.62	-4.15	76.50	-2.00	41.95	-4.38
76.80	-1.50	43.97	-4.38	77.00	-1.50	44.71	-4.64
77.10	-1.20	45.74	-4.55	77.30	-1.20	46.93	-4.85
77.40	-0.90	46.42	-4.61	77.60	-0.90	47.41	-4.90
77.70	-0.60	46.69	-4.64	77.90	-0.60	47.82	-4.93
78.00	-0.30	45.07	-4.47	78.20	-0.30	47.28	-4.87
78.30	0.00	43.84	-4.35	78.50	0.00	46.06	-4.74
78.60	0.30	45.58	-4.52	78.80	0.30	47.44	-4.87
78.90	0.60	46.55	-4.61	79.10	0.60	47.94	-4.91
79.20	0.90	45.70	-4.52	79.40	0.90	47.85	-4.90
79.50	1.20	44.94	-4.44	79.70	1.20	45.75	-4.68
79.80	1.50	44.01	-4.35	80.00	1.50	45.05	-4.60
80.30	2.00	41.18	-4.06	80.50	2.00	43.35	-4.42

Horizontal position (cm)	<i>r</i> (cm)	Depth reading (mm)	<i>ε</i> (cm)
80.80	2.50	36.88	-3.62
81.30	3.00	33.54	-3.28
81.80	3.50	29.89	-2.91
82.30	4.00	26.48	-2.57
82.80	4.50	23.02	-2.22
83.30	5.00	18.27	-1.74
83.80	5.50	14.79	-1.38
84.30	6.00	10.68	-0.97
84.80	6.50	6.26	-0.52
85.30	7.00	2.95	-0.18
85.50	7.20	1.15	0.00
<hr/>			

Test No. 0.6/-6.35/3.58

<i>z</i> ₀ (cm)	<i>d</i> (cm)	<i>r</i> _i (cm)+ve	<i>r</i> _i (cm)-ve	<i>ε</i> _n (cm)+ve	<i>ε</i> _n (cm)-ve	<i>Q</i> (L/s)
	0.97	10.00	17.00	2.46	2.88	0.26
		average <i>r</i> _i (cm)	average <i>r</i> _i (cm)	2.67	2.67	
Water temp (°C)		76.70	76.70	-7.22	-7.22	
Tube position (cm)		44.18	44.18	-7.32	-7.32	
Time to fill (s)						
<i>Q</i> (L/s)				-7.27	-7.27	
<hr/>						

Test No. 0.6/-3.81/3.79

<i>z</i> ₀ (cm)	<i>d</i> (cm)	<i>r</i> _i (cm)+ve	<i>r</i> _i (cm)-ve	<i>ε</i> _m (cm)+ve	<i>ε</i> _m (cm)-ve	<i>Q</i> (L/s)
		10.00	10.00	0.97	0.97	0.28
		average <i>r</i> _i (cm)	average <i>r</i> _i (cm)	10.00	10.00	0.67
Water temp (°C)		76.70	76.70	20.00	average <i>r</i> _i (cm)	2.73
Tube position (cm)		44.18	44.18	80.10	<i>ε</i> _m (cm)+ve	-4.84
Time to fill (s)				41.67	<i>ε</i> _m (cm)-ve	-4.82
<i>Q</i> (L/s)				0.28	average <i>ε</i> _m (cm)	-4.83
<hr/>						

Horizontal position (cm)	<i>r</i> (cm)	Depth reading (mm)	<i>ε</i> (cm)
65.40	-11.30	1.59	0.00
66.20	-10.50	7.74	-0.62
67.20	-9.50	14.37	-1.29
68.20	-8.50	23.30	-2.18
69.20	-7.50	29.67	-2.82
70.20	-6.50	37.48	-3.61
71.20	-5.50	45.33	-4.40
72.20	-4.50	53.33	-5.20
73.20	-3.50	61.00	-5.97
<hr/>			

Horizontal position (cm)	<i>r</i> (cm)	Depth reading (mm)	<i>ε</i> (cm)	Horizontal position (cm)	<i>r</i> (cm)	Depth reading (mm)	<i>ε</i> (cm)
74.20	-2.50	67.02	-6.58	78.00	-2.10	40.92	-4.21
75.20	-1.50	72.62	-7.15	78.30	-1.80	43.52	-4.46
75.50	-1.20	73.41	-7.23	78.60	-1.50	43.76	-4.48
75.80	-0.90	74.12	-7.30	78.90	-1.20	46.65	-4.77
76.10	-0.60	74.35	-7.32	79.20	-0.90	47.15	-4.82
76.40	-0.30	73.82	-7.27	79.50	-0.60	47.11	-4.81
76.70	0.00	72.49	-7.14	79.80	-0.30	46.97	-4.79
77.00	0.30	73.16	-7.21	80.10	0.00	45.51	-4.64
77.30	0.60	73.28	-7.22	80.40	0.30	46.13	-4.70
77.60	0.90	72.07	-7.10	80.70	0.60	47.14	-4.80
77.90	1.20	71.50	-7.05	81.00	0.90	47.56	-4.84
78.20	1.50	70.50	-6.95	81.30	1.20	46.68	-4.74
79.10	2.40	64.93	-6.39	81.60	1.50	44.46	-4.52
80.10	3.40	57.00	-5.60	81.90	1.80	44.20	-4.49
81.10	4.40	49.56	-4.87	82.20	2.10	41.65	-4.23
82.10	5.40	43.79	-4.29	82.50	2.40	39.60	-4.02
83.10	6.40	34.75	-3.39	83.50	3.40	34.35	-3.49
84.10	7.40	28.23	-2.75	84.50	4.40	26.41	-2.68
85.10	8.40	20.46	-1.97	85.50	5.40	18.54	-1.88
86.10	9.40	10.23	-0.95	86.50	6.40	11.12	-1.13
87.10	10.40	2.19	-0.15	87.50	7.40	2.48	-0.25
87.30	10.60	0.64	0.00	87.80	7.70	0.00	0.00

Test No. 0.6/-5.08/3.58

<i>z</i> ₀ (cm)	-5.08	<i>z</i> ₀ (cm)	-1.27
<i>d</i> (cm)	0.97	<i>r</i> ₁ (cm)+ve	2.23
Time to Equilibrium (min)	10.00	<i>r</i> ₁ (cm)-ve	2.77
Water temp (°C)	17.00	average <i>r</i> ₁ (cm)	2.50
Tube position (cm)	76.60	<i>ε</i> _m (cm)+ve	-5.97
Time to fill (s)	44.20	<i>ε</i> _m (cm)-ve	-5.93
<i>Q</i> (L/s)	0.26	average <i>ε</i> _m (cm)	-5.95

Test No. 0.6/-1.27/2.94

<i>z</i> ₀ (cm)	0.97	<i>r</i> ₁ (cm)+ve	0.97
<i>d</i> (cm)		<i>r</i> ₁ (cm)-ve	2.22
Time to Equilibrium (min)	10.00	<i>r</i> ₁ (cm)-ve	2.23
Water temp (°C)	18.00	average <i>r</i> ₁ (cm)	2.22
Tube position (cm)	79.30	<i>ε</i> _m (cm)+ve	-2.15
Time to fill (s)	53.69	<i>ε</i> _m (cm)-ve	-2.16
<i>Q</i> (L/s)	0.22	average <i>ε</i> _m (cm)	-2.15

	Horizontal position (cm)	<i>r</i> (cm)	Depth reading (mm)	<i>e</i> (cm)	Horizontal position (cm)	<i>r</i> (cm)	Depth reading (mm)	<i>e</i> (cm)
67.30	-9.30	-2.67	0.00	75.50	-3.80	-1.25	0.00	0.00
68.10	-8.50	3.94	-0.65	76.00	-3.30	1.64	-0.28	-0.28
69.10	-7.50	12.88	-1.52	76.30	-3.00	4.88	-0.60	-0.60
70.10	-6.50	19.37	-2.15	76.60	-2.70	6.34	-0.73	-0.73
71.10	-5.50	28.88	-3.08	76.90	-2.40	10.26	-1.12	-1.12
72.10	-4.50	35.67	-3.74	77.20	-2.10	12.97	-1.38	-1.38
73.10	-3.50	44.24	-4.58	77.50	-1.80	15.64	-1.64	-1.64
74.10	-2.50	51.29	-5.27	77.80	-1.50	17.62	-1.84	-1.84
75.10	-1.50	56.60	-5.78	78.10	-1.20	19.35	-2.00	-2.00
75.40	-1.20	57.74	-5.89	78.40	-0.90	20.47	-2.11	-2.11
75.70	-0.90	58.01	-5.91	78.70	-0.60	21.03	-2.16	-2.16
76.00	-0.60	58.25	-5.93	79.00	-0.30	20.00	-2.05	-2.05
76.30	-0.30	57.85	-5.88	79.30	0.00	18.38	-1.88	-1.88
76.60	0.00	54.73	-5.56	79.60	0.30	19.96	-2.03	-2.03
76.90	0.30	58.90	-5.97	79.90	0.60	21.23	-2.15	-2.15
77.20	0.60	58.30	-5.91	80.20	0.90	20.52	-2.07	-2.07
77.50	0.90	57.86	-5.86	80.50	1.20	19.25	-1.94	-1.94
77.80	1.20	56.12	-5.68	80.80	1.50	17.92	-1.80	-1.80
78.10	1.50	54.84	-5.54	81.10	1.80	15.89	-1.59	-1.59
79.10	2.50	48.65	-4.91	81.40	2.10	13.97	-1.39	-1.39
80.10	3.50	40.75	-4.10	81.70	2.40	10.94	-1.08	-1.08
81.10	4.50	31.65	-3.17	82.00	2.70	8.31	-0.81	-0.81
82.10	5.50	25.53	-2.54	82.30	3.00	6.09	-0.58	-0.58
83.10	6.50	17.81	-1.75	82.60	3.30	3.55	-0.32	-0.32
84.10	7.50	9.24	-0.87	83.00	3.70	0.41	0.00	0.00
85.10	8.50	0.73	0.00					

Horizontal position (cm)	<i>r</i> (cm)	Depth reading (mm)	<i>e</i> (cm)	Horizontal position (cm)	<i>r</i> (cm)	Depth reading (mm)	<i>e</i> (cm)
67.30	-9.30	-2.67	0.00	75.50	-3.80	-1.25	0.00
68.10	-8.50	3.94	-0.65	76.00	-3.30	1.64	-0.28
69.10	-7.50	12.88	-1.52	76.30	-3.00	4.88	-0.60
70.10	-6.50	19.37	-2.15	76.60	-2.70	6.34	-0.73
71.10	-5.50	28.88	-3.08	76.90	-2.40	10.26	-1.12
72.10	-4.50	35.67	-3.74	77.20	-2.10	12.97	-1.38
73.10	-3.50	44.24	-4.58	77.50	-1.80	15.64	-1.64
74.10	-2.50	51.29	-5.27	77.80	-1.50	17.62	-1.84
75.10	-1.50	56.60	-5.78	78.10	-1.20	19.35	-2.00
75.40	-1.20	57.74	-5.89	78.40	-0.90	20.47	-2.11
75.70	-0.90	58.01	-5.91	78.70	-0.60	21.03	-2.16
76.00	-0.60	58.25	-5.93	79.00	-0.30	20.00	-2.05
76.30	-0.30	57.85	-5.88	79.30	0.00	18.38	-1.88
76.60	0.00	54.73	-5.56	79.60	0.30	19.96	-2.03
76.90	0.30	58.90	-5.97	79.90	0.60	21.23	-2.15
77.20	0.60	58.30	-5.91	80.20	0.90	20.52	-2.07
77.50	0.90	57.86	-5.86	80.50	1.20	19.25	-1.94
77.80	1.20	56.12	-5.68	80.80	1.50	17.92	-1.80
78.10	1.50	54.84	-5.54	81.10	1.80	15.89	-1.59
79.10	2.50	48.65	-4.91	81.40	2.10	13.97	-1.39
80.10	3.50	40.75	-4.10	81.70	2.40	10.94	-1.08
81.10	4.50	31.65	-3.17	82.00	2.70	8.31	-0.81
82.10	5.50	25.53	-2.54	82.30	3.00	6.09	-0.58
83.10	6.50	17.81	-1.75	82.60	3.30	3.55	-0.32
84.10	7.50	9.24	-0.87	83.00	3.70	0.41	0.00
85.10	8.50	0.73	0.00				

Test No. 0.6/-6.35/3.12**Test No. 0.6/-2.54/3.47**

z_0 (cm)	-6.35	r_t (cm)+ve	0.97	d (cm)	2.61	z_0 (cm)	-2.54
d (cm)		r_t (cm)-ve	10.00	Time to Equilibrium (min)	2.54	r_t (cm)+ve	0.97
Time to Equilibrium (min)	21.00	average r_t (cm)		Water temp (°C)	2.57	r_t (cm)-ve	10.00
Water temp (°C)		ε_m (cm)+ve	78.40	Tube position (cm)	-7.18	average r_t (cm)	19.00
Tube position (cm)		ε_m (cm)-ve	50.67	Time to fill (s)	-7.13	ε_m (cm)+ve	78.40
Time to fill (s)		average ε_m (cm)	0.23	Q (L/s)	-7.15	ε_m (cm)-ve	45.52
Q (L/s)						average ε_m (cm)	-3.64
Horizontal position (cm)	r (cm)	Depth reading (mm)	ε (cm)	Horizontal position (cm)	r (cm)	Depth reading (mm)	ε (cm)
67.90	-10.50	-1.70	0.00	72.30	-6.10	-1.22	0.00
68.40	-10.00	1.86	-0.35	72.40	-6.00	-0.71	-0.05
69.40	-9.00	11.22	-1.28	72.90	-5.50	4.65	-0.58
70.40	-8.00	19.41	-2.08	73.40	-5.00	9.00	-1.01
71.40	-7.00	28.25	-2.96	73.90	-4.50	13.19	-1.42
72.40	-6.00	37.53	-3.87	74.40	-4.00	16.78	-1.78
73.40	-5.00	45.17	-4.63	74.90	-3.50	21.51	-2.25
74.40	-4.00	53.16	-5.42	75.40	-3.00	25.31	-2.62
75.40	-3.00	60.24	-6.11	75.90	-2.50	27.64	-2.85
75.90	-2.50	62.86	-6.37	76.40	-2.00	31.64	-3.24
76.40	-2.00	67.19	-6.80	76.90	-1.50	34.80	-3.55
76.90	-1.50	69.09	-6.98	77.20	-1.20	35.08	-3.58
77.20	-1.20	69.45	-7.01	77.50	-0.90	35.77	-3.65
77.50	-0.90	70.00	-7.07	77.80	-0.60	35.35	-3.60
77.80	-0.60	70.64	-7.13	78.10	-0.30	34.01	-3.46
78.10	-0.30	70.47	-7.11	78.40	0.00	32.34	-3.29
78.40	0.00	69.42	-7.00	78.70	0.30	34.46	-3.50
78.70	0.30	70.77	-7.13	79.00	0.60	35.75	-3.63
79.00	0.60	71.29	-7.18	79.30	0.90	35.04	-3.55
79.30	0.90	70.24	-7.07	79.60	1.20	33.46	-3.39
79.60	1.20	67.90	-6.83	79.90	1.50	33.16	-3.36
79.90	1.50	67.43	-6.78	80.40	2.00	31.15	-3.15
80.40	2.00	65.16	-6.55	80.90	2.50	26.85	-2.72
80.90	2.50	64.44	-6.47	81.40	3.00	22.13	-2.24

Horizontal position (cm)	<i>r</i> (cm)	Depth reading (mm)	ε (cm)
81.40	3.00	58.67	-5.89
82.40	4.00	50.01	-5.01
83.40	5.00	42.95	-4.30
84.40	6.00	35.50	-3.54
85.40	7.00	27.83	-2.76
86.40	8.00	19.33	-1.90
87.40	9.00	11.36	-1.10
88.30	9.90	0.50	0.00

Test No. 0.6/-1.27/2.55

Horizontal position (cm)	<i>r</i> (cm)	Depth reading (mm)	ε (cm)
74.60	-3.80	1.85	0.00
75.10	-3.30	2.79	-0.10
75.60	-2.80	8.56	-0.67
76.10	-2.30	12.72	-1.09
76.60	-1.80	17.35	-1.56
76.90	-1.50	19.21	-1.74
77.20	-1.20	20.21	-1.84
77.50	-0.90	21.30	-1.95
77.80	-0.60	22.46	-2.07

Test No. 0.6/-1.27/3.12

z_0 (cm)	<i>d</i> (cm)	r_i (cm)+ve	r_i (cm)-ve
	0.97	r_i (cm)+ve	0.97
Time to Equilibrium (min)	10.00	r_i (cm)-ve	10.00
Water temp (°C)	22.00	average r_i , (cm)	average r_i , (cm)
Tube position (cm)	78.40	ε_m (cm)+ve	18.00
Time to fill (s)	61.98	ε_m (cm)-ve	average r_i , (cm)
Q (L/s)	0.19	average ε_m (cm)	2.23
		-2.02	78.30
		-2.07	50.66
		-2.05	0.23
		-2.12	average ε_m (cm)
		-2.11	-2.11
		-2.12	-2.12
Horizontal position (cm)	<i>r</i> (cm)	Depth reading (mm)	ε (cm)
			2.36
			2.11
			2.23
			2.13
			2.11
			2.12
Horizontal position (cm)	<i>r</i> (cm)	Depth reading (mm)	ε (cm)
			2.36
			2.11
			2.23
			2.13
			2.11
			2.12

Horizontal position (cm)	<i>r</i> (cm)	Depth reading (mm)	<i>ε</i> (cm)
78.10	-0.30	21.70	-2.00
78.40	0.00	21.49	-1.98
78.70	0.30	21.66	-1.99
79.00	0.60	21.91	-2.02
79.30	0.90	20.88	-1.92
79.60	1.20	18.69	-1.70
79.90	1.50	17.71	-1.60
80.40	2.00	15.23	-1.36
80.90	2.50	10.75	-0.91
81.40	3.00	5.66	-0.40
81.90	3.50	2.42	-0.08
82.00	3.60	1.61	0.00
		82.00	3.70
			-0.17
			0.00

Test No. 0.6/-5.08/2.58

<i>z</i> ₀ (cm)	<i>z</i> ₀ (cm)	<i>r</i> _t (cm)+ve	2.45	-3.81
<i>d</i> (cm)	<i>d</i> (cm)	<i>r</i> _t (cm)-ve	2.41	0.97
Time to Equilibrium (min)	10.00	average <i>r</i> _t (cm)	2.43	<i>r</i> _t (cm)+ve
Water temp (°C)	20.00	<i>ε</i> _m (cm)+ve	-5.90	<i>r</i> _t (cm)-ve
Tube position (cm)	78.40	<i>ε</i> _m (cm)-ve	-5.97	average <i>r</i> _t (cm)
Time to fill (s)	61.36	average <i>ε</i> _m (cm)	-5.93	2.49
<i>Q</i> (L/s)	0.19			-4.77
				-4.71
				-4.74

Horizontal position (cm)	<i>r</i> (cm)	Depth reading (mm)	<i>ε</i> (cm)	Horizontal position (cm)	<i>r</i> (cm)	Depth reading (mm)	<i>ε</i> (cm)
69.90	-8.50	-0.38	0.00	71.20	-7.20	-0.01	0.00
70.40	-8.00	4.66	-0.50	71.40	-7.00	1.65	-0.17
71.40	-7.00	12.91	-1.31	72.40	-6.00	10.26	-1.03
72.40	-6.00	21.61	-2.18	73.40	-5.00	19.08	-1.91
73.40	-5.00	31.05	-3.11	74.40	-4.00	26.35	-2.64
74.40	-4.00	38.81	-3.88	75.40	-3.00	34.38	-3.44
75.40	-3.00	46.20	-4.61	75.90	-2.50	38.43	-3.85

Horizontal position (cm)	<i>r</i> (cm)	Depth reading (mm)	ε (cm)	Horizontal position (cm)	<i>r</i> (cm)	Depth reading (mm)	ε (cm)
75.90	-2.50	50.34	-5.01	76.40	-2.00	40.60	-4.07
76.40	-2.00	54.21	-5.40	76.90	-1.50	45.31	-4.54
76.90	-1.50	57.07	-5.68	77.20	-1.20	45.68	-4.58
77.20	-1.20	58.89	-5.86	77.50	-0.90	46.39	-4.65
77.50	-0.90	60.00	-5.97	77.80	-0.60	46.98	-4.71
77.80	-0.60	59.54	-5.92	78.10	-0.30	45.82	-4.59
78.10	-0.30	59.20	-5.88	78.40	0.00	45.36	-4.55
78.40	0.00	58.21	-5.78	78.70	0.30	46.86	-4.70
78.70	0.30	59.18	-5.87	79.00	0.60	47.60	-4.77
79.00	0.60	59.37	-5.89	79.30	0.90	47.40	-4.75
79.30	0.90	59.48	-5.90	79.60	1.20	45.47	-4.56
79.60	1.20	58.42	-5.79	79.90	1.50	43.55	-4.37
79.90	1.50	58.07	-5.75	80.40	2.00	42.78	-4.29
80.40	2.00	54.67	-5.40	80.90	2.50	37.13	-3.73
80.90	2.50	51.12	-5.05	81.40	3.00	34.36	-3.45
81.40	3.00	47.87	-4.72	81.90	3.50	31.12	-3.13
82.40	4.00	39.79	-3.90	82.90	4.50	23.49	-2.37
83.40	5.00	32.61	-3.17	83.90	5.50	14.55	-1.47
84.40	6.00	25.03	-2.40	84.90	6.50	7.98	-0.82
85.40	7.00	15.45	-1.44	85.90	7.50	1.52	-0.17
86.40	8.00	7.19	-0.60	86.00	7.60	-0.21	0.00
87.20	8.80	1.27	0.00				

Test No. 0.6/-7.62/2.50	z_0 (cm)	d (cm)	r_t (cm)+ve	r_t (cm)-ve	Time to Equilibrium (min)	Water temp (°C)	Tube position (cm)	ε_m (cm)+ve	ε_m (cm)-ve	average r_t (cm)	average ε_m (cm)
	-7.62	-6.35									
z_0 (cm)	0.97	0.97	r_t (cm)+ve	r_t (cm)-ve							
d (cm)	2.04	2.24	r_t (cm)+ve	r_t (cm)-ve	10.00	22.00					
Time to Equilibrium (min)	10.00	2.24			average r_t (cm)						
Water temp (°C)	22.00	2.14									
Tube position (cm)	78.50	-8.38	ε_m (cm)+ve	ε_m (cm)-ve	78.50	63.25					
Time to fill (s)	63.22	-8.31	ε_m (cm)-ve								
Q (L/s)	0.18	-8.35	average ε_m (cm)		0.18						

Horizontal position (cm)	<i>r</i> (cm)	Depth reading (mm)	<i>ε</i> (cm)	Horizontal position (cm)	<i>r</i> (cm)	Depth reading (mm)	<i>ε</i> (cm)
66.50	-12.00	-1.00	0.00	67.90	-10.60	-0.23	0.00
67.50	-11.00	5.60	-0.66	68.50	-10.00	4.04	-0.43
68.50	-10.00	12.90	-1.38	69.50	-9.00	13.57	-1.38
69.50	-9.00	21.74	-2.26	70.50	-8.00	21.17	-2.14
70.50	-8.00	31.35	-3.22	71.50	-7.00	29.01	-2.92
71.50	-7.00	40.14	-4.10	72.50	-6.00	38.53	-3.87
72.50	-6.00	47.37	-4.82	73.50	-5.00	46.24	-4.64
73.50	-5.00	55.21	-5.60	74.50	-4.00	54.67	-5.48
74.50	-4.00	61.30	-6.21	75.50	-3.00	61.31	-6.15
75.50	-3.00	70.29	-7.10	76.00	-2.50	65.44	-6.56
76.00	-2.50	72.89	-7.36	76.50	-2.00	68.32	-6.85
76.50	-2.00	77.98	-7.87	77.00	-1.50	71.94	-7.21
77.00	-1.50	79.12	-7.98	77.30	-1.20	72.29	-7.24
77.30	-1.20	80.15	-8.08	77.60	-0.90	73.63	-7.38
77.60	-0.90	82.27	-8.29	77.90	-0.60	72.40	-7.25
77.90	-0.60	82.48	-8.31	78.20	-0.30	72.37	-7.25
78.20	-0.30	81.54	-8.22	78.50	0.00	71.50	-7.16
78.50	0.00	81.42	-8.21	78.80	0.30	72.43	-7.25
78.80	0.30	81.69	-8.23	79.10	0.60	72.48	-7.26
79.10	0.60	83.17	-8.38	79.40	0.90	72.34	-7.24
79.40	0.90	81.66	-8.23	79.70	1.20	72.27	-7.24
79.70	1.20	80.70	-8.13	80.00	1.50	68.92	-6.90
80.00	1.50	79.86	-8.04	80.50	2.00	66.77	-6.69
80.50	2.00	75.85	-7.64	81.00	2.50	62.54	-6.26
81.00	2.50	73.28	-7.38	81.50	3.00	60.09	-6.02
81.50	3.00	69.68	-7.02	82.50	4.00	50.93	-5.10
82.50	4.00	63.45	-6.40	83.50	5.00	41.59	-4.16
83.50	5.00	53.89	-5.44	84.50	6.00	35.50	-3.55
84.50	6.00	47.07	-4.75	85.50	7.00	29.22	-2.93
85.50	7.00	39.97	-4.04	86.50	8.00	21.08	-2.11
86.50	8.00	31.72	-3.21	87.50	9.00	12.42	-1.24
87.50	9.00	23.70	-2.41	88.50	10.00	1.77	-0.18

Horizontal position (cm)	<i>r</i> (cm)	Depth reading (mm)	<i>ε</i> (cm)
88.50	10.00	16.68	-1.70
89.50	11.00	7.60	-0.79
90.50	12.00	-0.26	0.00

Test No. 0.6/-2.54/0.53

<i>z</i> ₀ (cm)	-1.27	<i>r</i> _t (cm)+ve	2.08
<i>d</i> (cm)	2.04	<i>r</i> _t (cm)-ve	2.24
Time to Equilibrium (min)	10.00	<i>r</i> _t (cm)-ve	2.16
Water temp (°C)	21.00	average <i>r</i> _t (cm)	-1.92
Tube position (cm)	76.20	<i>ε</i> _m (cm)+ve	-1.93
Time to fill (s)	66.79	<i>ε</i> _n (cm)-ve	0.17
<i>Q</i> (L/s)	average <i>ε</i> _m (cm)	<i>Q</i> (L/s)	0.17

Horizontal position (cm)	<i>r</i> (cm)	Depth reading (mm)	<i>ε</i> (cm)	Horizontal position (cm)	<i>r</i> (cm)	Depth reading (mm)	<i>ε</i> (cm)
72.30	-3.90	1.03	0.00	68.80	-7.40	-1.23	0.00
72.60	-3.60	2.91	-0.19	69.20	-7.00	0.56	-0.18
72.90	-3.30	4.86	-0.39	70.20	-6.00	11.07	-1.22
73.20	-3.00	8.31	-0.74	71.20	-5.00	17.74	-1.88
73.50	-2.70	10.17	-0.93	72.20	-4.00	27.42	-2.84
73.80	-2.40	12.06	-1.13	73.20	-3.00	35.01	-3.59
74.10	-2.10	14.65	-1.39	73.70	-2.50	38.50	-3.93
74.40	-1.80	17.44	-1.67	74.20	-2.00	41.89	-4.27
74.70	-1.50	19.02	-1.84	74.70	-1.50	44.21	-4.49
75.00	-1.20	19.59	-1.90	75.00	-1.20	45.91	-4.66
75.30	-0.90	19.89	-1.93	75.30	-0.90	45.72	-4.64
75.60	-0.60	18.95	-1.84	75.60	-0.60	44.86	-4.55
75.90	-0.30	18.68	-1.82	75.90	-0.30	43.45	-4.41
76.20	0.00	17.62	-1.72	76.20	0.00	43.08	-4.37
76.50	0.30	18.40	-1.80	76.50	0.30	44.08	-4.47
76.80	0.60	19.09	-1.88	76.80	0.60	44.78	-4.53
77.10	0.90	19.47	-1.92	77.10	0.90	45.79	-4.63

Horizontal position (cm)	<i>r</i> (cm)	Depth reading (mm)	<i>ε</i> (cm)
77.40	1.20	18.33	-1.81
77.70	1.50	17.87	-1.77
78.00	1.80	16.12	-1.60
78.30	2.10	12.56	-1.25
78.60	2.40	11.78	-1.17
78.90	2.70	9.34	-0.93
79.20	3.00	7.58	-0.76
79.50	3.30	6.02	-0.61
79.80	3.60	4.10	-0.42
80.10	3.90	-0.18	0.00

Horizontal position (cm)	<i>r</i> (cm)	Depth reading (mm)	<i>ε</i> (cm)	Horizontal position (cm)	<i>r</i> (cm)	Depth reading (mm)	<i>ε</i> (cm)
77.40	1.20	18.33	-1.81	77.40	1.20	45.38	-4.59
77.70	1.50	17.87	-1.77	77.70	1.50	44.73	-4.52
78.00	1.80	16.12	-1.60	78.20	2.00	42.27	-4.27
78.30	2.10	12.56	-1.25	78.70	2.50	39.87	-4.03
78.60	2.40	11.78	-1.17	79.20	3.00	36.01	-3.64
78.90	2.70	9.34	-0.93	80.20	4.00	28.85	-2.91
79.20	3.00	7.58	-0.76	81.20	5.00	20.46	-2.07
79.50	3.30	6.02	-0.61	82.20	6.00	12.96	-1.31
79.80	3.60	4.10	-0.42	83.20	7.00	3.87	-0.39
80.10	3.90	-0.18	0.00	83.60	7.40	0.00	0.00

Test No. 0.6/-5.08/0.54

<i>z</i> ₀ (cm)	<i>d</i> (cm)	<i>r</i> _f (cm)+ve	<i>r</i> _f (cm)-ve	<i>d</i> (cm)	<i>r</i> _f (cm)+ve	<i>r</i> _f (cm)-ve	<i>z</i> ₀ (cm)	<i>d</i> (cm)	<i>r</i> _f (cm)+ve	<i>r</i> _f (cm)-ve	average <i>r</i> _f (cm)	average <i>r</i> _f (cm)	<i>z</i> ₀ (cm)	<i>d</i> (cm)	<i>r</i> _f (cm)+ve	<i>r</i> _f (cm)-ve	average <i>r</i> _f (cm)							
Time to Equilibrium (min)	10.00	<i>r</i> _f (cm)-ve	2.60	2.77	2.04	2.04	-6.35	2.77	2.04	2.04	2.84	2.84	2.77	2.04	2.04	2.04	2.35							
Water temp (°C)	22.00	average <i>r</i> _f (cm)	2.69	2.69	10.00	10.00	2.35	2.69	15.00	15.00	2.59	2.59	2.69	10.00	10.00	10.00	2.59							
Tube position (cm)	76.10	<i>ε</i> _m (cm)+ve	5.92	5.92	75.90	75.90	-7.16	5.92	66.04	66.04	-7.16	-7.16	-7.16	75.90	75.90	75.90	-7.16							
Time to fill (s)	65.64	<i>ε</i> _m (cm)-ve	-5.82	-5.82	<i>ε</i> _m (cm)-ve	<i>ε</i> _m (cm)-ve	-7.07	-5.82	44.09	44.09	-7.07	-7.07	-7.07	66.04	66.04	66.04	-7.07							
<i>Q</i> (L/s)	0.18	average <i>ε</i> _m (cm)	-5.87	-5.87	0.18	0.18	-7.11	-5.87	0.18	0.18	average <i>ε</i> _m (cm)	average <i>ε</i> _m (cm)	average <i>ε</i> _m (cm)	44.09	44.09	44.09	-7.11							
Horizontal position (cm)	<i>r</i> (cm)	Depth reading (mm)	<i>ε</i> (cm)	Horizontal position (cm)	<i>r</i> (cm)	Depth reading (mm)	<i>ε</i> (cm)	Horizontal position (cm)	<i>r</i> (cm)	Depth reading (mm)	<i>ε</i> (cm)	Horizontal position (cm)	<i>r</i> (cm)	Depth reading (mm)	<i>ε</i> (cm)	Horizontal position (cm)	<i>r</i> (cm)	Depth reading (mm)	<i>ε</i> (cm)					
67.00	-9.10	-0.54	0.00	65.50	-10.40	7.66	0.00	67.10	-9.00	-10.00	10.39	67.10	-9.00	-10.00	10.39	68.10	-8.00	-9.00	20.21	68.10	-8.00	-9.00	20.21	-1.25
68.10	-8.00	0.00	-0.05	65.90	-8.00	-9.00	-0.27	69.10	-7.00	17.90	-1.84	69.10	-7.00	-8.00	-2.02	70.10	-6.00	25.65	-2.61	70.10	-6.00	-7.00	37.21	-2.94
69.10	-7.00	8.33	-0.88	66.90	67.90	68.90	-3.63	71.10	-5.00	33.43	-3.38	69.90	-6.00	-6.00	-3.63	72.10	-4.00	40.72	-4.11	72.10	-4.00	-5.00	52.71	-4.49
70.10	-6.00	25.65	-2.61	68.90	68.90	68.90	44.09	73.10	-3.00	48.00	-4.84	71.90	-3.00	-4.00	58.96	73.60	-2.50	51.07	-5.14	73.60	-2.50	-3.00	66.93	-5.11
71.10	-5.00	33.43	-3.38	69.90	69.90	69.90	44.09	74.10	-2.00	55.21	-5.55	73.40	-2.50	-2.50	70.28	74.10	-2.00	55.21	-5.55	74.10	-2.00	-2.50	70.28	-6.23

Horizontal position (cm)	<i>r</i> (cm)	Depth reading (mm)	<i>ε</i> (cm)	Horizontal position (cm)	<i>r</i> (cm)	Depth reading (mm)	<i>ε</i> (cm)
74.60	-1.50	57.34	-5.77	73.90	-2.00	74.05	-6.61
74.90	-1.20	57.90	-5.82	74.40	-1.50	76.98	-6.90
75.20	-0.90	57.50	-5.78	74.70	-1.20	78.65	-7.07
75.50	-0.60	57.42	-5.77	75.00	-0.90	78.53	-7.05
75.80	-0.30	57.34	-5.76	75.30	-0.60	77.65	-6.96
76.10	0.00	56.00	-5.63	75.60	-0.30	77.09	-6.91
76.40	0.30	56.30	-5.66	75.90	0.00	76.68	-6.87
76.70	0.60	57.17	-5.74	76.20	0.30	77.73	-6.97
77.00	0.90	58.94	-5.92	76.50	0.60	78.76	-7.07
77.30	1.20	56.47	-5.67	76.80	0.90	79.64	-7.16
77.60	1.50	56.37	-5.66	77.10	1.20	79.56	-7.15
78.10	2.00	56.03	-5.62	77.40	1.50	78.70	-7.06
78.60	2.50	52.22	-5.24	77.90	2.00	75.73	-6.76
79.10	3.00	49.25	-4.94	78.40	2.50	74.08	-6.60
80.10	4.00	39.89	-4.00	78.90	3.00	70.46	-6.23
81.10	5.00	33.37	-3.35	79.90	4.00	63.81	-5.56
82.10	6.00	27.46	-2.76	80.90	5.00	54.81	-4.66
83.10	7.00	19.24	-1.93	81.90	6.00	48.62	-4.04
84.10	8.00	11.98	-1.20	82.90	7.00	42.20	-3.39
85.10	9.00	1.14	-0.11	83.90	8.00	34.23	-2.59
85.20	9.10	0.00	0.00	84.90	9.00	25.80	-1.75
				85.90	10.00	17.57	-0.92
				86.80	10.90	8.41	0.00
Test No. 0.6/-5.08/3.12							
<i>z</i> ₀ (cm)	-5.08	<i>z</i> ₀ (cm)	-2.54				
<i>d</i> (cm)	0.97	<i>r</i> _t (cm)+ve	2.36	<i>d</i> (cm)	2.04	<i>r</i> _t (cm)+ve	3.01
Time to Equilibrium (min)	10.00	<i>r</i> _t (cm)-ve	2.64	Time to Equilibrium (min)	10.00	<i>r</i> _t (cm)-ve	2.90
Water temp (°C)	17.00	average <i>r</i> _t (cm)	2.50	Water temp (°C)	21.00	average <i>r</i> _t (cm)	2.96
Tube position (cm)	78.30	<i>ε</i> _m (cm)+ve	-6.07	Tube position (cm)	77.00	<i>ε</i> _m (cm)+ve	-3.53
Time to fill (s)	50.69	<i>ε</i> _m (cm)-ve	-5.95	Time to fill (s)	46.18	<i>ε</i> _m (cm)-ve	-3.45
<i>Q</i> (L/s)	0.23	average <i>ε</i> _m (cm)	-6.01	<i>Q</i> (L/s)	0.25	average <i>ε</i> _m (cm)	-3.49

Horizontal position (cm)	<i>r</i> (cm)	Depth reading (mm)	<i>ε</i> (cm)
69.10	-9.20	-0.77	0.00
69.80	-8.50	3.86	-0.46
70.80	-7.50	13.57	-1.42
71.80	-6.50	21.47	-2.20
72.80	-5.50	29.65	-3.01
73.80	-4.50	38.17	-3.85
74.80	-3.50	44.08	-4.43
75.80	-2.50	51.68	-5.19
76.80	-1.50	57.52	-5.76
77.10	-1.20	58.25	-5.83
77.40	-0.90	58.42	-5.85
77.70	-0.60	59.44	-5.95
78.00	-0.30	59.12	-5.91
78.30	0.00	58.98	-5.89
78.60	0.30	60.16	-6.01
78.90	0.60	60.75	-6.07
79.20	0.90	59.06	-5.89
79.50	1.20	58.65	-5.85
79.80	1.50	57.66	-5.75
80.80	2.50	50.00	-4.97
81.80	3.50	44.57	-4.42
82.80	4.50	36.14	-3.57
83.80	5.50	27.87	-2.73
84.80	6.50	21.58	-2.10
85.80	7.50	12.53	-1.18
86.80	8.50	1.78	-0.10
87.10	8.80	0.81	0.00

Horizontal position (cm)	<i>r</i> (cm)	Depth reading (mm)	<i>r</i> (cm)	Depth reading (mm)	<i>ε</i> (cm)
70.70	70.70	-6.30	-0.15	0.00	0.00
71.00	-6.00	1.78	-0.20	-0.20	-0.20
72.00	-5.00	9.66	-0.99	-0.99	-0.99
73.00	-4.00	17.87	-1.82	-1.82	-1.82
74.00	-3.00	24.06	-2.44	-2.44	-2.44
74.50	-2.50	28.68	-2.91	-2.91	-2.91
75.00	-2.00	31.74	-3.22	-3.22	-3.22
75.50	-1.50	33.82	-3.43	-3.43	-3.43
75.80	-1.20	33.97	-3.45	-3.45	-3.45
76.10	-0.90	34.03	-3.45	-3.45	-3.45
76.40	-0.60	33.67	-3.42	-3.42	-3.42
76.70	-0.30	32.35	-3.29	-3.29	-3.29
77.00	0.00	32.08	-3.27	-3.27	-3.27
77.30	0.30	32.88	-3.35	-3.35	-3.35
77.60	0.60	33.62	-3.42	-3.42	-3.42
77.90	0.90	34.68	-3.53	-3.53	-3.53
78.20	1.20	33.74	-3.44	-3.44	-3.44
78.50	1.50	33.40	-3.41	-3.41	-3.41
79.00	2.00	31.20	-3.19	-3.19	-3.19
79.50	2.50	28.42	-2.92	-2.92	-2.92
80.00	3.00	24.75	-2.55	-2.55	-2.55
80.50	4.00	16.16	-1.70	-1.70	-1.70
81.00	5.00	9.75	-1.07	-1.07	-1.07
81.50	6.00	2.22	-0.32	-0.32	-0.32
82.00	6.30	-1.00	0.00	0.00	0.00

Test No. 0.6/-5.08/1.85

z_0 (cm)	-5.08	r_t (cm)	-9.40	ε (cm)	Depth reading (mm)
d (cm)	1.39	r_t (cm)+ve	-1.07	0.00	67.70
Time to Equilibrium (min)	10.00	r_t (cm)-ve	-9.00	-0.23	68.00
Water temp (°C)	22.00	average r_t (cm)	11.08	-1.21	69.00
Tube position (cm)	77.00	ε_m (cm)+ve	19.25	-2.02	70.00
Time to fill (s)	41.37	ε_m (cm)-ve	27.13	-2.80	71.00
Q (L/s)	0.28	average ε_m (cm)	-6.16	-6.13	72.00
Horizontal position (cm)	r (cm)			Horizontal position (cm)	r (cm)
					Depth reading (mm)
67.60	-9.40	-1.07	0.00	-9.30	-0.61
68.00	-9.00	1.30	-0.23	-9.00	5.76
69.00	-8.00	11.08	-1.21	-8.00	-0.64
70.00	-7.00	19.25	-2.02	-7.00	14
71.00	-6.00	27.13	-2.80	-6.00	-1.46
72.00	-5.00	35.19	-3.60	-5.00	-2.17
73.00	-4.00	43.11	-4.39	-4.00	-2.19
74.00	-3.00	50.17	-5.09	-3.00	-2.19
74.50	-2.50	53.83	-5.45	-2.50	-2.28
75.00	-2.00	56.92	-5.76	-2.00	-2.28
75.50	-1.50	59.56	-6.02	-1.50	-3.07
75.80	-1.20	60.07	-6.07	-1.20	-3.55
76.10	-0.90	60.96	-6.16	-0.90	-4.38
76.40	-0.60	60.43	-6.10	-0.60	-5.07
76.70	-0.30	60.03	-6.06	-0.30	-5.07
77.00	0.00	59.10	-5.96	0.00	-5.35
77.30	0.30	60.09	-6.06	77.30	-5.35
77.60	0.60	60.21	-6.07	77.60	-5.68
77.90	0.90	60.46	-6.09	77.90	-5.85
78.20	1.20	60.31	-6.08	78.20	-5.93
78.50	1.50	58.92	-5.94	78.50	-5.93
79.00	2.00	56.31	-5.67	79.00	-5.68
79.50	2.50	53.33	-5.37	79.50	-5.65
80.00	3.00	49.93	-5.03	80.00	-5.89

Test No. 0.6/-5.08/0.77

z_0 (cm)	-5.08	d (cm)	2.93	Time to Equilibrium (min)	10.00	r_t (cm)+ve	2.04	r_t (cm)-ve	2.66
d (cm)	1.39	r_t (cm)+ve	3.01	Water temp (°C)	21.00	average r_t (cm)	10.00	r_t (cm)-ve	2.98
Time to Equilibrium (min)	10.00	r_t (cm)-ve	2.97	Tube position (cm)	77.00	ε_m (cm)+ve	21.00	average r_t (cm)	2.82
Water temp (°C)	22.00	average r_t (cm)	-6.09	Time to fill (s)	45.77	ε_m (cm)-ve	77.00	ε_m (cm)+ve	-5.90
Tube position (cm)	77.00	ε_m (cm)+ve	-6.16	Q (L/s)	0.25	average ε_m (cm)	45.77	ε_m (cm)-ve	-5.93
Time to fill (s)	41.37	ε_m (cm)-ve	-6.13				0.25	average ε_m (cm)	-5.92
Q (L/s)	0.28	average ε_m (cm)	-6.13					3.00	47.17

Horizontal position (cm)	<i>r</i> (cm)	Depth reading (mm)	<i>ε</i> (cm)
81.00	4.00	43.73	-4.40
82.00	5.00	36.56	-3.68
83.00	6.00	28.18	-2.84
84.00	7.00	21.83	-2.20
85.00	8.00	13.39	-1.35
86.00	9.00	7.21	-0.72
86.60	9.60	0.00	0.00

Test No. 0.6/-6.35/0.77

<i>z_o</i> (cm)	-6.35	<i>r_i</i> (cm)+ve	2.59	<i>z_o</i> (cm)	-7.62	<i>r_i</i> (cm)+ve	2.04
<i>d</i> (cm)	2.04	<i>r_i</i> (cm)-ve	2.98	<i>d</i> (cm)	2.74	<i>r_i</i> (cm)-ve	3.02
Time to Equilibrium (min)	10.00	average <i>r_i</i> (cm)	2.78	Time to Equilibrium (min)	10.00	<i>r_i</i> (cm)-ve	3.02
Water temp (°C)	21.00	<i>ε_m</i> (cm)+ve	-7.17	Water temp (°C)	21.00	average <i>r_i</i> (cm)	2.88
Tube position (cm)	77.00	<i>ε_m</i> (cm)-ve	-7.13	Tube position (cm)	75.00	<i>ε_m</i> (cm)+ve	-8.50
Time to fill (s)	46.24	<i>ε_m</i> (cm)-ve	-7.15	Time to fill (s)	45.81	<i>ε_m</i> (cm)-ve	-8.49
<i>Q</i> (L/s)	0.25	average <i>ε_m</i> (cm)	-7.15	<i>Q</i> (L/s)	0.25	average <i>ε_m</i> (cm)	-8.50
Horizontal position (cm)	<i>r</i> (cm)	Depth reading (mm)	<i>ε</i> (cm)	Horizontal position (cm)	<i>r</i> (cm)	Depth reading (mm)	<i>ε</i> (cm)
65.30	-11.70	-0.81	0.00	61.60	-13.40	-1.53	0.00
66.00	-11.00	4.88	-0.55	62.00	-13.00	-0.64	-0.09
67.00	-10.00	11.7	-1.23	63.00	-12.00	8	-0.95
68.00	-9.00	19.04	-1.96	64.00	-11.00	16.27	-1.77
69.00	-8.00	26.34	-2.69	65.00	-10.00	23.75	-2.52
70.00	-7.00	33.94	-3.45	66.00	-9.00	30.98	-3.24
71.00	-6.00	41.16	-4.17	67.00	-8.00	38.83	-4.02
72.00	-5.00	47.70	-4.82	68.00	-7.00	46.12	-4.75
73.00	-4.00	55.18	-5.56	69.00	-6.00	53.65	-5.50
74.00	-3.00	62.96	-6.34	70.00	-5.00	60.62	-6.19
74.50	-2.50	66.05	-6.65	71.00	-4.00	68.16	-6.94
75.00	-2.00	69.00	-6.94	72.00	-3.00	75.16	-7.64

Test No. 0.6/-7.62/0.77

<i>z_o</i> (cm)	-7.62	<i>r_i</i> (cm)+ve	2.04	<i>z_o</i> (cm)	-7.62	<i>r_i</i> (cm)-ve	2.74
<i>d</i> (cm)	2.04	<i>r_i</i> (cm)-ve	3.02	<i>d</i> (cm)	2.74	<i>r_i</i> (cm)-ve	3.02
Time to Equilibrium (min)	10.00	average <i>r_i</i> (cm)	21.00	Time to Equilibrium (min)	10.00	<i>r_i</i> (cm)-ve	3.02
Water temp (°C)	21.00	<i>ε_m</i> (cm)+ve	75.00	Water temp (°C)	21.00	average <i>r_i</i> (cm)	2.88
Tube position (cm)	75.00	<i>ε_m</i> (cm)-ve	45.81	Tube position (cm)	75.00	<i>ε_m</i> (cm)+ve	-8.50
Time to fill (s)	45.81	<i>ε_m</i> (cm)-ve	0.25	Time to fill (s)	45.81	<i>ε_m</i> (cm)-ve	-8.49
<i>Q</i> (L/s)	0.25	average <i>ε_m</i> (cm)	-8.50	<i>Q</i> (L/s)	0.25	average <i>ε_m</i> (cm)	-8.50
Horizontal position (cm)	<i>r</i> (cm)	Depth reading (mm)	<i>ε</i> (cm)	Horizontal position (cm)	<i>r</i> (cm)	Depth reading (mm)	<i>ε</i> (cm)

Horizontal position (cm)	<i>r</i> (cm)	Depth reading (mm)	<i>ε</i> (cm)	Horizontal position (cm)	<i>r</i> (cm)	Depth reading (mm)	<i>ε</i> (cm)
75.50	-1.50	70.44	-7.08	72.50	-2.50	78.80	-8.00
75.80	-1.20	70.92	-7.13	73.00	-2.00	81.35	-8.25
76.10	-0.90	70.32	-7.07	73.50	-1.50	83.23	-8.44
76.40	-0.60	69.82	-7.02	73.80	-1.20	83.40	-8.46
76.70	-0.30	69.74	-7.01	74.10	-0.90	83.73	-8.49
77.00	0.00	69.30	-6.97	74.40	-0.60	83.36	-8.45
77.30	0.30	69.63	-7.00	74.70	-0.30	83.27	-8.44
77.60	0.60	70.88	-7.12	75.00	0.00	82.10	-8.32
77.90	0.90	71.35	-7.17	75.30	0.30	83.09	-8.42
78.20	1.20	69.51	-6.98	75.60	0.60	83.94	-8.50
78.50	1.50	69.42	-6.97	75.90	0.90	83.68	-8.48
79.00	2.00	67.25	-6.76	76.20	1.20	83.07	-8.41
79.50	2.50	63.76	-6.40	76.50	1.50	82.63	-8.37
80.00	3.00	60.58	-6.09	77.00	2.00	80.25	-8.13
81.00	4.00	52.88	-5.31	77.50	2.50	77.04	-7.81
82.00	5.00	45.62	-4.58	78.00	3.00	73.22	-7.42
83.00	6.00	39.39	-3.96	79.00	4.00	66.49	-6.75
84.00	7.00	31.88	-3.20	80.00	5.00	59.49	-6.05
85.00	8.00	25.68	-2.58	81.00	6.00	51.34	-5.23
86.00	9.00	18.59	-1.87	82.00	7.00	45.12	-4.60
87.00	10.00	12.22	-1.23	83.00	8.00	39.25	-4.01
88.00	11.00	4.76	-0.48	84.00	9.00	31.65	-3.25
88.70	11.70	-0.82	0.08	85.00	10.00	24.85	-2.57
				86.00	11.00	17.19	-1.80
				87.00	12.00	8.73	-0.95
				88.00	13.00	2.19	-0.29
				88.40	13.40	-0.70	0.00

Horizontal position (cm)	<i>r</i> (cm)	Depth reading (mm)	<i>ε</i> (cm)
75.50	-1.50	70.44	-7.08
75.80	-1.20	70.92	-7.13
76.10	-0.90	70.32	-7.07
76.40	-0.60	69.82	-7.02
76.70	-0.30	69.74	-7.01
77.00	0.00	69.30	-6.97
77.30	0.30	69.63	-7.00
77.60	0.60	70.88	-7.12
77.90	0.90	71.35	-7.17
78.20	1.20	69.51	-6.98
78.50	1.50	69.42	-6.97
79.00	2.00	67.25	-6.76
79.50	2.50	63.76	-6.40
80.00	3.00	60.58	-6.09
81.00	4.00	52.88	-5.31
82.00	5.00	45.62	-4.58
83.00	6.00	39.39	-3.96
84.00	7.00	31.88	-3.20
85.00	8.00	25.68	-2.58
86.00	9.00	18.59	-1.87
87.00	10.00	12.22	-1.23
88.00	11.00	4.76	-0.48
88.70	11.70	-0.82	0.08

Test No. 0.6/-2.54/2.57

z_0 (cm)	-2.54	r_i (cm)+ve	2.23	z_0 (cm)	-2.54
d (cm)	0.97	r_i (cm)-ve	-0.14	d (cm)	1.39
Time to Equilibrium (min)	10.00	average r_i (cm)	2.25	Time to Equilibrium (min)	r_i (cm)+ve
Water temp (°C)	22.00		2.24	Water temp (°C)	10.00
Tube position (cm)	78.40	ε_m (cm)+ve	-3.32	Tube position (cm)	r_i (cm)-ve
Time to fill (s)	61.62	ε_m (cm)-ve	-3.30	Time to fill (s)	22.00
Q (L/s)	0.19	average ε_m (cm)	-3.31	Q (L/s)	average ε_m (cm)

Horizontal position (cm)	r (cm)	Depth reading (mm)	ε (cm)	Horizontal position (cm)	r (cm)	Depth reading (mm)	ε (cm)
73.10	-5.30	1.37	0.00	73.20	-5.80	-0.54	0.00
73.40	-5.00	2.77	-0.14	73.50	-5.50	2.01	-0.26
73.90	-4.50	8.11	-0.68	74.00	-5.00	7.06	-0.76
74.40	-4.00	12.39	-1.11	74.50	-4.50	10.72	-1.13
74.90	-3.50	16.52	-1.52	75.00	-4.00	15.09	-1.56
75.40	-3.00	20.58	-1.93	75.50	-3.50	19.37	-1.99
75.90	-2.50	24.33	-2.31	76.00	-3.00	23.05	-2.36
76.40	-2.00	28.82	-2.76	76.50	-2.50	26.65	-2.72
76.90	-1.50	31.58	-3.04	77.00	-2.00	30.73	-3.13
77.20	-1.20	33.52	-3.24	77.50	-1.50	33.68	-3.43
77.50	-0.90	34.02	-3.29	77.80	-1.20	34.66	-3.52
77.80	-0.60	34.15	-3.30	78.10	-0.90	34.76	-3.53
78.10	-0.30	33.47	-3.23	78.40	-0.60	35.21	-3.58
78.40	0.00	31.71	-3.06	78.70	-0.30	34.74	-3.53
78.70	0.30	33.36	-3.23	79.00	0.00	33.61	-3.42
79.00	0.60	34.26	-3.32	79.30	0.30	34.51	-3.51
79.30	0.90	33.94	-3.29	79.60	0.60	34.69	-3.53
79.60	1.20	33.16	-3.21	79.90	0.90	34.80	-3.54
79.90	1.50	32.00	-3.10	80.20	1.20	34.51	-3.51
80.40	2.00	28.38	-2.74	80.50	1.50	33.67	-3.43
80.90	2.50	24.11	-2.31	81.00	2.00	31.70	-3.23
81.40	3.00	20.98	-2.00	81.50	2.50	28.23	-2.88
81.90	3.50	15.86	-1.49	82.00	3.00	23.53	-2.41

Test No. 0.6/-2.54/1.84

z_0 (cm)	-2.54	r_i (cm)+ve	2.23	z_0 (cm)	-2.54
d (cm)	0.97	r_i (cm)-ve	-0.14	d (cm)	1.39
Time to Equilibrium (min)	10.00	average r_i (cm)	2.25	Time to Equilibrium (min)	r_i (cm)+ve
Water temp (°C)	22.00		2.24	Water temp (°C)	10.00
Tube position (cm)	78.40	ε_m (cm)+ve	-3.32	Tube position (cm)	r_i (cm)-ve
Time to fill (s)	61.62	ε_m (cm)-ve	-3.30	Time to fill (s)	22.00
Q (L/s)	0.19	average ε_m (cm)	-3.31	Q (L/s)	average ε_m (cm)

Horizontal position (cm)	<i>r</i> (cm)	Depth reading (mm)	<i>ε</i> (cm)
82.40	4.00	12.04	-1.11
82.90	4.50	8.00	-0.71
83.40	5.00	3.60	-0.27
83.80	5.40	0.84	0.00
			84.50
			5.50
			4.59
			-0.52

Test No. 0.6/-3.81/1.84

Horizontal position (cm)	<i>r</i> (cm)	Depth reading (mm)	<i>ε</i> (cm)
71.10	-7.90	0.39	0.00
72.00	-7.00	6.71	-0.63
73.00	-6.00	13.79	-1.34
74.00	-5.00	21.86	-2.15
75.00	-4.00	30.57	-3.02
76.00	-3.00	37.61	-3.73
76.50	-2.50	41.79	-4.15
77.00	-2.00	45.18	-4.49
77.50	-1.50	47.34	-4.70
77.80	-1.20	48.45	-4.81
78.10	-0.90	49.41	-4.91

Test No. 0.6/-3.81/0.77

<i>z</i> ₀ (cm)	<i>r</i> _t (cm)+ve	<i>d</i> (cm)	<i>z</i> ₀ (cm)	<i>r</i> _t (cm)+ve
1.39	<i>r</i> _t (cm)-ve	3.06	2.70	<i>r</i> _t (cm)+ve
10.00	<i>r</i> _t (cm)-ve	2.90	3.08	<i>r</i> _t (cm)-ve
22.00	average <i>r</i> _t (cm)	2.98	Time to Equilibrium (min)	10.00
79.00	<i>ε</i> _m (cm)+ve	-4.85	Water temp (°C)	21.00
41.63	<i>ε</i> _m (cm)-ve	-4.91	Tube position (cm)	75.00
0.28	average <i>ε</i> _m (cm)	-4.88	Time to fill (s)	45.84
			<i>Q</i> (L/s)	0.25
				average <i>ε</i> _m (cm)
				-4.75

Horizontal position (cm)	<i>r</i> (cm)	Depth reading (mm)	ε (cm)	Horizontal position (cm)	<i>r</i> (cm)	Depth reading (mm)	ε (cm)
78.40	-0.60	48.95	-4.86	74.10	-0.90	46.98	-4.69
78.70	-0.30	48.18	-4.79	74.40	-0.60	46.76	-4.67
79.00	0.00	47.60	-4.73	74.70	-0.30	46.22	-4.61
79.30	0.30	47.73	-4.74	75.00	0.00	45.20	-4.51
79.60	0.60	48.25	-4.80	75.30	0.30	46.00	-4.59
79.90	0.90	48.82	-4.85	75.60	0.60	47.29	-4.72
80.20	1.20	48.04	-4.78	75.90	0.90	47.71	-4.76
80.50	1.50	47.50	-4.72	76.20	1.20	47.21	-4.71
81.00	2.00	44.98	-4.47	76.50	1.50	45.83	-4.57
81.50	2.50	42.65	-4.24	77.00	2.00	43.28	-4.32
82.00	3.00	38.89	-3.86	77.50	2.50	39.73	-3.96
83.00	4.00	30.31	-3.01	78.00	3.00	35.96	-3.58
84.00	5.00	22.59	-2.23	79.00	4.00	28.13	-2.80
85.00	6.00	14.58	-1.43	80.00	5.00	21.12	-2.10
86.00	7.00	6.46	-0.62	81.00	6.00	13.42	-1.33
86.80	7.80	0.21	0.00	82.00	7.00	6.83	-0.67
				82.90	7.90	0.19	0.00

Test No. 0.6/-6.35/1.89	z_0 (cm)	r_t (cm)+ve	d (cm)	r_t (cm)+ve	r_t (cm)-ve	Time to Equilibrium (min)	Time to Equilibrium (min)	average r_t (cm)	average r_t (cm)	Test No. 0.6/-2.54/4.85
		1.39	2.93	0.97	-2.54					
<i>d</i> (cm)		1.00	2.95	10.00	3.02					
Time to Equilibrium (min)		22.00	average r_t (cm)	20.00	3.16					
Water temp (°C)			2.94	20.00	3.09					
Tube position (cm)	77.00	ε_m (cm)+ve	-7.34	76.30						
Time to fill (s)	40.45	ε_m (cm)-ve	-7.36	33.14						
Q (L/s)	0.29	average ε_m (cm)	-7.35	0.35						
				0.19	3.68					
				0.00	3.69					

Horizontal position (cm)	<i>r</i> (cm)	Depth reading (mm)	<i>ε</i> (cm)
65.70	-11.30	-1.02	0.00
66.00	-11.00	1.47	-0.25
67.00	-10.00	10.03	-1.10
68.00	-9.00	17.21	-1.81
69.00	-8.00	24.39	-2.53
70.00	-7.00	32.34	-3.32
71.00	-6.00	40.22	-4.10
72.00	-5.00	47.63	-4.84
73.00	-4.00	52.25	-5.29
74.00	-3.00	62.42	-6.31
74.50	-2.50	67.16	-6.78
75.00	-2.00	70.03	-7.06
75.50	-1.50	71.95	-7.25
75.80	-1.20	72.44	-7.30
76.10	-0.90	73.09	-7.36
76.40	-0.60	72.86	-7.34
76.70	-0.30	72.63	-7.31
77.00	0.00	71.61	-7.21
77.30	0.30	72.33	-7.28
77.60	0.60	72.49	-7.30
77.90	0.90	72.90	-7.34
78.20	1.20	71.80	-7.22
78.50	1.50	71.17	-7.16
79.00	2.00	68.74	-6.92
79.50	2.50	66.48	-6.69
80.00	3.00	62.55	-6.29
81.00	4.00	53.93	-5.43
82.00	5.00	47.76	-4.80
83.00	6.00	40.36	-4.06
84.00	7.00	31.77	-3.20
85.00	8.00	24.51	-2.46
86.00	9.00	16.07	-1.62

Horizontal position (cm)	<i>r</i> (cm)	Depth reading (mm)	<i>ε</i> (cm)	Horizontal position (cm)	<i>r</i> (cm)	Depth reading (mm)	<i>ε</i> (cm)
69.90	69.90	-6.40	-0.40	69.90	69.90	-6.40	0.00
70.30	70.30	-6.00	2.13	70.30	70.30	-6.00	-0.25
70.80	70.80	-5.50	6.97	70.80	70.80	-5.50	-0.74
71.30	71.30	-5.00	11.10	71.30	71.30	-5.00	-1.15
71.80	71.80	-4.50	13.81	71.80	71.80	-4.50	-1.43
72.30	72.30	-4.00	18.61	72.30	72.30	-4.00	-1.91
72.80	72.80	-3.50	22.74	72.80	72.80	-3.50	-2.32
73.30	73.30	-3.00	25.9	73.30	73.30	-3.00	-2.64
73.80	73.80	-2.50	29.81	73.80	73.80	-2.50	-3.03
74.30	74.30	-2.00	33	74.30	74.30	-2.00	-3.35
74.80	74.80	-1.50	35.07	74.80	74.80	-1.50	-3.56
75.10	75.10	-1.20	35.49	75.10	75.10	-1.20	-3.60
75.40	75.40	-0.90	36.28	75.40	75.40	-0.90	-3.68
75.70	75.70	-0.60	35.81	75.70	75.70	-0.60	-3.64
76.00	76.00	-0.30	34.66	76.00	76.00	-0.30	-3.52
76.30	76.30	0.00	34.5	76.30	76.30	0.00	-3.51
76.60	76.60	0.30	36	76.60	76.60	0.30	-3.66
76.90	76.90	0.60	36.35	76.90	76.90	0.60	-3.69
77.20	77.20	0.90	36.12	77.20	77.20	0.90	-3.67
77.50	77.50	1.20	35.58	77.50	77.50	1.20	-3.62
77.80	77.80	1.50	34.28	77.80	77.80	1.50	-3.49
78.30	78.30	2.00	31.75	78.30	78.30	2.00	-3.24
78.80	78.80	2.50	28.39	78.80	78.80	2.50	-2.90
79.30	79.30	3.00	24.93	79.30	79.30	3.00	-2.56
79.80	79.80	3.50	20.71	79.80	79.80	3.50	-2.14
80.30	80.30	4.00	16.74	80.30	80.30	4.00	-1.74
80.80	80.80	4.50	13.28	80.80	80.80	4.50	-1.39
81.30	81.30	5.00	9.71	81.30	81.30	5.00	-1.04
81.80	81.80	5.50	4.61	81.80	81.80	5.50	-0.53
82.30	82.30	6.00	1.21	82.30	82.30	6.00	-0.19
82.50	82.50	6.20	0.00	82.50	82.50	6.20	0.00

Horizontal position (cm)	<i>r</i> (cm)	Depth reading (mm)	<i>ε</i> (cm)
87.00	10.00	7.72	-0.78
88.00	11.00	0.00	0.00

Test No. 0.6/-2.54/4.29

<i>z</i> ₀ (cm)	-2.54	<i>z</i> ₀ (cm)	-5.08
<i>d</i> (cm)	0.97	<i>r</i> _t (cm)+ve	0.97
Time to Equilibrium (min)	10.00	<i>r</i> _t (cm)-ve	10.00
Water temp (°C)	20.00	average <i>r</i> _t (cm)	21.00
Tube position (cm)	76.00	<i>ε</i> _m (cm)+ve	76.50
Time to fill (s)	37.44	<i>ε</i> _m (cm)-ve	28.79
<i>Q</i> (L/s)	0.31	average <i>ε</i> _m (cm)	0.40
Horizontal position (cm)	<i>r</i> (cm)	Depth reading (mm)	<i>ε</i> (cm)
69.70	-6.30	-0.59	0.00
70.00	-6.00	0.97	-0.15
70.50	-5.50	5.09	-0.56
71.00	-5.00	8.67	-0.91
71.50	-4.50	12.06	-1.24
72.00	-4.00	15.66	-1.60
72.50	-3.50	19.35	-1.96
73.00	-3.00	23.48	-2.37
73.50	-2.50	27.16	-2.73
74.00	-2.00	29.70	-2.98
74.50	-1.50	33.56	-3.36
74.80	-1.20	34.60	-3.46
75.10	-0.90	35.17	-3.51
75.40	-0.60	35.74	-3.56
75.70	-0.30	35.12	-3.50
76.00	0.00	33.71	-3.35
76.30	0.30	34.25	-3.40
Horizontal position (cm)	<i>r</i> (cm)	Depth reading (mm)	<i>ε</i> (cm)
67.00	67.00	-9.50	0.54
68.00	68.00	-8.50	9.74
69.00	69.00	-7.50	16.72
70.00	70.00	-6.50	24.91
71.00	71.00	-5.50	32.71
72.00	72.00	-4.50	40.32
73.00	73.00	-3.50	48.50
73.50	73.50	-3.00	52.24
74.00	74.00	-2.50	55.71
74.50	74.50	-2.00	58.90
75.00	75.00	-1.50	60.71
75.30	75.30	-1.20	62.00
75.60	75.60	-0.90	62.74
75.90	75.90	-0.60	63.21
76.20	76.20	-0.30	62.93
76.50	76.50	0.00	62.08
76.80	76.80	0.30	62.77
Horizontal position (cm)	<i>r</i> (cm)	Depth reading (mm)	<i>ε</i> (cm)

Horizontal position (cm)	<i>r</i> (cm)	Depth reading (mm)	<i>ε</i> (cm)	Horizontal position (cm)	<i>r</i> (cm)	Depth reading (mm)	<i>ε</i> (cm)
76.60	0.60	35.34	-3.51	77.10	0.60	62.91	-6.25
76.90	0.90	35.58	-3.53	77.40	0.90	63.53	-6.31
77.20	1.20	34.93	-3.46	77.70	1.20	62.11	-6.17
77.50	1.50	33.85	-3.35	78.00	1.50	61.62	-6.12
78.00	2.00	31.62	-3.12	78.50	2.00	60.12	-5.97
78.50	2.50	27.76	-2.73	79.00	2.50	55.62	-5.52
79.00	3.00	25.10	-2.46	79.50	3.00	52.54	-5.21
79.50	3.50	19.83	-1.92	80.00	3.50	49.45	-4.90
80.00	4.00	16.43	-1.58	81.00	4.50	42.02	-4.16
80.50	4.50	13.52	-1.28	82.00	5.50	34.55	-3.41
81.00	5.00	9.11	-0.83	83.00	6.50	26.30	-2.59
81.50	5.50	6.56	-0.57	84.00	7.50	18.58	-1.82
82.00	6.00	2.59	-0.17	85.00	8.50	10.96	-1.06
82.40	6.40	0.94	0.00	86.00	9.50	1.66	-0.13
				86.20	9.70	0.38	0.00

Test No. 0.6/-1.27/1.84

<i>z</i> ₀ (cm)	-1.27	<i>z</i> ₀ (cm)	-1.27
<i>d</i> (cm)	1.39	<i>r</i> _t (cm)+ve	2.90
Time to Equilibrium (min)	10.00	<i>r</i> _t (cm)-ve	2.98
Water temp (°C)	21.00	average <i>r</i> _t (cm)	2.94
Tube position (cm)	77.00	<i>ε</i> _m (cm)+ve	-2.43
Time to fill (s)	41.72	<i>ε</i> _m (cm)-ve	-2.42
<i>Q</i> (L/s)	0.28	average <i>ε</i> _m (cm)	-2.42

Test No. 0.6/-1.27/5.95

<i>z</i> ₀ (cm)	0.97	<i>r</i> _t (cm)+ve	3.27
<i>d</i> (cm)	2.90	<i>r</i> _t (cm)-ve	3.29
Time to Equilibrium (min)	10.00	average <i>r</i> _t (cm)	3.28
Water temp (°C)	22.00	Tube position (cm)	80.60
Tube position (cm)	80.60	<i>ε</i> _m (cm)+ve	-2.50
Time to fill (s)	27.04	<i>ε</i> _m (cm)-ve	-2.47
<i>Q</i> (L/s)	0.43	average <i>ε</i> _m (cm)	-2.48

	Horizontal position (cm)	<i>r</i> (cm)	Depth reading (mm)	<i>ε</i> (cm)	Horizontal position (cm)	<i>r</i> (cm)	Depth reading (mm)	<i>ε</i> (cm)
72.60	-4.40	0.00	0.00	75.90	-4.70	1.96	0.00	0.00
73.00	-4.00	3.15	-0.32	76.10	-4.50	4.36	-0.24	-0.24
73.50	-3.50	8.07	-0.81	76.60	-4.00	9.15	-0.72	-0.72
74.00	-3.00	12.48	-1.25	77.10	-3.50	13.15	-1.12	-1.12
74.50	-2.50	15.92	-1.60	77.60	-3.00	16.64	-1.47	-1.47
75.00	-2.00	19.83	-1.99	78.10	-2.50	20.82	-1.89	-1.89
75.50	-1.50	22.12	-2.22	78.60	-2.00	23.62	-2.17	-2.17
75.80	-1.20	22.78	-2.29	79.10	-1.50	25.78	-2.39	-2.39
76.10	-0.90	24.04	-2.42	79.40	-1.20	26.03	-2.41	-2.41
76.40	-0.60	23.61	-2.37	79.70	-0.90	26.26	-2.44	-2.44
76.70	-0.30	22.57	-2.27	80.00	-0.60	26.57	-2.47	-2.47
77.00	0.00	22.42	-2.26	80.30	-0.30	26.05	-2.42	-2.42
77.30	0.30	22.71	-2.29	80.60	0.00	25.32	-2.34	-2.34
77.60	0.60	23.06	-2.32	80.90	0.30	26.65	-2.48	-2.48
77.90	0.90	24.12	-2.43	81.20	0.60	26.71	-2.48	-2.48
78.20	1.20	23.03	-2.32	81.50	0.90	26.89	-2.50	-2.50
78.50	1.50	22.58	-2.28	81.80	1.20	26.40	-2.45	-2.45
79.00	2.00	19.61	-1.98	82.10	1.50	25.00	-2.31	-2.31
79.50	2.50	15.18	-1.54	82.60	2.00	23.10	-2.12	-2.12
80.00	3.00	11.78	-1.20	83.10	2.50	19.29	-1.74	-1.74
80.50	3.50	8.27	-0.85	83.60	3.00	17.00	-1.51	-1.51
81.00	4.00	3.47	-0.38	84.10	3.50	12.39	-1.05	-1.05
81.40	4.40	-0.31	0.00	84.60	4.00	8.49	-0.67	-0.67
				85.10	4.50	2.94	-0.11	-0.11
				85.30	4.70	1.83	0.00	0.00

Horizontal position (cm)	<i>r</i> (cm)	Depth reading (mm)	<i>ε</i> (cm)
72.60	-4.40	0.00	0.00
73.00	-4.00	3.15	-0.32
73.50	-3.50	8.07	-0.81
74.00	-3.00	12.48	-1.25
74.50	-2.50	15.92	-1.60
75.00	-2.00	19.83	-1.99
75.50	-1.50	22.12	-2.22
75.80	-1.20	22.78	-2.29
76.10	-0.90	24.04	-2.42
76.40	-0.60	23.61	-2.37
76.70	-0.30	22.57	-2.27
77.00	0.00	22.42	-2.26
77.30	0.30	22.71	-2.29
77.60	0.60	23.06	-2.32
77.90	0.90	24.12	-2.43
78.20	1.20	23.03	-2.32
78.50	1.50	22.58	-2.28
79.00	2.00	19.61	-1.98
79.50	2.50	15.18	-1.54
80.00	3.00	11.78	-1.20
80.50	3.50	8.27	-0.85
81.00	4.00	3.47	-0.38
81.40	4.40	-0.31	0.00

Test No. 0.6/-5.08/4.34

Horizontal position (cm)	<i>r</i> (cm)	Depth reading (mm)	<i>ε</i> (cm)
66.50	-9.50	-0.25	0.00
67.00	-9.00	3.04	-0.33
68.00	-8.00	10.91	-1.11
69.00	-7.00	19.23	-1.94
70.00	-6.00	26.78	-2.70
71.00	-5.00	34.58	-3.47
72.00	-4.00	42.17	-4.23
73.00	-3.00	50.13	-5.02
73.50	-2.50	53.67	-5.38
74.00	-2.00	56.87	-5.70
74.50	-1.50	59.75	-5.98
74.80	-1.20	60.28	-6.03
75.10	-0.90	60.69	-6.07
75.40	-0.60	61.29	-6.13
75.70	-0.30	60.00	-6.00
76.00	0.00	59.35	-5.94
76.30	0.30	59.58	-5.96
76.60	0.60	60.71	-6.07
76.90	0.90	60.62	-6.06
77.20	1.20	59.79	-5.98
77.50	1.50	59.04	-5.90
77.80	1.80	56.82	-5.68
78.50	2.50	53.78	-5.38
79.00	3.00	49.75	-4.97

Test No. 0.6/-2.54/5.32

<i>r</i> (cm)	<i>z</i> ₀ (cm)	<i>d</i> (cm)	<i>r</i> _t (cm)+ve	<i>r</i> _t (cm)-ve	<i>z</i> ₀ (cm)	<i>d</i> (cm)	<i>r</i> _t (cm)+ve	<i>r</i> _t (cm)-ve	<i>z</i> ₀ (cm)	<i>d</i> (cm)	<i>r</i> _t (cm)+ve	<i>r</i> _t (cm)-ve
5.08	-5.08	2.87	2.92	2.89	-5.08	2.92	Time to Equilibrium (min)	Time to Equilibrium (min)	-5.08	2.92	0.97	-2.54
0.97	0.97	10.00	<i>r</i> _t (cm)-ve	average <i>r</i> _t (cm)	0.97	10.00	<i>r</i> _t (cm)-ve	average <i>r</i> _t (cm)	0.97	10.00	0.97	3.11
<i>d</i> (cm)	<i>d</i> (cm)	22.00	average <i>r</i> _t (cm)	2.89	Water temp (°C)	22.00	average <i>r</i> _t (cm)	2.89	Water temp (°C)	22.00	average <i>r</i> _t (cm)	3.20
Time to Equilibrium (min)	Time to Equilibrium (min)	22.00	average <i>r</i> _t (cm)	2.92	Tube position (cm)	75.50	average <i>r</i> _t (cm)	2.92	Tube position (cm)	75.50	average <i>r</i> _t (cm)	3.16
Water temp (°C)	Water temp (°C)	76.00	<i>ε</i> _m (cm)+ve	-6.07	Time to fill (s)	30.22	<i>ε</i> _m (cm)-ve	-6.13	Time to fill (s)	30.22	<i>ε</i> _m (cm)-ve	-3.68
Tube position (cm)	Tube position (cm)	76.00	<i>ε</i> _m (cm)-ve	-6.07	<i>Q</i> (L/s)	0.38	average <i>ε</i> _m (cm)	-6.10	<i>Q</i> (L/s)	0.38	average <i>ε</i> _m (cm)	-3.69
Time to fill (s)	Time to fill (s)	37.02	average <i>ε</i> _m (cm)	-6.13								
<i>Q</i> (L/s)	<i>Q</i> (L/s)	0.31	average <i>ε</i> _m (cm)	-6.10								

Horizontal position (cm)	<i>r</i> (cm)	Depth reading (mm)	<i>ε</i> (cm)
80.00	4.00	40.88	-4.08
81.00	5.00	34.82	-3.47
82.00	6.00	27.37	-2.73
83.00	7.00	19.55	-1.94
84.00	8.00	12.07	-1.19
85.00	9.00	2.93	-0.28
85.40	9.40	0.17	0.00

Test No. 0.6/-7.62/5.69

Horizontal position (cm)	<i>r</i> (cm)	Depth reading (mm)	<i>ε</i> (cm)	Horizontal position (cm)	<i>r</i> (cm)	Depth reading (mm)	<i>ε</i> (cm)
63.50	-12.50	1.40	0.00	60.90	-13.40	-0.21	0.00
63.70	-12.30	2.87	-0.15	61.30	-13.00	2.79	-0.30
64.70	-11.30	14.6	-1.32	62.30	-12.00	12.67	-1.29
65.70	-10.30	23.11	-2.17	63.30	-11.00	21.01	-2.12
66.70	-9.30	31.07	-2.96	64.30	-10.00	28.71	-2.89
67.70	-8.30	40.84	-3.93	65.30	-9.00	36.05	-3.62
68.70	-7.30	49.44	-4.79	66.30	-8.00	44.30	-4.45
69.70	-6.30	58.42	-5.69	67.30	-7.00	51.97	-5.21
70.70	-5.30	66.71	-6.51	68.30	-6.00	59.29	-5.94
71.70	-4.30	73.79	-7.22	69.30	-5.00	66.93	-6.71
72.70	-3.30	81.38	-7.97	70.30	-4.00	73.86	-7.40

Test No. 0.6/-7.62/5.53

<i>z</i> ₀ (cm)	<i>d</i> (cm)	<i>r</i> _t (cm)+ve	<i>r</i> _t (cm)-ve	<i>Time to Equilibrium</i> (min)	<i>Water temp</i> (°C)	<i>Tube position</i> (cm)	<i>ε</i> _m (cm)+ve	<i>ε</i> _m (cm)-ve	<i>Time to fill</i> (s)	<i>Q</i> (L/s)	<i>average ε_m</i> (cm)	<i>average ε_m</i> (cm)
7.62	2.98	3.77	10.00	20.00	74.30	29.04	0.40	-8.97	-7.62	0.97	3.11	3.70
0.97	1.00	3.37	20.00	74.30	29.04	0.40	-8.97	-7.62	0.97	3.11	3.70	
10.00	21.00	21.00	average <i>r</i> _t (cm)	average <i>ε_m</i> (cm)								
<i>r</i> _t (cm)-ve	<i>ε_m</i> (cm)+ve	<i>ε_m</i> (cm)-ve										
average <i>r</i> _t (cm)												
average <i>ε_m</i> (cm)												

	Horizontal position (cm)	<i>r</i> (cm)	Depth reading (mm)	<i>ε</i> (cm)	Horizontal position (cm)	<i>r</i> (cm)	Depth reading (mm)	<i>ε</i> (cm)
73.20	-2.80	85.00	-8.33		71.30	-3.00	81.12	-8.12
73.70	-2.30	87.87	-8.62		71.80	-2.50	84.42	-8.45
74.20	-1.80	89.90	-8.82		72.30	-2.00	86.66	-8.68
74.50	-1.50	90.60	-8.89		72.80	-1.50	88.46	-8.86
74.80	-1.20	90.75	-8.91		73.10	-1.20	89.27	-8.94
75.10	-0.90	91.66	-9.00		73.40	-0.90	89.57	-8.97
75.40	-0.60	90.06	-8.83		73.70	-0.60	90.00	-9.01
75.70	-0.30	87.82	-8.61		74.00	-0.30	89.98	-9.01
76.00	0.00	82.29	-8.06		74.30	0.00	88.77	-8.89
76.30	0.30	89.84	-8.81		74.60	0.30	88.96	-8.91
76.60	0.60	89.35	-8.76		74.90	0.60	89.02	-8.91
76.90	0.90	89.01	-8.73		75.20	0.90	89.12	-8.92
77.20	1.20	88.41	-8.66		75.50	1.20	88.05	-8.81
77.70	1.70	86.02	-8.42		75.80	1.50	86.53	-8.66
78.20	2.20	82.44	-8.07		76.30	2.00	83.30	-8.34
78.70	2.70	79.92	-7.81		76.80	2.50	80.52	-8.06
79.70	3.70	73.02	-7.12		77.30	3.00	76.89	-7.70
80.70	4.70	65.30	-6.34		78.30	4.00	69.95	-7.00
81.70	5.70	58.84	-5.70		79.30	5.00	62.41	-6.25
82.70	6.70	51.83	-4.99		80.30	6.00	55.38	-5.54
83.70	7.70	45.00	-4.31		81.30	7.00	47.24	-4.73
84.70	8.70	37.02	-3.51		82.30	8.00	40.71	-4.08
85.70	9.70	30.00	-2.80		83.30	9.00	33.12	-3.32
86.70	10.70	22.86	-2.08		84.30	10.00	27.22	-2.72
87.70	11.70	15.20	-1.32		85.30	11.00	18.81	-1.88
88.70	12.70	6.34	-0.43		86.30	12.00	10.38	-1.04
89.30	13.30	2.08	0.00		87.30	13.00	2.94	-0.29
						13.20	0.00	0.00
					87.50			

Test No. 0.6/-2.54/5.69

z_0 (cm)	-2.54	r (cm)	Horizontal position (cm)	Depth reading (mm)	ε (cm)
d (cm)	0.97	r_i (cm)+ve	69.70	0.23	0.00
Time to Equilibrium (min)	10.00	r_i (cm)-ve	69.80	-6.50	-0.09
Water temp (°C)	21.00	average r_i (cm)	70.30	-6.00	4.55
Tube position (cm)	76.30	ε_m (cm)+ve	70.80	-5.50	8.73
Time to fill (s)	28.27	ε_m (cm)-ve	71.30	-5.00	12.14
Q (L/s)	0.41	average ε_m (cm)	71.80	-4.50	16.38
			72.30	-4.00	20.62
			72.80	-3.50	24.32
			73.30	-3.00	27.96
			73.80	-2.50	31.71
			74.30	-2.00	34.26
			74.80	-1.50	35.35
			75.10	-1.20	36.56
			75.40	-0.90	36.90
			75.70	-0.60	36.01
			76.00	-0.30	35.45
			76.30	0.00	35.29
			76.60	0.30	35.91
			76.90	0.60	36.08
			77.20	0.90	36.97
			77.50	1.20	36.49
			77.80	1.50	35.55
			78.30	2.00	32.44
			78.80	2.50	30.51

Test No. 0.6/-5.08/6.51

z_0 (cm)	-2.54	r (cm)	Horizontal position (cm)	r (cm)	Depth reading (mm)	ε (cm)
d (cm)	0.97	r_i (cm)+ve	68.90	-9.50	-0.67	0.00
Time to Equilibrium (min)	10.00	r_i (cm)-ve	69.40	-9.00	3.59	-0.34
Water temp (°C)	21.00	average r_i (cm)	70.40	-8.00	12.94	-1.28
Tube position (cm)	76.30	ε_m (cm)+ve	71.40	-7.00	21.64	-2.14
Time to fill (s)	28.27	ε_m (cm)-ve	72.40	-6.00	29.42	-2.92
Q (L/s)	0.41	average ε_m (cm)	73.40	-5.00	38.54	-3.83
			74.40	-4.00	46.01	-4.57
			75.40	-3.00	54.16	-5.38
			75.90	-2.50	57.62	-5.72
			76.40	-2.00	60.52	-6.01
			76.90	-1.50	62.46	-6.20
			77.20	-1.20	62.63	-6.22
			77.50	-0.90	63.47	-6.30
			77.80	-0.60	63.35	-6.29
			78.10	-0.30	62.18	-6.17
			78.40	0.00	61.16	-6.07
			78.70	0.30	61.46	-6.10
			79.00	0.60	62.02	-6.15
			79.30	0.90	61.44	-6.09
			79.60	1.20	61.04	-6.05
			79.90	1.50	59.26	-5.87
			80.40	2.00	57.92	-5.74
			80.90	2.50	55.30	-5.47
			81.40	3.00	51.54	-5.10

Horizontal position (cm)	<i>r</i> (cm)	Depth reading (mm)	ε (cm)
79.30	3.00	27.20	-2.66
79.80	3.50	23.03	-2.24
80.30	4.00	18.70	-1.81
80.80	4.50	15.52	-1.49
81.30	5.00	11.55	-1.09
81.80	5.50	7.39	-0.67
82.30	6.00	3.36	-0.27
82.60	6.30	0.70	0.00

Test No. 0.6/-5.08/4.42

z_0 (cm)	<i>r</i> (cm)+ve	ε (cm)	Horizontal position (cm)	<i>r</i> (cm)	Depth reading (mm)	ε (cm)
5.08	0.97	2.94	82.40	4.00	44.04	-4.34
<i>d</i> (cm)	<i>r</i> (cm)-ve		83.40	5.00	36.79	-3.61
Time to Equilibrium (min)	10.00	3.20	84.40	6.00	29.35	-2.87
Water temp (°C)	average <i>r</i> (cm)	3.07	85.40	7.00	21.73	-2.10
Tube position (cm)	77.70	ε_m (cm)+ve	86.40	8.00	14.68	-1.39
Time to fill (s)	36.37	ε_m (cm)-ve	87.40	9.00	5.51	-0.47
Q (L/s)	0.32	average ε_m (cm)	88.00	9.60	0.17	0.07

Test No. 0.6/-2.54/4.50

z_0 (cm)	<i>d</i> (cm)	r (cm)+ve	r (cm)-ve	Horizontal position (cm)	<i>r</i> (cm)	Depth reading (mm)	ε (cm)
2.54			0.97	82.40	4.00	44.04	-4.34
<i>d</i> (cm)				83.40	5.00	36.79	-3.61
Time to Equilibrium (min)		3.20		84.40	6.00	29.35	-2.87
Water temp (°C)		3.07		85.40	7.00	21.73	-2.10
Tube position (cm)		-6.18		86.40	8.00	14.68	-1.39
Time to fill (s)		-6.17		87.40	9.00	5.51	-0.47
Q (L/s)		-6.17		88.00	9.60	0.17	0.07

Horizontal position (cm)	r (cm)	Depth reading (mm)	ε (cm)	Horizontal position (cm)	r (cm)	Depth reading (mm)	ε (cm)
75.70	-2.00	57.29	-5.84	73.60	-2.00	33.97	-3.39
76.20	-1.50	59.63	-6.07	74.10	-1.50	36.67	-3.65
76.50	-1.20	60.17	-6.12	74.40	-1.20	37.69	-3.75
76.80	-0.90	60.61	-6.16	74.70	-0.90	38.28	-3.80
77.10	-0.60	60.65	-6.17	75.00	-0.60	38.13	-3.79
77.40	-0.30	59.85	-6.08	75.30	-0.30	36.84	-3.65
77.70	0.00	59.50	-6.05	75.60	0.00	36.33	-3.60
78.00	0.30	60.00	-6.10	75.90	0.30	37.40	-3.70
78.30	0.60	60.86	-6.18	76.20	0.60	38.33	-3.79
78.60	0.90	60.47	-6.14	76.50	0.90	38.30	-3.78
78.90	1.20	59.88	-6.08	76.80	1.20	37.22	-3.67
79.20	1.50	59.16	-6.01	77.10	1.50	36.85	-3.63
79.70	2.00	56.73	-5.76	77.60	2.00	34.20	-3.36
80.20	2.50	53.65	-5.45	78.10	2.50	31.48	-3.08
80.70	3.00	49.44	-5.03	78.60	3.00	28.04	-2.73
81.70	4.00	42.72	-4.35	79.10	3.50	23.19	-2.24
82.70	5.00	35.14	-3.58	79.60	4.00	19.13	-1.83
83.70	6.00	28.92	-2.96	80.10	4.50	15.96	-1.51
84.70	7.00	21.47	-2.21	80.60	5.00	12.22	-1.13
85.70	8.00	13.92	-1.45	81.10	5.50	9.20	-0.82
86.70	9.00	4.97	-0.54	81.60	6.00	5.56	-0.45
87.40	9.70	-0.44	0.00	82.20	6.60	1.15	0.00

Test No. 0.6/-2.54/4.68

z_0 (cm)	-2.54	z_0 (cm)	-5.08
d (cm)	0.97	r_t (cm)+ve	3.04
Time to Equilibrium (min)	10.00	r_t (cm)-ve	3.24
Water temp (°C)	18.00	average r_t (cm)	3.14
Tube position (cm)	77.60	ε_m (cm)+ve	-3.74
Time to fill (s)	34.33	ε_m (cm)-ve	-3.71
\underline{Q} (L/s)	0.34	average ε_m (cm)	-3.72

Test No. 0.6/-5.08/4.79

z_0 (cm)	-5.08
d (cm)	0.97
Time to Equilibrium (min)	10.00
Water temp (°C)	18.00
Tube position (cm)	77.70
Time to fill (s)	33.58
\underline{Q} (L/s)	0.34

Horizontal position (cm)	<i>r</i> (cm)	Depth reading (mm)	<i>ε</i> (cm)	Horizontal position (cm)	<i>r</i> (cm)	Depth reading (mm)	<i>ε</i> (cm)
71.30	-6.30	0.09	0.00	68.40	-9.30	-1.32	0.00
71.60	-6.00	2.14	-0.21	68.70	-9.00	1.29	-0.26
72.10	-5.50	6.87	-0.68	69.70	-8.00	11.32	-1.25
72.60	-5.00	10.71	-1.06	70.70	-7.00	19.38	-2.05
73.10	-4.50	15.62	-1.55	71.70	-6.00	28.04	-2.91
73.60	-4.00	20	-1.99	72.70	-5.00	35.08	-3.61
74.10	-3.50	23.44	-2.34	73.70	-4.00	43.13	-4.40
74.60	-3.00	27.32	-2.72	74.70	-3.00	51.09	-5.19
75.10	-2.50	30.52	-3.04	75.20	-2.50	55.71	-5.65
75.60	-2.00	33.77	-3.37	75.70	-2.00	58.52	-5.93
76.10	-1.50	36	-3.59	76.20	-1.50	60.18	-6.09
76.40	-1.20	36.95	-3.69	76.50	-1.20	61.3	-6.20
76.70	-0.90	37.2	-3.71	76.80	-0.90	61	-6.17
77.00	-0.60	37	-3.69	77.10	-0.60	60.76	-6.14
77.30	-0.30	36.48	-3.64	77.40	-0.30	60.68	-6.13
77.60	0.00	36.29	-3.62	77.70	0.00	59.75	-6.04
77.90	0.30	36.39	-3.63	78.00	0.30	60.57	-6.12
78.20	0.60	37.21	-3.71	78.30	0.60	61.57	-6.21
78.50	0.90	37.46	-3.74	78.60	0.90	61.18	-6.17
78.80	1.20	36.7	-3.66	78.90	1.20	60.07	-6.06
79.10	1.50	35.63	-3.55	79.20	1.50	60.05	-6.05
79.60	2.00	32.74	-3.27	79.70	2.00	57.41	-5.79
80.10	2.50	30.3	-3.02	80.20	2.50	54.04	-5.45
80.60	3.00	25.75	-2.57	80.70	3.00	50.87	-5.13
81.10	3.50	22.29	-2.22	81.70	4.00	43.27	-4.36
81.60	4.00	17.43	-1.73	82.70	5.00	36	-3.62
82.10	4.50	14.81	-1.47	83.70	6.00	28.45	-2.86
82.60	5.00	9.91	-0.98	84.70	7.00	21.95	-2.20
83.10	5.50	6.64	-0.66	85.70	8.00	13.68	-1.37
83.60	6.00	0.72	-0.06	86.70	9.00	4.59	-0.45
83.80	6.20	0.08	0.00	87.20	9.50	0.11	0.00

Test No. 0.6/-5.08/2.21

Horizontal position (cm)	<i>r</i> (cm)	Depth reading (mm)	<i>ε</i> (cm)
70.10	-10.10	-5.33	0.00
70.70	-9.50	-0.21	-0.50
71.20	-9.00	4.51	-0.95
71.70	-8.50	8.94	-1.38
72.20	-8.00	12.11	-1.69
72.70	-7.50	16.01	-2.06
73.20	-7.00	20.08	-2.46
73.70	-6.50	24.06	-2.84
74.20	-6.00	27.89	-3.21
74.70	-5.50	32.34	-3.64
75.20	-5.00	35.28	-3.92
75.70	-4.50	38.68	-4.25
76.20	-4.00	42.20	-4.59
76.70	-3.50	46.81	-5.03
77.20	-3.00	50.81	-5.42
77.70	-2.50	53.98	-5.72
78.20	-2.00	56.20	-5.93
78.70	-1.50	58.10	-6.11
79.00	-1.20	59.23	-6.21
79.30	-0.90	59.31	-6.21
79.60	-0.60	59.20	-6.19

Test No. 0.6/-10.16/1.89

<i>z</i> ₀ (cm)	<i>z</i> ₀ (cm)	<i>r</i> _t (cm)+ve	<i>d</i> (cm)	<i>r</i> _t (cm)-ve	<i>d</i> (cm)	Time to Equilibrium (min)	<i>r</i> _t (cm)+ve	<i>r</i> _t (cm)-ve	<i>d</i> (cm)
10.00	1.39	<i>r</i> _t (cm)+ve	3.02	<i>r</i> _t (cm)-ve	3.44	10.00	10.00	10.00	2.61
22.00	10.00	<i>r</i> _t (cm)-ve	3.23	Water temp (°C)	22.00	average <i>r</i> _t (cm)	22.00	average <i>r</i> _t (cm)	2.75
80.20	80.20	average <i>r</i> _t (cm)	-6.21	Tube position (cm)	77.00	<i>ε_m</i> (cm)+ve	77.00	<i>ε_m</i> (cm)+ve	2.68
34.72	34.72	<i>ε_m</i> (cm)+ve	-6.21	Time to fill (s)	40.57	<i>ε_m</i> (cm)-ve	40.57	<i>ε_m</i> (cm)-ve	-11.08
<i>Q</i> (L/s)	0.33	average <i>ε_m</i> (cm)	-6.21	<i>Q</i> (L/s)	0.29	average <i>ε_m</i> (cm)	0.29	average <i>ε_m</i> (cm)	-11.14
									-11.11
Horizontal position (cm)	<i>r</i> (cm)	Depth reading (mm)	<i>ε</i> (cm)	Horizontal position (cm)	<i>r</i> (cm)	Depth reading (mm)	<i>r</i> (cm)	Depth reading (mm)	<i>ε</i> (cm)
60.50	60.50	0.00	60.50	60.50	-16.50	-2.02	-2.02	-2.02	0.00
61.00	61.00	-0.50	61.00	61.00	-16.00	1.47	1.47	1.47	-0.35
62.00	62.00	-0.95	62.00	62.00	-15.00	10.58	10.58	10.58	-1.25
63.00	63.00	-1.38	63.00	63.00	-14.00	16.94	16.94	16.94	-1.88
64.00	64.00	-1.69	64.00	64.00	-13.00	23.72	23.72	23.72	-2.55
65.00	65.00	-2.06	65.00	65.00	-12.00	31.91	31.91	31.91	-3.37
66.00	66.00	-2.46	66.00	66.00	-11.00	39.44	39.44	39.44	-4.11
67.00	67.00	-2.84	67.00	67.00	-10.00	45.82	45.82	45.82	-4.74
68.00	68.00	-3.21	68.00	68.00	-9.00	54.44	54.44	54.44	-5.60
69.00	69.00	-3.64	69.00	69.00	-8.00	60.12	60.12	60.12	-6.16
70.00	70.00	-3.92	70.00	70.00	-7.00	68.83	68.83	68.83	-7.03
71.00	71.00	-4.25	71.00	71.00	-6.00	77.39	77.39	77.39	-7.88
72.00	72.00	-4.59	72.00	72.00	-5.00	83.95	83.95	83.95	-8.53
73.00	73.00	-5.03	73.00	73.00	-4.00	90.48	90.48	90.48	-9.17
74.00	74.00	-5.42	74.00	74.00	-3.00	98.73	98.73	98.73	-9.99
75.00	75.00	-5.72	75.00	75.00	-2.50	102.10	102.10	102.10	-10.33
76.00	76.00	-5.93	76.00	76.00	-2.00	105.54	105.54	105.54	-10.67
77.00	77.00	-6.11	77.00	77.00	-1.50	107.91	107.91	107.91	-10.90
78.00	78.00	-6.21	78.00	78.00	-1.20	109.64	109.64	109.64	-11.07
79.00	79.00	-6.21	79.00	79.00	-0.90	110.31	110.31	110.31	-11.14
79.30	79.30	-6.19	79.30	79.30	-0.60	109.56	109.56	109.56	-11.06

	Horizontal position (cm)	<i>r</i> (cm)	Depth reading (mm)	ε (cm)	Horizontal position (cm)	<i>r</i> (cm)	Depth reading (mm)	ε (cm)
79.90	-0.30	58.57	-6.12	76.70	-0.30	109.39	-11.04	
80.20	0.00	57.42	-6.00	77.00	0.00	109.14	-11.01	
80.50	0.30	58.64	-6.11	77.30	0.30	109.44	-11.04	
80.80	0.60	59.64	-6.21	77.60	0.60	109.87	-11.08	
81.10	0.90	59.81	-6.21	77.90	0.90	109.08	-11.00	
81.40	1.20	59.15	-6.14	78.20	1.20	108.40	-10.93	
81.70	1.50	58.70	-6.09	78.50	1.50	107.33	-10.82	
82.20	2.00	55.56	-5.76	79.00	2.00	105.00	-10.59	
82.70	2.50	52.44	-5.43	79.50	2.50	101.31	-10.22	
83.20	3.00	49.16	-5.09	80.00	3.00	98.73	-9.95	
83.70	3.50	46.62	-4.82	81.00	4.00	91.40	-9.21	
84.20	4.00	41.39	-4.29	82.00	5.00	84.44	-8.51	
84.70	4.50	38.58	-3.99	83.00	6.00	76.69	-7.73	
85.20	5.00	35.01	-3.62	84.00	7.00	70.60	-7.12	
85.70	5.50	30.43	-3.15	85.00	8.00	62.19	-6.27	
86.20	6.00	27.01	-2.80	86.00	9.00	55.77	-5.62	
86.70	6.50	23.91	-2.47	87.00	10.00	47.84	-4.82	
87.20	7.00	19.06	-1.97	88.00	11.00	42.06	-4.24	
88.20	8.00	11.76	-1.22	90.00	13.00	25.20	-2.54	
88.70	8.50	7.61	-0.79	91.00	14.00	18.20	-1.83	
89.20	9.00	40.13	0.00	92.00	15.00	9.97	-1.00	
				93.00	16.00	0.86	-0.09	
				93.10	16.10	0.00	0.00	

Test No. T2/0.3048/1.842

Horizontal position (cm)	<i>r</i> (cm)	Depth reading (mm)	<i>ε</i> (cm)
79	-2.30	-0.2	0.00
79.2	-2.10	0.41	-0.06
79.5	-1.80	1.67	-0.19
79.8	-1.50	3.45	-0.37
80.1	-1.20	5.26	-0.55
80.4	-0.90	5.67	-0.60
80.7	-0.60	5.58	-0.59
81	-0.30	4.65	-0.50
81.3	0.00	4.1	-0.45
81.6	0.30	4.29	-0.47
81.9	0.60	5.3	-0.57
82.2	0.90	4.96	-0.54
82.5	1.20	4.58	-0.50
82.8	1.50	3.37	-0.38
83.1	1.80	2.77	-0.33
83.4	2.10	1.82	-0.23
83.6	2.30	-0.52	0.00

Test No. T2/0.3048/1.886

	<i>z₀</i> (cm)	<i>r_b</i> (cm)+ve	<i>z₀</i> (cm)	0.30	<i>r_b</i> (cm)+ve	2.30
	<i>d</i> (cm)	<i>r_b</i> (cm)-ve	<i>d</i> (cm)	1.37	<i>r_b</i> (cm)-ve	2.60
Time to Equilibrium (min)	15.00	average <i>r_b</i> (cm)	2.30	10.00	average <i>r_b</i> (cm)	2.45
Water temp (°C)	19.00	<i>ε_m</i> (cm)+ve	-0.57	20.00	<i>ε_m</i> (cm)+ve	-0.59
Tube position (cm)	81.30	<i>ε_m</i> (cm)-ve	-0.60	82.20	<i>ε_m</i> (cm)-ve	-0.58
Time to fill (s)	40.76	average <i>ε_m</i> (cm)	-0.58	40.86	average <i>ε_m</i> (cm)	-0.58
<i>Q</i> (L/s)	0.28	<i>ψ</i> (radian)	1.44	0.28	<i>ψ</i> (radian)	1.45
					Horizontal position (cm)	<i>r</i> (cm)
						Depth reading (mm)
						<i>ε</i> (cm)

Test No. T2/0.3048/1.842

Horizontal position (cm)	<i>r</i> (cm)	Depth reading (mm)	ε (cm)
79.2	-2.40	0	0.00
79.5	-2.10	1.67	-0.17
79.8	-1.80	3.45	-0.35
80.1	-1.50	5.26	-0.54
80.4	-1.20	5.67	-0.58
80.7	-0.90	5.58	-0.58
81	-0.60	4.65	-0.49
81.3	-0.30	5.06	-0.53
81.6	0.00	4.29	-0.46
81.9	0.30	5.76	-0.61
82.2	0.60	4.96	-0.53
82.5	0.90	4.58	-0.50
82.8	1.20	3.37	-0.38
83.1	1.50	2.77	-0.32
83.4	1.80	1.82	-0.23
83.6	2.00	-0.52	0.00

Test No. T2/0.508/1.881

	<i>r_b</i> (cm)+ve	<i>z₀</i> (cm)	<i>r_b</i> (cm)-ve	<i>d</i> (cm)	<i>d</i> (cm)	<i>r_b</i> (cm)+ve	<i>r_b</i> (cm)-ve	<i>r_b</i> (cm)
Time to Equilibrium (min)	15.00	average <i>r_b</i> (cm)	2.20			15.00	average <i>r_b</i> (cm)	2.50
Water temp (°C)	20.00	ε_m (cm)+ve	-0.61			20.00	ε_m (cm)+ve	-0.55
Tube position (cm)	81.60	ε_m (cm)-ve	-0.58			81.40	ε_m (cm)-ve	-0.52
Time to fill (s)	40.76	average ε_m (cm)	-0.59			39.91	average ε_m (cm)	-0.53
<i>Q</i> (L/s)	0.28	ψ (radian)	1.43			0.29	ψ (radian)	1.37
						Horizontal position (cm)	<i>r</i> (cm)	Depth reading (mm)
								ε (cm)

Test No. T2/0.508/1.888

Horizontal position (cm)	<i>r</i> (cm)	Depth reading (mm)	ε (cm)
77.3	-2.70	-0.37	0.00
77.6	-2.40	0.37	-0.07
77.9	-2.10	1.81	-0.21
78.2	-1.80	3.9	-0.42
78.5	-1.50	4.76	-0.50
78.8	-1.20	5.36	-0.56
79.1	-0.90	6.13	-0.64
79.4	-0.60	5.75	-0.60
79.7	-0.30	5.79	-0.60
80	0.00	4.47	-0.46
80.3	0.30	5.05	-0.52
80.6	0.60	6.1	-0.62
80.9	0.90	5.35	-0.54
81.2	1.20	5.32	-0.54
81.5	1.50	4.73	-0.48
81.8	1.80	2.38	-0.24
82.1	2.10	1.05	-0.10
82.4	2.40	0.03	0.00

Test No. T2/0.508/1.866

	r_b (cm)+ve	r_b (cm)-ve	z_o (cm)	r_b (cm)+ve	r_b (cm)-ve	d (cm)	d (cm)	z_o (cm)	r_b (cm)+ve	r_b (cm)-ve	d (cm)	Time to Equilibrium (min)	average r_b (cm)	r_b (cm)+ve	r_b (cm)-ve	d (cm)	Time to Equilibrium (min)	average r_b (cm)	r_b (cm)+ve	r_b (cm)-ve	d (cm)	Time to Equilibrium (min)	average r_b (cm)	r_b (cm)+ve	r_b (cm)-ve	d (cm)	Time to Equilibrium (min)	average r_b (cm)						
Water temp (°C)	20.00	ε_n (cm)+ve	2.70	r_b (cm)+ve	2.40	15.00	1.39	15.00	0.51	r_b (cm)+ve	2.60	2.55	1.39	0.51	r_b (cm)-ve	2.70	2.55	1.39	0.51	r_b (cm)+ve	2.60	2.55	1.39	0.51	r_b (cm)-ve	2.70	2.55							
Tube position (cm)	80.00	ε_m (cm)-ve	2.40	average r_b (cm)	2.55	20.00	20.00	20.00	15.00	average r_b (cm)	2.65	20.00	20.00	15.00	average r_b (cm)	2.65	20.00	20.00	15.00	average r_b (cm)	2.65	20.00	20.00	15.00	average r_b (cm)	2.65	20.00							
Time to fill (s)	39.76	average ε_m (cm)	2.40	-0.62	-0.64	80.50	80.50	80.50	80.50	average r_b (cm)	2.65	40.23	40.23	40.23	40.23	average r_b (cm)	2.65	40.23	40.23	40.23	average r_b (cm)	2.65	40.23	40.23	40.23	average r_b (cm)	2.65	40.23						
Q (L/s)	0.29	ψ (radian)	1.37	-0.63	-0.64	0.29	0.29	0.29	0.29	ψ (radian)	1.38	0.29	0.29	0.29	0.29	ψ (radian)	1.38	0.29	0.29	0.29	ψ (radian)	1.38	0.29	0.29	0.29	ψ (radian)	1.38	0.29						
Horizontal position (cm)				Horizontal position (cm)					Horizontal position (cm)				Horizontal position (cm)				Horizontal position (cm)				Horizontal position (cm)				Horizontal position (cm)				Horizontal position (cm)					

Test No. T2/0.508/1.861

Horizontal position (cm)	<i>r</i> (cm)	Depth reading (mm)	<i>ε</i> (cm)
77.6	-2.80	-1.21	0.00
78	-2.40	-0.83	-0.03
78.4	-2.00	2.41	-0.35
78.8	-1.60	3.51	-0.46
79.2	-1.20	4.39	-0.55
79.6	-0.80	5.79	-0.68
80	-0.40	4.88	-0.59
80.4	0.00	3.76	-0.47
80.8	0.40	4.31	-0.52
81.2	0.80	5.84	-0.67
81.6	1.20	4.4	-0.52
82	1.60	3.5	-0.43
82.4	2.00	2.05	-0.28
82.8	2.40	0.4	-0.11
83	2.60	-0.71	0.00

Test No. T2/0.508/1.492

	<i>r_b</i> (cm)+ve	<i>z₀</i> (cm)	<i>r_b</i> (cm)+ve	<i>z₀</i> (cm)	<i>d</i> (cm)	<i>r_b</i> (cm)-ve	<i>z₀</i> (cm)	<i>r_b</i> (cm)-ve	<i>d</i> (cm)	Time to Equilibrium (min)	average <i>r_b</i> (cm)	<i>z₀</i> (cm)	<i>r_b</i> (cm)+ve	<i>z₀</i> (cm)	<i>r_b</i> (cm)-ve	<i>z₀</i> (cm)	<i>d</i> (cm)	Time to Equilibrium (min)	average <i>r_b</i> (cm)	<i>z₀</i> (cm)	
<i>r_b</i> (cm)	0.51	<i>r_b</i> (cm)+ve	2.60	<i>r_b</i> (cm)-ve	2.80	average <i>r_b</i> (cm)	2.70	average <i>r_b</i> (cm)	20.00	20.00	20.00	20.00	<i>r_b</i> (cm)+ve	0.51	<i>r_b</i> (cm)-ve	1.39	1.39	1.39	1.39	1.90	
<i>d</i> (cm)	1.39	<i>r_b</i> (cm)-ve		average <i>r_b</i> (cm)									average <i>r_b</i> (cm)		average <i>r_b</i> (cm)					1.90	
Time to Equilibrium (min)	20.00	average <i>r_b</i> (cm)																			1.95
Water temp (°C)	20.00	<i>ε_m</i> (cm)+ve	-0.67	<i>ε_m</i> (cm)-ve	-0.68	Tube position (cm)	20.00	<i>ε_m</i> (cm)+ve	20.00	Water temp (°C)	20.00	Tube position (cm)	20.00	<i>ε_m</i> (cm)-ve	-0.38	<i>ε_m</i> (cm)+ve	20.00	Tube position (cm)	20.00	<i>ε_m</i> (cm)-ve	-0.38
Tube position (cm)	80.40	<i>ε_m</i> (cm)-ve		average <i>ε_m</i> (cm)		Time to fill (s)	80.30	<i>ε_m</i> (cm)-ve	80.30	Tube position (cm)	80.30	Time to fill (s)	80.30	average <i>ε_m</i> (cm)	-0.35	<i>ε_m</i> (cm)-ve	80.30	Tube position (cm)	80.30	average <i>ε_m</i> (cm)	-0.35
Time to fill (s)	40.34	average <i>ε_m</i> (cm)				<i>Q</i> (L/s)	1.38	<i>ψ</i> (radian)	0.23	Time to fill (s)	50.30	<i>Q</i> (L/s)	1.38	<i>ψ</i> (radian)	1.32	<i>ψ</i> (radian)	0.23	Time to fill (s)	50.30	<i>Q</i> (L/s)	1.32

Test No. T2/0.508/1.326

	Horizontal position (cm)	<i>r</i> (cm)	Depth reading (mm)	<i>ε</i> (cm)
78	-2.30	-0.91	0.00	78.4
78.7	-1.60	1.06	-0.20	78.5
79.1	-1.20	1.45	-0.24	78.7
79.5	-0.80	1.9	-0.28	79.1
79.9	-0.40	1.37	-0.23	79.5
80.3	0.00	0.78	-0.17	79.9
80.7	0.40	1.5	-0.24	80.3
81.1	0.80	1.95	-0.28	80.7
81.5	1.20	1.4	-0.23	81.1
81.9	1.60	0.18	-0.11	81.5
82.3	2.00	-0.88	0.00	81.9

Test No. T2/0.508/1.106

	<i>z₀</i> (cm)	<i>r_b</i> (cm)+ve	2.00	<i>z₀</i> (cm)	0.51	<i>r_b</i> (cm)+ve	1.80
	<i>d</i> (cm)	<i>r_b</i> (cm)-ve	2.30	<i>d</i> (cm)	1.39	<i>r_b</i> (cm)-ve	1.90
Time to Equilibrium (min)	20.00	average <i>r_b</i> (cm)	2.15	Time to Equilibrium (min)	20.00	average <i>r_b</i> (cm)	1.85
Water temp (°C)	20.00	<i>ε_m</i> (cm)+ve	-0.28	Water temp (°C)	20.00	<i>ε_m</i> (cm)+ve	-0.28
Tube position (cm)	80.30	<i>ε_m</i> (cm)-ve	-0.28	Tube position (cm)	80.30	<i>ε_m</i> (cm)-ve	-0.27
Time to fill (s)	56.63	average <i>ε_m</i> (cm)	-0.28	Time to fill (s)	67.88	average <i>ε_m</i> (cm)	-0.27
<i>Q</i> (L/s)	0.20	<i>ψ</i> (radian)	1.34	<i>Q</i> (L/s)	0.17	<i>ψ</i> (radian)	1.30

Test No. T2/0.508/0.916

z_o (cm)	0.51	r_b (cm)+ve	2.00	ε (cm)	0.00
d (cm)	1.39	r_b (cm)-ve	2.00	d (cm)	-0.19
Time to Equilibrium (min)	20.00	average r_b (cm)	2.00	Time to Equilibrium (min)	20.00
Water temp (°C)	20.00	ε_m (cm)+ve	-0.33	Water temp (°C)	20.00
Tube position (cm)	80.30	ε_m (cm)-ve	-0.32	Tube position (cm)	80.20
Time to fill (s)	81.93	average ε_m (cm)	-0.33	Time to fill (s)	55.45
Q (L/s)	0.14	ψ (radian)	1.32	Q (L/s)	0.21

Test No. T2/0.508/1.354

z_o (cm)	2.00	r_b (cm)+ve	0.51	r_b (cm)-ve	2.10
d (cm)	2.00	d (cm)	1.39	r_b (cm)-ve	2.00
Time to Equilibrium (min)	20.00	average r_b (cm)	20.00	average r_b (cm)	20.05
Water temp (°C)	20.00	ε_m (cm)+ve	20.00	ε_m (cm)+ve	20.27
Tube position (cm)	80.30	ε_m (cm)-ve	80.20	ε_m (cm)-ve	80.22
Time to fill (s)	81.93	average ε_m (cm)	55.45	average ε_m (cm)	55.24
Q (L/s)	0.14	ψ (radian)	0.21	ψ (radian)	1.33

Horizontal position (cm)	r (cm)	Depth reading (mm)	ε (cm)	Horizontal position (cm)	r (cm)	Depth reading (mm)	ε (cm)
78.3	-2.00	-1.31	0.00	78.2	-2.00	-1.74	0.00
78.7	-1.60	0.6	-0.19	78.6	-1.60	-1.11	-0.06
79.1	-1.20	1.73	-0.30	79	-1.20	-0.57	-0.22
79.5	-0.80	1.95	-0.32	79.4	-0.80	0.64	-0.22
79.9	-0.40	1.61	-0.28	79.8	-0.40	0.3	-0.18
80.3	0.00	0.55	-0.17	80.2	0.00	0.5	-0.19
80.7	0.40	1.89	-0.30	80.6	0.40	0.37	-0.17
81.1	0.80	2.21	-0.33	81	0.80	1.15	-0.24
81.5	1.20	1.92	-0.21	81.4	1.20	1.46	-0.27
81.9	1.60	-0.08	-0.10	81.8	1.60	-0.75	-0.04
82.3	2.00	-1.03	0.00	82.3	2.10	-1.04	0.00

Test No. T2/0.254/1.140

Horizontal position (cm)	<i>r</i> (cm)	Depth reading (mm)	ε (cm)
78	-2.20	-1.27	0.00
78.2	-2.00	0.54	-0.18
78.6	-1.60	3.26	-0.44
79	-1.20	4.73	-0.57
79.4	-0.80	5.7	-0.66
79.8	-0.40	5.19	-0.60
80.2	0.00	3.73	-0.44
80.6	0.40	5.28	-0.58
81	0.80	6.07	-0.65
81.4	1.20	5.81	-0.62
81.8	1.60	3.06	-0.33
82.2	2.00	1.41	-0.15
82.4	2.20	-0.08	0.00

Test No. T2/0.381/0.877

	z_o (cm)	r_b (cm)+ve	z_o (cm)	r_b (cm)+ve
<i>d</i> (cm)	1.39	r_b (cm)-ve	<i>d</i> (cm)	1.39
Time to Equilibrium (min)	20.00	average r_b (cm)	Time to Equilibrium (min)	20.00
Water temp (°C)	20.00	ε_m (cm)+ve	Water temp (°C)	20.00
Tube position (cm)	80.20	ε_m (cm)-ve	Tube position (cm)	80.30
Time to fill (s)	65.87	average ε_m (cm)	Time to fill (s)	85.57
Q (L/s)	0.18	ψ (radian)	Q (L/s)	0.14
				ψ (radian)
				1.38
				ε (cm)
			Horizontal position (cm)	<i>r</i> (cm)
				Depth reading (mm)

Test No. T2/0.127/1.036

Horizontal position (cm)	<i>r</i> (cm)	Depth reading (mm)	ε (cm)	Horizontal position (cm)	<i>r</i> (cm)	Depth reading (mm)	ε (cm)
77.8	-2.50	-1.15	0.00	77.5	-2.80	-1.08	0.00
77.9	-2.40	0.35	-0.15	77.9	-2.40	1.86	-0.29
78.3	-2.00	2.03	-0.31	78.3	-2.00	4.88	-0.59
78.7	-1.60	4.16	-0.51	78.7	-1.60	6.83	-0.78
79.1	-1.20	5.8	-0.66	79.1	-1.20	7.51	-0.85
79.5	-0.80	5.91	-0.67	79.5	-0.80	7.93	-0.89
79.9	-0.40	4.21	-0.49	79.9	-0.40	7.36	-0.83
80.3	0.00	4.05	-0.46	80.3	0.00	5.29	-0.62
80.7	0.40	5.86	-0.63	80.7	0.40	6.22	-0.71
81.1	0.80	6.09	-0.65	81.1	0.80	6.82	-0.77
81.5	1.20	5.1	-0.54	81.5	1.20	5.95	-0.68
81.9	1.60	3.21	-0.34	81.9	1.60	4.8	-0.56
82.3	2.00	0.84	-0.09	82.3	2.00	3.02	-0.38
82.6	2.30	-0.04	0.00	82.7	2.40	-0.76	0.00

Test No. T2/0.127/1.993

z_o (cm)	r_b (cm)+ve	z_o (cm)	r_b (cm)+ve
<i>d</i> (cm)	r_b (cm)-ve	<i>d</i> (cm)	r_b (cm)-ve
Time to Equilibrium (min)	20.00	average r_b (cm)	2.40
Water temp (°C)	20.00	ε_m (cm)+ve	-0.65
Tube position (cm)	80.30	ε_m (cm)-ve	-0.67
Time to fill (s)	72.42	average ε_m (cm)	-0.66
Q (L/s)	0.16	ψ (radian)	1.52
			0.31
			ψ (radian)

Horizontal position (cm)	<i>r</i> (cm)	Time to fill (s)	ε (cm)	Time to Equilibrium (min)	<i>d</i> (cm)	average r_b (cm)
77.5	-2.80	-1.08	0.00	20.00	2.40	2.40
77.9	-2.40	1.86	-0.29			
78.3	-2.00	4.88	-0.59			
78.7	-1.60	6.83	-0.78			
79.1	-1.20	7.51	-0.85			
79.5	-0.80	7.93	-0.89			
79.9	-0.40	7.36	-0.83			
80.3	0.00	5.29	-0.62			
80.7	0.40	6.22	-0.71			
81.1	0.80	6.82	-0.77			
81.5	1.20	5.95	-0.68			
81.9	1.60	4.8	-0.56			
82.3	2.00	3.02	-0.38			
82.6	2.30	-0.76	0.00			

Test No. T2/0.254/1.993

	Horizontal position (cm)	<i>r</i> (cm)	Depth reading (mm)	ε (cm)	
77.5	-2.80	-1.09	0.00	77.8	-2.40
77.9	-2.40	1.09	-0.22	78.2	-2.00
78.3	-2.00	2.83	-0.39	78.6	-1.60
78.7	-1.60	5.31	-0.64	79	-1.20
79.1	-1.20	6.25	-0.73	79.4	-0.80
79.5	-0.80	6.79	-0.78	79.8	-0.40
79.9	-0.40	6.68	-0.77	80.2	0.00
80.3	0.00	6	-0.70	80.6	0.40
80.7	0.40	6.5	-0.75	81	0.80
81.1	0.80	7.41	-0.84	81.4	1.20
81.5	1.20	7.3	-0.82	81.8	1.60
81.9	1.60	5.23	-0.62	82.2	2.00
82.3	2.00	2.29	-0.32	82.6	2.40
82.7	2.40	0.24	-0.11		-0.08
82.9	2.60	-0.9	0.00		0.00

Test No. T2/0.127/1.401

	Test No. T2/0.127/1.401															
z_0 (cm)	r_b (cm)+ve	2.60														
<i>d</i> (cm)	r_b (cm)-ve	2.80														
Time to Equilibrium (min)	average r_b (cm)	2.70														
Water temp (°C)	ε_m (cm)+ve	-0.84														
Tube position (cm)	ε_m (cm)-ve	-0.78														
Time to fill (s)	average ε_m (cm)	-0.81														
Q (L/s)	ψ (radian)	1.48														
	Horizontal position (cm)	<i>r</i> (cm)														
		Depth reading (mm)														
		ε (cm)														
	z_0 (cm)	r_b (cm)	average r_b (cm)	d (cm)	Time to Equilibrium (min)	Water temp (°C)	Tube position (cm)	Time to fill (s)	Q (L/s)	ε_m (cm)+ve	ε_m (cm)-ve	average r_b (cm)	ε_m (cm)+ve	ε_m (cm)-ve	average ε_m (cm)	ψ (radian)

Test No. T2/0.127/1.993

Horizontal position (cm)	<i>r</i> (cm)	Depth reading (mm)	ε (cm)
77.3	-3.00	-0.97	0.00
77.5	-2.80	0.76	-0.25
77.9	-2.40	3.12	-0.47
78.3	-2.00	5.24	-0.67
78.7	-1.60	7.57	-0.89
79.1	-1.20	8.88	-1.01
79.5	-0.80	9.01	-1.01
79.9	-0.40	9.59	-1.06
80.3	0.00	7.73	-0.86
80.7	0.40	9.11	-0.98
81.1	0.80	8.66	-0.92
81.5	1.20	7.69	-0.81
81.9	1.60	7.28	-0.76
82.3	2.00	3.64	-0.38
82.7	2.40	2.56	-0.26
83.1	2.80	0	0.00

Test No. T2/0.127/1.464

	<i>r_b</i> (cm)+ve	<i>z₀</i> (cm)	<i>r_b</i> (cm)-ve	<i>d</i> (cm)	<i>d</i> (cm)	<i>r_b</i> (cm)-ve	<i>r_b</i> (cm)+ve
Time to Equilibrium (min)	20.00	average <i>r_b</i> (cm)	2.90			20.00	average <i>r_b</i> (cm)
Water temp (°C)	20.00	ε_m (cm)+ve	-0.98			20.00	ε_m (cm)+ve
Tube position (cm)	80.30	ε_m (cm)-ve	-1.06			80.20	ε_m (cm)-ve
Time to fill (s)	37.66	average ε_m (cm)	-1.02			51.28	average ε_m (cm)
<i>Q</i> (L/s)	0.31	ψ (radian)	1.53			0.23	ψ (radian)
							1.52
							ε (cm)
							Depth reading (mm)
						<i>r</i> (cm)	
					Horizontal position (cm)		

Test No. T2/0.635/1.528

Horizontal position (cm)	<i>r</i> (cm)	Depth reading (mm)	ε (cm)
78.3	-2.00	-1.06	0.00
78.7	-1.60	-0.09	-0.09
79.1	-1.20	2.29	-0.31
79.5	-0.80	2.71	-0.35
79.9	-0.40	1.66	-0.23
80.3	0.00	0.56	-0.11
80.7	0.40	3.02	-0.35
81.1	0.80	3.41	-0.37
81.5	1.20	1.82	-0.20
81.9	1.60	0.56	-0.07
82.3	2.00	-0.02	0.00

Test No. T2/0.254/1

	r_b (cm)+ve	z_0 (cm)	r_b (cm)-ve	d (cm)	d (cm)	r_b (cm)-ve	r_b (cm)+ve
Time to Equilibrium (min)	20.00	average r_b (cm)	2.00	Time to Equilibrium (min)	21.00	average r_b (cm)	2.00
Water temp (°C)	20.00	ε_m (cm)+ve	-0.37	Water temp (°C)	20.00	ε_m (cm)+ve	-0.42
Tube position (cm)	80.30	ε_m (cm)-ve	-0.35	Tube position (cm)	80.20	ε_m (cm)-ve	-0.44
Time to fill (s)	49.14	average ε_m (cm)	-0.36	Time to fill (s)	94.19	average ε_m (cm)	-0.43
Q (L/s)	0.24	ψ (radian)	1.26	Q (L/s)	0.12	ψ (radian)	1.44
				Horizontal position (cm)	<i>r</i> (cm)	Depth reading (mm)	ε (cm)

Test No. T2/0.254/1.002

	Horizontal position (cm)	<i>r</i> (cm)	Depth reading (mm)	<i>ε</i> (cm)
78.1	-2.10	-1.09	0.00	78.8
78.6	-1.60	1.52	-0.26	79
79	-1.20	3.02	-0.41	79.3
79.4	-0.80	4.18	-0.53	79.6
79.8	-0.40	3.49	-0.46	79.9
80.2	0.00	2.91	-0.40	80.2
80.6	0.40	3.7	-0.48	80.5
81	0.80	3.58	-0.47	80.8
81.4	1.20	3.51	-0.46	81.1
81.8	1.60	1.8	-0.29	81.4
82.2	2.00	-1.1	0.00	81.7

Test No. T2/0.635/1.092

	<i>z₀</i> (cm)	<i>r_b</i> (cm)+ve	2.00	<i>z₀</i> (cm)	0.64	<i>r_b</i> (cm)+ve	1.70
	<i>d</i> (cm)	<i>r_b</i> (cm)-ve	2.10	<i>d</i> (cm)	1.39	<i>r_b</i> (cm)-ve	1.40
Time to Equilibrium (min)	21.00	average <i>r_b</i> (cm)	2.05	Time to Equilibrium (min)	21.00	average <i>r_b</i> (cm)	1.55
Water temp (°C)	20.00	<i>ε_m</i> (cm)+ve	-0.48	Water temp (°C)	20.00	<i>ε_m</i> (cm)+ve	-0.15
Tube position (cm)	80.20	<i>ε_m</i> (cm)-ve	-0.53	Tube position (cm)	80.20	<i>ε_m</i> (cm)-ve	-0.14
Time to fill (s)	74.95	average <i>ε_m</i> (cm)	-0.50	Time to fill (s)	68.73	average <i>ε_m</i> (cm)	-0.14
<i>Q</i> (L/s)	0.15	<i>ψ</i> (radian)	1.45	<i>Q</i> (L/s)	0.17	<i>ψ</i> (radian)	1.18
				Horizontal position (cm)	<i>r</i> (cm)	Depth reading (mm)	<i>ε</i> (cm)

Test No. T2/0.635/1.447

Horizontal position (cm)	<i>r</i> (cm)	Depth reading (mm)	ε (cm)
78	-2.30	-1.5	0.00
78.3	-2.00	0.4	-0.18
78.7	-1.60	1.27	-0.26
79.1	-1.20	2.57	-0.39
79.5	-0.80	3.04	-0.42
79.9	-0.40	2.21	-0.33
80.3	0.00	0.79	-0.18
80.7	0.40	2.66	-0.36
81.1	0.80	4.17	-0.51
81.5	1.20	3.04	-0.39
81.9	1.60	1.22	-0.20
82.3	2.00	0.41	-0.11
82.5	2.20	-0.62	0.00

Test No. T2/0.254/1.548

	z_0 (cm)	r_b (cm)+ve	z_0 (cm)	r_b (cm)+ve
<i>d</i> (cm)	0.64	r_b (cm)-ve	2.20	2.60
Time to Equilibrium (min)	1.39	r_b (cm)-ve	2.30	2.20
Time to Equilibrium (min)	21.00	average r_b (cm)	2.25	2.40
Water temp (°C)	20.00	ε_m (cm)+ve	-0.51	21.00
Tube position (cm)	80.30	ε_m (cm)-ve	-0.42	average r_b (cm)
Time to fill (s)	51.88	average ε_m (cm)	-0.47	20.00
Q (L/s)	0.22	ψ (radian)	1.30	ε_m (cm)+ve
	z_0 (cm)	d (cm)	r (cm)	ε (cm)
	z_0 (cm)	d (cm)	Depth reading (mm)	Depth reading (mm)
	z_0 (cm)	d (cm)	r (cm)	ε (cm)
	77.6		-2.20	-1.07
	77.8		-2.00	-0.54
	78.2		-1.60	1.47
	78.6		-1.20	3.73
	79.4		-0.80	5.75
	79.8		-0.40	6.36
	80.2		0.00	5.32
	80.6		0.40	5.45
	80.6		0.80	5.76
	81		1.20	6.81
	81.4		1.60	5.61
	81.8		2.00	3.36
	82.2		2.40	-0.35
	82.4		2.60	-0.24
			0	0.00

Test No. T2/0.254/1.296

Horizontal position (cm)	<i>r</i> (cm)	Depth reading (mm)	ε (cm)
78	-2.20	-0.76	0.00
78.2	-2.00	-0.72	0.00
78.6	-1.60	2.37	-0.30
79	-1.20	5.5	-0.61
79.4	-0.80	6.28	-0.68
79.8	-0.40	5.89	-0.64
80.2	0.00	2.8	-0.32
80.6	0.40	5.23	-0.56
81	0.80	6.19	-0.65
81.4	1.20	5.79	-0.61
81.8	1.60	3.13	-0.33
82.2	2.00	1.52	-0.17
82.5	2.30	-0.11	0.00

Test No. T2/0.127/1.216

	z_o (cm)	r_b (cm)+ve	z_o (cm)	r_b (cm)+ve
<i>d</i> (cm)	0.25	r_b (cm)-ve	2.30	0.13
Time to Equilibrium (min)	1.39	average r_b (cm)	2.20	r_b (cm)-ve
Water temp (°C)	21.00	average r_b (cm)	2.25	average r_b (cm)
Tube position (cm)	20.00	z_m (cm)+ve	21.00	2.20
Time to fill (s)	80.20	ε_m (cm)-ve	Water temp (°C)	20.00
Q (L/s)	57.94	average ε_m (cm)	Tube position (cm)	ε_m (cm)+ve
	0.20	ψ (radian)	Time to fill (s)	ε_m (cm)-ve
		1.46	Q (L/s)	average ε_m (cm)
				-0.54
				0.19
				ψ (radian)
			Horizontal position (cm)	<i>r</i> (cm)
				Depth reading (mm)
				ε (cm)

Test No. T2/0.381/1.736

Horizontal position (cm)	<i>r</i> (cm)	Depth reading (mm)	ε (cm)
77.8	-2.50	-1.89	0.00
77.9	-2.40	-1.21	-0.06
78.3	-2.00	0.28	-0.20
78.7	-1.60	3.01	-0.46
79.1	-1.20	4.16	-0.56
79.5	-0.80	5.58	-0.69
79.9	-0.40	4.98	-0.61
80.3	0.00	4.01	-0.50
80.7	0.40	5.18	-0.60
81.1	0.80	5.67	-0.64
81.5	1.20	4.36	-0.49
81.9	1.60	3.21	-0.37
82.3	2.00	0.36	-0.07
82.7	2.40	-0.16	0.00

Test No. T2/0.381/1.216

	Test No. T2/0.381/1.216
z_o (cm)	0.38
d (cm)	1.39
Time to Equilibrium (min)	21.00
Water temp (°C)	20.00
Tube position (cm)	80.30
Time to fill (s)	43.25
Q (L/s)	0.27
r_b (cm)+ve	2.40
r_b (cm)-ve	2.50
average r_b (cm)	2.45
ε_m (cm)+ve	-0.64
ε_m (cm)-ve	-0.69
average ε_m (cm)	-0.66
Q (L/s)	1.42
z_o (cm)	0.38
d (cm)	2.00
Time to Equilibrium (min)	21.00
Water temp (°C)	20.00
Tube position (cm)	80.20
Time to fill (s)	61.74
Q (L/s)	0.19
r_b (cm)+ve	1.39
r_b (cm)-ve	1.39
average r_b (cm)	2.00
ε_m (cm)+ve	-0.34
ε_m (cm)-ve	-0.38
average ε_m (cm)	-0.36
ψ (radian)	1.38

Test No. T2/0.381/1.051

Horizontal position (cm)	<i>r</i> (cm)	Depth reading (mm)	ε (cm)
78.3	-1.90	-0.06	0.00
78.6	-1.60	0.99	-0.10
79	-1.20	3.39	-0.34
79.4	-0.80	4.61	-0.47
79.8	-0.40	4.36	-0.44
80.2	0.00	2.75	-0.28
80.6	0.40	3.93	-0.40
81	0.80	5.09	-0.51
81.4	1.20	2.66	-0.27
81.8	1.60	2.13	-0.21
82.1	1.90	0	0.00

Test No. T2/0.381/1.58

		Test No. T2/0.381/1.58	
z_0 (cm)	0.38	r_b (cm)+ve	1.90
<i>d</i> (cm)	1.39	r_b (cm)-ve	1.90
Time to Equilibrium (min)	21.00	average r_b (cm)	1.90
Water temp (°C)	20.00	ε_m (cm)+ve	-0.51
Tube position (cm)	80.20	ε_m (cm)-ve	-0.47
Time to fill (s)	71.45	average ε_m (cm)	-0.49
<i>Q</i> (L/s)	0.16	ψ (radian)	1.37
		z_0 (cm)	0.38
		<i>d</i> (cm)	1.39
		Time to Equilibrium (min)	21.00
		Water temp (°C)	20.00
		Tube position (cm)	80.20
		Time to fill (s)	47.52
		<i>Q</i> (L/s)	0.24
		ψ (radian)	1.39
		r_b (cm)+ve	2.20
		r_b (cm)-ve	2.00
		average r_b (cm)	2.10
		ε_m (cm)+ve	-0.59
		ε_m (cm)-ve	-0.47
		average ε_m (cm)	-0.53
		ψ (radian)	1.39
		ε (cm)	0.00

Test No. T1/0.254/3.543**Test No. T1/0.127/3.62**

	z_o (cm)	r_b (cm)+ve	z_o (cm)	r_b (cm)+ve	d (cm)	d (cm)	r_b (cm)-ve	r_b (cm)-ve	ϵ_m (cm)+ve	ϵ_m (cm)+ve	ϵ_m (cm)-ve	ϵ_m (cm)-ve	average r_b (cm)	Time to Equilibrium (min)	Time to Equilibrium (min)	r (cm)	Depth reading (mm)	ϵ (cm)	
d (cm)	0.97	r_b (cm)-ve		2.50				0.97								2.40			
Time to Equilibrium (min)	21.00	average r_b (cm)		2.40				21.00								2.40			
Water temp (°C)	15.00	ϵ_m (cm)+ve		-0.69				12.00								-0.83			
Tube position (cm)	80.40	ϵ_m (cm)-ve		-0.57				80.40								-0.87			
Time to fill (s)	43.71	average ϵ_m (cm)		-0.63				43.49								-0.85			
Q (L/s)	0.26	ψ (radian)		1.47				0.27								1.52			
Horizontal position (cm)	r (cm)	Depth reading (mm)	ϵ (cm)	Horizontal position (cm)	r (cm)	Depth reading (mm)	ϵ (cm)	Horizontal position (cm)	r (cm)	Depth reading (mm)	ϵ (cm)	Horizontal position (cm)	r (cm)	Depth reading (mm)	ϵ (cm)	Horizontal position (cm)	r (cm)	Depth reading (mm)	ϵ (cm)
77.9	-2.50	0.03	0.00	77.9				77.9								-2.50		-1.09	0.00
78	-2.40	0.86	-0.08	78				78								-2.40		0.31	-0.14
78.3	-2.10	3.16	-0.31	78.3				78.3								-2.10		2.21	-0.32
78.6	-1.80	4.39	-0.44	78.6				78.6								-1.80		4.06	-0.50
78.9	-1.50	5.68	-0.57	78.9				78.9								-1.50		6.03	-0.69
79.2	-1.20	6.75	-0.67	79.2				79.2								-1.20		7.09	-0.79
79.5	-0.90	6.87	-0.69	79.5				79.5								-0.90		7.97	-0.87
79.8	-0.60	6.12	-0.61	79.8				79.8								-0.60		7.87	-0.85
80.1	-0.30	5.39	-0.54	80.1				80.1								-0.30		7.39	-0.80
80.4	0.00	5.54	-0.55	80.4				80.4								0.00		7.13	-0.77
80.7	0.30	5.7	-0.57	80.7				80.7								0.30		7.86	-0.83
81	0.60	6.66	-0.66	81				81								0.60		7.92	-0.83
81.3	0.90	6.54	-0.65	81.3				81.3								0.90		7.25	-0.76
81.6	1.20	5.25	-0.52	81.6				81.6								1.20		5.49	-0.57
81.9	1.50	3.77	-0.38	81.9				81.9								1.50		4.2	-0.44
82.2	1.80	2.54	-0.25	82.2				82.2								1.80		1.97	-0.21
82.5	2.10	0.74	-0.07	82.5				82.5								2.10		1.38	-0.14
82.7	2.30	0	0.00	82.7				82.7								2.30		0	0.00

Test No. T1/0.508/5.560

Horizontal position (cm)	<i>r</i> (cm)	Depth reading (mm)	ε (cm)
75.8	-2.50	1.28	0.00
75.9	-2.40	1.58	-0.03
76.2	-2.10	2.7	-0.15
76.5	-1.80	4.1	-0.29
76.8	-1.50	5.55	-0.43
77.1	-1.20	6.58	-0.54
77.4	-0.90	7.26	-0.61
77.7	-0.60	7.96	-0.68
78	-0.30	8.12	-0.70
78.3	0.00	6.6	-0.55
78.6	0.30	7.84	-0.68
78.9	0.60	7.7	-0.67
79.2	0.90	6.85	-0.58
79.5	1.20	6.67	-0.57
79.8	1.50	5.8	-0.48
80.1	1.80	3.92	-0.30
80.4	2.10	2	-0.11
80.8	2.50	0.9	0.00

Test No. T1/0.254/5.159

	<i>r_b</i> (cm)+ve	<i>z₀</i> (cm)	0.25	<i>r_b</i> (cm)+ve	2.80
	<i>r_b</i> (cm)-ve	<i>d</i> (cm)	0.97	<i>r_b</i> (cm)-ve	2.80
	average <i>r_b</i> (cm)	<i>d</i> (cm)	10.00	average <i>r_b</i> (cm)	2.80
Time to Equilibrium (min)	10.00				
Water temp (°C)	20.00	ε_m (cm)+ve	-0.68	ε_m (cm)+ve	-0.86
Tube position (cm)	78.30	ε_m (cm)-ve	-0.70	ε_m (cm)-ve	-0.87
Time to fill (s)	28.32	average ε_m (cm)	-0.69	average ε_m (cm)	-0.87
<i>Q</i> (L/s)	0.41	ψ (radian)	1.37	ψ (radian)	1.48
		Horizontal position (cm)	<i>r</i> (cm)	Horizontal position (cm)	<i>r</i> (cm)
		75.5		75.5	
				-2.80	0
				-2.70	0.36
				-2.40	1.55
				-2.10	3.39
				-1.80	4.91
				-1.50	6.74
				-1.20	7.3
				-0.90	8.07
				-0.60	8.61
				-0.30	7.22
				0.00	6.94
				0.30	7.28
				0.60	8.53
				0.90	8.35
				1.20	8.02
				1.50	6.91
				1.80	5.19
				2.10	3.97
				2.40	1.68
				2.70	0.84
				2.80	-0.17
				81.1	0.00
				81.1	

Test No. T1/0.508/5.2

	Horizontal position (cm)	<i>r</i> (cm)	Depth reading (mm)	ε (cm)
73.6	-2.60	0.51	0.00	
73.8	-2.40	1.54	-0.10	75.5
74.1	-2.10	2.91	-0.24	75.6
74.4	-1.80	4.55	-0.40	75.9
74.7	-1.50	5.84	-0.53	76.2
75	-1.20	6.54	-0.60	76.5
75.3	-0.90	6.74	-0.62	76.8
75.6	-0.60	6.88	-0.63	77.1
75.9	-0.30	6.26	-0.57	77.4
76.2	0.00	5.32	-0.47	77.7
76.5	0.30	6.12	-0.55	78
76.8	0.60	6.22	-0.56	78.3
77.1	0.90	6.29	-0.57	78.6
77.4	1.20	5.5	-0.49	78.9
77.7	1.50	3.84	-0.32	79.2
78	1.80	2.96	-0.23	79.5
78.3	2.10	1.8	-0.11	79.8
78.7	2.50	0.69	0.00	80.1

Test No. T1/0.508/6.283

	Horizontal position (cm)	<i>r</i> (cm)	Depth reading (mm)	ε (cm)
z ₀ (cm)	0.51	<i>r_b</i> (cm)+ve	2.50	z ₀ (cm)+ve
<i>d</i> (cm)	0.97	<i>r_b</i> (cm)-ve	2.60	<i>d</i> (cm)
Time to Equilibrium (min)	10.00	average <i>r_b</i> (cm)	2.55	Time to Equilibrium (min)
Water temp (°C)	20.00	ε_m (cm)+ve	-0.57	Water temp (°C)
Tube position (cm)	76.20	ε_m (cm)-ve	-0.63	Tube position (cm)
Time to fill (s)	30.28	average ε_m (cm)	-0.60	Time to fill (s)
<i>Q</i> (L/s)	0.38	ψ (radian)	1.37	<i>Q</i> (L/s)
	Horizontal position (cm)	<i>r</i> (cm)	Depth reading (mm)	ε (cm)
z ₀ (cm)	0.51	<i>r_b</i> (cm)+ve	2.50	z ₀ (cm)+ve
<i>d</i> (cm)	0.97	<i>r_b</i> (cm)-ve	2.60	<i>d</i> (cm)-ve
Time to Equilibrium (min)	10.00	average <i>r_b</i> (cm)	2.55	average <i>r_b</i> (cm)
Water temp (°C)	20.00	ε_m (cm)+ve	-0.57	ε_m (cm)+ve
Tube position (cm)	76.30	ε_m (cm)-ve	-0.63	ε_m (cm)-ve
Time to fill (s)	30.28	average ε_m (cm)	-0.60	average ε_m (cm)
<i>Q</i> (L/s)	0.38	ψ (radian)	1.37	ψ (radian)

Test No. T1/0.254/6.299

Horizontal position (cm)	<i>r</i> (cm)	Depth reading (mm)	ε (cm)
75.3	-3.00	-0.17	0.00
75.6	-2.70	2.04	-0.22
75.9	-2.40	3.81	-0.39
76.2	-2.10	5.36	-0.54
76.5	-1.80	7.16	-0.72
76.8	-1.50	7.8	-0.78
77.1	-1.20	8.92	-0.89
77.4	-0.90	9.26	-0.92
77.7	-0.60	9	-0.89
78	-0.30	8.56	-0.85
78.3	0.00	7.3	-0.72
78.6	0.30	8.56	-0.84
78.9	0.60	8.9	-0.87
79.2	0.90	8.92	-0.87
79.5	1.20	8.69	-0.84
79.8	1.50	7.18	-0.69
80.1	1.80	5.75	-0.54
80.4	2.10	3.67	-0.33
80.7	2.40	1.87	-0.15
81	2.70	0.83	-0.04
81.1	2.80	0.43	0.00

Test No. T1/0.254/5.481

	z_0 (cm)	r_b (cm)+ve	z_0 (cm)	r_b (cm)+ve
	<i>d</i> (cm)	r_b (cm)-ve	<i>d</i> (cm)	r_b (cm)-ve
Time to Equilibrium (min)	10.00	average r_b (cm)	2.90	average r_b (cm)
Water temp (°C)	22.00	ε_m (cm)+ve	-0.87	ε_m (cm)+ve
Tube position (cm)	78.30	ε_m (cm)-ve	-0.92	ε_m (cm)-ve
Time to fill (s)	25.00	average ε_m (cm)	-0.90	average ε_m (cm)
<i>Q</i> (L/s)	0.46	ψ (radian)	1.48	ψ (radian)

	Horizontal position (cm)	<i>r</i> (cm)	Horizontal position (cm)	<i>r</i> (cm)	Depth reading (mm)	ε (cm)
	75.4	75.4	75.4	75.4	-2.90	1.07

Test No. T2/0.635/2.014

	Horizontal position (cm)	<i>r</i> (cm)	Depth reading (mm)	<i>ε</i> (cm)	
7.8	1.80	-0.84	0.00	77.7	
78.3	2.10	1.06	0.18	77.8	-2.50
78.7	2.50	2.16	0.05	78.2	-2.40
79.1	2.90	3.17	-0.07	78.6	-2.00
79.5	3.30	3.77	-0.15	79	-1.60
79.9	3.70	2.19	-0.01	79.4	-1.20
80.3	4.10	1.08	0.09	79.8	-0.80
80.7	4.50	1.88	-0.01	80.2	-0.40
81.1	4.90	3.62	-0.20	80.6	0.00
81.5	5.30	3.05	-0.16	81	0.40
81.9	5.70	0.91	0.03	81.4	0.80
82.3	6.10	0.17	0.09	81.8	1.20
82.5	6.30	-0.8	0.18	82.2	1.60
				82.4	3.14
					-0.33
					-0.61
					-0.67
					-0.61
					-0.11
					-0.08
					-0.03
					0.00

Test No. T2/0.127/1.128

	<i>z</i> ₀ (cm)	<i>r_b</i> (cm)+ve	2.20	<i>z</i> ₀ (cm)	0.13	<i>r_b</i> (cm)+ve	2.20
	<i>d</i> (cm)	<i>r_b</i> (cm)-ve	2.30	<i>d</i> (cm)	1.39	<i>r_b</i> (cm)-ve	2.50
	Time to Equilibrium (min)	20.00	average <i>r_b</i> (cm)	2.25	Time to Equilibrium (min)	21.00	average <i>r_b</i> (cm)
Water temp (°C)	20.00	<i>ε_m</i> (cm)+ve	-0.44	Water temp (°C)	20.00	<i>ε_m</i> (cm)+ve	-0.67
Tube position (cm)	80.30	<i>ε_m</i> (cm)-ve	-0.46	Tube position (cm)	80.20	<i>ε_m</i> (cm)-ve	-0.75
Time to fill (s)	37.27	average <i>ε_m</i> (cm)	-0.45	Time to fill (s)	66.52	average <i>ε_m</i> (cm)	-0.71
<i>Q</i> (L/s)	0.31	ψ (radian)	1.30	<i>Q</i> (L/s)	0.17	ψ (radian)	1.52
				Horizontal position (cm)	<i>r</i> (cm)	Depth reading (mm)	<i>ε</i> (cm)

Test No. T2/0.254/1.126

	Horizontal position (cm)	<i>r</i> (cm)	Depth reading (mm)	ε (cm)
77.9	-2.30	-1.48	0.00	
78.2	-2.00	-0.1	-0.13	77.9
78.6	-1.60	1.69	-0.29	78.3
79	-1.20	2.95	-0.41	78.7
79.4	-0.80	4.48	-0.55	79.1
79.8	-0.40	4.03	-0.49	79.5
80.2	0.00	3.09	-0.38	79.9
80.6	0.40	4.86	-0.54	80.3
81	0.80	5.65	-0.61	80.7
81.4	1.20	4.81	-0.51	81.1
81.8	1.60	2.59	-0.28	81.5
82.2	2.00	1.03	-0.11	81.9
82.6	2.40	0.08	0.00	82.3

Test No. T2/0.254/1.965

	Horizontal position (cm)	<i>r</i> (cm)	Depth reading (mm)	ε (cm)	Horizontal position (cm)	<i>r</i> (cm)	Depth reading (mm)	ε (cm)
<i>z₀</i> (cm)	0.25	<i>r_b</i> (cm)+ve	2.40		<i>z₀</i> (cm)	0.25	<i>r_b</i> (cm)+ve	2.60
<i>d</i> (cm)	1.39	<i>r_b</i> (cm)-ve	2.30		<i>d</i> (cm)	1.39	<i>r_b</i> (cm)-ve	2.70
Time to Equilibrium (min)	20.00	average <i>r_b</i> (cm)	2.35		Time to Equilibrium (min)	20.00	average <i>r_b</i> (cm)	2.65
Water temp (°C)	20.00	ε_m (cm)+ve	-0.61		Water temp (°C)	20.00	ε_m (cm)+ve	-0.69
Tube position (cm)	80.20	ε_m (cm)-ve	-0.55		Tube position (cm)	80.30	ε_m (cm)-ve	-0.88
Time to fill (s)	66.68	average ε_m (cm)	-0.58		Time to fill (s)	38.19	average ε_m (cm)	-0.79
<i>Q</i> (L/s)	0.17	ψ (radian)	1.46		<i>Q</i> (L/s)	0.30	ψ (radian)	1.48

Test No. T2/0.254/1.365

	z_0 (cm)	d (cm)	Time to Equilibrium (min)	Water temp (°C)	Tube position (cm)	Time to fill (s)	Q (L/s)	r_b (cm)+ve	r_b (cm)-ve	average r_b (cm)	ε_m (cm)+ve	ε_m (cm)-ve	average ε_m (cm)	ψ (radian)	r_b (cm)+ve	r_b (cm)-ve	average r_b (cm)	ε_m (cm)+ve	ε_m (cm)-ve	average ε_m (cm)	ψ (radian)
77.8								-2.40	-2.40	-2.40	-0.56	-0.56	-0.56		2.20	2.20	2.20	0.00	0.00	0.00	
78.2								-2.00	-2.00	-2.00	0.22	0.22	0.22		2.40	2.40	2.40	-0.08	-0.08	-0.08	
78.6								-1.60	-1.60	-1.60	2.82	2.82	2.82		2.30	2.30	2.30	-0.34	-0.34	-0.34	
79								-1.20	-1.20	-1.20	4.76	4.76	4.76		-0.65	-0.65	-0.65	-0.63	-0.63	-0.63	
79.4								-0.80	-0.80	-0.80	5.21	5.21	5.21		-0.53	-0.53	-0.53	-0.58	-0.58	-0.58	
79.8								-0.40	-0.40	-0.40	5.73	5.73	5.73		-0.63	-0.63	-0.63	-0.63	-0.63	-0.63	
80.2								0.00	0.00	0.00	3.97	3.97	3.97		-0.46	-0.46	-0.46	-0.46	-0.46	-0.46	
80.6								0.40	0.40	0.40	4.88	4.88	4.88		-0.55	-0.55	-0.55	-0.55	-0.55	-0.55	
81								0.80	0.80	0.80	5.86	5.86	5.86		-0.65	-0.65	-0.65	-0.65	-0.65	-0.65	
81.4								1.20	1.20	1.20	5.43	5.43	5.43		-0.61	-0.61	-0.61	-0.61	-0.61	-0.61	
81.8								1.60	1.60	1.60	3.8	3.8	3.8		-0.44	-0.44	-0.44	-0.44	-0.44	-0.44	
82.2								2.00	2.00	2.00	1.74	1.74	1.74		-0.24	-0.24	-0.24	-0.24	-0.24	-0.24	
82.4								2.20	2.20	2.20	-0.64	-0.64	-0.64		0.00	0.00	0.00	0.00	0.00	0.00	

APPENDIX B
Explanation of the Derived Equations

The following provides explanations of the derived theory on page 70-75. Applied shear stress on a point horizontal plane equivalent to that at point A

$$\tau_c = K''(\varphi) \rho \sqrt{\frac{v U_0^3 d^6}{r_{t1}^7}}$$

Eq. 4.37 on page 70

Threshold shear stress of the sediment

$$\tau_{*c} = 0.5 \tan \varphi ; \text{ when } D_* < 0.3$$

Eq. 2.19 on page 17

$$\text{where, } \tau_{*c} = \frac{\tau_c}{(\rho_s - \rho) D g}$$

$$\text{or, } \tau_c = (\rho_s - \rho) D g \times 0.5 \tan \varphi$$

putting the above value of τ_c in Eq. 4.37, we get

$$K''(\varphi) \rho \sqrt{\frac{v U_0^3 d^6}{r_{t1}^7}} = (\rho_s - \rho) D g \times 0.5 \tan \varphi$$

Eq. 2.38 on page 71

Multiplying both side by $d^{1/2}$

$$K''(\varphi) \rho \sqrt{\frac{v U_0^3 d^7}{r_{t1}^7}} = (\rho_s - \rho) D g \times (0.5 \tan \varphi) d^{1/2}$$

$$\text{or, } K''(\varphi) \frac{\sqrt{v U_0^3}}{\left(\frac{\rho_s - \rho}{\rho} \right) D g \times (0.5 \tan \varphi) d^{1/2}} = \left(\frac{r_{t1}}{d} \right)^{7/2}$$

$$\text{or, } \frac{K''(\varphi)}{(0.5 \tan \varphi) \left(\frac{\rho_s - \rho}{\rho} \right) D g} \sqrt{\frac{v}{U_0 d}} = \left(\frac{r_{t1}}{d} \right)^{7/2}$$

$$\text{or, } \frac{r_{tl}}{d} = \left[\frac{K''(\varphi)}{(0.5 \tan \varphi)} \frac{U_0^2}{\left(\frac{\rho_s - \rho}{\rho} \right) Dg} \sqrt{\frac{v}{U_0 d}} \right]^{2/7}$$

$$\text{or, } \frac{r_{tl}}{d} = [K''(\varphi)]^{2/7} \left[\frac{F_0^4}{(0.5 \tan \varphi)^2 R_0} \right]^{1/7}$$

Using Eq. 4.24 on page 67 we get

$$\frac{r_t}{d} = C_1 + [K''(\varphi)]^{2/7} \left[\frac{F_0^4}{(0.5 \tan \varphi)^2 R_0} \right]^{1/7}$$

Eq. 4.40 on page 71

Again when $0.3 < D_* < 19$

$$\tau_{*c} = 0.25 D_*^{-0.6} \tan \varphi$$

Eq. 2.20 on page 17

Using Eq. 4.37 and 2.20, we get

$$K''(\varphi) \rho \sqrt{\frac{v U_0^3 d^6}{r_{tl}^7}} = (\rho_s - \rho) Dg \times 0.25 D_*^{-0.6} \tan \varphi$$

$$\text{or, } K''(\varphi) \rho \sqrt{\frac{v U_0^3 d^7}{r_{tl}^7}} = (0.25 \tan \varphi) \times d^{1/2} (\rho_s - \rho) Dg \left[D \left\{ \frac{(\rho_s - \rho) g}{\rho v^2} \right\}^{1/3} \right]^{-0.6}$$

$$\text{or, } \frac{K''(\varphi)}{(0.25 \tan \varphi)} \frac{U_0^2}{\left(\frac{\rho_s - \rho}{\rho} \right) Dg} \left[D \left\{ \frac{(\rho_s - \rho) g}{\rho v^2} \right\}^{1/3} \right]^{0.6} \sqrt{\frac{v}{U_0 d}} = \left(\frac{r_{tl}}{d} \right)^{7/2}$$

$$\text{or, } \frac{K''(\varphi)}{(0.25 \tan \varphi)} \frac{U_0^2}{\left(\frac{\rho_s - \rho}{\rho} \right) Dg} \left[\frac{D^{0.4}}{v^{0.4}} \left\{ \frac{(\rho_s - \rho) Dg}{\rho} \right\}^{0.2} \right] \sqrt{\frac{v}{U_0 d}} = \left(\frac{r_{tl}}{d} \right)^{7/2}$$

$$\text{or, } \frac{K''(\varphi)}{(0.25 \tan \varphi)} \frac{U_0^{1.6}}{\left\{ \left(\frac{\rho_s - \rho}{\rho} \right) Dg \right\}^{0.8}} \left[\frac{U_0^{0.4} D^{0.4}}{v^{0.4}} \right] \sqrt{\frac{v}{U_0 d}} = \left(\frac{r_{tl}}{d} \right)^{7/2}$$

$$\text{or, } \frac{K''(\varphi)}{(0.25 \tan \varphi)} \frac{F_0^{1.6} R_s^{0.4}}{R_0^{1/2}} = \left(\frac{r_{t1}}{d} \right)^{7/2}$$

$$\text{or, } \frac{r_{t1}}{d} = \left[\frac{K''(\varphi)}{(0.25 \tan \varphi)} \frac{F_0^{1.6} R_s^{0.4}}{R_0^{1/2}} \right]^{2/7}$$

$$\text{or, } \frac{r_{t1}}{d} = [K''(\varphi)]^{2/7} \left[\frac{F_0^{3.2} R_s^{0.8}}{(0.25 \tan \varphi)^2 R_0} \right]^{1/7}$$

Using Eq. 4.24,

$$\frac{r_t}{d} = C_1 + [K''(\varphi)]^{2/7} \left[\frac{F_0^{3.2} R_s^{0.8}}{(0.25 \tan \varphi)^2 R_0} \right]^{1/7}$$

Eq. 4.41 on page 72

when $19 < D_* < 50$

$$\tau_{*c} = 0.013 D_*^{0.4} \tan \varphi$$

Eq. 2.21 on page 17

Now from Eq. 4.37 and 2.21, we get

$$K''(\varphi) \rho \sqrt{\frac{v U_0^3 d^6}{r_{t1}^7}} = (\rho_s - \rho) D g \times 0.013 D_*^{0.4} \tan \varphi$$

$$\text{or, } K''(\varphi) \rho \sqrt{\frac{v U_0^3 d^7}{r_{t1}^7}} = (0.013 \tan \varphi) \times d^{1/2} (\rho_s - \rho) D g \times D_*^{0.4}$$

$$\text{or, } \frac{K''(\varphi)}{(0.013 \tan \varphi)} \frac{1}{\left(\frac{\rho_s - \rho}{\rho} \right) D g} \sqrt{\frac{v U_0^3}{d}} = \left[D \left\{ \frac{(\rho_s - \rho) g}{\rho v^2} \right\}^{1/3} \right]^{0.4} \left(\frac{r_{t1}}{d} \right)^{7/2}$$

$$\text{or, } \frac{K''(\varphi)}{(0.013 \tan \varphi)} \frac{1}{\left(\frac{\rho_s - \rho}{\rho} \right) D g} \left[\frac{D^{2/3}}{v^{2/3}} \left\{ \frac{(\rho_s - \rho) D g}{\rho} \right\}^{1/3} \right]^{-0.4} \sqrt{\frac{v U_0^3}{d}} = \left(\frac{r_{t1}}{d} \right)^{7/2}$$

$$\text{or, } \frac{K''(\phi)}{(0.013 \tan \phi)} \left[\frac{U_0^{6.8}}{\left\{ \left(\frac{\rho_s - \rho}{\rho} \right) Dg \right\}^{3.4}} \right]^{1/3} \left(\frac{v^{0.8}}{U_0^{0.8} D^{0.8}} \right)^{1/3} \sqrt{\frac{v}{U_0 d}} = \left(\frac{r_{tl}}{d} \right)^{7/2}$$

$$\text{or, } \frac{K''(\phi)}{(0.013 \tan \phi)} \frac{[F_0^{6.8}]^{1/3}}{[R_s^{0.8}]^{1/3} R_0^{1/2}} = \left(\frac{r_{tl}}{d} \right)^{7/2}$$

$$\text{or, } \frac{r_{tl}}{d} = \left[\frac{K''(\phi)}{(0.013 \tan \phi)} \frac{[F_0^{6.8}]^{1/3}}{[R_s^{0.8}]^{1/3} R_0^{1/2}} \right]^{2/7}$$

Now, using Eq. 4.24, the above equation becomes

$$\frac{r_t}{d} = C_1 + [K''(\phi)]^{2/7} \left[\frac{F_0^{6.8}}{(0.013 \tan \phi) R_s^{0.8} R_0^{1.5}} \right]^{2/21}$$

Eq. 4.42 on page 72

Again, for $D_* > 50$ the threshold shear stress

$$\tau_{*c} = 0.06 \tan \phi$$

Eq. 2.22 on page 17

Now comparing Eq. 2.22 and 2.19 and using Eq. 4.37, similarly as in Eq. 4.40, we can derive

$$\frac{r_t}{d} = C_1 + [K''(\phi)]^{2/7} \left[\frac{F_0^4}{(0.06 \tan \phi)^2 R_0} \right]^{1/7}$$

Eq. 4.43 on page 72

$$v_r = -\frac{Q}{2\pi} \frac{r}{[z_0^2 + r^2]^{3/2}}$$

Eq. 4.44 on page 73

$$v_{rb} = g_1(\theta, i)v_r$$

$$\left(\frac{\partial u'}{\partial z'} \right)_A = \frac{2}{\sqrt{3}} \sqrt{\frac{-v_{rb}^3}{(z_0^2 + r^2)^{1/2} v}} = \frac{2}{\sqrt{3}} \sqrt{\frac{-v_{rb}^3}{r_{a0} v}}$$

Eq. 4.45 on page 73

Eq. 4.47 on page 74

Using Eq. 4.44 and 4.45

$$\therefore v_{rb} = -g_1(\theta, i) \frac{Q}{2\pi} \frac{r}{[z_0^2 + r^2]^{3/2}}$$

Assuming that the seepage flow has little effect on scouring and using the above value of v_{rb} in Eq. 4.47, we get

$$\left(\frac{\partial u'}{\partial z'} \right)_A = \frac{2}{\sqrt{3}} \sqrt{\frac{-v_{rb}^3}{(z_0^2 + r^2)^{1/2} v}} = \frac{2}{\sqrt{3}} \sqrt{\frac{\left[g_1(\theta) \frac{Q}{2\pi} \frac{r}{r_{a0}^3} \right]^3}{r_{a0} v}}$$

since $r = r_{a0} \sin \psi$

Eq. 4.50 on page 75

$$\text{or, } \left(\frac{\partial u'}{\partial z'} \right)_A = \frac{2[g_1(\theta)]^{3/2}}{\sqrt{3}} \sqrt{\frac{\left[\frac{U_0 \pi d^2}{8\pi} \sin \psi \right]^3}{r_{a0}^9 v}} \quad \because r = r_b$$

$$\text{or, } \left(\frac{\partial u'}{\partial z'} \right)_A = \frac{[g_1(\theta)]^{3/2}}{\sqrt{384}} \sqrt{\frac{[U_0 d^2 \sin \psi]^3}{r_{a0}^9 v}}$$

Multiplying both sides by μ

$$\mu \left(\frac{\partial u'}{\partial z'} \right)_A = \tau_{c\theta s} = \rho v \frac{[g_1(\theta)]^{3/2}}{19.6} \sqrt{\frac{[U_0 d^2 \sin \psi]^3}{r_{a0}^9 v}}$$

$$\text{or, } \tau_{c\theta s} = \frac{[g_1(\theta)]^{3/2}}{19.6} \rho \sqrt{\frac{\nu U_0^3 d^6 \sin^3 \psi}{r_{a0}^9}}$$

Eq. 4.52 on page 75

VITA AUCTORIS

Syeed Mahbub Ullah was born in 1975, in Dhaka, Bangladesh. He graduated from Bangladesh University of Engineering and Technology (BUET), Dhaka, Bangladesh, in October, 1999 with a Bachelor of Science in Civil Engineering.

He was accepted in the Faculty of Graduate Studies and Research, University of Windsor, in 2001 leading to the degree of Master of Applied Science in Civil Engineering.